

# **New methods for the synthesis of *N*-heteroaromatics and imines**



The  
University  
Of  
Sheffield.

**Kenji Philippe M. Kopf**

A thesis submitted in partial fulfilment of the requirements for the degree of  
Doctor of Philosophy

The University of Sheffield  
Faculty of Sciences  
Department of chemistry

February 2021

## Abstract

This thesis is divided into four chapters containing the work conducted at two universities, and it describes new methods for the synthesis of nitrogen-containing compounds.

The first chapter describes the project undertaken at The University of Sheffield. In this part, the scope of alkynylboronate cycloadditions with aromatic substrates was explored, to obtain highly functionalised heteroaromatic compounds. The aza-Diels-Alder cycloaddition reactions of 1,2,4-triazines with alkynes offered a rapid synthesis of highly substituted pyridineboronic esters. With these substrates, the possibility of controlling axial chirality through chiral tethers favouring one atropisomer over the other was envisaged. The scope was explored to establish empirical selectivity data relating the importance of the interaction between the functional group *ortho* to the biaryl axis and the chiral boronic ester on the diastereomeric excess.

In the second chapter of this thesis, the work done at Stockholm University is described. In this project, an efficient method for the oxidative coupling of a diverse variety of benzylamines with other nucleophilic partners was developed. This process is catalysed by a transition-metal functionalized MOF (Metal-organic framework), namely PCN-222(Pd), under light irradiation. Importantly, a side reaction arising from the self-condensation of two identical molecules of benzyl amine was avoided. This increased the scope of the reaction, as well as the usefulness of the process. Catalytic conditions to achieve this goal were found, and the substrate scope was investigated.

The third part describes the work done during the industrial secondment at AstraZeneca. This was focused on a recently developed Ni-catalysed benzannulation method for the mild and selective synthesis of functionalised phenols. During the secondment, the optimisation of the formation of heterocyclic compounds resulting from the Ni-catalysed coupling of cyclobutenone with different substrates such aldehydes, imines and nitriles was explored.

Finally, the last chapter describes a new approach to an unusual class of pyrimidine derivatives. Pyrimidines are amongst the most widely represented class of heterocycles in the chemical sciences. Based on this, we explored the synthesis of pyrimidine boronates via the condensation of stable ynone trifluoroborates with various guanidines to have access to aryl-, heteroaryl-, and alkyl- substituted aminopyrimidines containing the valuable boron functional handle.

## **Other documents based on this work**

This thesis summarizes the work performed at the University of Sheffield, at Stockholm University and at AstraZeneca within the multi-partner Innovative Training Network (ITN) European Joint Doctorate (EJD) “Catalytic Methods for Sustainable Synthesis. A Merged Experimental and Computational Approach” (CATMEC). Within this program, I aim to obtain a double PhD degree, from the University of Sheffield and from Stockholm University. Therefore, the content of this thesis will also be part of a report for the thesis defence at Stockholm University.

## Acknowledgements

I would like to thank my thesis supervisors, Professor Joseph Harrity and Professor Belén Martín-Matute for all the help they provided me with while writing this thesis and for letting me be a part of their team. Thank you for all for your advice and for teaching me everything that makes me a proud scientist. I would like to thank Dr. Werngard Czechtizky and Dr. Stefan Schiesser for supervising me during my time at AstraZeneca and make this secondment a real pleasure for me.

I would like to express my thanks to Professor Pher Andersson and to Aitor Bermejo-López for reading this thesis and providing valuable feedback.

I also wish to thank all the members of my research group for their collaboration but also for all the fun we have had at the lab and outside of work (the pub lunches, the pub evenings). Thank you for your advice and your help. Thank you for standing my singing in the lab, as well (Chris, I still dream of our amazing soprano duo). Larry and his *théories du complot* (conspiracy theories), I wish you the best. Marie, your swag and your hips that don't lie when saying "Putain !". I want to thank you, too. Matt, also known as the British agent, thank you for your help during this thesis and for having always been nice. Special thanks to you for your sense of humour after a pint! Keep going! Aitor, for your help, your kindness, your humour, your honesty, to your help for my thesis, during my time at SU and to always be happy to share a beer! I want to thank everyone else: Sophie, David, Samuel, Sergio and many more! You guys rock!

I would also thank my teacher who gave me the will and the desire to do a PhD. Dr. Marianne Wiaux, you are a great teacher and I hope you can inspire more students to continue! (Quote: *De la régularité Kenji* ☺)

Now, on the other side of the Channel, thanks to all my family and friends from home. I will now turn to French:

*Mes chers parents, je pars... Je vous aime, mais je pars... Non, mais ne vous inquiétez pas, je reviens ! Merci à vous deux, car sans vous je ne serais pas là où j'en suis. Votre soutien depuis le début de mes études jusqu'à maintenant n'a pas de prix. Les vrais héros des temps modernes sont nos parents et j'en suis fier ! Je vous aime !*

*Ma sister, sista, sisi pour les intimes (non maman, pas l'impératrice... quoi que...), je suis sûr que nous sommes jumeaux mais j'ai juste profité du forfait « all inclusive » un peu plus longtemps. Nous sommes tellement pareils et différents par la même occasion. Juste merci, ma sœur, nos souvenirs sont de l'or, so is your heart!*

*Mes grands-parents chéris. Les souvenirs chaleureux de mon enfance jusqu'à maintenant. Vous faites partie intégrante de mon éducation. Je vous remercie de tous ces moments : des jeux de sociétés, des poulets-purée-compote, des balades en forêt. Tout est gravé dans la roche. Je vous aime !*

*Merci à tous mes amis, ma belle-famille choisie. Timothée, ma moule, on se connaît depuis nos deux ans et maintenant, regarde nous... Au secours ! Non, je plaisante ! Merci, mon mollusque préféré. Tu es un véritable ami and I am so proud of you ! The best doctor ever !*

*Merci à toi, Nath ! On ne s'est plus vu pendant un moment, mais les retrouvailles étaient comme la suite d'un livre, amazing! Ou plutôt devrais-je dire une trilogie : TNK ou ENFP pour les intimes. Tellement merci de faire partie de mes amis.*

*J'enchaîne maintenant avec Louise, ma miss préférée ! Un cœur d'or dans une veste en jean ! Home-made, of course! Tu es une amie comme on les rencontre rarement. La droiture artistique ou un modèle contemporain ou bien les deux ? Merci, miss !*

*Mon cher guillaume, tu es un vrai rock ! Base solide sur qui on peut compter et dont l'amitié ne change pas avec le temps. Sans toi, je ne saurais pas assumer complètement la folie de ma quatrième personnalité. Tu gères, merci, old friend! Bien sûr, je remercie également tous les autres qui font partie intégrante de ma vie et de mes souvenirs.*

*Alexandre, mon mister lova lova ! L'amitié qui se déclenche à retardement mais, mon père, ce que tu me fais rire ! Merci, mon grand brun des neiges !*

*Guy, mon bel estomac. Malcolm, mon faquin des bois. Pablo, mon faquin des champs. Pauline, girl you know it's true (chorégraphie à la Rihanna sans vomir). Gael et mimi, mes cousins d'ammouuuuur (c'est sexyyyyy).*

But also, I cannot not mention you, Caffeine, always with me in the morning. Thanks for getting me through the day. Tea, much more British, but after three, you are my dream.

X. Anax, E. Fitose and S. T. IlNocte, thank you for all the time I was down during this thesis (nights together are always the best parties). P. Araceta and I. Buprofen, when the pain hit me in the face or when work was too much, you were always there for me. Thank you.

*Bien sûr*, the best for the end. I wish to thank my amazing man. Thank you for standing by me, for supporting and helping me. You are the ground of my life and the sky of my dreams. With you I feel so much better than ever have. My soul is finally complete. Thank you, my beautiful husband. Forever and after. I love you

This project has received funding from the European Union's Horizon 2020 research innovative programme under grant agreement No 721223

# Table of Contents

Abstract.....	i
Other documents based on this work.....	ii
Acknowledgements .....	iii
Table of Contents .....	v
Abbreviations .....	vi
List of publications.....	vii
Network Overview .....	1
General introduction .....	1
<b>1. Chapter I. Synthesis of heteroaromatic atropisomers.....</b>	<b>3</b>
1.1. Introduction.....	3
1.1.1. Pyridine in organic chemistry .....	3
1.1.2. Diels-Alder cycloaddition.....	5
1.1.3. Atropisomerism.....	10
1.2. Aim of Chapter I.....	12
1.3. Results and discussion .....	13
1.3.1. Synthesis routes to cycloaddition.....	13
1.3.2. Resolution of atropisomers .....	17
1.4. Conclusion and outlook .....	22
<b>2. Chapter II. Synthesis of imines via MOF-catalysed oxidative condensation of amines ....</b>	<b>23</b>
2.1. Introduction.....	23
2.1.1. Synthesis of imines .....	23
2.1.2. Metal-organic frameworks for catalytic applications .....	27
2.1.3. Synthesis of imines catalysed by MOFs .....	30
2.2. Aim of this chapter .....	32
2.3. Results and discussion .....	32
2.4. Conclusion and outlook .....	42
<b>3. Chapter III. Synthesis of heterocyclic compounds via Ni-catalysed benzannulation.....</b>	<b>43</b>
3.1. Introduction.....	43
3.1.1. Base-mediated benzannulation .....	43
3.1.2. Transition metal-mediated benzannulation.....	44
3.2. Aim of this chapter .....	45
3.3. Results and discussion .....	46
3.4. Conclusion .....	51
<b>4. Chapter IV. Synthesis of Pyrimidin-6-yl Trifluoroborate Salts as Heterocyclic Boronic Acid Derivatives .....</b>	<b>52</b>
4.1. Introduction.....	52
4.2. Aim of this chapter .....	54
4.3. Results and discussion .....	54
4.4. Conclusion .....	58
<b>5. Chapter V. Experimental part.....</b>	<b>59</b>
5.1. General consideration .....	59
5.2. Chapter I .....	60
5.3. Chapter II.....	84
5.4. Chapter IV.....	92
<b>References.....</b>	<b>99</b>
<b>Appendix.....</b>	<b>97</b>

## Abbreviations

BINOL	1,1'-bi-2,2'-naphthol
br	broad
calcd	calculated
cat.	catalytic
Cp	Cyclopentadiene
CPME	cyclopentyl methyl ether
$\delta$	chemical shift
d	doublet
DCM	dichloromethane
DG	directing group
DMF	dimethylformamide
DMSO	dimethyl sulfoxide
Dppb	1,4-Bis(diphenylphosphino)butane
DppBz	1,2-Bis(diphenylphosphanyl)benzene
Dppe	1,2-Bis(diphenylphosphino)ethane
E <sup>+</sup>	electrophile
eq	equivalent
FTIR	Fourier transform infrared
HAP	Hydroxyapatite
HOMO	highest occupied molecular orbital
HTs	Hydrotalcites
h	hour
LCCT	Ligand-to-cluster charge transfer
LUMO	Lowest unoccupied molecular orbital
m	multiplet
Me	Methyl
MOF	Metal organic framework
NMR	nuclear magnetic resonance
Nu	nucleophile
O.N	over night
PCy <sub>3</sub>	Tricyclohexylphosphine
Ph	phenyl
py	pyridine
q	quadruplet (NMR)
rt	room temperature
s	singlet (NMR), strong (FTIR)
sat.	saturated
SDAs	structure directing agents
SM	starting material
t	triplet
TBAF	tetra- <i>n</i> -butylammonium fluoride
TCPP	tetrakis(4-carboxyphenyl)porphyrin
THF	tetrahydrofuran
TMDA	N,N,N',N'-Tetramethyl ethylenediamine
Tol	toluene
t <sub>R</sub>	retention time

# List of publications

## List of publications

This report is based on the following publications/manuscripts:

### PAPER I:

**Development of a thermodynamic dynamic thermodynamic resolution of atropisomeric boronic ester**

K. P. M. Kopf, S. Bachollet, L. Valdez-Perez, N. Orlov, J.P.A. Harrity.

*Manuscript in preparation*

### PAPER II:

**Photoinduced selective synthesis of imines via amine condensation catalyzed by Pd@PCN-222**

A. Bermejo-López, K. P. M. Kopf, S. Carrasco, A. Sanz-Marco, M.S Hvid, B. Martín-Matute.

*Manuscript in preparation*

### PAPER III:

**Novel Pyrimidin-6-yl Trifluoroborate Salts as Highly Air- and Moisture-stable Heterocyclic Boronic Acid Derivatives.**

D. L. Cousins, K. P. M. Kopf, P. Fricero, E. J. McColl, W. Czechtizky, Y. H. Lim, J. P. A. Harrity

*Manuscript accepted*

## Author contribution:

### PAPER I:

- The synthesis of highly substituted N-heteroaromatic compounds under mild conditions via substrate directed aza-Diels-Alder cycloaddition reactions.
- Using a chiral resolving agent such (R)-BINOL to control the product axial chirality, favouring one atropisomer over the other via dynamic processes.
- Engaging chiral atropisomeric boronic esters in further catalytic cross-coupling processes.
- Establishing empirical stereoselectivity data relating the importance of the interaction between the functional group on the alkyne and the chiral boronic ester

### PAPER II:

- Developing the optimization of the reaction after the initial findings.
- Expanding the scope using the best conditions found.

### PAPER III:

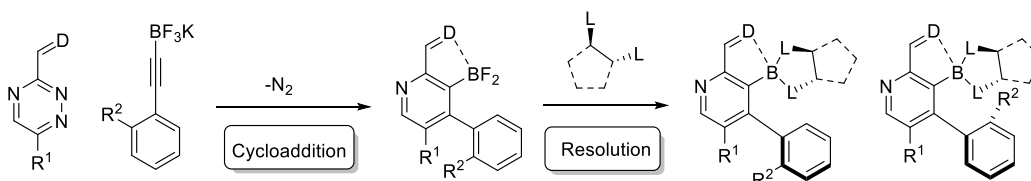
- Developing the optimization of the condensation after the initial findings.
- Expanding the scope of the synthesis of pyrimidine using the best conditions found.
- Investigate the potential of these compounds for further organic synthesis

## Network Overview

The work presented in this report has been performed within the multi-partner Innovative Training Network (ITN) European Joint Doctorate (EJD) “Catalytic Methods for Sustainable Synthesis. A Merged Experimental and Computational Approach” (CATMEC). This ITN network aimed to offer state-of-the-art training to early stage researchers (ESRs) in sustainable chemical synthesis, catalysis, computational chemistry and bioactive molecule synthesis design on both traditional and non-traditional (e.g. flow) platforms. The network comprised three full academic partners and three industrial partners. This thesis presents the research undertaken towards a European Joint doctorate between the University of Sheffield (group of Prof. J. P. Harrity, home university) and Stockholm University (group of B. Martín-Matute, host university). The aim of this project was the synthesis of nitrogen containing compounds and comprised four distinct parts, which describe the work performed at the home university and at the host university.

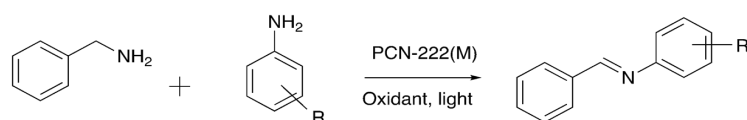
## General introduction

Nitrogen-containing compounds are common building blocks for the synthesis of organic compounds. Whether the nitrogen atom is located in a heterocycle or as part of an amine functional group, its derivatives are *ubiquitous* in agrochemicals and pharmaceuticals and they play a role in the constitution of biologically active compounds. This thesis will cover different routes for the synthesis of nitrogen-containing compounds. In the first project we investigated the development of a new and efficient strategy for the stereoselective synthesis of highly functionalised heteroaromatic compounds. This method comprises two different steps, as shown in Scheme 1. First, an aza Diels-Alder cycloaddition leading to a difluoroboron intermediate. The substituents on the aryl groups provide atropisomerism, and at this stage it is possible to resolve the atropisomers by reacting this intermediate with a chiral ligand.



**Scheme 1.** Key reactions involved in Chapter I.

The second part of this thesis, Chapter II, was conducted at Stockholm University. The goal of this project was to study the photocatalytic oxidative coupling of two different amines catalyzed by the MOF PCN-222(M) [M = Co, Ni, Cu, Zn, Pd] (Scheme 2). In particular, we wanted to identify which metal (M) on the PCN-222 would give the best performance, with a view to developing a protocol that gives high selectivity (cross-condensation *vs* self-condensation). This would dramatically increase the scope of the reaction, as well as the utility of the process. We also wanted to identify the advantages of using the current method compared to those described in the literature.



**Scheme 2.** Photocatalytic oxidative coupling of two different amines (Chapter II).

Chapter III described the work done during the industrial secondment at AstraZeneca. Our group have developed a Ni-catalysed benzannulation method for the mild and selective synthesis of functionalised phenols.<sup>1</sup> This chemistry offers an effective way to generate benzene-based target molecules from simple starting materials. However, it is currently limited with regard to the synthesis of heterocyclic compounds, such as lactones. During the secondment, optimal conditions have been investigated for the formation of heterocyclic compounds resulting from the Ni-catalysed coupling of cyclobutenone with different substrates such aldehydes, imines and nitriles. Finally, the last chapter describes a new approach to an unusual class of pyrimidine derivatives. Pyrimidines are amongst the most widely represented class of heterocycles in the chemical sciences. A significant proportion of marketed pyrimidines contain a 2-amino group, and so we investigated the scope of an ynone (potassium (3-oxo-3-phenylprop-1-yn-1-yl)trifluoroborate) condensation with various *N*-substituted guanidines. In particular, we explored the potential of this method to allow access to aryl-, heteroaryl-, and alkyl- substituted aminopyrimidines.

# 1. Chapter I. Synthesis of heteroaromatic atropisomers

## 1.1. Introduction

### 1.1.1. Pyridine in organic chemistry

Pyridines are an important class of molecules which continue to attract attention as they play a role in the preparation of biologically active compounds.<sup>2</sup> Pharmaceuticals containing pyridines appeared in the 1930s with the recognition of niacin's activity in the prevention of dermatitis and dementia. Nicotinic acid and its derivatives exhibit the biological activity of nicotinamide, which acts as an electron acceptor in many biological redox reactions.<sup>3</sup>

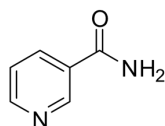


**Figure 1.** Structure of niacinamide (nicotinamide).

Over subsequent decades, many examples were shown to have applications in medicinal chemistry. Some of these organic compounds have anticancer properties, as well as activity against *Plasmodium falciparum*, a parasite responsible for many diseases in humans, such as malaria (Figure 2).<sup>4</sup>

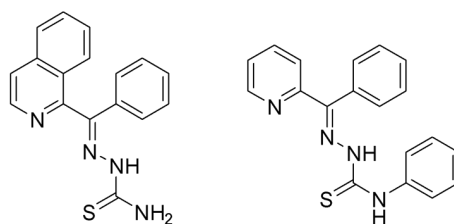


**Figure 2.** Thiosemicarbazones derived from quinoline (left) and pyridine (right) as anticancer drugs.

The heterocyclic structure based on pyridine was found useful in coordination chemistry as ligand in complexes of Ru and Os. For example, as fluorescence probes for DNA analysis and researching for mutations.<sup>5</sup>

From a structural point of view, pyridine is a 6 membered ring with six  $\pi$ -electrons that are delocalized over the ring (Figure 3). The molecule is planar and satisfies the Hückel rule for an aromatic system. Pyridine is a reasonable nucleophile for carbonyl groups and is often used

as a nucleophilic catalyst in acylation reactions. The nucleophilicity arises from the lone pair on the nitrogen atom which cannot interact in the aromaticity of the ring because the  $sp^2$  orbital is orthogonal to the conjugated  $\pi$ -system.<sup>6</sup>

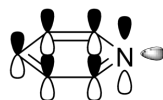
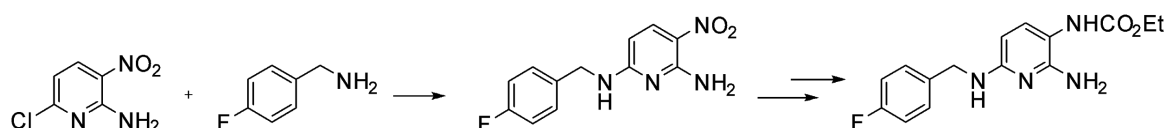


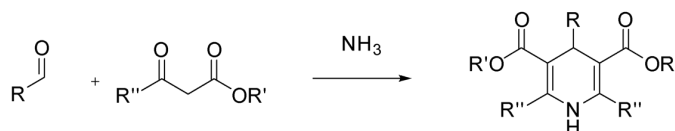
Figure 3. Orbital description of pyridine.

Pyridine is a poor substrate for electrophilic aromatic substitution since the nitrogen atom destabilizes potential Wheland intermediates and lowers the energy of the orbitals of pyridine's  $\pi$  system means that electrophilic attack on the ring is difficult. The carbons on the ring are unreactive, and the electrophilic reagents attack the nitrogen atom leading to a stable pyridinium cation, making the ring even less reactive. Thus, electrophilic aromatic substitution reactions such as nitration become very slow.<sup>5</sup> On the other hand, pyridine is more prone to undergo nucleophilic aromatic substitution than benzene. The intermediate anion generated by attack at the 2- and 4-positions is stabilized by the electronegative nitrogen atom and by delocalization inside the ring. Nucleophiles like thiolates or amines work well for this kind of reaction. Such reactions have been used for the synthesis of medicinal compounds such as the analgesic Flupirtine (Scheme 3).<sup>7</sup>



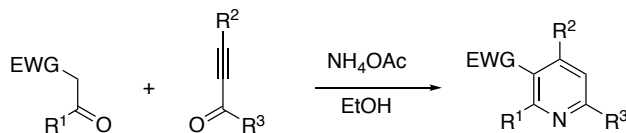
**Scheme 3.** Nucleophilic substitution on a chloropyridine in the nine-step synthesis of Flupirtine.

Because of its general utility, a wide range of syntheses have been reported to provide substituted pyridines, such as the Hantzsch reaction, which gives dihydropyridine derivatives by condensation of an aldehyde with two equivalents of a ketoester with ammonia (Scheme 4). An oxidation of the dihydropyridine can next lead to a substituted pyridine.



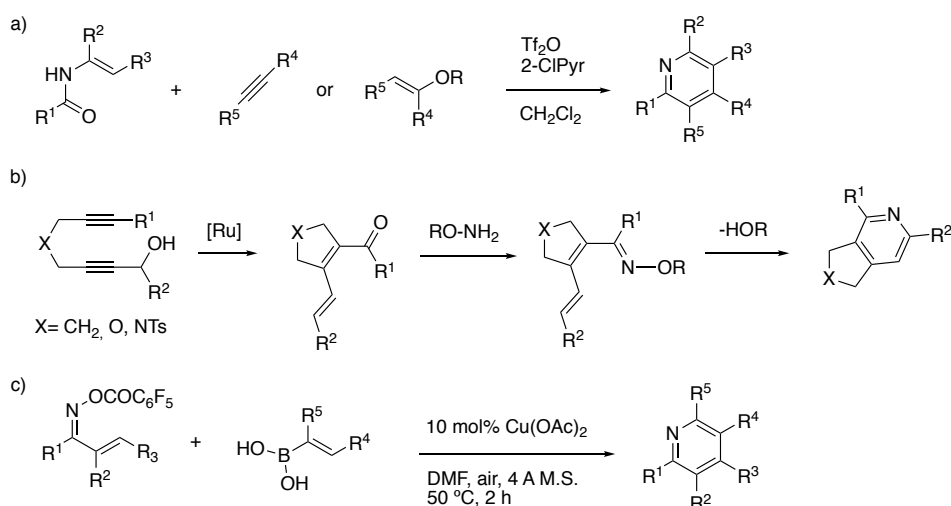
#### Scheme 4. General synthesis of Hantzsch ester.

The Bohlmann-Rahtz pyridine synthesis allows the generation of simply substituted pyridines by condensation of enamines with ethynylketones, which then undergo a cyclodehydration (Scheme 5).<sup>8</sup>



#### Scheme 5. General Bohlmann-Rahtz pyridine synthesis.

At this point, many researchers attempted the development of mild and efficient methods for the synthesis of highly substituted pyridines. Many syntheses are based on condensation reactions,<sup>9</sup> metal-catalysed cycloaddition reactions<sup>10</sup> or by thermal electrocyclizations<sup>11</sup> (Scheme 6).



**Scheme 6.** A) Single-step synthesis of pyridine derivatives by condensation of nucleophiles with amides. B) Ruthenium-catalyzed cycloisomerization–6 $\pi$ -cyclization. C) Cascade reaction comprising thermal electrocyclization.

### 1.1.2. Diels-Alder cycloaddition

Cycloadditions are an important class of reactions which can provide complex cyclic compounds in a one-step process. The Diels-Alder reaction is a cycloaddition where a conjugated diene reacts with a dienophile.<sup>12</sup> This reaction is classified as a [4+2] cycloaddition where the 4 and 2 represent the number of atoms involved in the ring forming process.

Two species are involved in this reaction (a diene and a dienophile) and the substituents in these two species can influence the cycloaddition rate.<sup>13</sup> In the case of a normal electron-demand Diels-Alder reaction, an electron rich substituted diene (HOMO raised in energy) accelerates the reaction with electron-withdrawing substituted dienophiles (LUMO lowered in energy). In another case, an electron-withdrawing groups on the diene (LUMO lowered in energy) accelerate the cycloaddition with dienophiles having electron-donating groups (HOMO raised in energy). For this last one, the reaction is called an inverse electron-demand Diels-Alder process (Figure 4).<sup>14,15</sup>

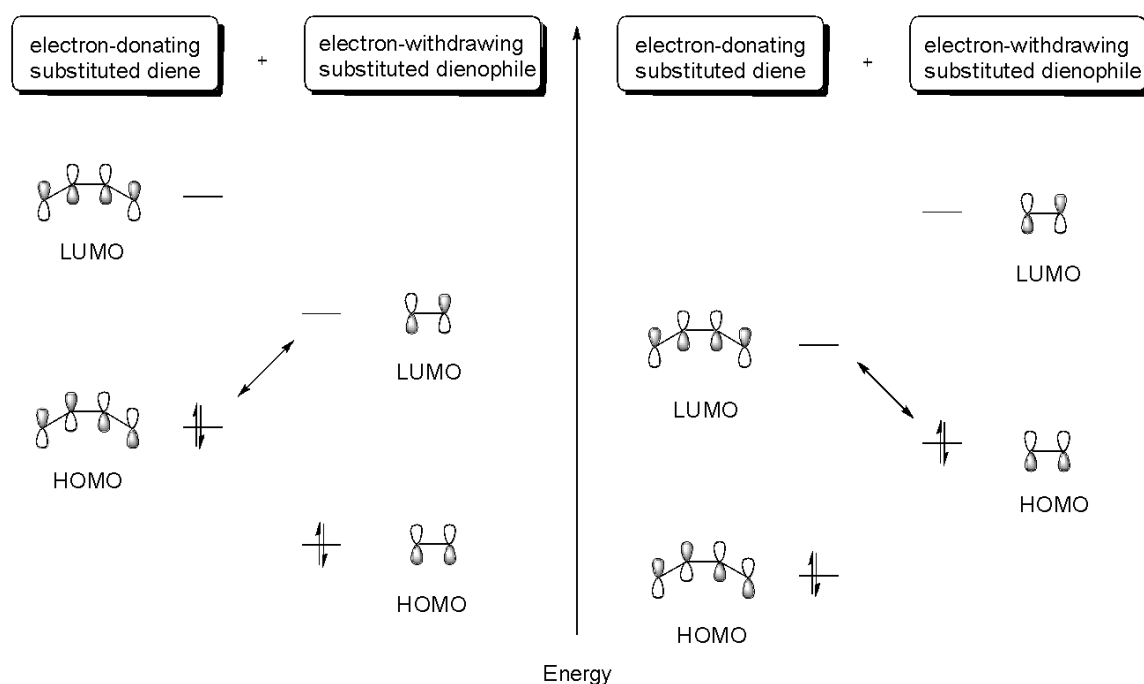
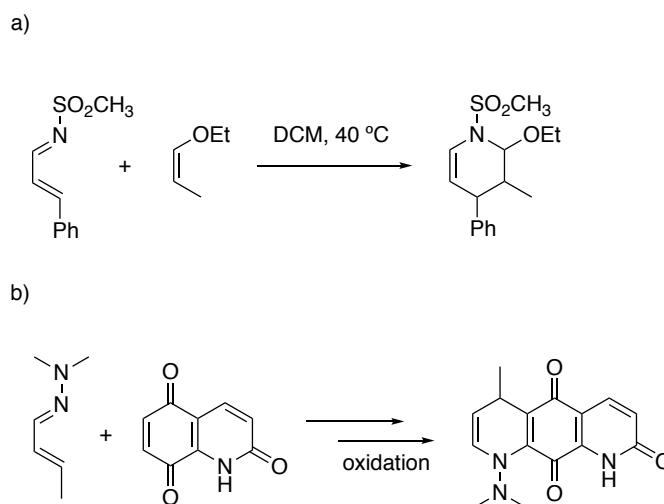


**Figure 4.** Frontier orbital interactions in Diels-Alder reactions.

This reaction is atom economical and a very powerful method to synthesize six-membered rings. There are many examples in organic chemistry using this reaction, like the synthesis of steroids by Woodward in 1952<sup>16</sup> or the synthesis of Morphine by Gates and Schudi<sup>17</sup> in 1952 and represent a powerful tool for biomedical applications as drug delivery systems.<sup>18</sup>

Because of its broad utility, the Diels-Alder reaction has been used to prepare heterocyclic compounds. Many reports highlight the use of 1-azadienes in hetero Diels-Alder reactions, such as in Behforouz and Ahmadian's work in 2000<sup>19</sup> or Mahajan and co-workers in 2002 (Scheme 7).<sup>20</sup>



**Scheme 7.** Diels-Alder reaction using electron deficient A) or electron rich B) 1-azadienes.

Depending on the substituent on the nitrogen atom, the reaction occurs via a normal electron demand (electron-rich 1-azadienes) or inverse electron demand (electron-deficient 1-azadiene) process.<sup>21</sup>

A particularly popular heterocycle forming variant of the Diels-Alder reaction uses substituted 1,2,4-triazines with enamines.<sup>22</sup> This represents the most thoroughly investigated heteroaromatic azadiene system capable of  $4\pi$  diene participation.<sup>23, 24</sup> An example of this application was based on the synthesis of Streptonigrin by Weinreb and co-workers in a 34-step route in 1980.<sup>25</sup> A few years after, Boger *et al.* reported the potential utility of the inverse electron demand Diels-Alder reaction of 1,2,4-triazines with an enamine for the construction of the Streptonigrin biaryl C ring.<sup>26</sup>

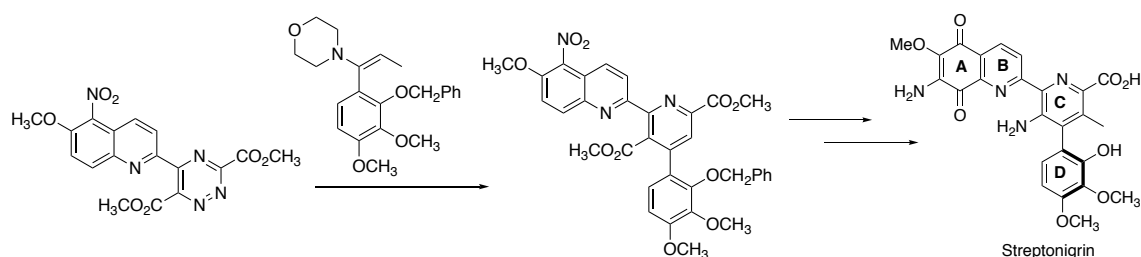


**Figure 5.** Inverse electron Diels-Alder for the construction of ring C of Streptonigrin.

Based on preceding studies for a cycloaddition route to substituted pyridines, they analysed the potential of an enamine in an inverse electron demand Diels-Alder process (Figure 6).<sup>27</sup>

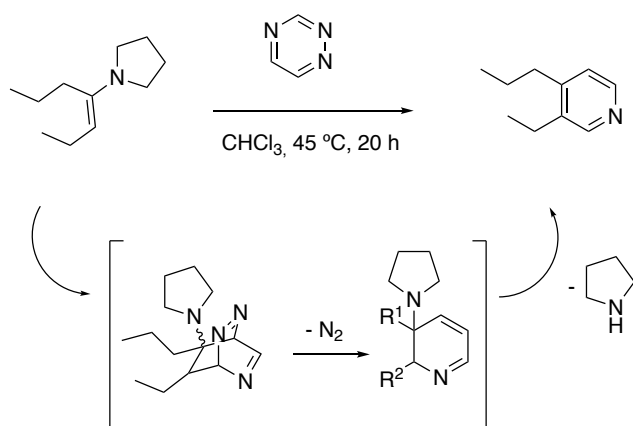


**Figure 6.** Example of an aza Diels-Alder of 1,2,4 triazine with an enamine.

We have recently become interested in this kind of reaction for the mild and regiocontrolled synthesis of heteroaromatic compounds by directed cycloadditions. In this strategy we used an alkyne bearing a Lewis acid that would promote pre-association with a diene bearing a complementary Lewis base (Figure 7).<sup>28</sup>

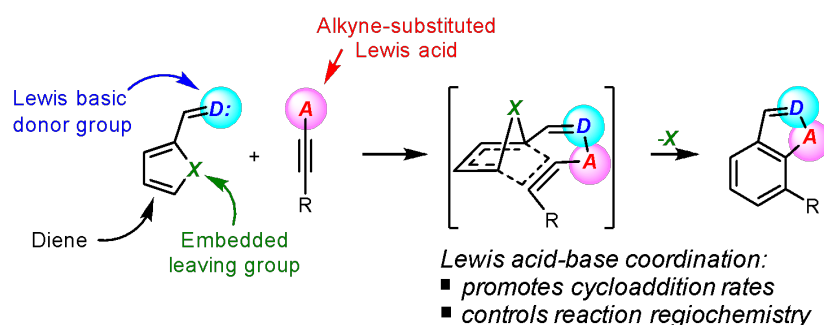


**Figure 7.** Directed cycloaddition via Lewis acid-base coordination.

Several examples of this type of reaction have been studied in our group, highlighting clear advantages of this strategy for the synthesis of aromatic and heteroaromatic compounds. For example, tetrazines, 2-pyrones and sydnone have all been found to undergo cycloadditions under mild conditions using this concept.<sup>29</sup> After this, our research group focused on establishing the reactivity of non-activated triazines with alkynes. A comparative study showed that the reaction of an alkynylboronic ester required harsh conditions and provided the corresponding product in low yield. In contrast, the use of an alkyne bearing a Lewis acid offered better conversion in only 20 min at moderate temperature with  $\text{BF}_3 \cdot \text{OEt}_2$  as a fluoride scavenger (Figure 8).

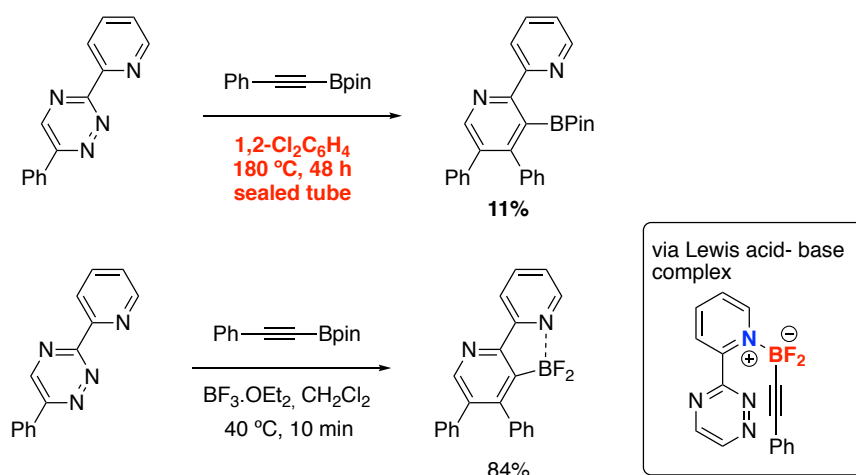
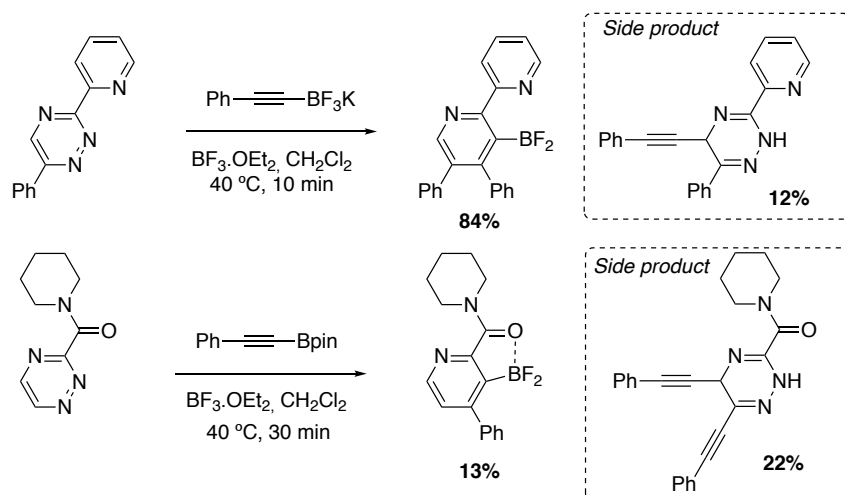


**Figure 8.** Inverse Diels-Alder cycloaddition of triazine. The insertion of a Lewis acid promoter generates the activate species in situ.

During a study on the reaction scope it was noted that when unsubstituted triazines were used, the corresponding products were obtained with a moderate yield. The reason was found to be a direct acetylide addition to the heteroaromatic ring leading to a minor side product. In the case where both C5 and C6 were unsubstituted, a double addition product was obtained leading to a lower yield of the desired product (Scheme 8).



**Scheme 8.** Directed cycloaddition with 1,2,4 triazines.

### 1.1.3. Atropisomerism

Atropisomerism results from restricted rotation about a single bond due to steric effects, where the energy barrier is high enough to isolate the different isomeric species.<sup>30, 31</sup> Based on this, we can classify three different types of atropisomerism. Class one concerns molecules which do not have atropisomeric properties because they show very fast axial rotation (Figure 9). Class three encompasses classical atropisomers: molecules which are kinetically inert meaning that no interconversion or racemisation is expected. Between these classes is the second class: with an interconversion energy of between 20 and 30 kcal/mol, these molecules have the potential to form atropisomers but the stereochemical integrity can be compromised over time.

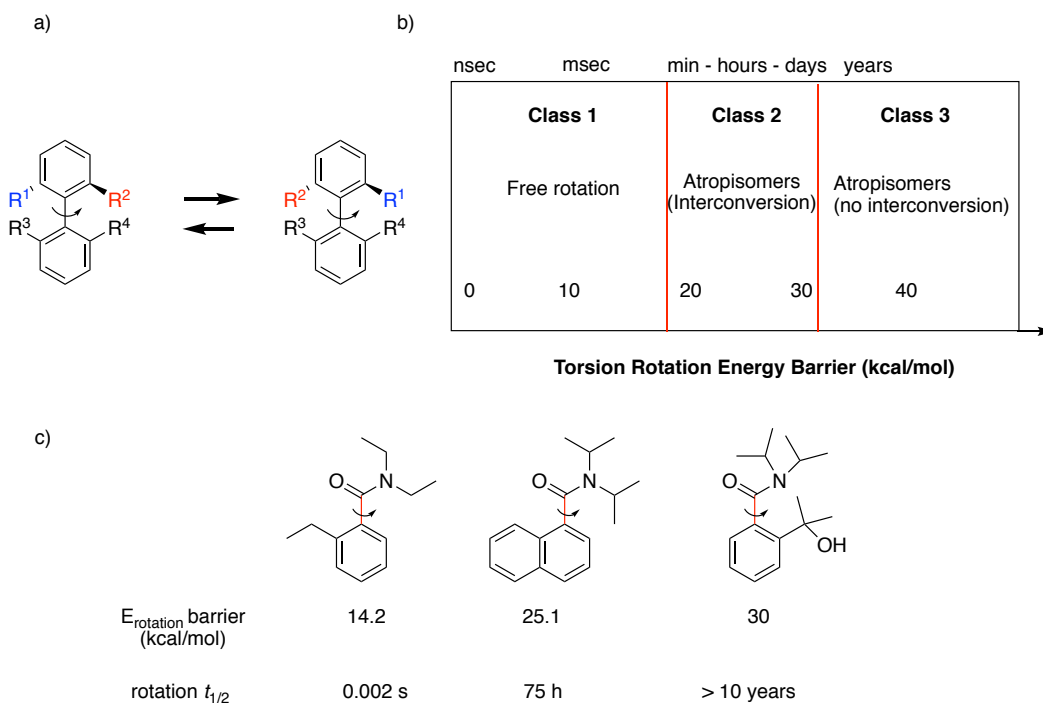


**Figure 9.** A) Interconversion of atropisomers. B) Atropisomers divided into different classes on the basis of the interconversion energy barrier. C) Example of different compounds from class 1, 2 and 3 represented with their energy of axial rotation barrier and their half-life time.<sup>30</sup>

Atropisomerism is not just an academic phenomenon, we can find this property in natural products, pharmaceuticals and agrochemicals. Several examples have been reported such as Stenagacin, a natural product which possesses significant activity against cells derived from human carcinoma of the nasopharynx, or Streptonigrin, used for treatment of cancer (Figure 10).<sup>32</sup> Some pharmaceutically important products have been synthesised in industry such as the Bcl-2 ligand by UCB celltech<sup>33</sup> for the regulation of cell death, or a CCR5 inhibitor by GSK as treatment for HIV infection.<sup>34</sup>

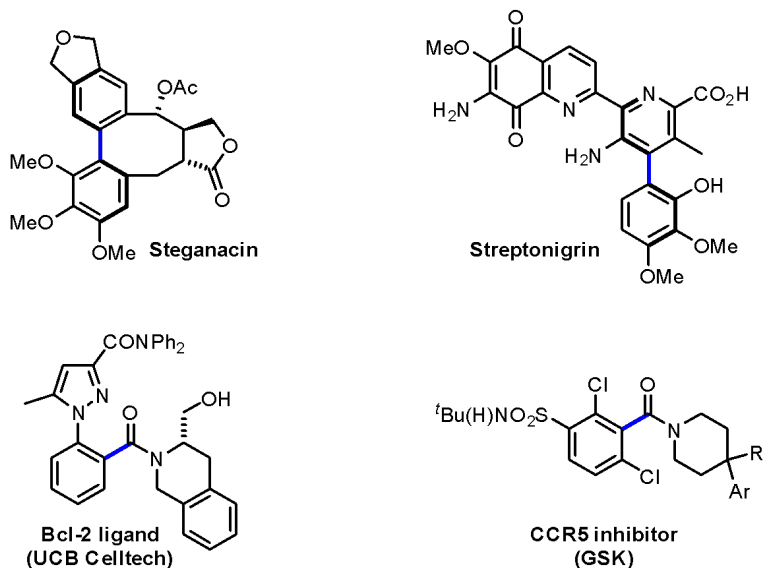
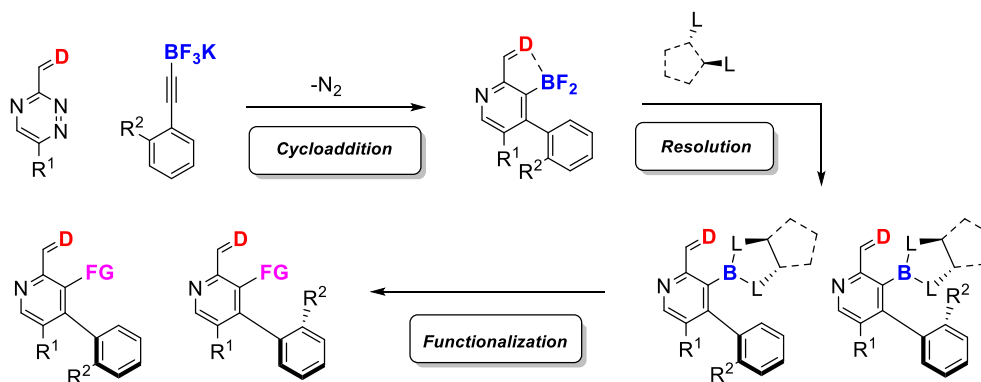


**Figure 10.** Examples of atropisomeric natural products and pharmaceutical compounds.

## 1.2. Aim of Chapter I

In this project, we plan to devise an efficient method for the stereoselective synthesis of functionalised atropisomers. This method will comprise three important steps, as shown in Scheme 9. First, an aza Diels-Alder cycloaddition produces a difluoroboron intermediate. The substituents on the molecule provide atropisomerism and at this stage it is possible to resolve the atropisomers by adding a chiral ligand to the molecule. The role of the boron is not only to act as Lewis acid promoting the association of the alkyne with the triazine, it also provides a site for the addition of the chiral ligand and also as a handle to further elaborate the products.

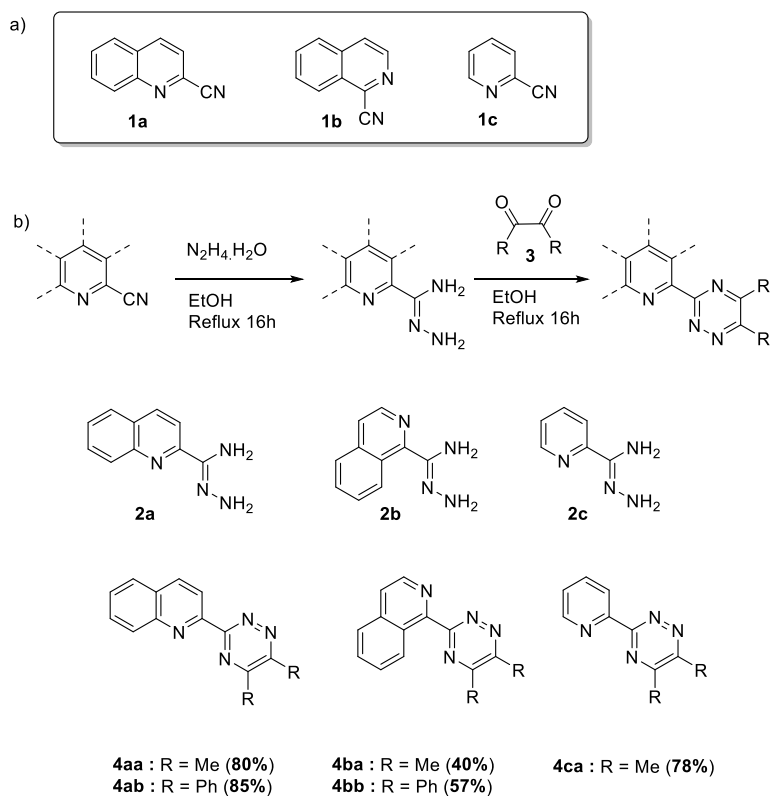


**Scheme 9.** The key reactions involved in this project.

## 1.3. Results and discussion

### 1.3.1. Synthesis routes to cycloaddition

This project started with the synthesis of the required dienes for the cycloaddition step. The condensation between an amidrazone with a 1,2-dicarbonyl derivative is a well-established way to synthesise triazines.<sup>35, 36</sup> This pathway has been explored by our group and allows analogues bearing quinoline or pyridine fragments to be easily prepared (Scheme 10).<sup>37</sup> Accordingly, the synthesis of these substrates was performed. This procedure began with the reaction of a cyanoquinoline derivative and hydrazine to obtain the corresponding amidrazone. The condensation was then performed with different 1,2-dicarbonyl structures.

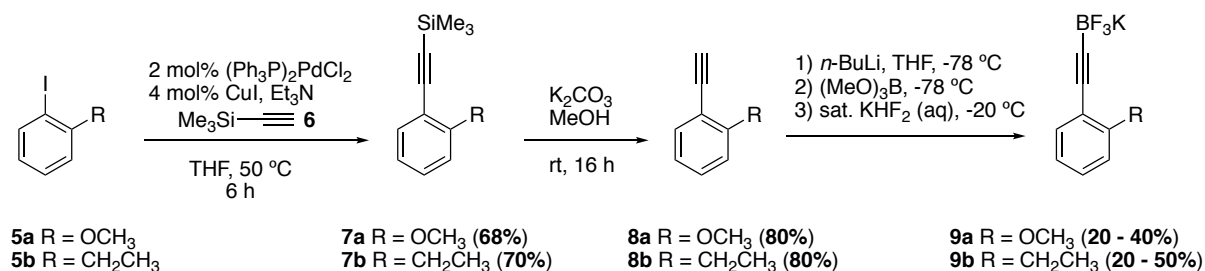


**Scheme 10.** a) Starting material used for the synthesis of 1,2,4-triazine. b) Formation of the amidrazone by reaction with hydrazine and condensation with 1,2-dicarbonyl compounds to form the corresponding triazine.

The formation of the quinoline and pyridine amidrazones **2a** and **2c** proceeded in quantitative yield and produced solid products that could be easily isolated by filtration. A similar outcome was observed during the condensation reaction with the 1,2-dicarbonyl compounds, and these processes took place in very good yields (Scheme 10).

Notably, the isoquinoline substituted amidrazone **2b** required a longer reaction time and it was not possible to isolate the product from **1b**. However, the crude was used directly for the next step to afford the compounds **4ba** and **4bb**.

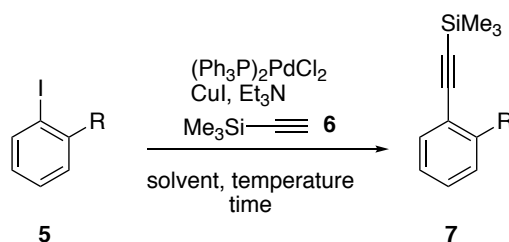
The synthesis of the alkynyltrifluoroborate salts was carried out next so that the cycloaddition reactions could be studied with the available 1,2,4-triazines. Iodobenzene compounds were chosen as precursors because of their commercial availability and their high reactivity in alkyne cross-coupling reactions.



**Scheme 11.** Synthesis routes toward the alkynyltrifluoroborate salts

The synthesis commenced with a Sonogashira coupling with ethynyltrimethylsilane followed by removal of the trimethylsilyl group leading to the ethynylbenzene precursors **8a** and **8b** (Scheme 11). An increase in catalyst loading led to a better yield of the reaction (Table 1, entry 2 & 5). When triethylamine was also used as solvent, no effect on the reaction yield was observed (Table 1, entry 3).

**Table 1.** Optimisation of the Sonogashira coupling<sup>a</sup>

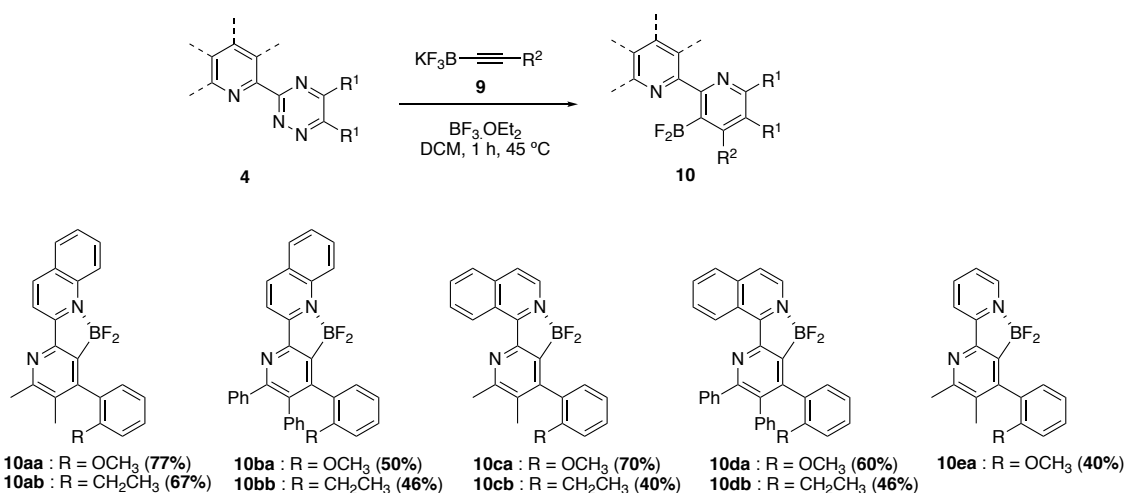


Entry	mol (mmol)	5	[Pd] (mol%)	[Cu] (mol%)	Solvent	7 (%) <sup>b</sup>
1	17.2	<b>5b</b>	2	4	THF	50
2	21.4	<b>5b</b>	4	8	THF	70
3 <sup>c</sup>	14.2	<b>5b</b>	4	8	--	65
4	14.1	<b>5a</b>	2	4	THF	55
5	21.4	<b>5a</b>	4	8	THF	68

a) Reaction conditions: **6** (2 equiv.), NEt<sub>3</sub> (6 equiv.), THF, 6 h, 50 °C. b) Yield c) Triethylamine used as solvent.

We next attempted to obtain the trifluoroborate salts by first deprotonating the alkyne (**8a**, **8b**) with *n*-butyllithium and adding an excess of trimethylboronate. An excess of KHF<sub>2</sub> dissolved in water, led to the product (**9a**, **9b**) in moderate yields.

The synthesis of both coupling partners was followed by the first cycloaddition with the triazine **4aa** with the alkynylboronate salts **9a**. This reaction was successful and so we continued this study by using different triazines (Scheme 12).



**Scheme 12.** Cycloaddition of the triazine **4** with the alkynylboronate salts **9**. Reaction conditions: 1) trifluoroborate salt **9** (3 equiv.), BF<sub>3</sub>·OEt<sub>2</sub> (3 equiv.), CH<sub>2</sub>Cl<sub>2</sub>, 40 °C, 30 min.

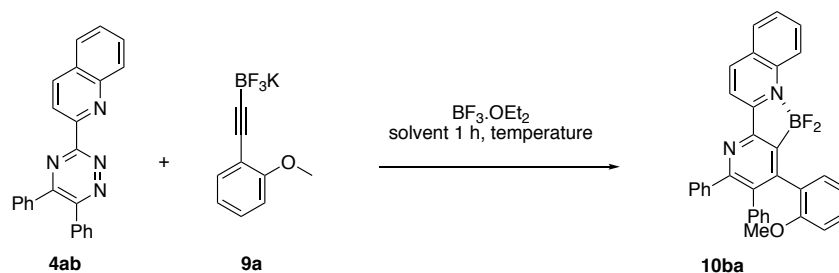
Different purification protocols were generally required across the examples shown in Scheme 12, and these are summarised in Table 2. The product **10ab** and **10aa** were purified by column chromatography over silica gel to afford a good yield (Table 2, entry 1-2). The isoquinoline **10ca** and **10cb** required the use of florisil column to afford a respectable yield of 40% and 70%, respectively (Table 2, entry 5-6).

**Table 2.** Purification method

Entry	Compound	Yield (%)	Purification method
1	<b>10ab</b>	67	Silica gel column (DCM: EtOAc) - (8 : 2)
2	<b>10aa</b>	77	Silica gel column (Hex: EtOAc) - (6 : 4)
3	<b>10bb</b>	46	Slow crystallisation in DCM
4	<b>10ba</b>	15	Slow crystallisation in DCM
5	<b>10cb</b>	40	Florisil column (Hex: EtOAc) - (8 : 2)
6	<b>10ca</b>	70	Florisil column (Gradient Cyclohexane, ending DCM)

During this study, we noted that product **10ba** was obtained in very low yield (Table 2, entry 4). In order to improve the yield, we varied reaction conditions and purification procedures (Table 3). Finally, a recrystallization of the alkynylboronate<sup>38</sup> **9a** was found to deliver the product in acceptable yield (Table 3). This result highlighted the importance of using pure alkyne substrate for optimal product yields.

**Table 3.** Optimisation of cycloaddition reaction<sup>a</sup>



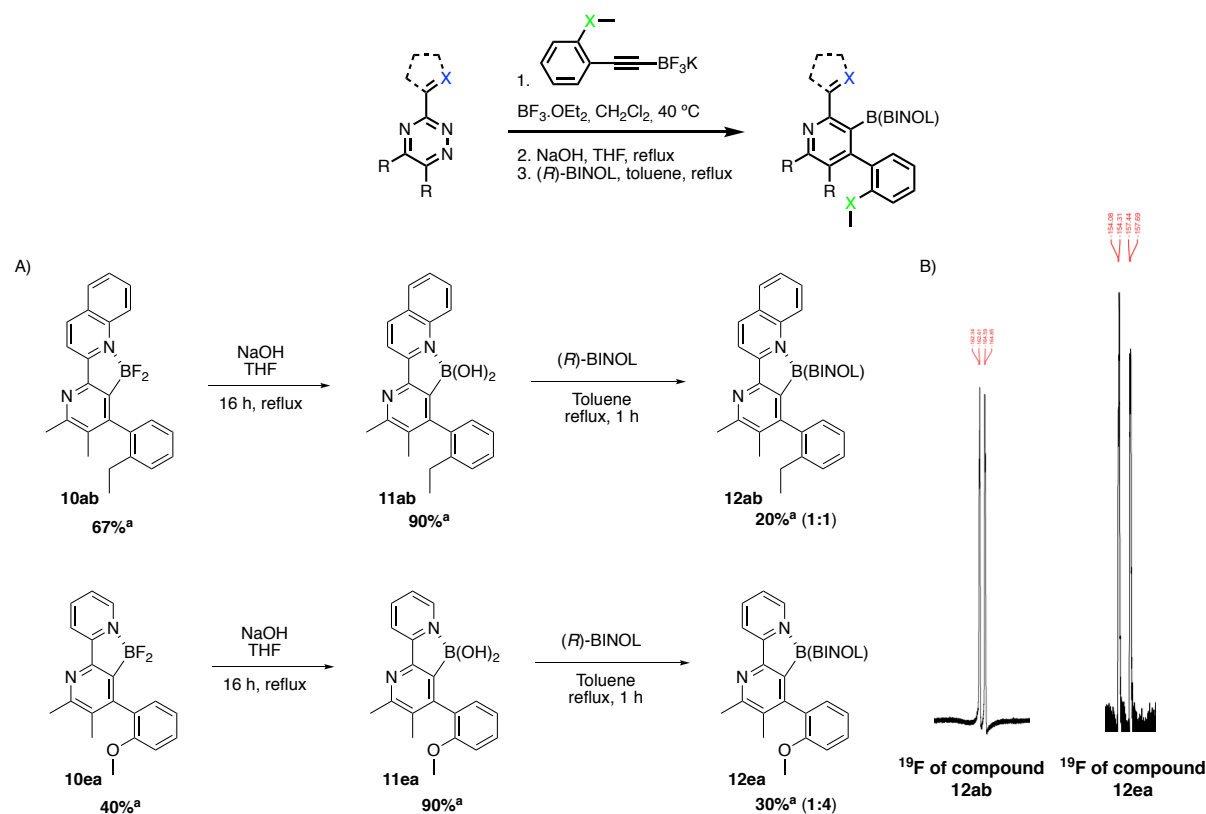
Entry	<b>9a</b> (equiv.)	<b>BF<sub>3</sub>·OEt<sub>2</sub></b> (equiv.)	Solvent	T (°C)	Yield (%) <sup>b</sup>
1	2.5	2.5	DCM	45	13
2	2.5	5	CHCl <sub>3</sub>	60	15
3	2.5	5	Toluene	85	Trace
4	2.5	5	THF	45	Trace
5 <sup>c</sup>	3	3	DCM	45	50

a) Reaction conditions: **9a** (2.5 equiv.), BF<sub>3</sub>·OEt<sub>2</sub> (2.5 equiv.), CH<sub>2</sub>Cl<sub>2</sub>, 1 h at 45 °C. b) Isolated yield .c) Recrystallisation of **9a** in hot acetone.

### 1.3.2. Resolution of atropisomers

The last part of this chapter concerns the resolution of the atropisomeric pyridines synthesised by cycloaddition. As described in the introduction, these molecules possess chirality that results from a hindrance of rotation about the biaryl bond. Indeed, evidence for atropisomerism was apparent from the <sup>19</sup>F NMR spectra of all the cycloadducts; two AB doublets could be discerned which was indicative of diastereotopic F-atoms. We then envisaged that the substitution of the fluorides for a chiral ligand could provide separable diastereoisomers. For this part, the boron played another major role because it provided a convenient handle to introduce chiral groups.

(*R*)-Binol was used as the chiral ligand of choice for the resolution step. The binol ester was generated from the corresponding boronic acid, which was in turn formed by addition of sodium hydroxide to the BF<sub>2</sub>-cycloadducts (Scheme 13).



**Scheme 13.** A) Cycloaddition and resolution of the atropisomers by insertion of chiral tether (*R*)-BINOL, B) <sup>19</sup>F NMR spectra of the cycloadducts **12ab** and **12ea** showing two AB doublets. Reaction conditions: 1) trifluoroborate salt (3 equiv.), BF<sub>3</sub>·OEt<sub>2</sub> (3 equiv.), CH<sub>2</sub>Cl<sub>2</sub>, 40 °C, 30 min; 2) NaOH (5 equiv.), THF, reflux, 16 h; 3) (*R*)-BINOL (1 equiv.), toluene, reflux, 1 h. a) Isolated yield.

Although the chiral boronic esters were formed in low yield, the stereochemical outcomes were surprisingly different. Specifically, **12ab** was formed as a mixture of two diastereoisomers in equal ratios, as expected. In contrast, compound **12ea** generated a measurable excess (**1:4**) of one diastereoisomer. A rationale for this latter result could be (i) the reaction proceeded to <100% conversion and that a kinetic resolution took place; (ii) the reaction proceeded with high conversion and that a dynamic thermodynamic resolution (or DTR) has taken place (albeit with a low yield of product).

With the work described in this chapter, we believe that a DTR takes place whereby the methoxy group can coordinate to boron to form a planar intermediate around the biaryl bond.

This mechanism provides a route to equilibration of the two diastereoisomers, and the one with the lower energy will be the major one (Figure 11).

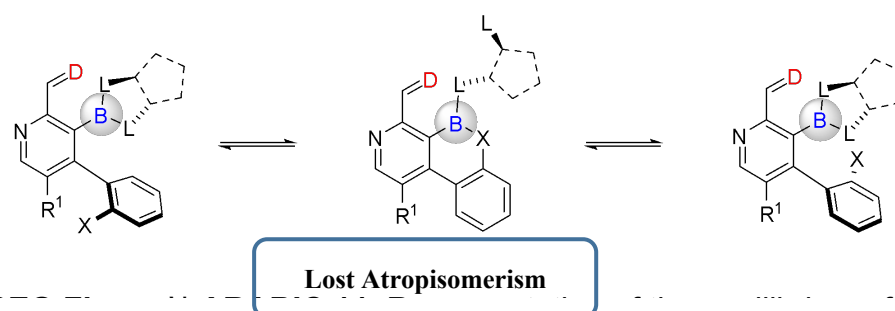
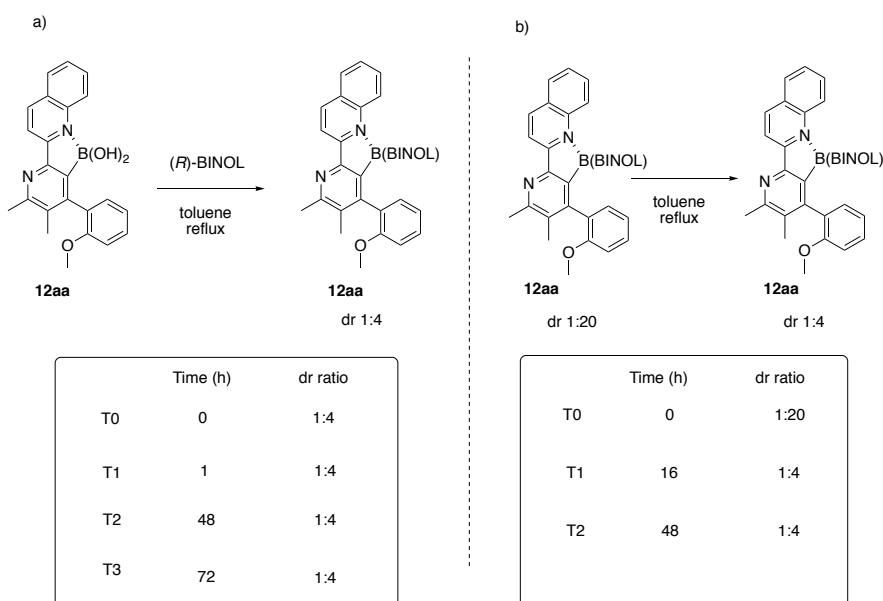


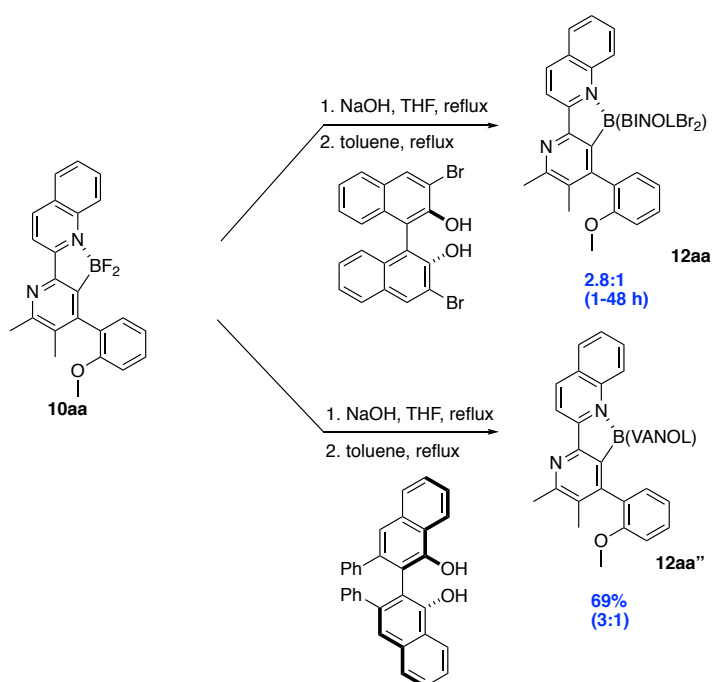
**Figure 11.** Lost atropisomerism. Coordination of the boron to the heteroatom, leading to a planar intermediate.

After this initial result, we analysed the change in diastereomer ratio of **10aa** in the reaction mixture over time. After formation of the corresponding boronic acid **11aa** under the same conditions as before, we used (*R*)-BINOL to form both stereoisomers. NMR analysis was used to monitor the variation of the diastereomer ratio over time (Scheme 14a). No change of the ratio was observed but after letting the mixture cool down, we observed precipitation in a ratio of 1:20 of the major diastereoisomer, which was confirmed by proton NMR. We decided to dissolve the solid in hot toluene and left the reaction for 16 h. Another NMR analysis showed that the diastereomeric ratio had returned to 1:4, suggesting that there is a dynamic equilibrium in the reaction (Scheme 14b).



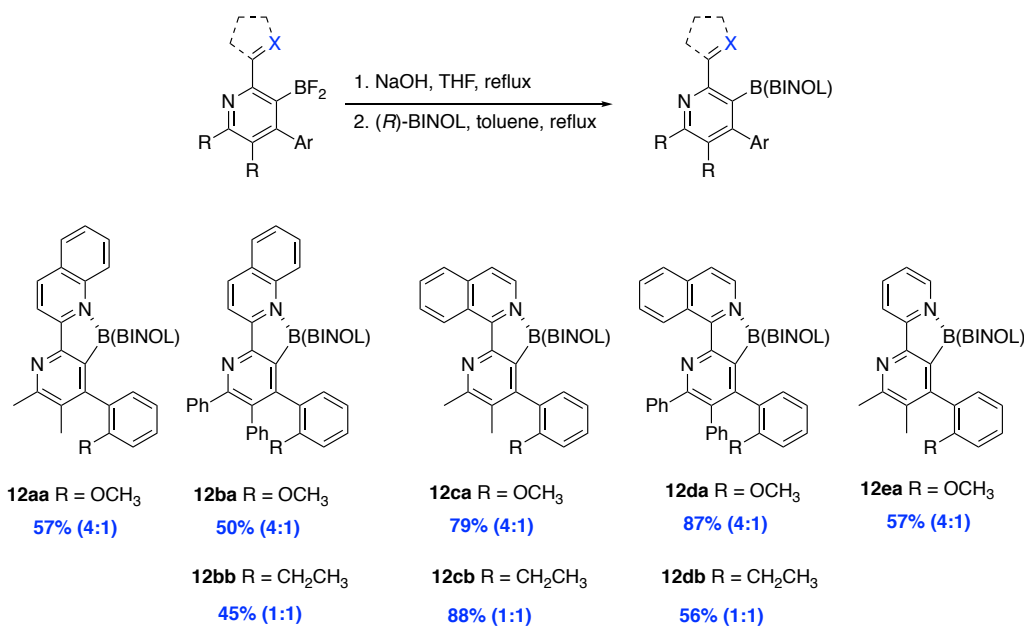
**Scheme 14.** Analysis of the changing diastereomeric ratio during time. a) Insertion of the chiral group on the boronic acid from **12aa** gave a ratio 1:4 of both diastereoisomers without any change after 3 days. b) The major diastereoisomer precipitated after cooling down the mixture to give a ratio of 1:20. This new ratio was heated again in toluene overnight, returning the ratio to 1:4.

Furthermore, we tried to add alternative chiral diols in order to improve the ratio of diastereomers. First, (*R*)-dibromo-BINOL was used but unfortunately the reaction offered a poorer ratio of 2.8:1 of **12aa'**. Based on that, we chose another ligand (*R*)-VANOL, but unfortunately this offered a similar ratio of products of 3:1 (Scheme 15). We therefore decided to proceed to the exploration of the scope with (*R*)-BINOL.



**Scheme 15.** Chiral ligand insertion for the resolution of the molecule. Hindered ligand was used to see the impact on the ratio of the diastereoisomers. <sup>a</sup>Isolated yield.

The resolution was extended to other boronic acid derivatives to generate the corresponding boronic esters. An excellent yield was obtained for the isoquinoline derivative **12ca** and **12cb** with respectively 79% and 88%. The other compounds afford a yield of 50% to 45% for the quinoline **12ba** and **12bb** bearing the phenyl group and 57% for the product **12aa** (Scheme 16). In these different cases, the diastereoisomers were not separable.



**Scheme 16.** Scope of the boronic ester synthesis. Reaction conditions: 1) **10** (1 equiv.), NaOH (10 equiv.), THF, reflux, 16 h 2) **11** (1 equiv.), (*R*)-BINOL (1 equiv.), toluene, reflux, 1 h.

After some optimisation, we were able to isolate both stereoisomers of **12cb** by preparative HPLC. One of them was next dissolved in toluene and heated at reflux for 2 h (Figure 12). Interestingly, in this case we did not observe any change of the ratio, which suggests that this substrate cannot undergo DTR.

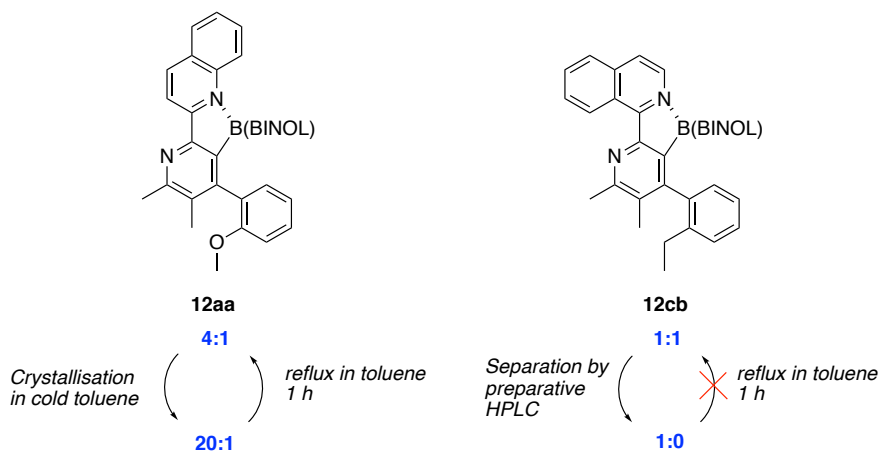


**Figure 12.** Analysis of the diastereomeric ratio over time. Left, the major diastereoisomer precipitated after cooling down the mixture to give a ratio of 1:20. This new ratio was heated again in toluene for 1 h, returning the ratio to 1:4. Right, the diastereoisomers were separated by preparative HPLC and one of them was then heated in toluene for 1 h, affording the same diastereoisomer ratio.

Finally, X-ray crystal structure was obtained of compound **12aa** after crystallization in cold toluene (Figure 13). The proton NMR of the resulting 20:1 mixture could confirm that the major diastereoisomer of the ratio 4:1 was the one isolate after crystallization by comparing the proton of the methoxy group of the two spectra. Also, the X-ray crystal structure highlighted a possible potential for  $\pi$ -stacking between the anisole and one of the biaryl rings of the BINOL. We could speculate that the minor diastereomer in these cases could have an unfavourable steric interaction of the ortho-substituent and the Binol ester oxygen atom favoring one diastereomer over the other.

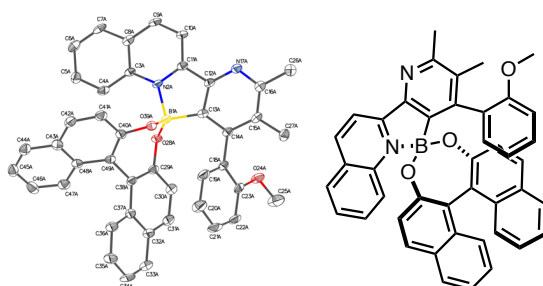


**Figure 13.** X-ray crystal structure of compounds **12aa** (left) and representation of the corresponding major diastereoisomer (right)

## 1.4. Conclusion and outlook

We have shown that the aza-Diels-Alder cycloaddition reactions of 1,2,4-triazines with alkynyltrifluoroborate salts offer a rapid method for the synthesis of atropisomeric pyridines bearing a boronic ester. The purity of the alkyne  $\text{BF}_3\text{K}$  salts or the  $\text{BF}_3\cdot\text{OEt}_2$  played an important role in the yield of the reaction. We also worked on the resolution of the molecules by addition of a chiral ligand and speculate that the interaction of an adjacent oxygen atom with the boron promotes equilibration of the diastereomers. The experiments suggest that the ratio is the result of dynamic thermodynamic resolution (or DTR).

As expected, when an ethyl group replaced a methoxy group, a diastereomeric ratio of 1:1 was obtained. After separation of both ethyl-substituted isomers, one was dissolved in toluene and heated at reflux for 1 h. Interestingly, in this case we did not observe any change of the diastereomeric ratio, which suggests that this substrate cannot undergo DTR.

As discussed, the role of the boron is not only to act as a Lewis acid that promotes association of the alkyne with the triazine, it also provides a site for the addition of a chiral ligand and also as a handle to further elaborate the products. This functionality could be use in cross coupling reactions, such as Suzuki coupling to afford a new panel of highly substituted aromatic compounds.

## 2. Chapter II. Synthesis of imines *via* MOF-catalysed oxidative condensation of amines

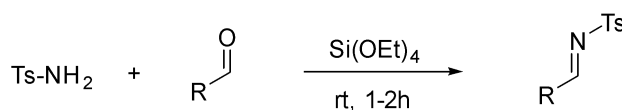
### 2.1. Introduction

In this section, synthesis of imines will be described. Imines are analogous to ketones and aldehydes but contain a C=N bond instead of a C=O bond. Imines are also known as Schiff bases, and are common synthetic intermediates in the preparation of heterocycles and other nitrogen-containing organic molecules.<sup>39</sup>

#### 2.1.1. Synthesis of imines

##### 2.1.1.1. Classical methods

Imines can be prepared by condensing carbonyl compounds (aldehydes and ketones) with primary or *sec*-amines under acidic conditions.<sup>40</sup> Even though this is the most straightforward method to prepare imines, it gives poor yields when using non-nucleophilic amines or acid-sensitive carbonyl compounds. Several alternatives have been developed to overcome these difficulties. For example, Love,<sup>41</sup> Look<sup>42</sup> and coworkers found that tetraethyl orthosilicate can be used to synthesise imines in these difficult cases, through their ability to act as desiccant to remove the water and shift the equilibrium towards the imine product (Scheme 17).



R = Alkyl, Aryl

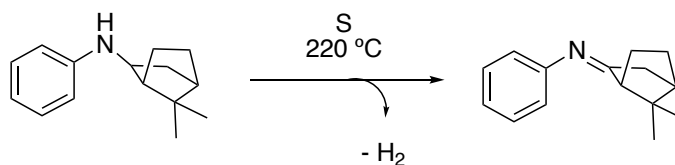
**Scheme 17.** Preparation of N-tosylaldimines.

Several different methods have been introduced to promote what is still essentially a condensation of an amine and aldehyde. But in this report, I will focus on alternative routes, namely those involving oxidation of alcohols or of amines.

## 2.1.1.2. Catalytic methods

### 2.1.1.2.1. C-N bond oxidation

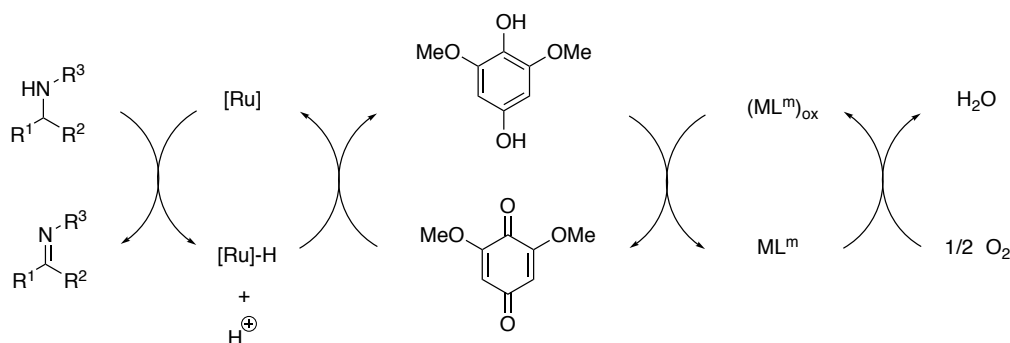
Imines can be prepared through oxidation of carbon-nitrogen single bonds. For example, Ritter and co-workers reported the dehydrogenation of isobornylaniline (Scheme 18) in the presence of sulfur.<sup>43</sup>



**Scheme 18.** Dehydrogenation of isobornylaniline to obtain the camphor anil.

In recent decades, it has been shown that the use of metal catalysts offers an efficient route for the synthesis of imines. A pioneering example was reported in 1988 by Nishinaga and co-workers, who demonstrated the use of Co(salen) complexes to dehydrogenate amines under aerobic conditions.<sup>44</sup> At this time, the dehydrogenation was not well documented and this pathway was proposed as a new route towards the synthesis of imines.

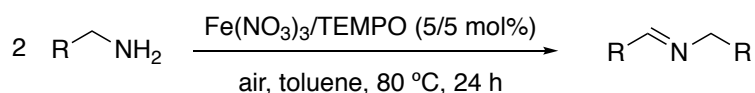
As mentioned, imines can be produced *via* the aerobic oxidation of amines under transition metal catalysis, in which the metal shuttles between an oxidized and a reduced form. A common challenge here is the high-energy barrier that must be overcome to re-oxidize the metal under aerobic conditions. This has been solved in some instances by using electron-transfer mediators. For example, Bäckvall and co-workers described a mild and efficient biomimetic ruthenium-catalysed pathway to generate aldimines and ketimines.<sup>45</sup> This design was inspired by the role of NAD<sup>+</sup> and ubiquinone in the biological oxidation of alcohols. By replacing nicotinamide by a ruthenium complex and cytochrome C by a metal macrocycle, they provided a route to oxidise secondary amines using oxygen as the final oxidant (Scheme 19).



**Scheme 19.** Aerobic oxidation of amines. As metal macrocycle ( $ML^m$ ), a  $[Co(salen)]$ -type complex, was used for the  $O_2$  activation.

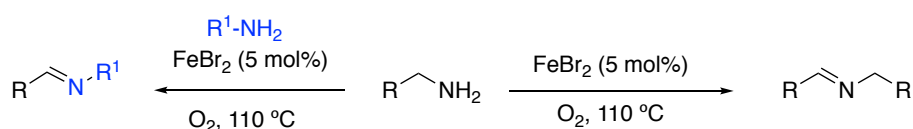
#### 2.1.1.2.2. Dehydrogenative coupling of amines

A different approach to produce imines consists of the dehydrogenative coupling of two different amines. Instead of oxidizing a C–N bond, two amines are reacted under catalytic conditions forming an imine and liberating ammonia. Numerous examples exist, using both homogeneous and heterogeneous catalysts. An example is shown in Scheme 20, where an iron / TEMPO catalytic system was used.<sup>46</sup>



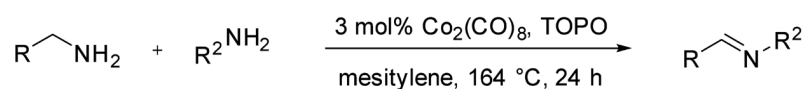
**Scheme 20.** Aerobic oxidation catalysed by iron

Gopalaiah and co-workers have also used iron catalysts under aerobic conditions for the dehydrogenative coupling of amines, which could lead to the self- or cross-condensation (Scheme 21).<sup>47</sup>



**Scheme 21.** Iron-catalysed oxidative condensation of primary amines to imines

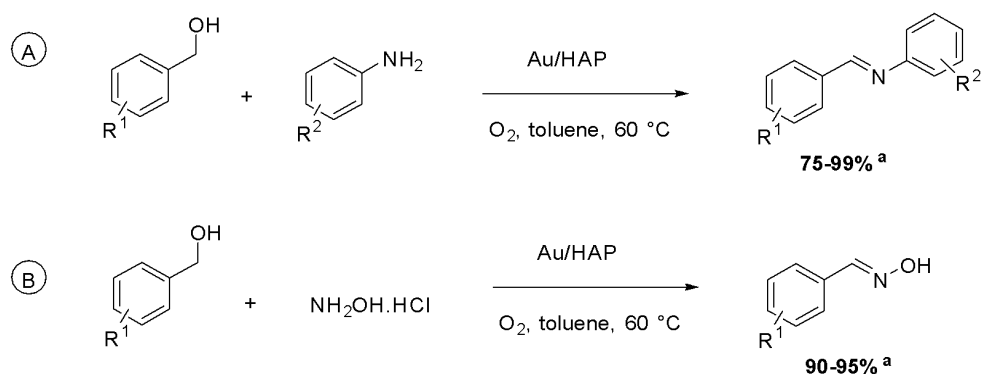
Another example has been reported by Madsen and co-workers, where cobalt nanoparticles are formed in situ for the coupling of amines into imines (Scheme 22).<sup>48</sup>



**Scheme 22.** Dehydrogenative coupling of primary amines into imines. Nanoparticles of cobalt formed in situ and stabilised by trioctylphosphine oxide (TOPO).

### 2.1.1.2.3. Dehydrogenative coupling of alcohols and amines

One of the great advances in this field was brought about by Haruta's use of CO (carbon monoxide) oxidation and alkene epoxidation, catalysed by supported gold nanoclusters.<sup>49</sup> Following this work, the use of gold has since become more important in the catalytic oxidation of alcohols<sup>50,51</sup> but also in the synthesis of imines and oximes via supported gold nanoparticles.<sup>52</sup> The effect of the gold immobilized onto hydroxyapatite (HAP,  $\text{Ca}_{10}(\text{PO}_4)_6(\text{OH})_2$ ) provided an efficient way to synthesise imines by a tandem oxidation-condensation reaction (Scheme 23). It has been demonstrated that HAP shows great potential as a catalyst support.<sup>53, 54</sup>

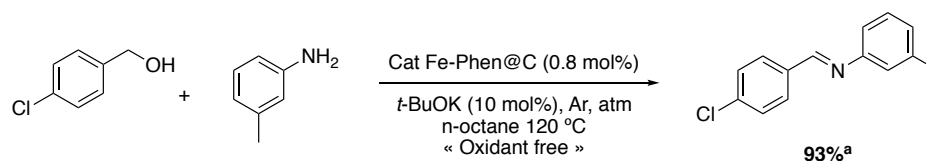


**Scheme 23.** Reactions catalysed by gold/hydroxyapatite for the synthesis of a) imines (Au/HAP 1 mol%), and b) oxime (Au/ HAP, 2 mol%). <sup>a</sup>Conversion (%) based on the conversion of alcohols to imines.

The acceptorless dehydrogenation (AD) is another pathway used for the amination or imination of alcohols. The development of homogeneous catalysts for this method has been well documented<sup>55</sup> but they possess several disadvantages such as extensive use of ligands, low sensitivity or poor catalyst recovery.<sup>56</sup> However, modified hydrotalcites (HTs) have been synthesised as an efficient, cheap and recyclable heterogeneous catalyst.<sup>57</sup> Hydrotalcite-like compounds are mineral hydroxide based with the general formula  $[\text{M}^{2+}_{1-x}\text{M}^{3+}_x(\text{OH})_2]^{x+}(\text{A}^{n-})_{x/n} \cdot m\text{H}_2\text{O}$  composed often of magnesium and aluminium.<sup>58</sup> Voutchkova-Kostal and co-workers reported good catalytic activity for Mg–Al HTs impregnated with  $\text{Pd}^0$  in alcohol imination reactions, proceeding through acceptorless alcohol dehydrogenation.<sup>56</sup>

Until now, few methods involved reusable heterogeneous catalysts based on earth-abundant eco-friendly metals for the direct imine synthesis. Inspired by the application of N-doped

graphene,<sup>59</sup> the group of Raman described for the first time the dehydrogenative coupling of alcohols and amines in the presence of an iron-based graphene catalyst (Scheme 24).<sup>56</sup>



**Scheme 24.** Iron-catalysed direct imine formation by acceptorless dehydrogenative coupling of alcohols with amines. <sup>a</sup>Isolated yield.

These examples highlight the great attention that has been paid to heterogeneous catalysis, an area which is in perpetual improvement. Similarly, metal-organic frameworks (MOFs) have shown tremendous potential to act as heterogeneous catalysts for synthetic organic chemistry,<sup>60</sup> and examples using a MOF catalyst for the synthesis of imines are given below in Section 2.1.2.

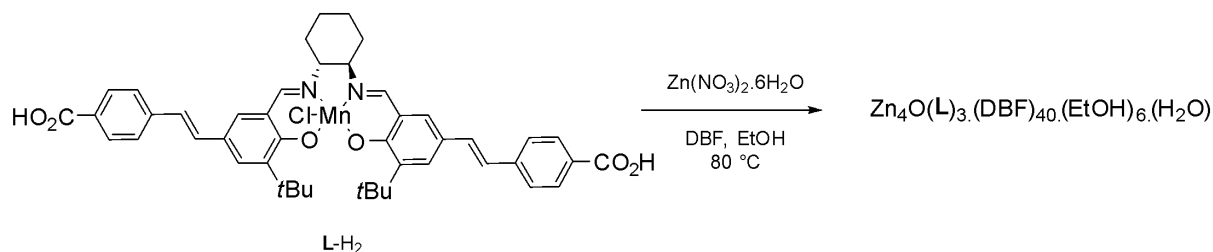
### 2.1.2. Metal-organic frameworks for catalytic applications

Metal-organic frameworks (MOFs) are porous compounds involving strong metal-ligand interactions. Many of them possess a particular robustness due to their strong bonding, and they can be easily modified by for example incorporation of functional groups or active sites.<sup>61</sup> Since the 90s, MOFs have been studied for their applications,<sup>62</sup> physical<sup>63</sup> and catalytic properties.<sup>60,64</sup>

The pore size or the crystalline structure can be controlled by the choice of metal and organic linkers and how they are connected. According to the metal-ligand combination, it is possible to obtain different structures; this is called polymorphism. An example of this principle is given by Tian and co-workers.<sup>65</sup> They synthesised diverse zinc imidazoles by modifying reaction parameters (such as solvent) or by incorporating small substituents that play the role of structure directing agents (SDAs).

Different approaches to the use of MOFs as catalysts have been studied.<sup>60,66</sup> Namely, using the structural metal as the catalytic center (i), use of the MOF as a host for immobilizing catalysts (ii), and finally using the porous structure of the MOFs to host different metal nanoparticles (iii). The first case refers to an open shell metal center amenable to the introduction of labile ligands, which can be easily exchanged during catalysis. The use of HKUST-1 as a MOF for the storage of H<sub>2</sub> is a good example due to its Cu<sup>2+</sup> metal sites accessible by thermal activation.

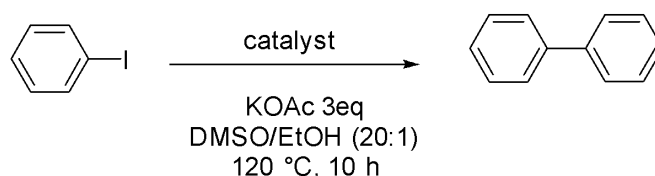
An example where the catalysis takes place at an additional metal center is shown in Scheme 25. In this case, a metalolinker containing a Mn(III) center was used for the stereoselective epoxidation of alkenes and for epoxide ring-opening reactions.<sup>67</sup>



**Scheme 25.** Synthesis of CMOF-1. Design built from [Zn<sub>4</sub>(μ<sub>4</sub>-O)(O<sub>2</sub>CR)<sub>6</sub>] SBUs and a Mn-Salen derived dicarboxylate.

In the last case, the porous framework provides an efficient space to the catalytic activities of the metal nanoparticles. An example was reported by Haruta et al., where the use of gold nanoparticles inside the MOF allow the aerobic oxidation of alcohols.<sup>68</sup> Martín-Matutes' group reported also the C–C bond-formation (Mizoroki-Heck reaction) mediated by Pd(II)@MIL-101-NH<sub>2</sub>. In this last example, the mononuclear Pd(II) species were coordinated to the linkers of the MOF and gradually converted to Pd nanocluster under the reaction conditions. A mixture of the both species (Pd(II) complexes and Pd nanoclusters) coexisted and became the active species of the process.<sup>69</sup>

MOFs have also been used as catalysts to construct C–C bonds through Suzuki-Miyaura cross-couplings or Ullman-type couplings. These reactions are well known for the assembly of biaryl structures. Chen and co-workers compared the performance of homogeneous catalysts with palladium-based MOFs, such as MOF-253 containing bipyridine linkers functionalized with PdCl<sub>2</sub>.<sup>70</sup> They studied the Ullman-type reaction and observed that the catalytic activity was substantially improved when using the heterogeneous catalyst (Scheme 26).



Catalyst	conversion (%)	Yield(%) <sup>a</sup>
MOF-253·0.05PdCl <sub>2</sub>	>99	>99
Pd(bpy)Cl <sub>2</sub>	56	50
PdCl <sub>2</sub> (CH <sub>3</sub> CN) <sub>2</sub>	12	10

**Scheme 26.** Ullmann coupling of iodobenzene over MOF-253·0.05PdCl<sub>2</sub>. <sup>a</sup>Based on by GC-MS analysis.

The authors suggested that this effect was due to the 2,2'-bipyridine linker of the MOF catalyst increases the electron density on Pd and facilitates the oxidative addition of the aryl halide on the Pd active site. Moreover, this difference of activity with the homogeneous system could be the result of the electron configuration of the bpy moiety in the MOF due to the presence of charge transfer between bordering ligands and metals in MOFs. This resulted in a higher catalytic activity with the MOF than that with homogeneous systems, such as Pd(bpy)Cl<sub>2</sub> (possessing a single bpy molecule) and PdCl<sub>2</sub>(CH<sub>3</sub>CN)<sub>2</sub>. Martín-Matute's group has also used Pd(0)-functionalized MOFs, in particular, Pd@MIL-101, for the Suzuki-Miyaura cross-coupling of highly functionalized aryl halides and boronic acids under very mild reaction conditions,<sup>71</sup> as well as in the aerobic homocoupling of boronic acids.<sup>72</sup>

MOFs are often described as a porous crystalline structure but in fact they can be found in other physical states. Amorphous metal-organic frameworks (aMOFs) keep the same pattern of building block and connectivity of their crystalline siblings but do not possess any long-range periodic order.<sup>73</sup> Cheetham *et al.*<sup>74</sup> characterised a zeolitic crystalline structure, ZIF-4, which undergoes a morphology change on heating to over 300 °C to an amorphous system. Related work revealed the promising abilities of amorphous ZIFs to trap guest molecules, showing good molecular uptake capacity.<sup>75</sup> It also appears that this kind of compounds show biomedical applications as drug storage capacities and drug delivery vehicles.<sup>76</sup>

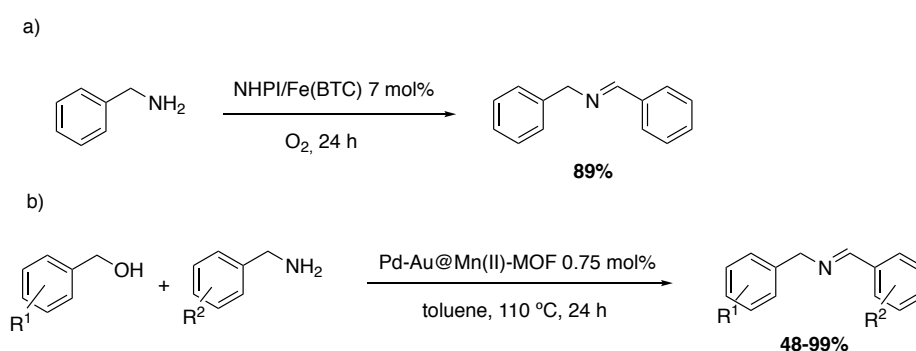
MOFs have been used with great success in a number of synthetic transformations, where the MOF composition plays a pivotal role on the outcome of the reaction. For example, Fe- and Cr- MIL-100 and MIL-101 have been used in allylic oxidations of alkenes in the presence of molecular oxygen.<sup>77</sup> It was revealed that the product selectivity depends of the nature of the

metal. Whilst the Fe based MOF produced unsaturated alcohols, the Cr-based MOF favoured the formation of unsaturated ketones.

Other classical organic reactions can take place with the use of MOFs, and the role of the MOF structure on the catalysis outcome has been discussed to some extent.<sup>60,78</sup>

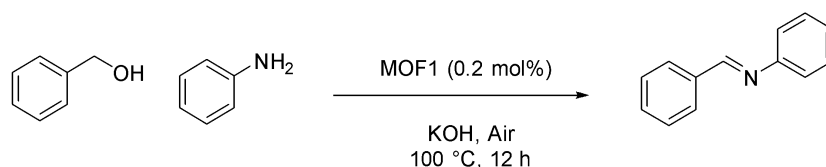
### 2.1.3. Synthesis of imines catalysed by MOFs

In this section examples using MOF catalysts to synthesize imines are described. Fe(BTC) (BTC: 1,3,5-benzenetricarboxylate) was used for the synthesis of *N*-benzylimines from the corresponding benzylamines under aerobic conditions.<sup>79</sup> The authors compared this protocol to previous results<sup>80</sup> for the oxidation of benzylic compounds in the presence of peroxide, but in this case, with the incorporation of *N*-hydroxyphthalimide (NHPI). They reported a number of advantages of the MOF system: the only oxidant source is molecular oxygen, and the reaction can be performed without a solvent. Additionally, this material does not require any pre-activation step, alleviating reproducibility issues. Chen, Dong and co-workers developed a new porous Pd-Au@Mn(II)-MOF for the one-pot tandem synthesis of imines from benzyl alcohols and anilines, and from benzyl alcohols and benzylamine. This catalyst demonstrated excellent recyclability (Scheme 27).<sup>81</sup>



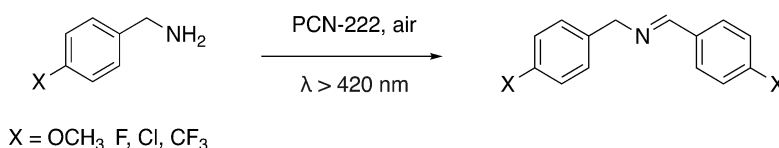
**Scheme 27.** Synthesis of imine via aerobic oxidation. a) Oxidation condensation of benzylamine b) One-pot tandem synthesis of imines from alcohols and amines.

Following this work, new catalysts were prepared in an effort to combine high recyclability in a solvent-free system. A Ni<sub>3</sub>(OH)(COO)<sub>6</sub>-based MOF from C<sub>3</sub> symmetric ligands (MOF1) was used in a solvent-free system for the one-pot synthesis of imines (Scheme 28).<sup>82</sup> The reaction requires activation by base.



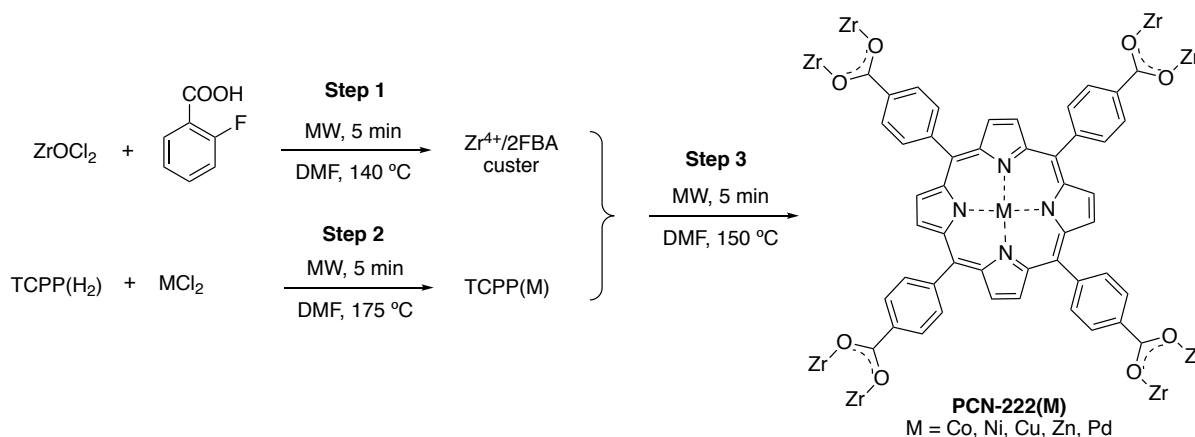
**Scheme 28.** One-pot solvent-free synthesis of *N*-benzylideneaniline from benzyl alcohol and aniline.

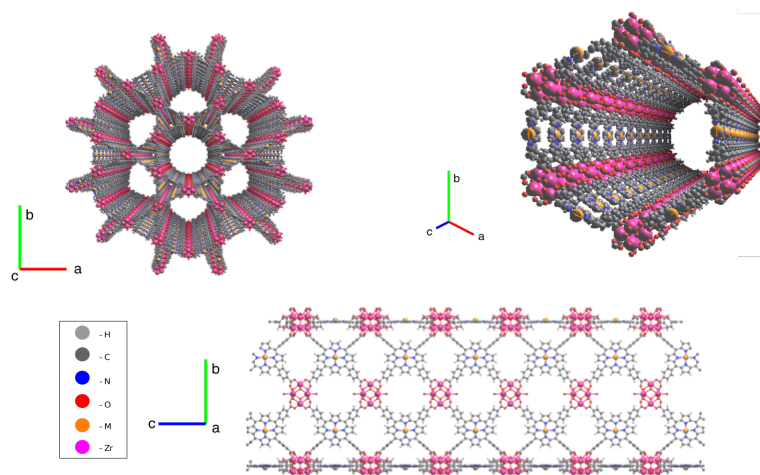
Recently, Jiang and co-workers reported an alternative method by which a diverse variety of benzylamines oxidatively couple in a process mediated by PCN-222 under visible light irradiation (Scheme 29).<sup>83</sup> PCN-222 is a mesoporous MOF which possess a tetrakis(4-carboxyphenyl)porphyrin (TCPP) as a heme-like organic linker and a Zr<sub>6</sub> clusters as nodes (structure determines by single X-ray diffraction).<sup>85</sup> A limitation with this system is that since the reaction occurs through auto condensation of two identical benzylamines, the aromatic groups in the final imine have the same substitution pattern.



**Scheme 29.** Condensation of benzylamine under visible light and air

The Martín-Matute group at Stockholm University has developed a straightforward method for the synthesis of PCN-222 and of metallated PCN-222(M),<sup>84</sup> (where M = Ni, Cu, Zn, Co, Pd) that overcome the limitations of the synthetic protocol reported by Zhou and co-workers<sup>85</sup> (Scheme 14). Since the new synthetic method is very straightforward, it enables the fast synthesis of PCN-222 functionalized with different metals (M), facilitating catalyst screening (Scheme 30).

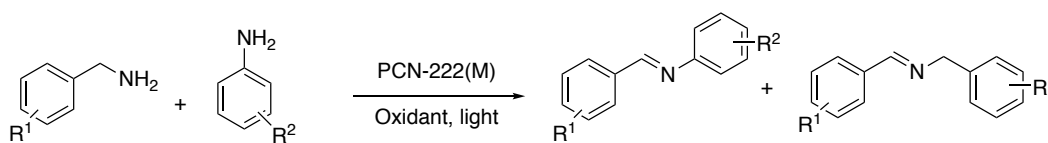




**Scheme 30.** Synthesis of PCN-222(M) [M = Co, Ni, Cu, Zn, Pd] and three-dimensional representation of PCN-222(M).

## 2.2. Aim of this chapter

The second part of this thesis was realised at Stockholm University. The goal of this project was to study the photocatalytic oxidative heterocoupling of two amines using PCN-222(M) [M = Co, Ni, Cu, Zn, Pd] (Scheme 31). In particular, we aimed to identify which metal (M) on the PCN-222 would give the best performance. In addition, we wanted to develop a protocol that gave high selectivity for cross-condensation *vs* self-condensation. This would dramatically increase the scope of the reaction, as well as the utility of the process. We also want to identify the advantages of using the current method when compared to those described in the literature.



**Scheme 31.** Photocatalytic oxidative coupling of two different amines.

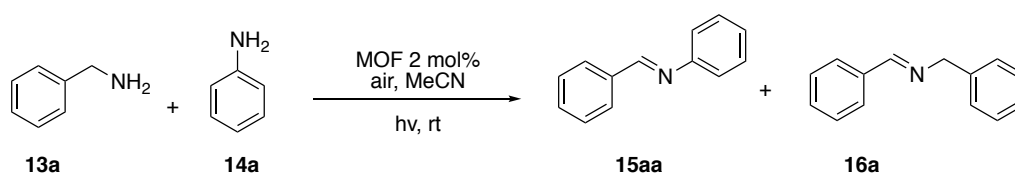
## 2.3. Results and discussion

The PCN-222 and PCN-222(M) used in this project was synthesised by other member of our group *via* a three-step, one-pot microwave-assisted. The first step allows the synthesis of the Zr preclusters through the reaction of ZrOCl<sub>2</sub> with 2-fluorobenzoic acid (2FBA). The second

step includes the metalation of tetrakis(4-carboxyphenyl)porphyrin under microwave irradiation. The preparation of non-metalated PCN-222, step could be obtained in the absence of metal salts. Finally, the last step of the synthesis was carried out by combination of the two mixtures from steps 1 and 2 and treated with trifluoroacetic acid (Scheme 30).

Preliminary investigations performed in the group using benzylamine **13a** and aniline **14a** as model substrates demonstrated that PCN-222 and PCN-222(Pd) are able to mediate the oxidative cross-condensation reaction (Table 4). Despite this, conversions were rather limited and large amounts of the unwanted auto condensation product **16a** were formed (Table 4, entries 2 and 4).

**Table 4.** Influence of the MOF and the reaction time on the photocatalytic oxidative cross-condensation of amines.<sup>a</sup>



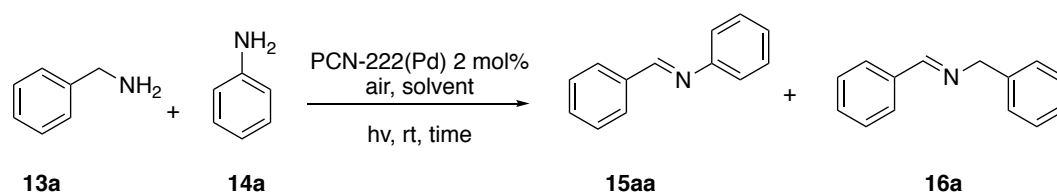
Entry	13a:14a	MOF	Time (h)	MOF (mol %)	15aa:16a	15aa + 16a (%) <sup>b</sup>
1	1:5	PCN-222	90	12	1: 12	5
2	1:1	PCN-222	90	2	1: 12	22
3	1:5	PCN-222	90	2	1: 2	37
4	1:5	PCN-222	24	2	1: 6	12
5	1:5	PCN-222(Pd)	24	2	1: 3	15

a) Reaction conditions: benzylamine **13a** (0.3 mmol, 1 equiv.), aniline **14a** (1.5 mmol, 5 equiv.), MOF (2 mol%), MeCN (3 mL), hv (11 W household lightbulb), rt, for the time indicated. b) Yield determined by <sup>1</sup>H NMR spectroscopy in comparison to the benzylamine.

A close look at these results reveals that by decreasing the time of the reaction, the selectivity increases in favour of the undesired product **16a** (90 h vs 24 h; Table 1, entries 3 vs 4). When PCN-222(Pd) was used instead of PCN-222, a better ratio **15aa** / **16a** was obtained, although still in favour of the unwanted **16a** (Table 4, entry 5).

With these preliminary results, I first investigated the effect of the solvent on the outcome of the reaction (Table 5). Cyclopentyl methyl ether (CPME) brought a poor conversion and a poor

selectivity (**15aa:16a** = 1:20, Table 5, entry 3), whereas dichloroethane (DCE) was marginally better than acetonitrile (Table 5, entry 4 vs 1 and 2). On the other hand, increasing the reaction temperature to 60-65 °C (by inserting the reaction tube in an oil bath heated at 65 °C) afforded a very good yield of 75% and a better selectivity (**15aa:16a** = 2:1, Table 5, entry 6). It is important to notice that the reaction system is covered with a box where the lightbulb is directed on the reaction tube.

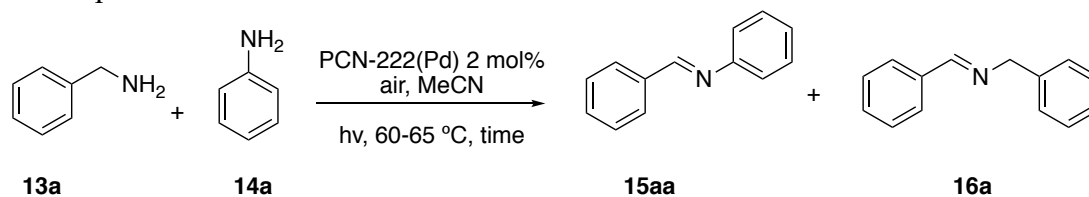
**Table 5.** Condition optimization for photocatalytic oxidation: Influence of solvent.<sup>a</sup>

Entry	2a (equiv.)	t (h)	Solvent	15aa:16a	15aa + 16a (%) <sup>b</sup>
1	1:5	24	Dry MeCN	1: 6	12
2	1:5	24	MeCN / H <sub>2</sub> O (2/1)	1: 6	13
3	1:5	24	CPME	1: 20	3
4	1:5	24	DCE	1: 2.3	13
5 <sup>c</sup>	1:5	24	MeCN	1: 2.8	30
6 <sup>c</sup>	1:5	80	MeCN	2: 1	75

a) Reaction conditions: benzylamine **13a** (0.3 mmol, 1 equiv.), aniline **14a** (1.5 mmol, 5 equiv.), PCN-222(Pd) (2 mol%), solvent (3 mL), hv (11 W household lightbulb), rt.; b) Yield determined by proton NMR spectroscopy in comparison to the benzylamine of **1a**; c) 60–65 °C (oil bath).

Next a slow addition of benzylamine **13a** to the reaction mixture was explored (0.4 mL/h, 0.125 M) at room temperature and after only 20 h, a better product selectivity was obtained in favour of **15aa** (Table 6, entry 1). By using the best conditions from Table 5 (entry 6) and using a longer reaction time, a ratio **15aa:16a** of 30:1 was obtained, in a quantitative yield (Table 6, entry 2). Unfortunately, these results could not be reproduced when the reaction was run on a larger scale (Table 6, entries 3-5).

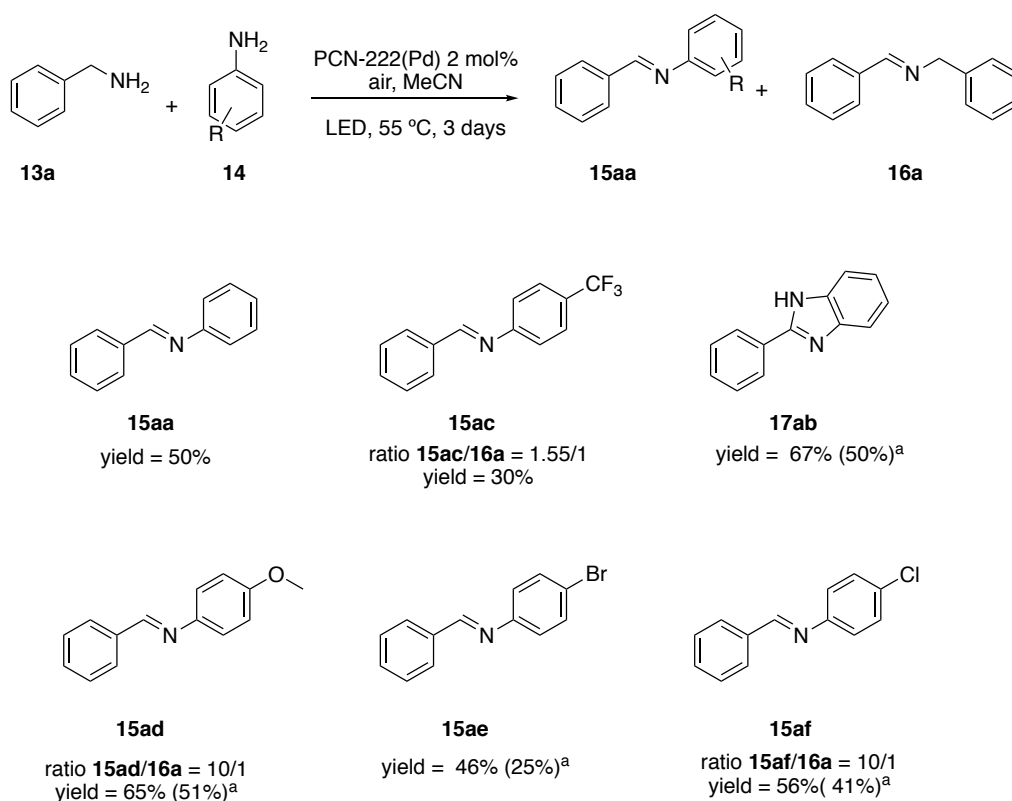
When non-metalated PCN-222 was used under the conditions shown in Table 5, entry 6, a lower conversion and a higher ratio in favour of **16a** was obtained (Table 6, entry 6). Reducing the temperature to 55 °C (Table 6, entry 7) gave high conversion in favour of the product after 120 h, but the selectivity was decreased in comparison to entry 2. Under oxygen-free conditions, a moderate yield was obtained (Table 6, entry 8) after 68 h.

**Table 6.** Optimization *via* slow addition of **13a**.<sup>a</sup>

Entry	<b>13a</b> (mmol)	t (h)	<b>13a</b> Addition flow (mL/h)	<b>13a</b> Addition time (h)	<b>15aa:16a</b>	<b>15aa + 16a</b> (%) <sup>b</sup>
1 <sup>c</sup>	0.3	20	0.4	6	1.3: 1	15
2	0.3	100	0.4	6	30: 1	99
3 <sup>d</sup>	0.9	72	0.4	6	3: 1	80
4 <sup>d</sup>	0.9	144	0.8	3	1: 1.15	50
5	0.9	96	0.3	24	1.8: 1	75
6 <sup>e</sup>	0.3	72	0.4	6	1: 1.8	45
7 <sup>f</sup>	0.3	120	0.4	6	15: 1	98
8 <sup>g</sup>	0.3	68	0.4	6	1: 1.1	56

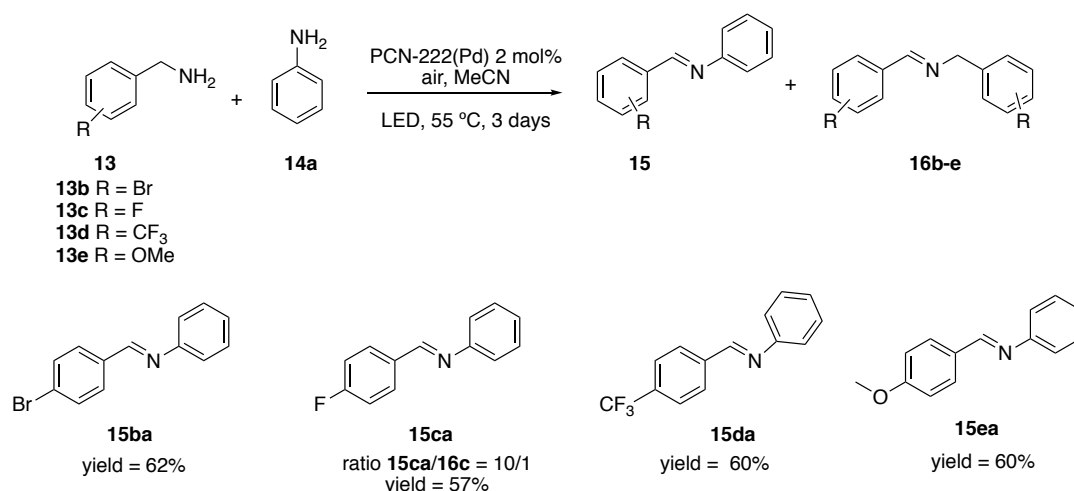
a) Reaction conditions: A solution of benzylamine **13a** (0.3 mmol, 1 equiv., 0.125 M) in 2.4 mL of MeCN, is added to a suspension of aniline **14a** (1.5 mmol, 5 equiv.), and PCN-222(Pd) (2 mol%), in MeCN (1 mL). The mixture is stirred under hv irradiation (11 W household lightbulb immobilized in a cardboard box), at 65 °C. b) Yield determined by <sup>1</sup>H NMR spectroscopy in comparison to the benzylamine; c) Room temperature; d) **13a** (0.9 mmol, 1 equiv., 0.375 M); e) PCN-222 as catalyst; f) 55 °C; g) Under O<sub>2</sub>.

The next idea was to use the same protocol but replace the visible light lamp (11 W household lightbulb) by a more powerful LED strip (*North light*, 12 W, 1.5 A). This new light source provided complete conversion of compound **13a** (0.125 M, slow addition: 0.4 mL/h) in 80 h. Thus, the scope was then investigated using PCN-222(Pd), 2 mol%, in MeCN under an atmosphere of air with the new light source. These conditions afforded a full conversion after three days for the different substituted imines (Scheme 32). Compounds **15aa** and **15ae** were obtained in yields of 50% and 46%, respectively. Importantly, in these instances, self-condensation of **16a** was not detected. Imine **15af** was obtained as a mixture of **15af** and **16a** in a ratio of 10:1 in favour of the former. The same ratio was obtained for **15ad**, albeit in a higher yield of 65%. The imine **15ac** was formed in the lowest yield (30%), with a modest ratio of 1.55:1. Interestingly, benzimidazole **17ab** was obtained by condensation of benzylamine **13a** with *o*-phenylene diamine (**14b**).



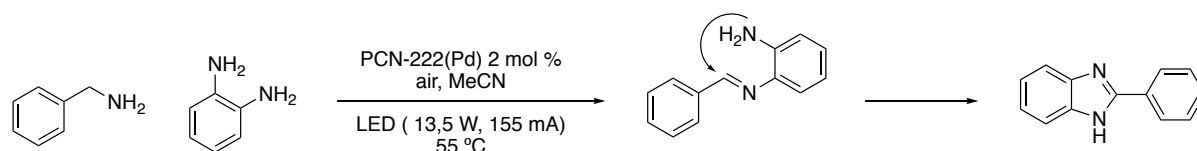
**Scheme 32.** Scope of the reaction based on the substituents of the aniline. Reaction conditions: **13a** (1 equiv., 0.3 mmol, 0.125 M), in 2.4 mL of MeCN, is added in 6 h to a suspension of aniline **14a** (1.5 mmol, 5 equiv.), and PCN-222(Pd) (2 mol%), in MeCN (1 mL). The mixture is stirred under *h $\nu$*  irradiation (LED strip (*North light*, 12 W, 1.5 A)) for 3 days. Yield determined by <sup>1</sup>H NMR spectroscopy. Yield determined by <sup>1</sup>H NMR spectroscopy against an internal standard. a) Isolated yield.

Substituted benzylamines were then subjected to the reaction conditions (Scheme 33). Both electron-withdrawing and electron-donating groups were well tolerated on the aryl ring of the benzyl amines (Scheme 33). Imine **15ca** was obtained together with the corresponding self-condensation product, although only a small amount of the latter was formed.



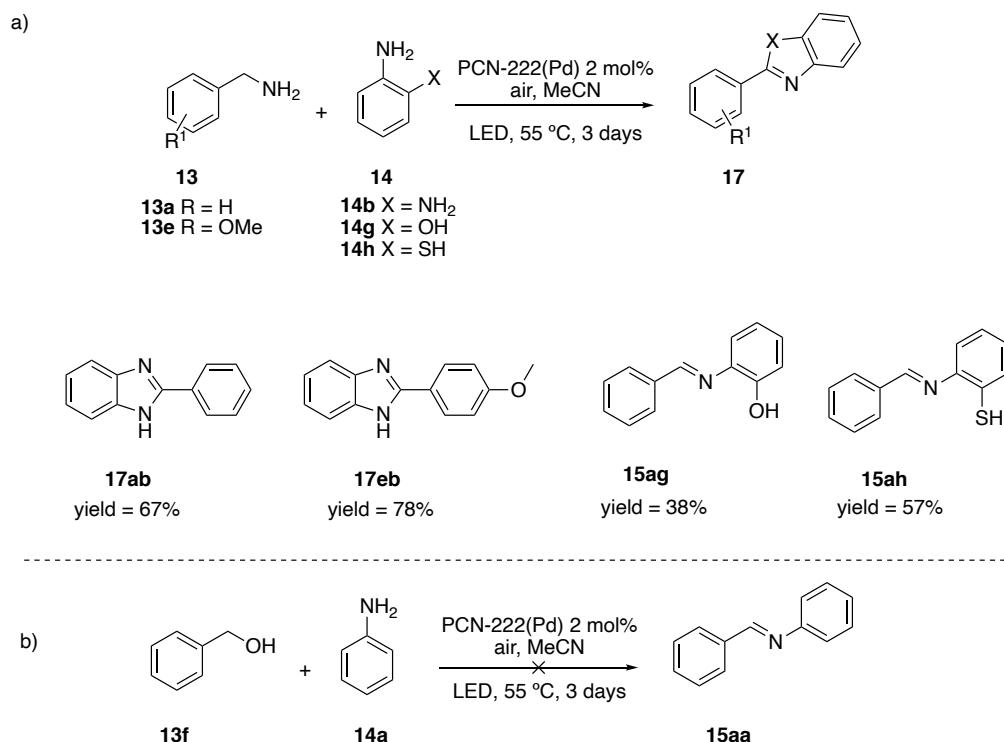
**Scheme 33.** Reaction of benzylamines **13b-13e** with aniline **14a**. Reaction condition: **13** (1 equiv., 0.3 mmol), **14a** (5 equiv., 1.5 mmol), PCN-222(Pd) (2 mol%), LED strip (*North light*, 12 W, 1.5 A), MeCN, under air, 3 days. Yield determined by <sup>1</sup>H NMR spectroscopy.

To further expand the scope of the reaction, we then reacted benzyl amines with 2-aminophenol **14g** and with 2-aminobenzenethiol **14h**, providing the oxidative cross-coupled products **15ag** and **15ah** in 38% and 57% yield, respectively. When benzylamines **13a** and **13e** were reacted with *o*-phenylenediamine **14b**, benzimidazoles **17ab** and **17eb** were obtained in good yields of 67% and 78%, respectively (Scheme 35a). In these last cases, the reaction is not limited to the oxidative condensation. A cyclization occurs upon nucleophilic attack of the nitrogen to the imine formed in the first step, affording the benzimidazole (Scheme 34).



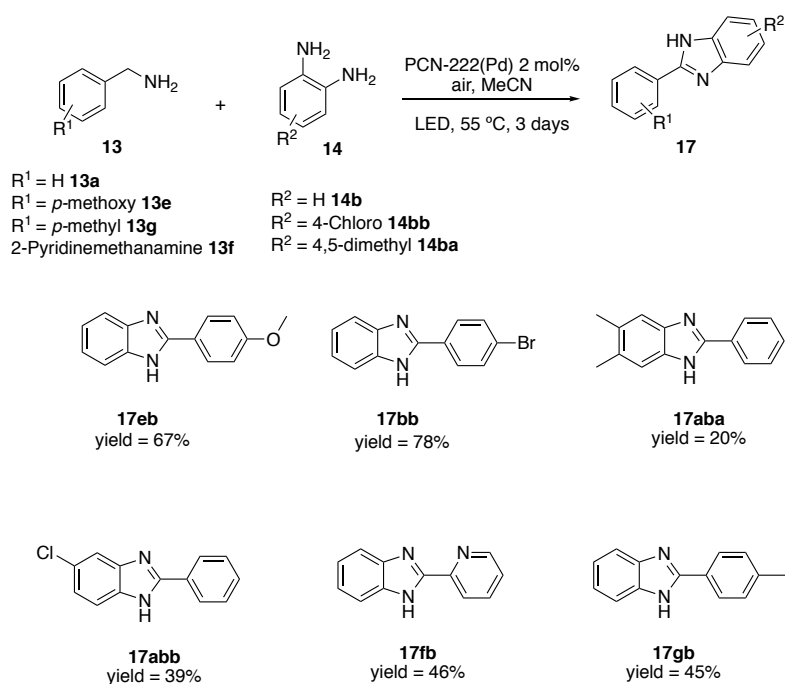
**Scheme 34.** Oxidative condensation followed by oxidative cyclization affording the corresponding benzimidazole.

The oxidative cross-coupling of benzyl alcohols with anilines was also attempted (Scheme 35 b). Unfortunately, no product was observed and only the starting materials (SM) remained after reaction.



**Scheme 35.** a) Reaction of benzylamines **13a**, **13e** with *ortho*-substituted anilines **14b**, **14g**, **14h**. b) Oxidative cross-coupling of benzyl alcohols with aniline **14a**. Reaction condition: **13** (1 equiv., 0.3 mmol), **14** (5 equiv., 1.5 mmol), PCN-222(Pd) (2 mol%), LED strip (*North light*, 12 W, 1.5 A), MeCN, under air, 3 days. Yields calculated by <sup>1</sup>H NMR spectroscopy against with an internal standard.

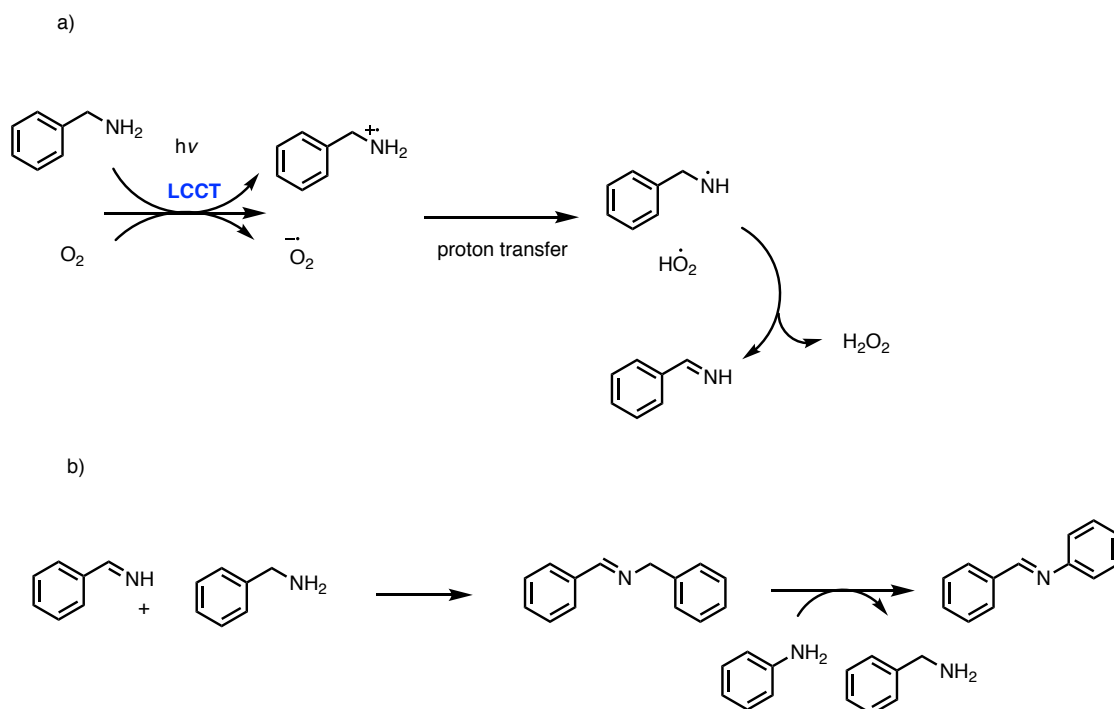
We then explored the scope of the oxidative cross-coupling / cyclization reactions. The results are shown in Scheme 36. In a general way, the benzimidazole obtained from the different substituted benzylamines **13** offered the same range of yields. The best yields, 63% and 78%, respectively, were obtained for **17eb** and **17bb**. When the *o*-phenylene diamine contained a chlorine atom (**14bb**) or two methyl group (**14ba**), yields of 39% for **17abb** and of 20% for **17aba** were obtained.



**Scheme 36.** Reaction of benzylamines **13a**, **13b**, **13e-13g** with *ortho*-substituted anilines **14b**, **14ba**, **14bb**. Isolated yield. a) Yield determined by  $^1\text{H}$  NMR spectroscopy.

Based on the mechanistic proposals reported in the literature,<sup>86</sup> we suggested the mechanism shown in Scheme 37. The first step involves the photoexcitation of the organic linkers, followed by electron transfer to the metal cluster (ligand-to-cluster charge transfer, LCCT). This route generates electrons and holes showing oxidative and reductive properties (e-h separation). The photogeneration of electrons and holes is a model described in the literature<sup>87</sup> and proposed to be operative for imine formation by the Jiang group.<sup>83</sup>

Upon photoexcitation, the PCN-222 gives rise to a e-h separation, reducing the  $\text{O}_2$  to  $\text{O}_2^{\cdot-}$  and oxidizing benzylamine **13a** to  $\text{PhCH}_2\text{NH}_2^{\cdot+}$ . A proton transfer from the  $\text{PhCH}_2\text{NH}_2^{\cdot+}$  to  $\text{O}_2^{\cdot-}$  generate the benzylamine radicals ( $\text{PhCH}^{\cdot}\text{NH}_2$  and  $\text{PhCH}_2\text{NH}^{\cdot}$ ) and hydroperoxyl radicals ( $\text{HO}_2^{\cdot}$ ) which leads to benzylideneamine and  $\text{H}_2\text{O}_2$  (Scheme 37a). This intermediate is attacked by benzylamine (**13a**) to afford the imine **16a** resulting as the side-product from auto condensation. Finally, the attack of the aniline **14a** gave the desired imine **15aa** (Scheme 37b).



**Scheme 37.** Proposed mechanism to the oxidative condensation of the benzylamine **13a** with aniline **14a**. a) Ligand-to-cluster charge transfer (LCCT). This route generated a hole possessing redox properties allowing to reduce the  $O_2$  to  $O_2^{\cdot-}$  and oxidize the benzylamine **13a** to  $PhCH_2NH_2^{\cdot+}$ . b) Attack of the benzylamine **13a** on the benzylideneimine to generate the side product **16a** which, by attack of the aniline, lead to the product **15aa**.

## **2.4. Conclusion and outlook**

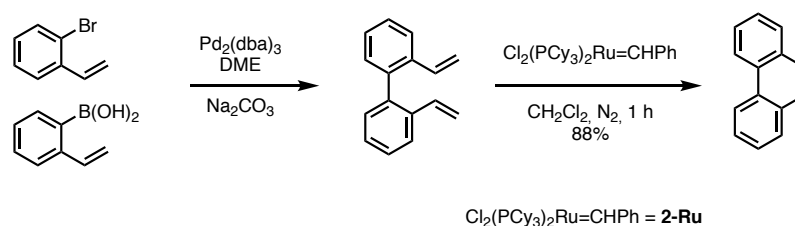
It has been shown that the oxidative cross-condensation of benzyl amines with anilines can be achieved under photocatalytic conditions using the MOF PCN-222(Pd) as the catalyst. The best results were obtained by slow addition of the benzylamine on a solution containing the MOF catalyst and an excess of the aniline. Importantly, the intensity of the light source played an important role on the reaction outcome. The scope and limitations of the reaction have been investigated. These results need further optimization to improve the yields of some of the substrates. Moreover, the recyclability of the MOF catalyst needs to be investigated.

### 3. Chapter III. Synthesis of heterocyclic compounds via Ni-catalysed benzannulation

#### 3.1.Introduction

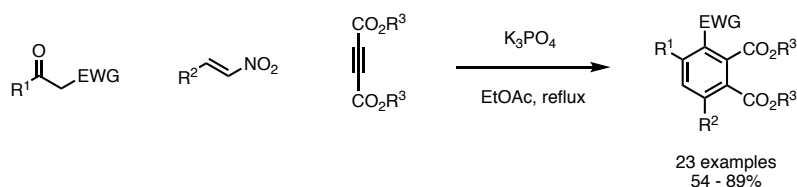
##### 3.1.1. Base-mediated benzannulation

Benzannulation is one of the most important methods to synthesize highly substituted benzene derivatives<sup>88</sup> and it includes many different processes such as Diels–Alder [4+2] cycloadditions (cf. Chapter I), Bergman cyclization, the Dötz reaction or even ring-closing metathesis via Grubbs first- or second-generation catalysts (Scheme 38).<sup>89</sup>



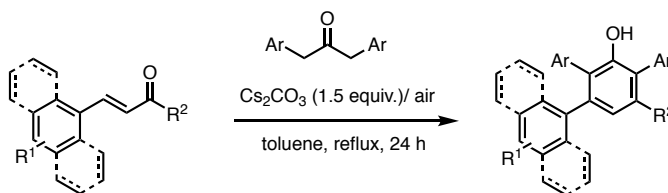
**Scheme 38.** Synthesis of phenanthrene via ring closing metathesis.

More recently, transition-metal-free benzannulation reactions have been developed to offer benzene type structures. For example, Wu and co-workers developed an efficient synthesis of polysubstituted phthalic acid derivatives in presence of potassium phosphate (Scheme 39).<sup>90</sup>



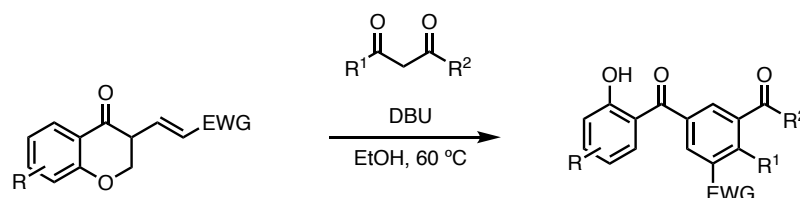
**Scheme 39.** Multicomponent transition-metal-free benzannulation reaction in presence of potassium phosphate.

Lee et al. reported an aerobic oxidative benzannulation reaction by using cesium carbonate base, offering polysubstituted phenols with antioxidant properties via Michael addition, intramolecular aldol and oxidation (Scheme 40).<sup>91</sup>



**Scheme 40.** Benzannulation reaction for the construction of polyarylphenols.

Organic bases can also be used for the synthesis of polyfunctionalized aromatics. A series of DBU-mediated domino reactions, such as Michael addition, cyclization, elimination, was explored by Hu and co-workers for the synthesis of polysubstituted 2-hydroxybenzophenones. In this sequence, substituted chromone and 1,3-dicarbonyl compounds were used for the benzannulation process (Scheme 41).<sup>92,93</sup>

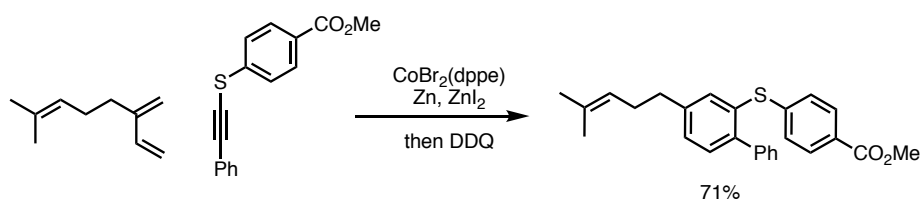


**Scheme 11.** Synthesis of 2-hydroxybenzophenones from chromones and 1,3-dicarbonyl compounds.

### 3.1.2. Transition metal-mediated benzannulation

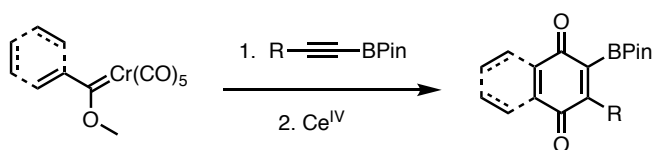
Classical approaches to the synthesis of aromatic compounds have been dominated by electrophilic and nucleophilic substitution reactions, and these are often controlled by pre-existing directing groups which deliver specific substitution patterns. This approach significantly limits the range of aromatic products that can be produced, prompting researchers to devise alternative methods using ring synthesis approaches.

Metal mediated cyclization reactions of alkynes has been a very effective approach for the assembly of aromatics rings.<sup>94</sup> A first example was reported by Reppe and co-worker, who revealed that the cyclotrimerization of alkynes can afford benzene derivatives.<sup>95</sup> Other such cobalt-based complexes have been used for the synthesis of aromatic compounds by promoting the reaction of 1,3-dienes with alkynyl sulfides (Scheme 42).<sup>96</sup>



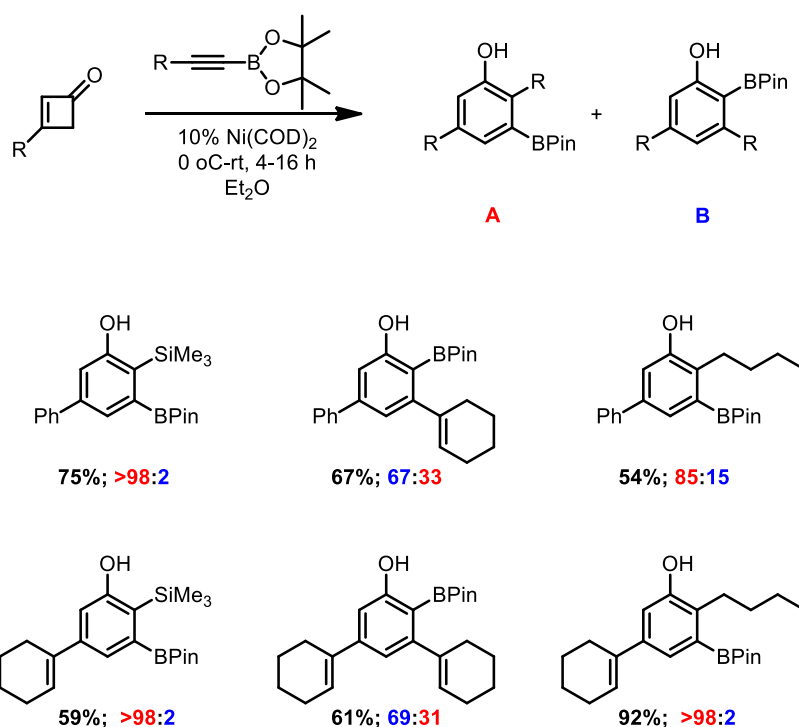
**Scheme 42.** Co-catalyzed reaction of 1,3-diene with alkynyl sulfides.

Metal promoted benzannulation strategies can bring challenges concerning chemoselectivity and regioselectivity. The Harrity group previously addressed this issue with regard to the Dötz benzannulation reaction. They were able to show that this chemistry could allow access to quinone boronic esters with high regiocontrol and in good yields (Scheme 43).<sup>97</sup>



**Scheme 43.** Dötz-type benzannulation. Pin=pinacol

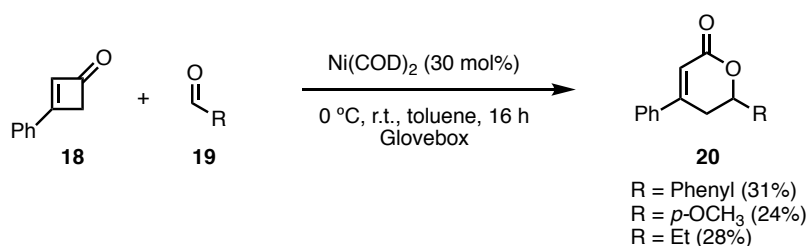
Based on this work and the literature, the group has developed a Ni-catalysed benzannulation method for the mild and selective synthesis of functionalised phenols.<sup>98</sup> This chemistry offers an effective way to generate benzene-based target molecules from simple starting materials (Scheme 44).



**Scheme 44.** Synthesis of Heteroaromatic Boronic Esters

### 3.2. Aim of this chapter

While the chemistry outlined in the previous section offers a useful way to generate benzene derivatives, it is currently limited with regard to the synthesis of heterocyclic compounds, as illustrated by the low yields for the synthesis of lactones **20** (Scheme 45).<sup>99</sup>



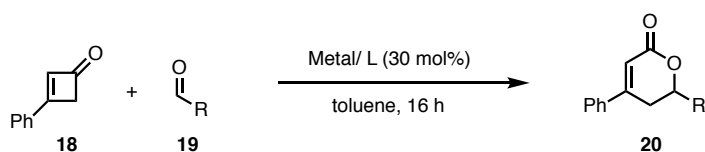
**Scheme 45.** Example of a cycloaddition reaction to form heterocyclic compounds

To overcome the limitation, we decided to explore this transformation further. In particular, we planned to: i) screen different catalysts and ligands to obtain the optimal conditions of the reaction; ii) investigate the suitability of imines and nitriles as reactants; iii) establish empirical scope relating to the different “R” substituents based on the best conditions.

### 3.3. Results and discussion

As mentioned, the previous method was limited with respect to the synthesis of heterocyclic compounds. In order to optimise this reaction, the study was initiated with cyclobutenone **18a** and benzaldehyde **19a** as coupling partners for the synthesis of lactone **20a**. Each metal was screened with all the ligands listed below (30 metal/ligand combinations – see Table 7) and the reaction was monitored by LCMS analysis to detect presence of the product.

**Table 7.** Screening conditions<sup>a</sup>



Ligand	Ni complex
<b>Dppb</b>	NiCp <sub>2</sub>
<b>PCy<sub>3</sub></b>	Ni(dppf)( <i>o</i> -tolyl)Cl
<b>Xantphos</b>	Ni(TMDA)( <i>o</i> -tolyl)Cl
<b>DppBz</b>	Ni( <i>o</i> -tolyl)(PCy <sub>3</sub> ) <sub>2</sub> Cl
<b>Dppe</b>	Ni(PPh <sub>3</sub> ) <sub>2</sub> ( <i>o</i> -naphthyl)Cl
<b>Bipyridine</b>	

a) Reaction conditions: **18** (0.01 mmol, 1 equiv.), **19a** (0.01 mmol, 1 equiv.), metal/ligand combination (30 mol%), toluene, 16 h, rt, in a glove box.

The presence of product was detected with three different metal sources (Ni(dppf)(*o*-tolyl)Cl, Ni(TMDA)(*o*-tolyl)Cl and NiCp<sub>2</sub>) coupled with 1,2-bis(diphenylphosphino)benzene (dppBz).

Unfortunately, no trace of product was observed with the other combination of precatalyst/ligands.

In a second step, the loading of the metal/dppBz was varied from 30 to 100 mol% and the impact on the reaction was evaluated after one and three days. 1,3,5-Trimethoxybenzene was used as an internal standard (IS) allowing us to rapidly estimate how much of the product was formed by calculating the ratio of the product to the IS. As identical stoichiometries of reagents and IS were used in each run, larger ratios were taken as an indication of greater product formation. Increasing the catalyst loading had a direct impact on the ratio in favour of the product up to 80 mol%, which provided the optimal results (Table 8, entry 6, 9). The Ni(dppf)(*o*-tolyl)Cl catalyst didn't provide any trace of product and was therefore removed from the further tests (Table 8, entry 1,4,7,10). These experiments revealed that the best ratio was obtained after one day and therefore, the reaction was stopped at this time in subsequent experiments.

**Table 8.** Screening conditions: Loading of catalysts over time<sup>a</sup>

Entry	Metal/dppBz	(Metal/L) (mol%)	LCMS <sup>b</sup> Product/IS 1 day	LCMS <sup>a</sup> Product/IS 3 days
1	Ni(dppf)( <i>o</i> -tolyl)Cl	30	Only S. M.	Only S. M.
2	Ni(TMDA)( <i>o</i> -tolyl)Cl	30	0.69	Trace of product
3	NiCp <sub>2</sub>	30	1.57	1.24
4	Ni(dppf)( <i>o</i> -tolyl)Cl	50	Only S. M.	Only S. M.
5	Ni(TMDA)( <i>o</i> -tolyl)Cl	50	0.8	0.7
6	NiCp <sub>2</sub>	50	3.17	1.53
7	Ni(dppf)( <i>o</i> -tolyl)Cl	80	Only S. M.	Only S. M.
8	Ni(TMDA)( <i>o</i> -tolyl)Cl	80	1.35	1.17
9	NiCp <sub>2</sub>	80	4.98	1.6
10	Ni(dppf)( <i>o</i> -tolyl)Cl	100	Only S. M.	Only S. M.
11	Ni(TMDA)( <i>o</i> -tolyl)Cl	100	1.75	0.9
12	NiCp <sub>2</sub>	100	4.65	4.8

Reaction condition: **18a** (0.01 mmol, 1 equiv.), **19a** (0.01 mmol, 1 equiv.), metal/ligand (30-100 mol%), toluene, time, rt, in a glove box b) Surface area of the product to the internal standard (IS)

The temperature was next investigated with the reaction conducted at 40, 60 and 80 °C with three different catalyst loadings (30, 50, 80 mol%). Generally, the ratio increased marginally with increasing temperature until 60 °C (Figure 14). For reasons that are unclear, no trace of products was detected at 60 °C at a catalyst loading 50 mol% and therefore, the ratio couldn't be calculated in these runs.

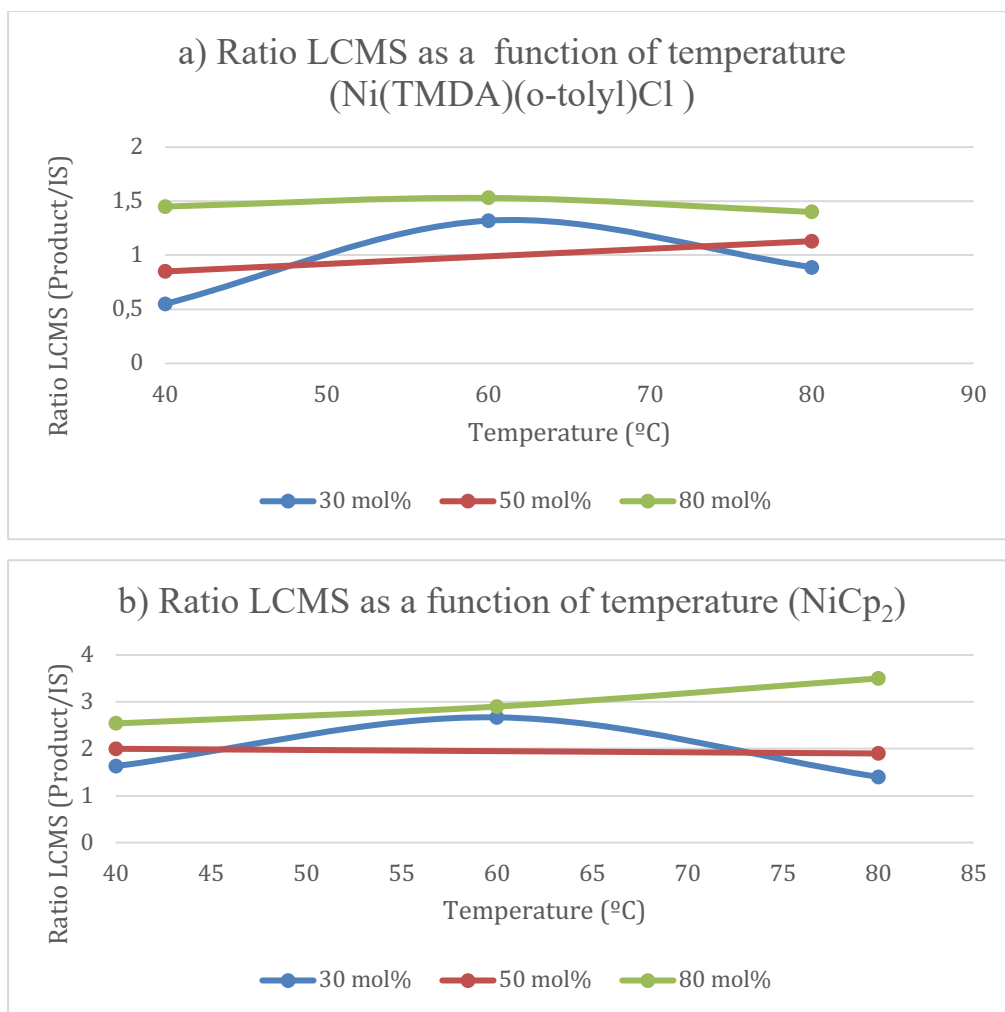


**Figure 14.** LCMS ratio as a function of the temperature for a) Ni(TMDA)(*o*-tolyl)Cl and b) NiCp<sub>2</sub> at three different catalyst loadings. The ratio could not be obtained at 60 °C at 50 mol% loading.

Based on these results, the NiCp<sub>2</sub>/dppBz catalyst system was introduced in batch-mode (higher quantity of mmol) to be able to analyse the reaction by NMR spectroscopy but only trace amounts of the product were observed (Table 9, entry 1 – 4). Surprisingly, switching to a catalyst system comprising Ni(TMDA)(*o*-tolyl)Cl/dppBz, we observed product formation in around 23% yield (table 9, entry 5).

The cyclobutanone **18a** was completely consumed in our best condition: (**18a** (0.01 mmol, 1 equiv.), **19a** (0.01 mmol, 1 equiv.), Ni(TMDA)(*o*-tolyl)Cl/dppBz (80 mol%), toluene, time, rt, in a glove box, Table 3, entry 5). Therefore, to improve the yield, the loading of the starting material **18a** was increased to 4 equivalents. Unfortunately, the product could not be observed in this case (Table 9, entry 6). A control experiment was performed without any catalysts or ligands and as expected, only starting materials was observed (Table 9, entry 7).

**Table 9.** Batch mode<sup>a</sup>

Entry	Metal/dppBz	Loading (%)	(Metal/L)	Temperature (°C)	Yields <sup>b</sup>
1	NiCp <sub>2</sub>	50		40	trace
2	NiCp <sub>2</sub>	80		40	trace
3	NiCp <sub>2</sub>	30		60	trace
4	NiCp <sub>2</sub>	80		60	trace
5	Ni(TMDA)( <i>o</i> -tolyl)Cl	80		60	23%
6 <sup>c</sup>	Ni(TMDA)( <i>o</i> -tolyl)Cl	80		60	No product
7	/	/		40	Only S.M.

a) Reaction conditions: **18** (0.2 mmol, 1 equiv.), **19a** (0.2 mmol, 1 equiv.), metal/ligand (30 – 80 mol%), toluene, 16 h, rt. in a glove box b) Yield calculated by NMR spectroscopy using 1,3,5 trimethoxybenzene as internal standard. c) 4 equiv. of **1** used in this case.

A microwave reactor was next used to accelerate the reaction, and using the conditions from table 9, entry 5 the time taken to completely consume the starting material was reduced to 6 hours giving the product in a 39% yield using 3 equivalents of the benzaldehyde (Table 10, entry 1). These conditions were next employed under both nitrogen and air which revealed that the catalytic activity seemed to decrease with increased oxygen levels (Table 10, entry 3 and 4).

**Table 10.** Cycloaddition of cyclobutenone **18** with benzaldehyde: Microwave system<sup>a</sup>

Entry	Metal	Atmosphere	Yield (%)
1 <sup>a</sup>	Ni(TMDA)( <i>o</i> -tolyl)Cl	Nitrogen	39%
2 <sup>a</sup>	NiCp <sub>2</sub>	Nitrogen	/
3	Ni(TMDA)( <i>o</i> -tolyl)Cl	Nitrogen	31%
4	Ni(TMDA)( <i>o</i> -tolyl)Cl	Air	15%

a) Reaction conditions: **18** (0.2 mmol, 1 equiv.), **19a** (0.6 mmol, 3 equiv.), metal/ligand (80 mol%), toluene, MW 6h, 60 °C, in a glove box. a) reaction set up inside a glove box under inert atmosphere.

The stability of the starting materials and the product under the reaction conditions was another parameter to observe. The same conditions, as reported in Table 10 (entry 1), was used on the product lactone **20a**, and the yield of recovered material was only 42% highlighting that product could be consumed over time (Figure 15).

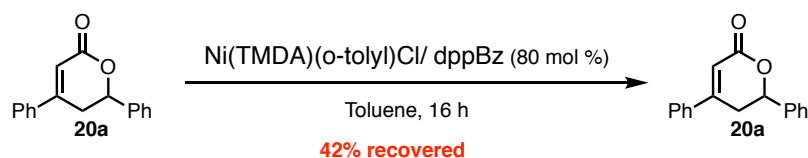


**Figure 15.** Analysis of the stability of the product inside the catalytic system.

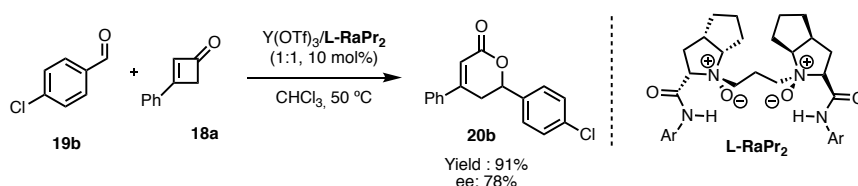
With the problems observed with these ‘optimal’ conditions, other catalysts were tested. Based on recent literature concerning the synthesis of coumarin derivatives from cyclobutenones, two different metals were used to extend the scope of the reactions.<sup>100</sup> Scandium(III) triflate was first analysed with different ligands but afforded poor yields of product (Table 1).

**Table 1.** Cycloaddition with cyclobutenone **1**: New catalyst system.<sup>a</sup>

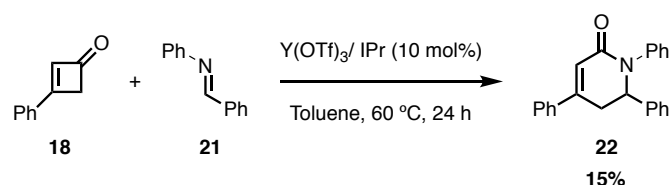
Entry	Ligand	NMR (%)	yield
1	IPr	8%	
2	Dppe	5%	
3	DppBz	5%	
4	Bipyridine	trace	
5	/	trace	

a) Reaction conditions: **18a** (0.2 mmol, 1 equiv.), **19a** (0.2 mmol, 1 equiv.), Sc(OTf)<sub>3</sub>/ligand (30 mol%), toluene, 16 h, N<sub>2</sub>, 60 °C.

Unfortunately, a recently reported and related process (Scheme 46) provided an enantioselective route to the synthesis of the same type of lactone with a much higher yield.<sup>100</sup>



**Scheme 46.** Enantioselective Synthesis of Lactone via Catalytic Ring Opening/Cycloaddition of Cyclobutenones



**Scheme 47.** Synthesis of lactam via Catalytic Ring Opening/Cycloaddition of Cyclobutenones with imine.

As the project was therefore stopped for now, we were interested to replace the benzaldehyde by an imine to the synthesis of lactam. The commercially available *N*-benzylideneaniline **21** was used as imine for the synthesis of lactam with the cyclobutenone **18** offering the product **22** in 15% yield, showing the potential of this system to be used on other functionalized molecules.

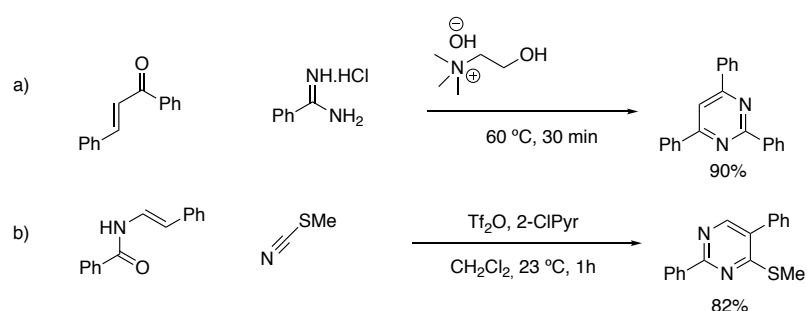
### 3.4. Conclusion

The Ni-catalysed cycloaddition of cyclobutenones with aldehydes offered a rapid way to synthesise heterocyclic compounds. However, this method is limited due to the instability of the product under the reaction conditions. Unfortunately, recent studies have highlighted yttrium (III) triflate has catalyst for the enantioselective synthesis of the same type of lactone. Therefore, this chemistry can still be improved to the synthesis of lactam type compounds by reaction of cyclobutanone **18** with functionalized imines to the synthesis of *N*-heteroaromatic boronates as intermediates for further coupling reactions.

## 4. Chapter IV. Synthesis of Pyrimidin-6-yl Trifluoroborate Salts as Heterocyclic Boronic Acid Derivatives

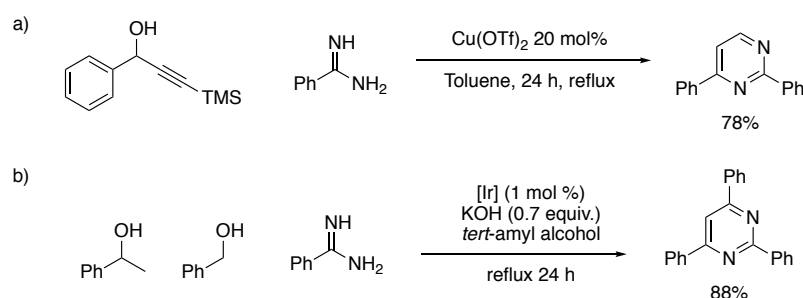
### 4.1.Introduction

Pyrimidines are amongst the most widely represented class of heterocycles in biological systems, and they are constituents of nucleic acids as well as many pharmaceuticals and agrochemicals.<sup>101</sup> Pyrimidines can be synthesised by condensation reaction such as amidines with  $\alpha,\beta$ -unsaturated ketones<sup>102</sup> or even condensation of cyanic acid derivatives with N-vinyl/aryl amides, reported by Ahmad et al (Scheme 47).<sup>103</sup>



**Scheme 47.** Synthesis of pyrimidines via condensation of a)  $\alpha,\beta$ -unsaturated ketones with amidine salts b) N-vinyl amides and nitriles

Transition metal catalysts have also been used to promote the synthesis of pyrimidines. Zhan and co-workers have reported the tandem reaction of propargylic alcohols and amidines using Cu(OTf)<sub>2</sub> as catalyst.<sup>104</sup> More recently, Kempe and co-workers developed a procedure using iridium-catalysis for the multicomponent synthesis of pyrimidines from amidines (Scheme 48).<sup>105</sup>

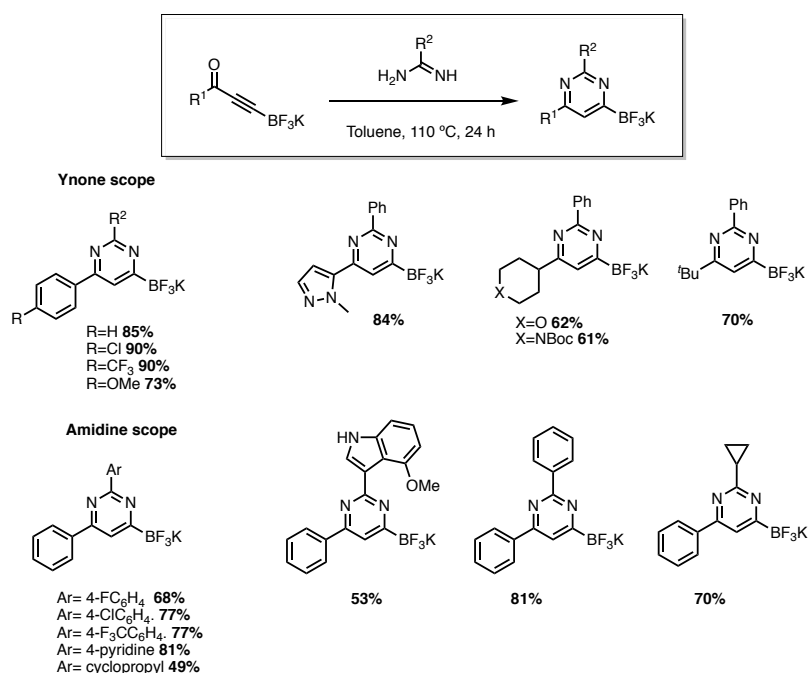


**Scheme 48.** Synthesis of pyrimidines a) from propargylic alcohols and amidines using Cu(OTf)<sub>2</sub> b) from amidines and alcohols.

However, many methods suffer from the use of expensive or toxic metal catalysts, multistep synthesis of precursors, expensive and sensitive reagents or strongly basic conditions.

Given the significance and the synthetic challenges posed by pyrimidines in the chemical sciences, the Harrity group set out to establish a robust strategy for the synthesis of pyrimidine 4-boronic acid derivatives via the condensation of amidines and ynone trifluoroborate salts, and to explore their utilization in organic synthesis.

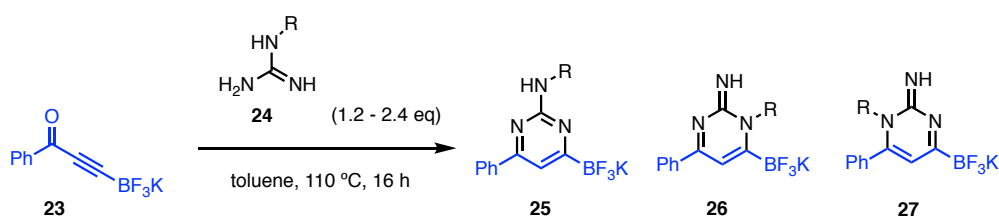
The previous studies investigated the condensation reaction of amidines and ynone trifluoroborate salts and these results are summarized in Scheme 47. Benzamidine was found to undergo smooth condensation with a range of ynone trifluoroborate salts to give the corresponding pyrimidine borates in good yield. The scope of the condensation included a range of aromatic, heteroaromatic and aliphatic substituents (Scheme 49).



**Scheme 49.** Scope of condensation of ynones trifluoroborate and benzamidine

## 4.2. Aim of this chapter

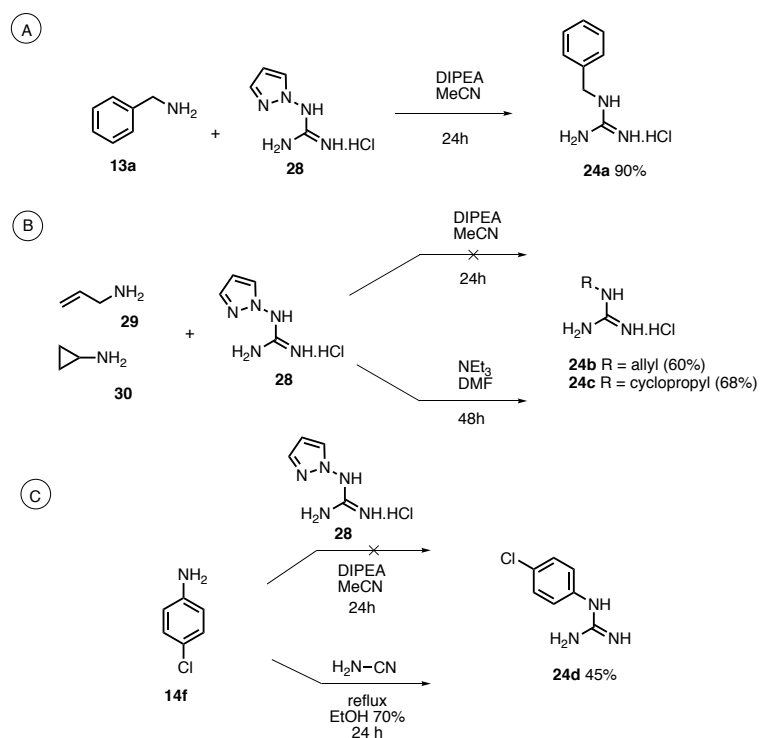
A significant proportion of marketed pyrimidines contain a 2-amino group, and so it was important to demonstrate the compatibility of guanidines in this chemistry. Following this, we investigated the scope of an ynone (potassium (3-oxo-3-phenylprop-1-yn-1-yl)trifluoroborate) condensation with various *N*-substituted guanidines. In particular, we wanted to explore the potential of this method to allow access to aryl-, heteroaryl-, and alkyl- substituted aminopyrimidines (Scheme 50). In addition, the issue of regioselectivity was also of interest.



**Scheme 50.** Synthesis of substituted aminopyrimidines via condensation of potassium (3-oxo-3-phenylprop-1-yn-1-yl)trifluoroborate with *N*-substituted guanidines.

## 4.3. Results and discussion

The first step was to synthesise the different guanidine precursors. Towards this end, 1*H*-pyrazole-1-carboxamide hydrochloride was reacted with the benzylamine to afford the corresponding guanidine **24** (Scheme 51a). The same reaction was used with the cyclopropylamine **30** and the 2-propen-1-ylamine **29**, however no conversion to the product was observed (Scheme 51b). Fortunately, by replacing the solvent from acetonitrile to dimethylformamide, the guanidine could be obtained after 48 h of reaction at room temperature. The same problem was observed with the synthesis of the precursor **24e** by using either acetonitrile or dimethylformamide as solvent. To overcome this problem, another route was considered by using the cyanamide as electrophile, leading in this case to the desired guanidine **24e** (Scheme 51c).



**Scheme 51.** Synthesis of the guanidine precursors

In parallel to the synthesis of the guanidine precursor, the ynone **23** was synthesized from benzaldehyde. The first step was the reaction of the benzaldehyde with a solution of ethynylmagnesium bromide to afford the propargylic alcohol **31** (figure 16). The second step was the borylation of the terminal alkyne and conversion to the alkynyl trifluoroborate salt **32** following by oxidation using  $\text{MnO}_2$  to finally give the ynone trifluoroborate **23** in a good overall yield.

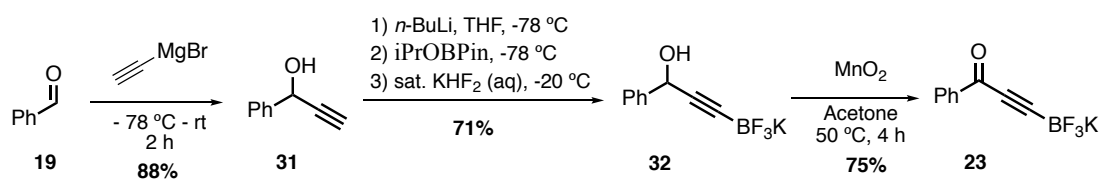
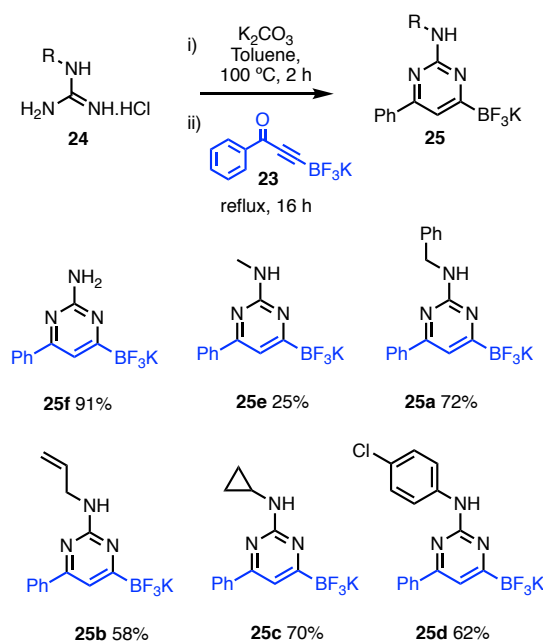


**Figure 16.** Synthesis of ynone **23** from benzaldehyde

After this, the corresponding pyrimidines were synthesised based on the previous condensation reactions of the amidines and the ynone trifluoroborate salts (Scheme 50). Unfortunately, the condensation of the guanidine hydrochloride salts was inefficient under the previously reported conditions (toluene, reflux). To overcome this difficulty, potassium carbonate was used as base promoter. Specifically, an excess potassium carbonate was stirred with the guanidine salt in

toluene at reflux for 2 h before adding the ynone trifluoroborate salts. Under these conditions, the different pyrimidines were successfully obtained via condensation (Scheme 52).



**Scheme 52.** Synthesis of pyrimidines via condensation of guanidines

Under these conditions, the products were isolated with high regioselectivities after recrystallization, and the regiochemistry was assigned on the basis of <sup>1</sup>H NMR spectroscopy, and by X-ray crystallography in the case of the compounds **25a** and **25e** (Figure 17). Minor compounds were observed in the crude which could correspond to regioisomeric condensation products, but these could not be isolated in sufficient purity or quantity to be characterized.

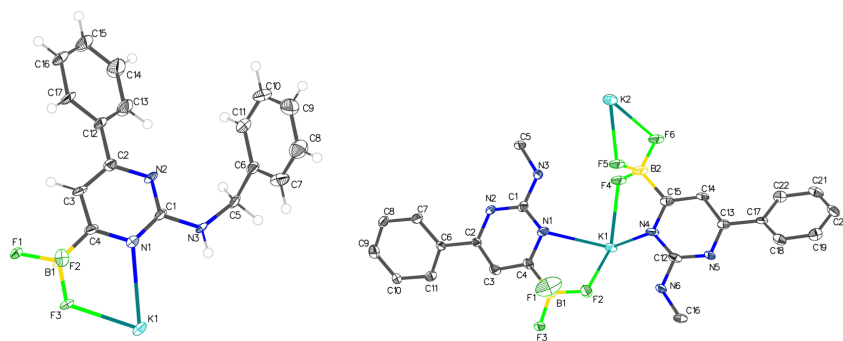
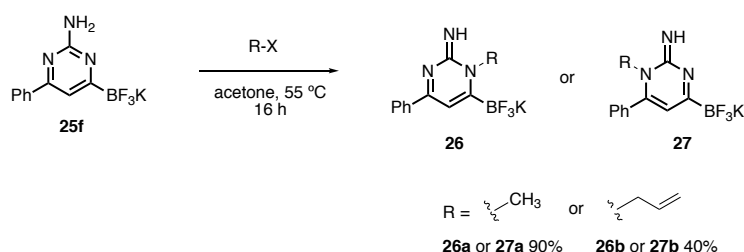


**Figure 17.** Crystal structure of products **25a** (left), **25e** (right) confirming the regiochemistry.

Following these results, we decided to functionalise the pyrimidine **25f** to confirm the regioselectivity of the condensation. As the alkylation could lead to three possible isomers, it would be interesting to see if the products obtained would be the same or different as the condensation.

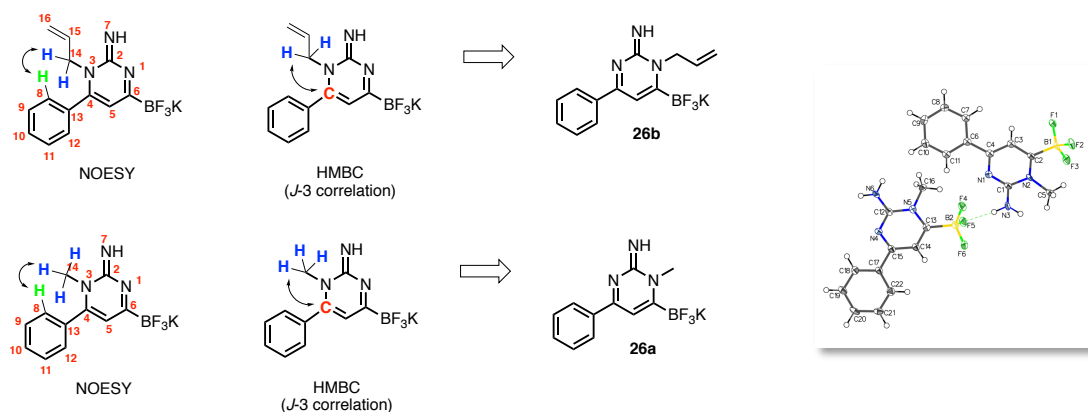
The alkylation proceeded smoothly to afford one regioisomer of the corresponding pyrimidine (Scheme 53). Comparing the NMR spectra of these compounds with the previous spectra of compounds **25b** and **25e** showed that the alkylation led to different product isomers as compared to the condensation reaction.



**Scheme 53.** Alkylation of the pyrimidine **25f**

Therefore, this reaction led to two possible products, **26** or **27**, and to obtain more information about the structure of these isomers, a range of NMR experiments were performed. First, 2D NOESY revealed that no correlation was observed between the side chain of **27a** (-CH<sub>3</sub>) or **27b** (-CH<sub>2</sub>-CH=CH<sub>2</sub>) with the phenyl group, suggesting that the regioisomer could be **26** (Scheme 54). Secondly, a combination of COSY, HSQC and HMBC NMR experiments were used to confirm the connectivity of the product with respect to the allyl group. A correlation between the allylic CH<sub>2</sub> and C<sub>2</sub> of the ring carbon was observed. However, no correlation with C<sub>4</sub> was observed, supporting the results of the NOESY analysis (Scheme 54).

In summary, the analysis revealed that for both compounds, the side chain should be away from the phenyl group, suggesting that the regioisomer **26** was obtained. Fortunately, we were able to obtain crystals of compound **26a** which provided an opportunity to confirm the regiochemistry of the product by X-ray crystallographic analysis, and which confirmed **26** as the only regioisomer.



**Scheme 54.** H-H and H-C correlation. No correlation of the hydrogen of the side chain (in blue) with the hydrogen of the phenyl group (in green) or the carbon (in red) was observed. A crystal structure of compound **26a** was obtained, confirming the regiochemistry.

#### 4.4. Conclusion

In conclusion, the ynone (potassium (3-oxo-3-phenylprop-1-yn-1-yl)trifluoroborate) was found to undergo condensation with substituted guanidines to afford a range of novel pyrimidin-6-yl trifluoroborate salts. The structure of these compounds was confirmed by a combination of single crystal X-ray analysis and NOESY and HMBC NMR spectroscopy, which confirmed that the condensation and alkylation reactions proceeded with different regiochemistries.

## 5. Chapter V. Experimental part

### 5.1. General consideration

All reactions were carried out in flame-dried glassware under an inert atmosphere unless otherwise specified.

Solvents and reagents were used as supplied or purified using standard laboratory techniques according to methods described by Perrin and Armarego.

Dry solvent was provided *via* a Grubbs type one manufactured by Innovative Technology. The solvent contained in a lined metal reservoir is forced through a couple of metals columns, containing either molecular sieve or activated alumina. The oxygen and water removal proceeds as the solvent passes through the drying agent.

The dried solvent is then collected to an appropriate vessel under vacuum via a Schlenk line system. The water content is monitored daily by coulometric Karl Fischer titration.

Thin layer chromatography (or TLC) was performed on aluminium-backed plates pre-coated with silica (Merck silica Kieselgel 60 F254), which were developed using standard visualizing agents: ultraviolet light or potassium permanganate.

Flash chromatography was performed on silica gel (60 Å, mesh 40-63 µm).

Melting points were obtained using a Stuart apparatus and are uncorrected.

<sup>1</sup>H spectra were recorded on a Bruker AVIII HD-400 (400 MHz), Bruker AVI-400 (400 MHz), Bruker AMX-400 (400 MHz) or DPX-400 (400 MHz). Proton magnetic resonance chemical shifts are reported from the residual protic solvent resonance as the internal standard (CDCl<sub>3</sub>: δ = 7.26 ppm or DMSO: δ = 2.50 ppm). Data are reported as follows: chemical shift (ppm), multiplicity (s = singlet, d = doublet, t = triplet, q = quartet, m = multiplet or br = broad), then coupling constant (Hz).

<sup>13</sup>C NMR spectra were recorded on a Bruker AVIII HD-400 (101 MHz), Bruker AVI-400 (101 MHz), Bruker AMX-400 (101 MHz) or DPX-400 (101 MHz).

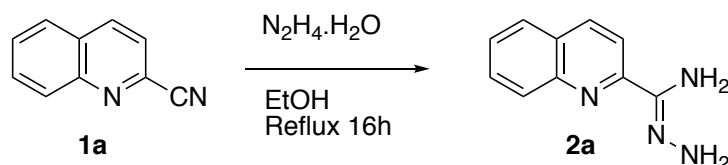
<sup>19</sup>F NMR spectra were recorded on a Bruker AMX-400 (376 MHz) or Bruker AVIII HD-400 (376 MHz) and the chemical shifts are uncorrected.

<sup>11</sup>B NMR spectra were recorded on a Bruker AVIII HD-400 (128 MHz), and the chemical shifts are uncorrected.

Infrared spectra were recorded on a Perkin-Elmer Paragon 100 FTIR spectrometer. The most structurally relevant bands are quoted in cm<sup>-1</sup>.

## 5.2. Chapter I

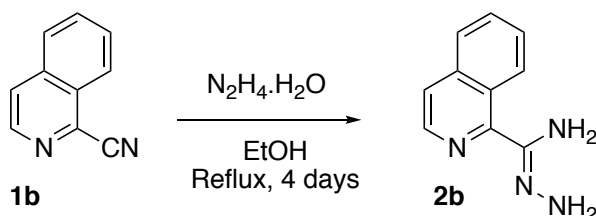
### Preparation of 2-Quinolylamidrazone 2a



To a stirred suspension of quinoline-2-carbonitrile (1 g, 6.48 mmol, 1 eq) in ethanol (4 mL) under nitrogen was added hydrazine hydrate (0.63 mL, 13 mmol, 2 eq) and the reaction was stirred overnight at room temperature. The yellow precipitate was filtered and washed with cold diethyl ether (3x10 mL) to afford 2-quinolylamidrazone as a yellow solid (1.66 g, 94%).  **$^1\text{H}$  NMR (400 MHz,  $\text{CDCl}_3$ ):** 8.25-8.23 (1H, m), 8.10-8.07 (1H, m), 8.01-7.99 (1H, m), 7.94-7.92 (1H, m), 7.726-7.72 (1H, m), 7.58-7.54 (1H, m), 5.91 (2H, br.), 5.65 (2H, br).

These data are in agreement with the previously reported spectral data.<sup>106</sup>

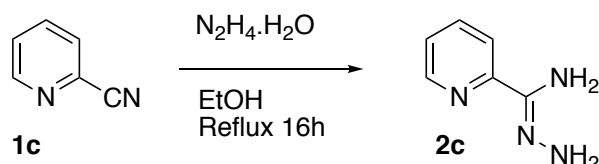
### Preparation of the isoquinoline-1-carbohydrazonamide 2b



To a stirred suspension of quinoline-2-carbonitrile (1 g, 6.48 mmol, 1 eq) in ethanol (4mL) under nitrogen was added hydrazine hydrate (0.63 mL, 13 mmol, 2 eq) and the reaction was stirred overnight at room temperature for 4 days. The solution was extracted with dichloromethane (3x40 mL) and washed with water (30 mL) and brine (30 mL). The organic layer was dried over  $\text{Na}_2\text{SO}_4$ , filtered and evaporated to dryness to give isoquinoline-1-carbohydrazonamide as a mixture used directly for the next step.  **$^1\text{H}$  NMR (400 MHz,  $\text{CDCl}_3$ ):** 9.46-9.42 (1H, m), 8.47-8.44 (1H, m), 7.83-7.80 (1H, m), 7.69-7.60 (3H, m), 5.37 (2H, br), 4.48 (2H, br).

These data are in agreement with the previously reported spectral data.<sup>106</sup>

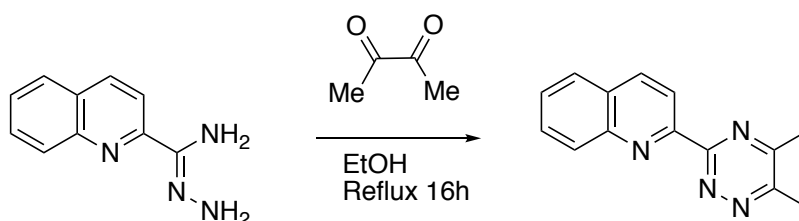
### Preparation of the (pyridine-2-yl)amidrazone 2c



To a stirred suspension of 2-cyanopyridine (5 g, 48.0 mmol, 1 eq) in ethanol (50 mL) under nitrogen was added hydrazine monohydrate (4.70 mL, 96 mmol, 2 eq) and the reaction was stirred overnight at room temperature. The yellow precipitate was filtered and washed with cold diethyl ether (3x10 mL) to afford (pyridine-2-yl)amidrazone as a yellow solid (4.5 g, 70%).  $^1\text{H NMR}$  (400 MHz,  $\text{CDCl}_3$ ): 8.53 (d,  $J = 5.0$  Hz, 1H), 8.02 (d,  $J = 8.0$  Hz, 1H), 7.71 (td,  $J = 8.0, 1.5$  Hz, 1H), 7.40 – 7.19 (m, 1H), 5.31 (s, 2H), 4.24 (s, 2H).

These data are in agreement with the previously reported spectral data.<sup>106</sup>

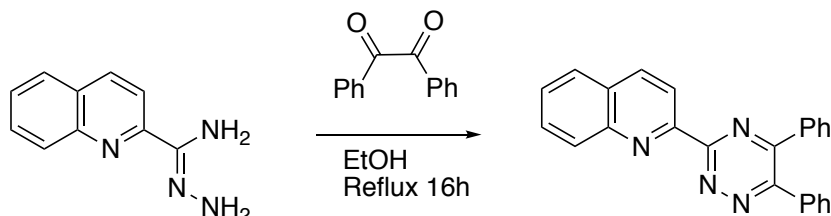
### Preparation of the 5,6-dimethyl-3-(2-quinoly)-1,2,4-triazine 4aa



To a stirred solution of butane-2,3-dione (0.494 mL, 5.64 mmol, 1 eq) in ethanol (40 mL) was added 2-quinolylamidrazone (1.05 g, 5.64 mmol, 1 eq) and the reaction was stirred overnight at reflux. Upon cooling, a yellow precipitate formed, which was filtered and washed with cold ethanol (3x10 mL) to afford the 5,6-dimethyl-3-(2-quinoly)-1,2,4-triazine (1.05 g, 80%) as a yellow solid.  $^1\text{H NMR}$  (400 MHz,  $\text{CDCl}_3$ ):  $\delta$  8.73 (d, 1H,  $J = 8.6$  Hz), 8.37 (dd, 2H,  $J = 8.4$  Hz, 2.6 Hz), 7.90 (d, 1H,  $J = 8.2$  Hz), 7.78 (ddd, 1H,  $J = 8.4$  Hz, 6.9 Hz, 1.4 Hz), 7.62 (ddd, 1H,  $J = 8.0$  Hz, 6.9 Hz, 1.2 Hz), 2.8 (s, 3H), 2.75 (s, 3H).

These data are in agreement with the previously reported spectral data.<sup>106</sup>

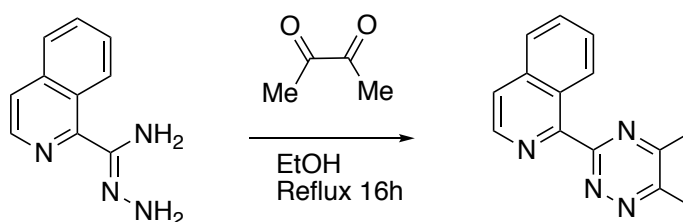
### Preparation of the 5,6-diphenyl-3-(2-quinoly)-1,2,4-triazine 4ab



To a stirred solution of benzil (5.15 g, 14.28 mmol, 1 eq) in ethanol (45 mL) was added 2-quinolyamidrazone (2.66 g, 14.28 mmol, 1 eq) and the reaction was stirred overnight at reflux. Upon cooling, a yellow precipitated formed, which was filtered and washed with cold ethanol (3x20 mL) to afford 5,6-diphenyl-3-(2-quinoly)-1,2,4-triazine (1.05 g, 80%) as a yellow solid (4.54 g, 85%).  $^1\text{H NMR}$  (400 MHz,  $\text{CDCl}_3$ ):  $\delta$  8.81 (d,  $J = 8.5$  Hz, 1H), 8.42 (d,  $J = 8.5$  Hz, 2H), 7.94 (d,  $J = 8.0$  Hz, 1H), 7.82 (t,  $J = 8.0$  Hz, 1H), 7.77 (d,  $J = 8.5$  Hz, 2H), 7.72-7.64 (m, 3H), 7.55-7.39 (m, 6H).

These data are in agreement with the previously reported spectral data.<sup>106</sup>

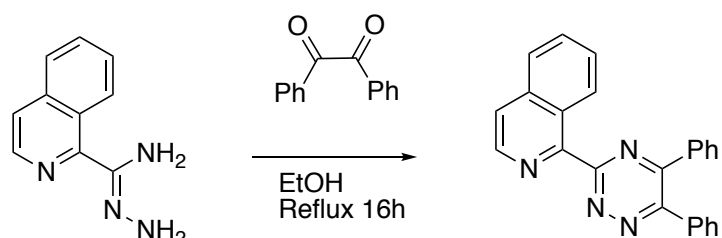
### Preparation of the 5,6-dimethyl-3-(2-isoquinoly)-1,2,4-triazine 4ba



To a stirred solution of butane-2,3-dione (1.40 mL, 16.21 mmol, 1 eq) in ethanol (35 mL) was added 2-isoquinolyamidrazone (3.0 g, 16.21 mmol, 1 eq) and the reaction was stirred overnight at reflux. Upon cooling, the solvent was removed in vacuo and the residue was purified chromatographically over silica gel with ethyl acetate to afford 5,6-dimethyl-3-(2-isoquinoly)-1,2,4-triazine (1.05 g, 40%) as a yellow solid.  $^1\text{H NMR}$  (400 MHz,  $\text{CDCl}_3$ )  $\delta$  8.77 (d,  $J = 5.5$  Hz, 1H), 8.55 (d,  $J = 8.5$  Hz, 1H), 7.93 (d,  $J = 8.5$  Hz, 1H), 7.82 (d,  $J = 5.5$  Hz, 1H), 7.76 – 7.71 (m, 1H), 7.66 – 7.61 (m, 1H), 2.84 (s, 3H), 2.73 (s, 3H).

These data are in agreement with the previously reported spectral data.<sup>106</sup>

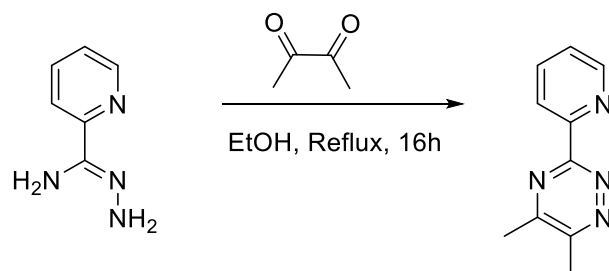
### Preparation of the 5,6-diphenyl-3-(2-isoquinoly)-1,2,4-triazine 4bb



To a stirred solution of benzil (3.09 g, 14.76 mmol, 1 eq) in ethanol (35 mL) was added 2-quinolyamidrazone (2.75 g, 14.76 mmol, 1 eq) and the reaction was stirred overnight at reflux. Upon cooling, a yellow precipitate formed, which was filtered and washed with cold ethanol (3x20 mL) to afford 5,6-diphenyl-3-(2-isoquinoly)-1,2,4-triazine (1.05 g, 80%) as a yellow solid (3.00 g, 57%). <sup>1</sup>H NMR (400 MHz, CDCl<sub>3</sub>): δ 8.83 (d, *J* = 5.5 Hz, 1H), 8.66 (d, *J* = 8.5 Hz, 1H), 7.99 (d, *J* = 8.5 Hz, 1H), 7.88 (d, *J* = 5.5 Hz, 1H), 7.82 – 7.66 (m, 6H), 7.52 – 7.42 (m, 4H), 7.41 – 7.33 (m, 2H).

These data are in agreement with the previously reported spectral data.<sup>[34]</sup>

### Preparation of the 5,6-dimethyl-3-(2-pyridyl)-1,2,4-triazine 4ca

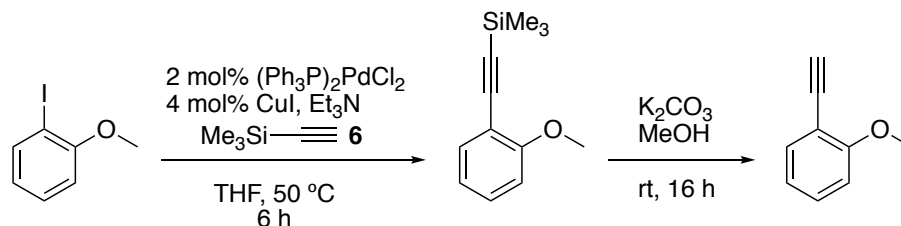


To a stirred solution of butan-2,3-dione (2.6 mL, 29.38 mmol, 1 eq) in ethanol (60 mL) was added 2-pyridylamidrazone (4.0 g, 29.38 mmol, 1 eq) and the reaction was stirred overnight at reflux. Upon cooling, the solvent was removed *in vacuo* and the residue purified chromatographically over silica gel with ethyl acetate to afford the product 5,6-dimethyl-3-(2-pyridyl)-1,2,4-triazine (1.05 g, 80%) as a yellow solid (4.7 g, 85%). <sup>1</sup>H NMR (400 MHz, CDCl<sub>3</sub>) δ 8.90-8.86 (m, 1H), 8.65 (d, *J* = 8.0 Hz, 1H), 7.91 (t, *J* = 8.0 Hz, 1H), 7.49 – 7.43 (m, 1H), 2.79 (s, 3H), 2.71 (s, 3H).

These data are in agreement with the previously reported spectral data.<sup>106</sup>

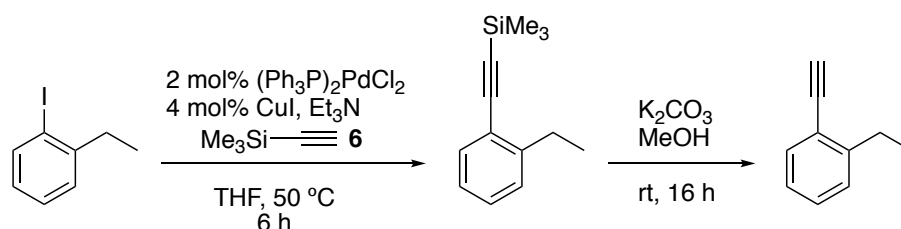


### Preparation of the 2-ethynylanisole **8a**



To a stirred solution of 1-ethyl-2-iodo benzene **5a** (5.0 g, 21.4 mmol, 1 equiv.) in degassed THF were added,  $\text{PdCl}_2(\text{PPh}_3)_2$  (0.6 g, 0.865 mmol, 0.04 equiv.),  $\text{CuI}$  (0.33 g, 0.172 mmol, 0.08 equiv.),  $\text{NEt}_3$  (15 mL, 101 mmol, 5 equiv.) and trimethylsilyl acetylene (4.5 mL 32.1 mmol, 1.5 equiv.). The reaction mixture was stirred at 50 °C under nitrogen and monitored by TLC analysis. After 5 h, the reaction mixture was cooled and the mixture triturated with pentane. The filtrate was collected, and the solvent was removed under vacuum to afford the product **7a** (3.0 g, 68%) as a yellow oil. The alkyne **7a** (3.0 g, 14.7 mmol, 1 equiv.) was added to methanol (30 mL) containing potassium carbonate (0.81 g, 5.87 mmol, 0.4 equiv.). The mixture was stirred at room temperature overnight and the solvent removed under vacuum. A solution 5% citric acid (50 mL) was added and the product was extracted with dichloromethane. The residue was purified chromatographically over silica gel with pentane to afford the product (1.6 g, 80%) as a pale yellow oil.  $^1\text{H NMR}$  ( $\text{CDCl}_3$ , 400 MHz)  $\delta$  7.47 (dd, 1H,  $J = 1.7, 7.5$  Hz), 6.94-6.89 (m, 2H), 3.92 (s, 3H), 3.23 (s, 1H). These data are in agreement with the previously reported spectral data.<sup>107</sup>

### Preparation of 1-ethyl-2-ethynylbenzene **8b**

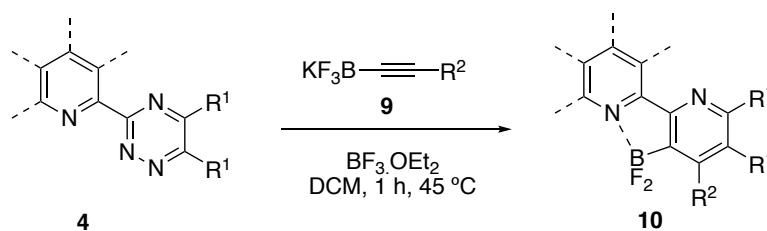


To a stirred solution of 1-ethyl-2-iodo benzene **5b** (5.0 g, 21.7 mmol, 1 equiv.) in degassed THF were added,  $\text{PdCl}_2(\text{PPh}_3)_2$  (0.6 g, 0.865 mmol, 0.04 equiv.), and  $\text{CuI}$  (0.33 g, 0.172 mmol, 0.08 equiv.),  $\text{NEt}_3$  (15 mL, 101 mmol, 5 equiv.) and added trimethylsilyl acetylene (4.5 mL, 32.1 mmol, 1.5 equiv.). The reaction mixture was stirred at 50 °C for 5 h under nitrogen and followed by TLC. The mixture was triturated with pentane and the solvent was removed in vacuum to afford the product (3.2 g, 70%) as a yellow oil.

The compound **7b** (3.2 g, 15.8 mmol, 1 equiv.) was added in a 30 mL of methanol containing potassium carbonate (0.9 g, 6.33 mmol, 0.4 equiv.). The mixture was stirred at room temperature for the night and the solvent removed in vacuum. 50 mL of a solution 5% citric acid was added, and the product was extracted with dichloromethane. the residue was purified chromatographically over silica gel with pentane to afford the product (1.6 g, 80%) as a pale-yellow oil. **<sup>1</sup>H NMR (400 MHz, CDCl<sub>3</sub>)** δ 7.49 (dd, 1H, J = 7.6 Hz, 1.2 Hz), 7.30 (td, 1H, J = 7.5 Hz, 1.4 Hz), 7.24 (d, 1H, J = 7.6 Hz), 7.16 (td, 1H, J = 7.5 Hz, 1.4 Hz), 3.26 (s, 1H), 2.84 (q, 2H, J = 7.6 Hz), 1.27 (t, 3H, J = 7.5 Hz).

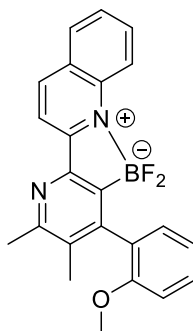
These data are in agreement with the previously reported spectral data.<sup>83</sup>

## Preparation of BINOL esters: Representative procedure



A solution of 5,6-dimethyl-3-(2-quinolyl)-1,2,4-triazine **4aa** (40 mg, 0.168 mmol, 1 equiv.) and potassium ((2-methoxyphenyl)ethynyl)trifluoroborate **8a** (120 mg, 0.504 mmol, 3 equiv.) in dichloromethane (4 mL) was treated with boron trifluoride diethyl etherate (0.104 mL, 0.84 mmol, 5 equiv.). The reaction was stirred for one hour at reflux and then quenched with brine (15 mL). The mixture was extracted with dichloromethane (4x15 mL) and the extract dried over MgSO<sub>4</sub>, filtered and the solvent evaporated. The residue was purified chromatographically silica gel using hexane/ethyl acetate (6:4) to afford 2-(3-(difluoroboranyl)-5,6-dimethyl-4-(2-ethylphenyl)pyridin-2-yl)quinoline **10aa** as a pale yellow amorphous solid (110 mg, 77%).

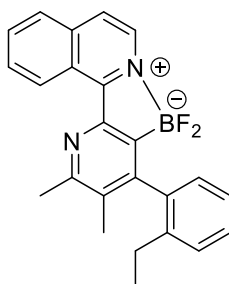
### Compound 10aa



Chemical Formula: C<sub>23</sub>H<sub>19</sub>BF<sub>2</sub>N<sub>2</sub>O

**<sup>1</sup>H NMR (400 MHz, CDCl<sub>3</sub>)** δ 8.57 (d, *J* = 8.5 Hz, 1H), 8.51 (d, *J* = 8.5 Hz, 1H), 8.41 (d, *J* = 8.5 Hz, 1H), 7.94 (d, *J* = 8.0 Hz, 1H), 7.84 (t, *J* = 8.0 Hz, 1H), 7.62 (t, *J* = 7.5 Hz, 1H), 7.46-7.36 (m, 2H), 7.13 (t, *J* = 7.5 Hz, 1H), 7.03 (d, *J* = 8.5 Hz, 1H), 3.78 (s, 3H), 2.66 (s, 3H), 2.14 (s, 3H). **<sup>13</sup>C NMR (101 MHz, CDCl<sub>3</sub>)** δ 158.3, 157.3, 156.5, 152.4, 149.6, 144.2, 140.3, 134.4, 133.2, 130.7, 129.4, 129.1, 128.6, 128.4, 127.7, 122.9, 120.8, 115.5, 111.1, 55.8, 23.7, 16.5. **<sup>19</sup>F (376.5 MHz, CDCl<sub>3</sub>)** δ -152.3 – -158.7 (2F, m). **<sup>11</sup>B NMR (128 MHz, CDCl<sub>3</sub>)** δ 9.1. **HRMS (ESI-TOF) *m/z* [MH<sup>+</sup>]** calcd for C<sub>23</sub>H<sub>20</sub><sup>11</sup>BF<sub>2</sub>N<sub>2</sub>O 389.1637, found 389.1640. **FTIR (neat)**  $\nu_{\max}$  / cm<sup>-1</sup> 2842, 1598, 1246, 1084.

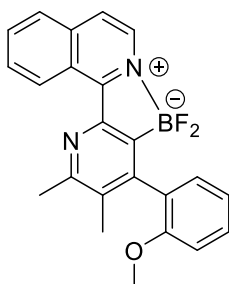
## Compound 10cb



Chemical Formula: C<sub>24</sub>H<sub>21</sub>BF<sub>2</sub>N<sub>2</sub>

Following the representative procedure, 5,6-dimethyl-3-(2-isoquinolyl)-1,2,4-triazine **4ba** (100 mg, 0.427 mmol, 1 equiv.), potassium ((2-ethylphenyl)ethynyl)trifluoroborate (290 mg, 1.27 mmol, 3 equiv.) and boron trifluoride diethyl etherate (0.26 mL, 2.14 mmol, 5 equiv.) were combined to give crude product **10cb**. The residue was purified chromatographically over florisil using hexane/ethyl acetate (8:2) to afford 2-(3-(difluoroboranyl)-5,6-dimethyl-4-(2-ethylphenyl)pyridin-2-yl)isoquinoline as a pale yellow amorphous solid (66 mg, 40%). **<sup>1</sup>H NMR (400 MHz, CDCl<sub>3</sub>)** δ 10.61-10.54 (1H, m), 8.29 (1H, d, *J* = 6.0 Hz), 7.96-7.93 (2H, m), 7.92-7.87 (1H, m), 7.84 (1H, d, *J* = 6.0 Hz), 7.42-7.37 (2H, m), 7.36-7.30 (1H, m), 7.22 (1H, d, *J* = 7.0 Hz), 2.76 (3H, s), 2.12 (3H, s), 2.06 (2H, q, *J* = 7.5 Hz), 1.11 (3H, t, *J* = 7.5 Hz). **<sup>13</sup>C NMR (100.6 MHz, CDCl<sub>3</sub>)** δ 157.8, 155.2, 154.4, 152.1, 141.2, 139.6, 138.2, 134.0, 132.4, 132.0, 130.1, 130.0, 128.7, 128.0, 127.9, 127.0, 125.5, 125.2, 123.0, 60.4, 26.1, 23.9, 21.1. **<sup>19</sup>F (376.5 MHz, CDCl<sub>3</sub>)** δ -162.6 – -164.6 (m, 2F). **<sup>11</sup>B (160.5 MHz, CDCl<sub>3</sub>)** δ 7.3. **HRMS (ESI-TOF) *m/z* [MH<sup>+</sup>]** calcd for C<sub>24</sub>H<sub>22</sub><sup>11</sup>BF<sub>2</sub>N<sub>2</sub>: 387.1844, found 387.1845. **FTIR (neat) *v*<sub>max</sub> / cm<sup>-1</sup>** 2961, 2925, 2874, 1597, 1447, 1269, 1087, 953, 846, 809.

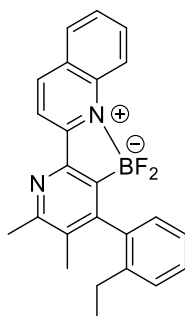
## Compound 10ca



Chemical Formula: C<sub>23</sub>H<sub>19</sub>BF<sub>2</sub>N<sub>2</sub>O

Following the representative procedure, 5,6-dimethyl-3-(2-isoquinolyl)-1,2,4-triazine **4ba** (100 mg, 0.427 mmol, 1 equiv.), potassium ((2-methoxyphenyl)ethynyl)trifluoroborate (250 mg, 1.07 mmol, 2.5 equiv.) and boron trifluoride diethyl etherate (0.13 mL, 1.07 mmol, 2.5 equiv.) were combined to give crude product **10ca**. The residue was precipitated slowly from dichloromethane to afford 2-(3-(difluoroboranyl)-5,6-dimethyl-4-(2-methoxyphenyl)pyridin-2-yl)isoquinoline as a pale brown amorphous solid (130 mg, 70%). **<sup>1</sup>H NMR** (400 MHz, CDCl<sub>3</sub>): δ 10.60 (d, *J* = 8.0 Hz, 1H), 8.30 (d, *J* = 6.0 Hz, 1H), 8.00 – 7.94 (m, 2H), 7.94 – 7.88 (m, 1H), 7.85 (d, *J* = 6.0 Hz, 1H), 7.46 – 7.36 (m, 2H), 7.13 (td, *J* = 7.5, 1.0 Hz, 1H), 7.04 (d, *J* = 8.5 Hz, 1H), 3.80 (s, 3H), 2.75 (s, 3H), 2.17 (s, 3H). **<sup>13</sup>C NMR** (100.6 MHz, CDCl<sub>3</sub>): δ 157.4, 156.3, 155.2, 154.6, 149.4, 139.5, 134.0, 133.4, 132.0, 130.6, 130.3, 129.7, 129.2, 128.4, 126.9, 125.2, 122.8, 120.7, 111.0, 55.7, 23.7, 16.3. **<sup>19</sup>F** (376.5 MHz, CDCl<sub>3</sub>) δ -158.8 – -168.3 (m, 2F). **<sup>11</sup>B** (160.5 MHz, CDCl<sub>3</sub>) δ 7.3. **HRMS (ESI-TOF)** *m/z* [MH<sup>+</sup>] calcd for C<sub>23</sub>H<sub>20</sub><sup>11</sup>BF<sub>2</sub>N<sub>2</sub>O: 389.1637, found 389.1632. **FTIR (neat)** ν<sub>max</sub> / cm<sup>-1</sup> 3079, 2953, 2836, 1600, 1553, 1494, 1353, 1243, 1089, 952, 832.

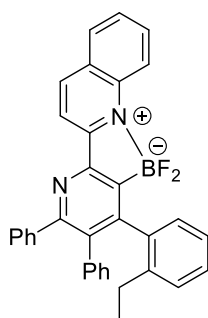
## Compound 10ab



Chemical Formula: C<sub>24</sub>H<sub>21</sub>BF<sub>2</sub>N<sub>2</sub>

Following the representative procedure, 5,6-dimethyl-3-(2-quinolyl)-1,2,4-triazine **4aa** (100 mg, 0.427 mmol, 1 equiv.), potassium ((2-ethylphenyl)ethynyl)trifluoroborate (290 mg, 1.27 mmol, 3 equiv.) and boron trifluoride diethyl etherate (0.26 mL, 2.14 mmol, 5 equiv.) were combined to give the crude **10ab**. The residue was purified chromatographically over silica gel using CH<sub>2</sub>Cl<sub>2</sub>/ethyl acetate (1:1) to afford 2-(3-(difluoroboranyl)-5,6-dimethyl-4-(2-ethylphenyl)pyridin-2-yl)quinoline as a beige amorphous solid (110 mg, 67%). **<sup>1</sup>H NMR (400 MHz, CDCl<sub>3</sub>)** δ 8.64 (d, *J* = 8.5 Hz, 1H), 8.53 (d, *J* = 9.0 Hz, 1H), 8.48 (d, *J* = 8.5 Hz, 1H), 7.99 (d, *J* = 7.5 Hz, 1H), 7.90 – 7.84 (m, 1H), 7.67 (t, *J* = 7.0 Hz, 1H), 7.42 – 7.38 (m, 2H), 7.36 – 7.31 (m, 1H), 7.21 (d, *J* = 7.0 Hz, 1H), 2.70 (s, 3H), 2.46 (q, *J* = 7.5 Hz, 2H), 2.11 (s, 3H), 1.09 (t, *J* = 7.5 Hz, 3H). **<sup>13</sup>C NMR (101 MHz, CDCl<sub>3</sub>)** δ 158.5, 157.1, 154.6, 152.3, 144.2, 141.2, 140.2, 138.1, 133.3, 133.2, 129.0, 128.7, 128.5, 128.0, 127.7, 125.6, 122.8, 116.6, 115.4, 26.1, 23.6, 16.4, 14.6. **<sup>19</sup>F (376.5 MHz, CDCl<sub>3</sub>)**: δ -155.0 – -157.0 (2F, m). **<sup>11</sup>B NMR (128 MHz, CDCl<sub>3</sub>)**: δ 8.7. **HRMS (ESI-TOF) *m/z* [MH<sup>+</sup>]** calcd for C<sub>24</sub>H<sub>22</sub><sup>11</sup>BF<sub>2</sub>N<sub>2</sub> 387.1844, found 387.1841. **FTIR (neat)** ν<sub>max</sub> / cm<sup>-1</sup> 2961, 2925, 2874, 1597, 1447, 1269, 1087, 953, 846, 809.

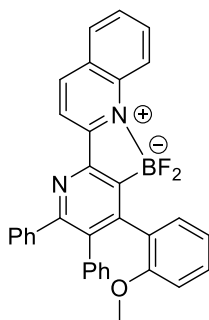
## Compound 10bb



Chemical Formula:  $C_{34}H_{25}BF_2N_2$

Following the representative procedure, 5,6-diphenyl-3-(2-quinolyl)-1,2,4-triazine **4ab** (85 mg, 0.236 mmol, 1 equiv.), potassium ((2-ethylphenyl)ethynyl)trifluoroborate (139 mg, 0.590 mmol, 2.5 equiv.) and boron trifluoride diethyl etherate (0.15 mL, 1.18 mmol, 5 equiv.) were combined to give the crude **10bb**. The residue was slowly precipitated from dichloromethane to afford 2-(3-(difluoroboranyl)-5,6-diphenyl-4-(2-ethylphenyl)pyridin-2-yl)quinoline as a beige amorphous solid (55 mg, 46%).  **$^1H$  NMR (400 MHz,  $CDCl_3$ )**  $\delta$  8.68 (d,  $J = 8.5$  Hz, 1H), 8.60 (d,  $J = 8.5$  Hz, 2H), 8.02 (d,  $J = 8.0$  Hz, 1H), 7.91 (t,  $J = 7.5$  Hz, 1H), 7.70 (t,  $J = 7.5$  Hz, 1H), 7.49 – 7.41 (m, 2H), 7.37 (d,  $J = 8.0$  Hz, 1H), 7.30 – 7.21 (m, 5H), 7.18 – 7.10 (m, 1H), 7.08 – 6.90 (m, 5H), 2.51 – 2.35 (m, 1H), 2.23 – 2.09 (m, 1H), 1.02 (t,  $J = 7.5$  Hz, 3H).  **$^{13}C$  NMR (101 MHz,  $CDCl_3$ )**  $\delta$  159.1, 156.5, 154.2, 153.4, 144.4, 140.8, 140.7, 140.2, 137.9 (x2 C) 137.5, 133.4, 131.1, 130.2, 129.9, 129.4, 128.6, 128.1, 127.8, 127.7 (x2 C) 127.3, 127.2, 126.6, 124.7, 123.0, 115.8, 25.9, 14.1.  **$^{19}F$  (376.5 MHz,  $CDCl_3$ )**  $\delta$  -153.3 – -156.1 (m, 2F).  **$^{11}B$  NMR (128 MHz,  $CDCl_3$ )**  $\delta$  8.7. **HRMS (ESI-TOF)  $m/z$  [ $MH^+$ ]** calcd for  $C_{34}H_{26}^{11}BF_2N_2$  511.2157, found 511.2166. **FTIR (neat)**  $\nu_{max}$  /  $cm^{-1}$  3273, 2924, 1628, 1553, 1492, 1243, 1089, 952, 832.

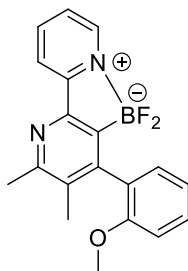
## Compound 10ba



Chemical Formula: C<sub>33</sub>H<sub>23</sub>BF<sub>2</sub>N<sub>2</sub>O

Following the representative procedure, 5,6-diphenyl-3-(2-quinolyl)-1,2,4-triazine **4ab** (85 mg, 0.236 mmol, 1 equiv.), potassium ((2-ethylphenyl)ethynyl)trifluoroborate (139 mg, 0.590 mmol, 2.5 equiv.) and boron trifluoride diethyl etherate (0.15 mL, 1.18 mmol, 5 equiv.) were combined to give the crude **10ba**. The residue was slowly precipitated from dichloromethane and washed with diethyl ether to afford 2-(3-(difluoroboranyl)-5,6-diphenyl-4-(2-methoxyphenyl)pyridin-2-yl)quinoline as a light grey amorphous solid (60 mg, 50%). **<sup>1</sup>H NMR (400 MHz, CDCl<sub>3</sub>)** δ 8.67 (d, *J* = 8.5 Hz, 1H), 8.61 (t, *J* = 8.0 Hz, 2H), 8.03 (d, *J* = 8.0 Hz, 1H), 7.92 (t, *J* = 8.0 Hz, 1H), 7.71 (t, *J* = 8.0 Hz, 1H), 7.48 – 7.43 (m, 1H), 7.43 – 7.38 (m, 2H), 7.30 – 7.23 (m, 5H), 7.06 – 6.92 (m, 5H), 6.69 (d, *J* = 8.5 Hz, 1H), 3.42 (s, 3H). **<sup>13</sup>C NMR (101 MHz, CDCl<sub>3</sub>)** δ 158.8, 156.5, 155.8, 154.4, 150.4, 144.8, 141.0, 140.1, 138.6, 138.5, 133.4, 131.1, 130.9, 130.5, 130.1, 129.5, 129.1, 128.9, 128.1, 127.5, 127.4, 126.8, 126.4, 122.6, 119.8, 115.7, 110.3, 54.9. **<sup>19</sup>F (376.5 MHz, CDCl<sub>3</sub>)** δ -151.5 (d, *J* = 102.0 Hz), -158.0 (d, *J* = 102.0 Hz). **<sup>11</sup>B NMR (128 MHz, CDCl<sub>3</sub>)**: δ 9.2. **HRMS (ESI-TOF) *m/z* [MH<sup>+</sup>]** calcd for C<sub>33</sub>H<sub>24</sub><sup>11</sup>B<sub>2</sub>N<sub>2</sub>O 513.1950, found 513.1959. **FTIR (neat)**  $\nu_{\text{max}}$  / cm<sup>-1</sup> 2925, 1597, 1240, 1103, 1006, 914, 825, 731, 699.

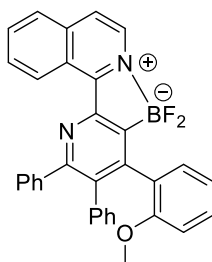
## Compound 10ea



Chemical Formula: C<sub>19</sub>H<sub>17</sub>BF<sub>2</sub>N<sub>2</sub>O

Following the representative procedure, 5,6-dimethyl-3-(2-pyridyl)-1,2,4-triazine **4ca** (100 mg, 0.424 mmol, 1 equiv.), potassium ((2-methoxyphenyl)ethynyl)trifluoroborate (197 mg, 1.06 mmol, 2.5 equiv.) and boron trifluoride diethyl etherate (0.13 mL, 1.06 mmol, 2.5 equiv.) were combined to give the crude **10ea**. The residue was purified chromatographically over silica gel with ethyl acetate to afford 2-(3-(difluoroboranyl)-5,6-dimethyl-4-(2-methoxyphenyl)pyridin-2-yl)pyridine as a pale yellow amorphous solid (60 mg, 30%). **<sup>1</sup>H NMR (400 MHz, CDCl<sub>3</sub>)** δ 8.45 (d, *J* = 5.5 Hz, 1H), 8.30 (t, *J* = 8.0 Hz, 1H), 8.15 (t, *J* = 8.0 Hz, 1H), 7.56 – 7.47 (m, 1H), 7.42 – 7.36 (m, 1H), 7.32 (d, *J* = 7.5 Hz, 1H), 7.09 (t, *J* = 7.5 Hz, 1H), 7.00 (d, *J* = 8.5 Hz, 1H), 3.76 (s, 3H), 2.63 (s, 3H), 2.10 (s, 3H). **<sup>13</sup>C NMR (101 MHz, CDCl<sub>3</sub>)** δ 158.3, 156.4, 156.0, 151.9, 149.9, 143.8, 141.3, 133.9, 130.6, 129.4, 128.4, 124.3, 120.8, 118.6, 111.0, 55.8, 23.7, 16.5. **<sup>19</sup>F (376.5 MHz, CDCl<sub>3</sub>)** δ -156.2 (d, *J* = 90.0 Hz), -163.2 (d, *J* = 90.0 Hz). **<sup>11</sup>B NMR (128 MHz, CDCl<sub>3</sub>)** δ 7.6. **HRMS (ESI-TOF) *m/z* [MH<sup>+</sup>]** calcd for C<sub>19</sub>H<sub>18</sub><sup>11</sup>BF<sub>2</sub>N<sub>2</sub>O 339.1480, found 339.1486. **FTIR (neat)**  $\nu_{\text{max}}$  / cm<sup>-1</sup> 2923, 1626, 1560, 1486, 1244, 1077, 946, 818, 756.

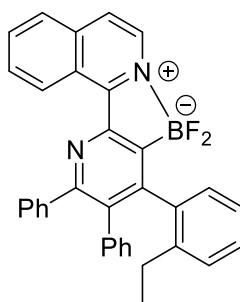
## Compound 10da



Chemical Formula: C<sub>33</sub>H<sub>23</sub>BF<sub>2</sub>N<sub>2</sub>O

Following the representative procedure, 5,6-diphenyl-3-(2-isoquinolyl)-1,2,4-triazine (121 mg, 0.336 mmol, 1 equiv.), potassium ((2-methoxyphenyl)ethynyl)trifluoroborate (240 mg, 1.0 mmol, 3 equiv.) and trifluoride diethyl etherate (0.13 mL, 1.0 mmol, 3 equiv.) were combined to give the crude **10da**. The residue was purified chromatographically over silica gel with dichloromethane to afford 2-(3-(difluoroboranyl)-5,6-diphenyl-4-(2-methoxyphenyl)pyridin-2-yl)isoquinoline as a light yellow amorphous solid (104 mg, 60%). <sup>1</sup>H NMR (400 MHz, CDCl<sub>3</sub>) δ 10.57 (d, *J* = 8.5 Hz, 1H), 8.40 (d, *J* = 6.0 Hz, 1H), 8.04 – 7.85 (m, 4H), 7.51 – 7.42 (m, 3H), 7.32 – 7.21 (m, 4H), 7.09 – 6.93 (m, 6H), 6.67 (d, *J* = 8.0 Hz, 1H), 3.41 (s, 3H). <sup>13</sup>C NMR (101 MHz, CDCl<sub>3</sub>) δ 158.0, 157.3, 155.7, 153.9, 150.5, 141.2, 139.6, 138.5, 137.8, 134.2, 132.1, 131.2, 130.9, 130.24, 130.20, 129.1, 128.0, 127.6, 127.4, 127.0, 126.9, 126.4, 125.3, 123.6, 120.1, 116.9, 110.3, 55.0. <sup>19</sup>F (376.5 MHz, CDCl<sub>3</sub>) δ -158.8 (d, *J* = 114.0 Hz), -165.9 (d, *J* = 114.0 Hz). <sup>11</sup>B NMR (128 MHz, CDCl<sub>3</sub>) δ 7.8. HRMS (ESI-TOF) *m/z* [MH<sup>+</sup>] calcd for C<sub>33</sub>H<sub>24</sub><sup>11</sup>BF<sub>2</sub>N<sub>2</sub>O 513.1950, found 513.1961. FTIR (neat) ν<sub>max</sub> / cm<sup>-1</sup> 3057, 2838, 1547, 1243, 1109, 1009, 914, 822, 753, 700.

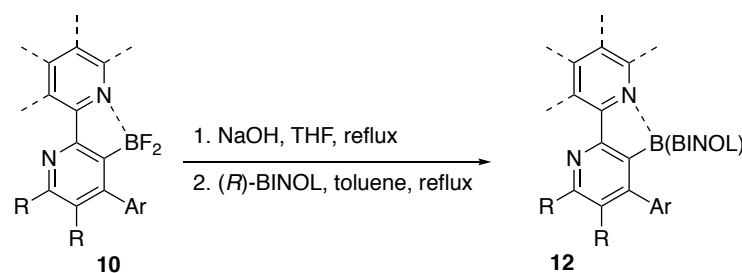
## Compound 10db



Chemical Formula:  $C_{34}H_{25}BF_2N_2$

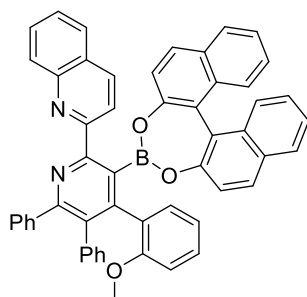
Following the representative procedure, 5,6-diphenyl-3-(2-isoquinolyl)-1,2,4-triazine (85 mg, 0.236 mmol, 1 equiv.), potassium ((2-ethylphenyl)ethynyl)trifluoroborate (139 mg, 0.590 mmol, 2.5 equiv.) and boron trifluoride diethyl etherate (0.15 mL, 1.18 mmol, 5 equiv.) were combined to give the crude **10db**. The residue was slowly precipitated from dichloromethane to afford 2-(3-(difluoroboranyl)-5,6-diphenyl-4-(2-ethylphenyl)pyridin-2-yl)isoquinoline as a light yellow amorphous solid (55 mg, 46%).  $^1H$  NMR (400 MHz)  $\delta$  10.60 (d,  $J$  = 8.5 Hz, 1H), 8.40 (d,  $J$  = 6.5 Hz, 1H), 8.07 – 7.88 (m, 4H), 7.51 – 7.45 (m, 2H), 7.34 – 7.18 (m, 6H), 7.15 – 7.08 (m, 1H), 7.06 – 6.89 (m, 5H), 2.46 – 2.34 (m, 1H), 2.19 – 2.07 (m, 1H), 0.99 (t,  $J$  = 7.6 Hz, 3H).  $^{13}C$  NMR (101 MHz,  $CDCl_3$ )  $\delta$  158.4, 157.0, 153.7, 153.2, 141.1, 140.7, 139.7, 137.8, 137.5, 137.1, 134.2, 132.2, 130.2 (x2 C), 130.2, 130.1, 129.8, 127.7 (x2 C), 127.5, 127.2 (x2 C), 127.1, 126.6, 125.4, 124.7, 123.7, 25.8, 14.1.  $^{19}F$  NMR (377 MHz,  $CDCl_3$ )  $\delta$  -161.05 (d,  $J$  = 111.5 Hz), -163.89 (d,  $J$  = 110.5 Hz).  $^{11}B$  NMR (128 MHz,  $CDCl_3$ ):  $\delta$  7.30. HRMS (ESI-TOF)  $m/z$  [ $MH^+$ ] calcd for  $C_{34}H_{26}^{11}BF_2N_2$  511.2152, found 511.2167. FTIR (neat)  $\nu_{max}$  /  $cm^{-1}$  3272, 2925, 1628, 1552, 1493, 1243, 1089, 952, 832.

## Preparation of BINOL esters: Representative procedure



To a solution of 2-(3-(difluoroboranyl)-5,6-diphenyl-4-(2-methoxyphenyl)pyridin-2-yl)quinoline **10ba** (0.14 g, 0.273 mmol, 1 equiv.) in THF (8 mL) was added NaOH (1.4 mL of a 1.0 M aqueous solution, 1.4 mmol, 5 equiv.). The reaction was stirred for 16 hours at reflux and the solvent was evaporated under reduced pressure. Brine solution (20 mL) was added and the organic phase was extracted with dichloromethane (4x 20 mL), dried over MgSO<sub>4</sub>, filtered and the solvent evaporated. The crude material was dissolved in toluene (8.0 mL) and (*R*)-BINOL (0.084 g, 0.295 mmol, 1 equiv.) was added. The reaction was stirred for 1 h at reflux and the solvent was evaporated under reduced pressure. The residue was purified chromatographically over silica gel using dichloromethane to afford the compound **12ba** as 4:1 mixture of diastereomers (111 mg, 50%).

### Compound 12ba

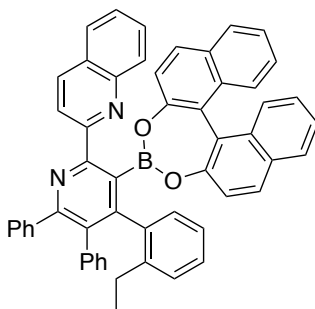


Chemical Formula: C<sub>53</sub>H<sub>35</sub>BN<sub>2</sub>O<sub>3</sub>

<sup>1</sup>H NMR (400 MHz, CDCl<sub>3</sub>): δ 8.76 – 8.71 (m, 1H), 8.63 – 8.57 (m, 1H), 8.01 (d, *J* = 9.0 Hz, 0.4H), 7.93 (d, *J* = 8.5 Hz, 0.4H), 7.89 – 7.82 (m, 1.6H), 7.81 – 7.71 (m, 2H), 7.65 (d, *J* = 8.0 Hz, 0.8H), 7.58 – 7.53 (m, 1.4H), 7.46 (d, *J* = 9.0 Hz, 0.2H), 7.43 – 7.39 (m, 1H), 7.39 – 7.31 (m, 4.6H), 7.29 – 7.15 (m, 6.6H), 6.95 – 6.85 (m, 4.6H), 6.84 – 6.72 (m, 1.4H), 6.70 – 6.65 (m, 0.8H), 6.62 – 6.53 (m, 1H), 6.43 (d, *J* = 9.0 Hz, 0.2H), 6.39 – 6.33 (m, 0.2H), 6.18 – 6.10 (m, 1H), 5.90 (d, *J* = 8.0 Hz, 0.8H), 5.75 (t, *J* = 7.5 Hz, 0.8H), 5.67 (d, *J* = 8.5 Hz, 0.2H), 3.30 (s, 0.6H), 3.24 (s, 2.4H). <sup>13</sup>C NMR (101 MHz, CDCl<sub>3</sub>) Major diastereomer only: δ 158.3, 157.5, 154.9, 154.8, 154.6, 150.5, 143.7, 141.3, 141.1, 139.2, 138.8, 133.7, 133.3, 131.9, 131.5, 130.3, 130.2, 130.1 (x2 C),

129.4, 129.2, 129.0, 128.4, 128.1, 127.8, 127.7, 127.5 (x2 C), 127.2 (x2 C), 127.1, 126.3, 126.2, 125.9, 125.2, 124.5, 124.3, 123.8, 123.5, 123.3, 122.8, 122.7, 122.3, 120.9, 118.3, 116.1, 109.2, 54.1. **<sup>11</sup>B NMR (128 MHz, CDCl<sub>3</sub>)** δ 13.5. **HRMS (ESI-TOF)** *m/z* [MH<sup>+</sup>] calcd for C<sub>53</sub>H<sub>36</sub><sup>11</sup>BN<sub>2</sub>O<sub>3</sub> 759.2819, found 759.2781. **FTIR (neat)**  $\nu_{\max}$  / cm<sup>-1</sup> 3056, 3002, 2956, 2924, 1594, 1546, 1335, 1251, 1097, 1005.

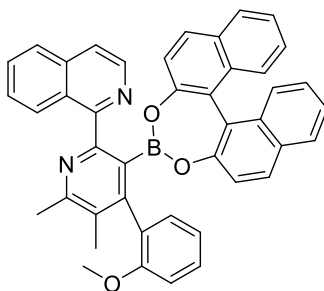
### Compound 12bb



Chemical Formula: C<sub>54</sub>H<sub>37</sub>BN<sub>2</sub>O<sub>2</sub>

Following the representative procedure, difluoroborane **10bb** (50 mg, 0.1 mmol, 1 equiv.), and (*R*)-BINOL (28 mg, 0.1 mmol, 1 equiv.) were combined to give crude product **12bb**. The residue was purified chromatographically over silica gel using petrol/AcOEt (7/3) to afford **12bb** as a 1:1 mixture of diastereomers (34 mg, 45%). **<sup>1</sup>H NMR (400 MHz, CDCl<sub>3</sub>)**: δ 8.73 (t, *J* = 9.0 Hz, 1H), 8.57 (t, *J* = 9.0 Hz, 1H), 7.98 (d, *J* = 9.0 Hz, 2H), 7.90 (d, *J* = 8.0 Hz, 2H), 7.87 – 7.69 (m, 4H), 7.51 (d, *J* = 8.5 Hz, 1H), 7.46 – 6.97 (m, 10H), 6.97 – 6.80 (m, 5H), 6.79 – 6.64 (m, 3H), 6.56 (d, *J* = 8.0 Hz, 0.5H), 6.52 – 6.44 (m, 1H), 6.23 – 6.15 (m, 0.5H), 6.09 (d, *J* = 8.0 Hz, 0.5H), 5.90 (t, *J* = 7.4 Hz, 0.5H), 2.65 – 2.54 (m, 0.5H), 2.38 – 2.27 (m, 0.5H), 2.17 – 2.10 (m, 0.5H), 2.03 – 1.94 (m, 0.5H), 0.92 (t, *J* = 7.5 Hz, 1.5H), 0.80 (t, *J* = 7.5 Hz, 1.5H). **<sup>13</sup>C NMR (101 MHz, CDCl<sub>3</sub>)** δ 158.8, 157.4, 155.00, 154.5, 154.4, 152.8, 152.6, 150.3, 143.7, 143.7, 141.4, 141.3, 140.2, 139.1, 139.0, 138.5, 138.2, 138.0, 134.7, 133.6, 133.4, 133.3, 132.4, 131.8, 131.5, 131.4, 131.1, 131.0, 130.2, 130.1(x2 C), 129.4, 129.3, 129.2 8x2 C), 129.0, 128.9, 128.4, 129.0, 127.8, 127.6 (x2 C), 127.5 8 (x2 C), 127.4, 127.3, 127.2, 127.1, 127.0, 126.9, 126.8, 126.2, 126.0, 125.2, 125.1, 124.9 (x 2C), 124.7, 124.5, 124.2, 124.0, 123.4, 123.3, 123.2, 123.1, 123.0, 123.0, 122.9, 122.2, 120.1, 117.8, 116.2, 116.1, 25.4, 13.3, 13.1. **<sup>11</sup>B NMR (128 MHz, CDCl<sub>3</sub>)**: δ 13.4. **HRMS (ESI-TOF)** *m/z* [MH<sup>+</sup>] calcd for C<sub>54</sub>H<sub>38</sub><sup>11</sup>BN<sub>2</sub>O<sub>2</sub> 759.2813, found 759.2781. **FTIR (neat)**  $\nu_{\max}$  / cm<sup>-1</sup> 3057, 2971, 2929, 2924, 1619, 1596, 1544, 1339, 1252, 1098, 995.

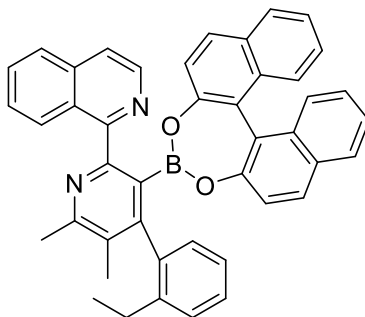
## Compound 12ca



Chemical Formula: C<sub>43</sub>H<sub>31</sub>BN<sub>2</sub>O<sub>3</sub>

Following the representative procedure, difluoroborane **10ca** (70 mg, 0.18 mmol, 1 equiv.), and (*R*)-BINOL (52 mg, 0.18 mmol, 1 equiv.) were combined to give crude product **12ca**. The residue was purified chromatographically over silica gel using petrol/AcOEt (7.5/2.5) to afford the compound **12ca** as a 4:1 mixture of diastereomers (89 mg, 79%). <sup>1</sup>H NMR (400 MHz, CDCl<sub>3</sub>) δ 10.74 (d, *J* = 8.5 Hz, 1H), 8.01 (d, *J* = 9.0 Hz, 0.4H), 7.96 – 7.85 (m, 4H), 7.82 – 7.77 (m, 1H), 7.75 – 7.72 (m, 1H), 7.54 – 7.13 (m, 9.4H), 7.02 – 6.97 (m, 1H), 6.85 (d, *J* = 7.5 Hz, 0.2H), 6.80 – 6.74 (m, 1H), 6.65 – 6.59 (m, 0.2H), 6.58 – 6.52 (m, 1H), 6.44 (t, *J* = 8.0 Hz, 0.8H), 5.95 (d, *J* = 8.0 Hz, 0.2H), 5.80 (t, *J* = 7.0 Hz, 0.8H), 3.88 (s, 2.4H), 3.29 (s, 0.6H), 2.77 – 2.73 (m, 3H), 2.06 – 2.01 (m, 3H). <sup>13</sup>C NMR (101 MHz, CDCl<sub>3</sub>) major diastereomer only: δ 159.6, 156.8, 155.6, 154.7, 154.5, 149.3, 146.1, 139.3, 133.8, 133.6, 133.1, 132.3, 131.9, 131.6, 130.5, 130.3, 130.1, 129.9, 129.2, 129.1, 128.6, 128.2, 128.1, 128.0, 127.6, 127.3, 126.9, 126.8, 125.1, 124.5, 124.2, 123.5, 123.3, 122.9, 122.6, 122.2, 121.5, 119.1, 109.7, 55.0, 23.8, 16.3. <sup>11</sup>B NMR (128 MHz, CDCl<sub>3</sub>): δ 10.6. HRMS (ESI-TOF) *m/z* [MH<sup>+</sup>] calcd for C<sub>43</sub>H<sub>31</sub><sup>11</sup>BN<sub>2</sub>O<sub>3</sub> 635.2506, found 635.2496. FTIR (neat) ν<sub>max</sub> / cm<sup>-1</sup> 3054, 3002, 2953, 2925, 1593, 1551, 1339, 1253, 1078, 1024, 960, 819.

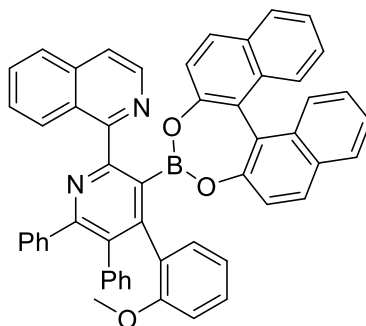
## Compound 12cb



Chemical Formula:  $C_{44}H_{33}BN_2O_2$

Following the representative procedure, difluoroborane **10cb** (80 mg, 0.21 mmol, 1 equiv.), and (*R*)-BINOL (60 mg, 0.21 mmol, 1 equiv.) were combined to give crude product **12cb**. The residue was purified chromatographically over silica gel using petrol/AcOEt (7.5/2.5) to afford the compound **12cb** as a 1:1 mixture of diastereomers (120 mg, 88%).  **$^1H$  NMR (400 MHz,  $CDCl_3$ ):**  $\delta$  10.74 (d,  $J = 8.0$  Hz, 1H), 7.97 – 7.84 (m, 4H), 7.82 – 7.71 (m, 2H), 7.58 – 7.55 (m, 0.5H), 7.54 – 7.48 (m, 1H), 7.48 – 7.02 (m, 8.5 H), 6.95 (d,  $J = 8.5$  Hz, 0.5H), 6.86 (d,  $J = 8.5$  Hz, 1H), 6.75 (d,  $J = 7.5$  Hz, 0.5H), 6.68 (d,  $J = 8.5$  Hz, 0.5H), 6.62 – 6.43 (m, 2H), 6.00 (t,  $J = 7.5$  Hz, 0.5H), 2.79 – 2.74 (m, 3H), 2.56 – 2.45 (m, 1H), 2.34 – 2.27 (m, 1H), 2.03 (s, 1.5H), 1.97 (s, 1.5H), 1.32 (t,  $J = 7.5$  Hz, 1.5H), 0.76 (t,  $J = 7.5$  Hz, 1.5H).  **$^{13}C$  NMR (101 MHz,  $CDCl_3$ ):**  $\delta$  157.4, 155.7, 154.4, 154.0, 152.6, 141.0, 139.7, 139.4, 138.2, 133.6, 133.4, 133.2, 133.1, 132.8, 130.3, 130.1, 129.7, 129.5, 129.3, 128.6, 128.0, 127.7, 127.2, 127.1, 126.9, 126.8, 126.5, 125.5, 125.1, 124.9, 124.6, 124.3, 123.4, 123.3, 123.1, 122.6, 122.1, 121.5, 120.4, 25.6, 24.0, 16.7, 14.1.  **$^{11}B$  NMR (128 MHz,  $CDCl_3$ ):**  $\delta$  12.2. **HRMS (ESI-TOF)  $m/z$  [ $MH^+$ ]** calcd for  $C_{44}H_{34}^{11}BN_2O_2$  633.2708, found 633.2710. **FTIR (neat)  $\nu_{max}$  /  $cm^{-1}$**  3055, 2963, 2934, 1593, 1505, 1466, 1339, 1254, 1098, 1023, 961, 819.

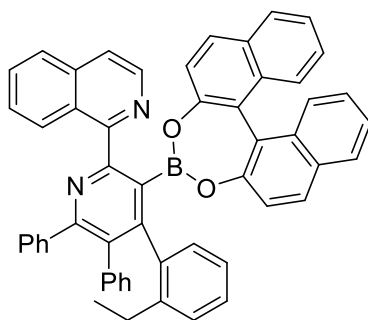
## Compounds 12da



Chemical Formula:  $C_{53}H_{35}BN_2O_3$

Following the representative procedure, difluoroborane **10da** (100 mg, 0.2 mmol, 1 equiv.), and (*R*)-BINOL (56 mg, 0.2 mmol, 1 equiv.) were combined to give crude product **12da**. The residue was purified chromatographically over silica gel using petrol/AcOEt (7.5/2.5) to afford the compound **12da** as a 4:1 mixture of diastereomers (124 mg, 83%). **<sup>1</sup>H NMR (400 MHz, CDCl<sub>3</sub>):** δ 10.78 – 10.65 (m, 1H), 7.98 – 7.85 (m, 4H), 7.82 (d, *J* = 8.5 Hz, 0.75H), 7.79 – 7.72 (m, 0.75H), 7.68 (d, *J* = 8.0 Hz, 0.75H), 7.58 – 7.50 (m, 2.25H), 7.46 – 7.12 (m, 12.5H), 7.07 – 7.03 (m, 1H), 7.02 – 6.81 (m, 4H), 6.79 – 6.69 (m, 1.5H), 6.66 (d, *J* = 8.5 Hz, 0.25H), 6.57 (d, *J* = 7.5 Hz, 0.25H), 6.53 – 6.48 (m, 0.25H), 6.39 – 6.33 (m, 0.75H), 6.30 (t, *J* = 7.5 Hz, 0.25H), 6.14 (d, *J* = 8.0 Hz, 0.75H), 5.72 (t, *J* = 7.0 Hz, 1H), 3.29 (s, 2.25H), 3.26 (s, 0.75H). **<sup>13</sup>C NMR (101 MHz, CDCl<sub>3</sub>)** major diastereomer only: δ 158.2, 157.9, 157.6, 154.9, 154.6, 154.3, 153.9, 150.3, 141.6, 139.4, 138.8, 138.2, 133.8, 133.6, 133.2, 133.0, 132.2, 130.4, 130.2 (x2 C), 129.9, 129.4, 128.7, 128.3, 128.0, 127.6 (x2 C), 127.5 (x2 C), 127.3, 127.2, 127.0, 126.8, 126.4, 126.0, 125.4, 125.2, 124.5, 123.4 (x2 C), 123.1, 122.6, 122.3, 122.0, 120.6, 118.6, 109.4, 54.3. **<sup>11</sup>B NMR (128 MHz, CDCl<sub>3</sub>):** δ 13.2. **HRMS (ESI-TOF) *m/z* [MH<sup>+</sup>]** calcd for  $C_{53}H_{36}^{11}BN_2O_3$  759.2819, found 759.2844. **FTIR (neat)  $\nu_{max}$  / cm<sup>-1</sup>** 3056, 2966, 2932, 1593, 1540, 1505, 1339, 1253, 1099, 995.

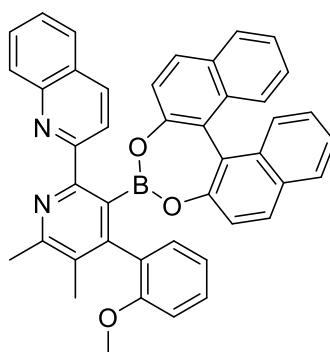
## Compound 12db



Chemical Formula:  $C_{54}H_{37}BN_2O_2$

Following the representative procedure, difluoroborane **10db** (70 mg, 0.14 mmol, 1 equiv.), and (*R*)-BINOL (40 mg, 0.14 mmol, 1 equiv.) were combined to give crude product **12db**. The residue was purified chromatographically over silica gel using petrol/AcOEt (7.5/2.5) to afford the compound **12db** as a 1:1 mixture of diastereomers (59 mg, 56%).  **$^1H$  NMR (400 MHz,  $CDCl_3$ ):**  $\delta$  10.76 – 10.69 (m, 1H), 8.03 – 7.83 (m, 4H), 7.80 – 7.70 (m, 2H), 7.61 – 7.56 (m, 1H), 7.55 – 7.46 (m, 2.5H), 7.43 – 7.37 (m, 1.5H), 7.35 – 7.07 (m, 10H), 7.00 – 6.73 (m, 6H), 6.70 (d,  $J = 8.0$  Hz, 0.5H), 6.68 – 6.64 (m, 0.5H), 6.62 (d,  $J = 8.5$  Hz, 0.5H), 6.43 (t,  $J = 7.5$  Hz, 0.5H), 6.37 – 6.32 (m, 1H), 6.29 – 6.25 (m, 0.5H), 5.94 (t,  $J = 7.0$  Hz, 0.5H), 2.66 – 2.57 (m, 0.5H), 2.40 – 2.31 (m, 0.5H), 2.23 – 2.14 (m, 0.5H), 2.07 – 1.99 (m, 0.5H), 0.95 (t,  $J = 7.5$  Hz, 1.5H), 0.78 (t,  $J = 7.5$  Hz, 1.5H).  **$^{13}C$  NMR (101 MHz,  $CDCl_3$ )**  $\delta$  158.1, 158.0, 157.6, 157.1, 154.4 (x2 C), 154.3, 153.9, 153.7, 153.6, 153.5, 152.5, 151.0, 142.7, 142.6, 141.6, 141.4, 140.6, 139.5, 139.4, 139.2, 138.5, 137.9, 137.7, 137.0, 133.8 (x2 C), 133.5, 133.2, 133.1 (x2 C), 132.3, 131.9, 131.2, 130.3, 130.2, 129.9, 129.6, 129.3, 129.1, 128.7 (x2 C), 128.0, 127.9, 127.6, 127.5, 127.4, 127.3, 127.2, 127.0, 126.9, 126.8, 126.7, 126.4 (x2 C), 126.3, 125.6, 125.5, 125.3, 125.2, 125.1, 124.6, 124.5, 124.0, 123.6, 123.4 (x2 C), 123.3, 123.2, 123.1, 122.7, 122.4, 122.2, 122.0, 25.4 (x2 C), 13.5, 13.0.  **$^{11}B$  NMR (128 MHz,  $CDCl_3$ ):**  $\delta$  11.2. **HRMS (ESI-TOF)  $m/z$  [ $MH^+$ ]** calcd for  $C_{54}H_{38}^{11}BN_2O_2Na$  779.2846, found 779.2846. **FTIR (neat)**  $\nu_{max}$  /  $cm^{-1}$  3055, 2963, 2934, 1593, 1505, 1466, 1339, 1254, 1098, 1023, 961, 819.

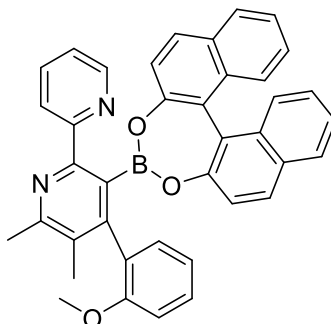
## Compound 12aa



Chemical Formula:  $C_{43}H_{31}BN_2O_3$

Following the representative procedure, difluoroborane **10aa** (53 mg, 0.13 mmol, 1 equiv.), and (*R*)-BINOL (39 mg, 0.13 mmol, 1 equiv.) were combined to give crude product **12aa**. The residue was purified chromatographically over silica gel using petrol/AcOEt (7/3) to afford the compound **12aa** as a 4:1 mixture of diastereomers (49 mg, 57%).  $^1H$  NMR (400 MHz,  $CDCl_3$ ) major diastereomer only:  $\delta$  8.61 (d,  $J = 8.5$  Hz, 1H), 8.55 (d,  $J = 8.5$  Hz, 1H), 7.85 – 7.79 (m, 2H), 7.76 – 7.66 (m, 2H), 7.55 (d,  $J = 8.5$  Hz, 1H), 7.39 (d,  $J = 8.5$  Hz, 1H), 7.37 – 7.14 (m, 7H), 7.12 (d,  $J = 7.5$  Hz, 1H), 6.90 (d,  $J = 8.5$  Hz, 1H), 6.84 (d,  $J = 8.5$  Hz, 1H), 6.72 – 6.66 (m, 1H), 6.32 (d,  $J = 8.0$  Hz, 1H), 6.29 – 6.23 (m, 1H), 5.88 (t,  $J = 7.5$  Hz, 1H), 3.83 (s, 3H), 2.38 (s, 3H), 1.96 (s, 3H).  $^{13}C$  NMR (101 MHz,  $CDCl_3$ ) major diastereomer only:  $\delta$  158.1, 157.7, 155.4, 155.1, 154.9, 141.0, 135.0, 133.7, 133.6, 133.5, 131.6, 131.5, 130.4, 130.1, 129.5, 123.0, 129.2, 128.5, 128.4, 127.8, 127.7, 127.6, 127.4, 127.3, 126.9, 125.2, 124.6, 124.4, 124.0, 123.8, 123.7, 123.2, 123.0, 122.6, 122.4, 121.3, 119.0, 118.0, 109.6, 54.9, 23.8, 16.5.  $^{11}B$  NMR (128 MHz,  $CDCl_3$ ):  $\delta$  12.9. FTIR (neat)  $\nu_{max} / cm^{-1}$  3059, 2952, 2922, 2849, 1594, 1523, 1467, 1337, 1253, 1083, 956, 746. HRMS (ESI-TOF)  $m/z$   $[MH^+]$  calcd for  $C_{43}H_{32}^{11}BN_2O_3$  635.2508, found 635.2511.

## Compound 12ea



Chemical Formula:  $C_{39}H_{29}BN_2O_3$

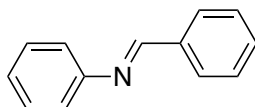
Following the representative procedure, difluoroborane **10ea** (60 mg, 0.18 mmol, 1 equiv.), and (*R*)-BINOL (51 mg, 0.18 mmol, 1 equiv.) were combined to give crude product **12ea**. The residue was purified chromatographically over silica gel using petrol/AcOEt (6/4) to afford the compound **12ea** as a 4:1 mixture of diastereoisomer (60 mg, 58%).  $^1\text{H NMR}$  (400 MHz,  $\text{CDCl}_3$ )  $\delta$  8.43 – 8.36 (m, 1H), 8.15 – 8.06 (m, 1H), 7.92 – 7.84 (m, 1H), 7.83 – 7.71 (m, 2H), 7.58 (d,  $J = 5.5$  Hz, 0.8H), 7.55 – 7.42 (m, 0.6H), 7.40 – 7.07 (m, 8.4H), 6.99 (d,  $J = 8.5$  Hz, 1H), 6.86 (d,  $J = 7.5$  Hz, 0.2H), 6.75 – 6.57 (m, 2.2H), 6.49 (t,  $J = 7.5$  Hz, 0.8H), 5.93 (d,  $J = 8.0$  Hz, 0.2H), 5.77 (t,  $J = 7.5$  Hz, 0.8H), 3.88 (s, 2.4H), 3.24 (s, 0.6H), 2.67 – 2.63 (m, 3H), 2.04 – 2.00 (m, 3H).  $^{13}\text{C NMR}$  (101 MHz,  $\text{CDCl}_3$ ) Major diastereomer only:  $\delta$  157.6, 156.1, 155.7, 154.5, 154.4, 154.1, 152.5, 149.7, 143.1, 141.7, 134.3, 133.5, 133.0, 131.9, 130.1, 129.9, 129.4, 129.1, 128.7, 128.3, 128.0, 127.8, 127.7, 127.3, 126.8, 125.3, 124.7, 123.5, 123.2, 122.8, 122.0, 120.9, 119.2, 118.4, 109.7, 55.1, 23.7, 16.5.  $^{11}\text{B NMR}$  (128 MHz,  $\text{CDCl}_3$ ):  $\delta$  11.4 HRMS (ESI-TOF)  $m/z$  [ $\text{MH}^+$ ] calcd for  $C_{39}H_{30}^{11}\text{BN}_2\text{O}_3$  585.2344, found 585.2358. FTIR (neat)  $\nu_{\text{max}}$  /  $\text{cm}^{-1}$  3056, 2995, 2924, 2832, 1624, 1492, 1466, 1339, 1252, 1076, 966, 751.

## 5.3. Chapter II

### Preparation of imines: Representative procedure

In a tube rack was added the aniline **14a** (0.137 mL, 5 equiv., 1.5 mmol) and the PCN-222(Pd) (0.012 g, 0.02 equiv.) in 1 mL of acetonitrile. The benzylamine **13a** (0.034 mL, 1 equiv., 0.3 mmol) was diluted in 2.4 mL of acetonitrile and added via a push syringe to the solution (0.4 mL/h, 6h). The mixture was left stirred inside a light box under visible light (LED lamp 13.5 W, 15 kW, 155 mA) for three days and then transferred in a falcon with 20 mL of acetonitrile. The solution was centrifuged (20 min, 10 °C, 10.000 RPM), decanted, and evaporated. The crude was finally purified chromatographically over silica gel column using AcOEt/NEt<sub>3</sub>/Pentane (0.5:1.5:8) to afford the imine **15aa** as a pale-yellow solid (27 mg, 50%).

### Compound 15aa

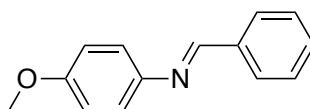


Chemical Formula: C<sub>13</sub>H<sub>11</sub>N

<sup>1</sup>H NMR (400 MHz, Chloroform-*d*) δ 8.50 (s, 1H), 7.97 – 7.92 (m, 2H), 7.53 – 7.48 (m, 3H), 7.46 – 7.40 (m, 2H), 7.31 – 7.23 (m, 3H). <sup>13</sup>C NMR (101 MHz, CDCl<sub>3</sub>) δ 160.45, 152.08, 136.22, 131.39, 129.15 (x2 C), 128.83 (x2 C), 128.78, 125.95, 120.88 (x2 C), 115.16.

These data are in agreement with the previously reported spectral data.<sup>108</sup>

### Compound 15ad



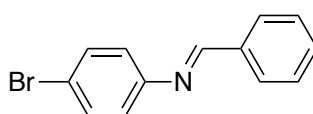
Chemical Formula: C<sub>14</sub>H<sub>13</sub>NO

Based on the representative procedure, aniline **14d** (184 mg, 1.5 mmol, 5 equiv.), and benzylamine **13a** (0.034 mL, 0.3 mmol, 1 equiv.) were combined to give the crude. The residue was finally

purified chromatographically over silica gel column using AcOEt/NEt<sub>3</sub>/Pentane (1.5:0.5:8.5) to afford the imine **15ad** as a pale-yellow solid (32 mg, 51%). <sup>1</sup>H NMR (400 MHz, Chloroform-*d*) δ 8.51 (s, 1H), 7.92 – 7.84 (m, 2H), 7.45 – 7.37 (m, 2H), 7.27 – 7.20 (m, 3H), 7.05 – 6.98 (m, 2H), 3.90 (s, 3H). <sup>13</sup>C NMR (101 MHz, CDCl<sub>3</sub>) δ 162.26, 159.67, 152.39, 130.50 (x2 C), 129.31, 129.09 (x2 C), 125.54, 120.86 (x2 C), 114.19 (x2 C), 55.43.

These data are in agreement with the previously reported spectral data.<sup>84</sup>

### Compound 15ae

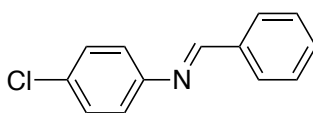


Chemical Formula: C<sub>13</sub>H<sub>10</sub>BrN

Based on the representative procedure, aniline **14e** (258 mg, 1.5 mmol, 5 equiv.), and benzylamine **13a** (0.034 mL, 0.3 mmol, 1 equiv.) were combined to give the crude. The residue was finally purified chromatographically over silica gel column using AcOEt/NEt<sub>3</sub>/Pentane (0.4:0.1:9.5) to afford the imine **15ae** as a brown solid (20 mg, 25%). <sup>1</sup>H NMR (400 MHz, Chloroform-*d*) δ 8.45 (s, 1H), 7.95 – 7.88 (m, 2H), 7.56 – 7.47 (m, 5H), 7.14 – 7.09 (m, 2H). <sup>13</sup>C NMR (101 MHz, CDCl<sub>3</sub>) δ 160.74, 151.03, 135.96, 132.19 (2x C), 131.64, 128.89 (x2 C), 122.59, 119.31 (2x C), 114.63.

<sup>109</sup> These data are in agreement with the previously reported spectral data.

### Compound 15af



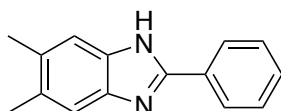
Chemical Formula: C<sub>13</sub>H<sub>10</sub>ClN

Based on the representative procedure, aniline **14f** (191 mg, 1.5 mmol, 5 equiv.), and benzylamine **13a** (0.034 mL, 0.3 mmol, 1 equiv.) were combined to give the crude. The residue was finally purified chromatographically over silica gel column using AcOEt/Pentane (4:6) to afford the imine **15af** as a pale-yellow solid (26 mg, 41%). <sup>1</sup>H NMR (400 MHz, Chloroform-*d*) δ 8.46 (s, 1H),

7.96 – 7.88 (m, 2H), 7.55 – 7.47 (m, 3H), 7.41 – 7.35 (m, 2H), 7.21 – 7.15 (m, 2H). <sup>13</sup>C NMR (101 MHz, CDCl<sub>3</sub>) δ 160.70, 150.53, 135.97, 131.62, 131.47, 129.24, 128.88 (x2 C), 128.82 (x2 C), 122.20 (x2 C).

These data are in agreement with the previously reported spectral data.<sup>85</sup>

### Compound 17aba

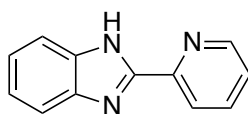


Chemical Formula: C<sub>15</sub>H<sub>14</sub>N<sub>2</sub>

Based on the representative procedure, aniline **14ba** (204 mg, 1.5 mmol, 5 equiv.), and benzylamine **13a** (0.034 mL, 0.3 mmol, 1 equiv.) were combined to give the crude. The residue crude was finally purified chromatographically over silica gel column using AcOEt/DCM (2:8) to afford the benzimidazole **17aba** as a pale-yellow solid (13 mg, 20%). <sup>1</sup>H NMR (400 MHz, Chloroform-*d*) δ 8.14 – 8.04 (m, 2H), 7.44 – 7.37 (m, 5H), 2.35 (s, 6H). <sup>13</sup>C NMR (101 MHz, CDCl<sub>3</sub>) δ 150.99, 137.54, 132.02, 129.93, 129.84 (2x C), 129.16 (2x C), 128.97, 126.57, 115.28, 29.71, 20.37 (2x C).

These data are in agreement with the previously reported spectral data.<sup>110</sup>

### Compound 17fb



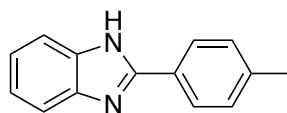
Chemical Formula: C<sub>12</sub>H<sub>9</sub>N<sub>3</sub>

Based on the representative procedure, aniline **14b** (162 mg, 1.5 mmol, 5 equiv.), and benzylamine **13f** (33 mg, 0.3 mmol, 1 equiv.) were combined to give the crude. The residue was finally purified chromatographically over silica gel column using AcOEt/DCM (1:1) to afford the benzimidazole **17fb** as a pale-yellow solid (26 mg, 46%). <sup>1</sup>H NMR (400 MHz, Chloroform-*d*) δ 8.66 (dd, *J* = 5.0, 1.0 Hz, 1H), 8.52 (dd, *J* = 8.0, 1.0 Hz, 1H), 7.89 (dd, *J* = 8.0, 2.0 Hz, 1H), 7.72 – 7.66 (m,

2H), 7.40 (dd,  $J = 7.5, 1.0$  Hz, 1H), 7.36 – 7.28 (m, 2H).  $^{13}\text{C}$  NMR (101 MHz,  $\text{CDCl}_3$ )  $\delta$  150.65, 149.12 (2x C), 148.10, 137.38 (2x C), 124.68 (2x C), 123.45 (2x C), 121.82 (2x C).

These data are in agreement with the previously reported spectral data.<sup>111</sup>

### Compound 17gb

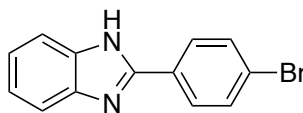


Chemical Formula:  $\text{C}_{14}\text{H}_{12}\text{N}_2$

Based on the representative procedure, aniline **14b** (162 mg, 1.5 mmol, 5 equiv.), and benzylamine **13g** (36 mg, 0.3 mmol, 1 equiv.) were combined to give the crude. The residue was finally purified chromatographically over silica gel column using AcOEt/Pentane (3:7) to afford the benzimidazole **17gb** as a pale-yellow solid (24 mg, 45%).  $^1\text{H}$  NMR (400 MHz, Chloroform-*d*)  $\delta$  8.02 – 7.94 (m, 2H), 7.68 (dd,  $J = 6.0, 3.0$  Hz, 2H), 7.33 – 7.25 (m, 4H), 2.42 (s, 3H).

These data are in agreement with the previously reported spectral data.<sup>87</sup>

### Compound 17bb

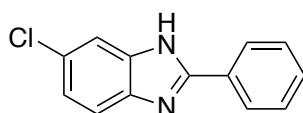


Chemical Formula:  $\text{C}_{13}\text{H}_9\text{BrN}_2$

Based on the representative procedure, aniline **14b** (162 mg, 1.5 mmol, 5 equiv.), and benzylamine **13b** (56 mg, 0.3 mmol, 1 equiv.) were combined to give the crude. The residue was finally purified chromatographically over silica gel column using AcOEt/Pentane (3:7) to afford the benzimidazole **17bb** as a pale-brown solid (32 mg, 38%).  $^1\text{H}$  NMR (400 MHz, MeOD)  $\delta$  7.99 (d,  $J = 8.6$  Hz, 2H), 7.70 (d,  $J = 8.5$  Hz, 2H), 7.64 – 7.57 (m, 2H), 7.31 – 7.28 (m, 2H).  $^{13}\text{C}$  NMR (101 MHz,  $\text{CDCl}_3$ )  $\delta$  154.78, 135.91 (x2 C), 132.64, 132.00 (x2 C), 128.08, 126.73 (x2 C), 118.55.

These data are in agreement with the previously reported spectral data.<sup>111</sup>

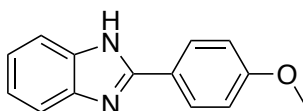
### Compound 17abb



Chemical Formula: C<sub>13</sub>H<sub>9</sub>ClN<sub>2</sub>

Based on the representative procedure, aniline **14bb** (214 mg, 1.5 mmol, 5 equiv.), and benzylamine **13a** (0.034 mL, 0.3 mmol, 1 equiv.) were combined to give the crude. The residue was finally purified chromatographically over silica gel column using AcOEt/Pentane (4:6) to afford the benzimidazole **17abb** as a pale-orange solid (26 mg, 39%). <sup>1</sup>H NMR (400 MHz, MeOD) δ 8.08 – 8.01 (m, 2H), 7.58 – 7.47 (m, 5H), 7.21 (dd, *J* = 8.5, 2.0 Hz, 1H). <sup>13</sup>C NMR (101 MHz, MeOD) δ 153.27, 130.25 (2x C), 129.18, 128.77, 128.00 (2x C), 126.46 (2x C), 122.89. These data are in agreement with the previously reported spectral data.<sup>112</sup>

### Compound 17eb

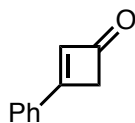


Chemical Formula: C<sub>14</sub>H<sub>12</sub>N<sub>2</sub>O

Based on the representative procedure, aniline **14b** (162 mg, 1.5 mmol, 5 equiv.), and benzylamine **13e** (41 mg, 0.3 mmol, 1 equiv.) were combined to give the crude. The residue was finally purified chromatographically over silica gel column using AcOEt/Pentane (3:7) to afford the benzimidazole **17eb** as a white solid (29 mg, 43%). <sup>1</sup>H NMR (400 MHz, DMSO-*d*) δ 8.15 – 8.06 (m, 2H), 7.54 (s, 2H), 7.16 (dd, *J* = 6.0, 3.0 Hz, 2H), 7.13 – 7.06 (m, 2H), 3.85 (s, 3H). <sup>13</sup>C NMR (101 MHz, DMSO) δ 161.11, 151.76, 128.50 (x2 C), 123.03, 122.28 (x2 C), 114.84 (x2 C), 55.81. These data are in agreement with the previously reported spectral data.<sup>113</sup>

## 5.4. Chapter III

### Synthesis of cyclobutanone **18**

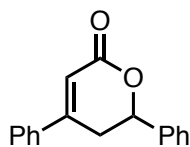


Chemical Formula: C<sub>10</sub>H<sub>8</sub>O

To a suspension of zinc-copper couple (9.60 g, 147 mmol) and phenylacetylene (5.00 g, 49 mmol) in diethyl ether (100 mL) was added a solution of trichloroacetyl chloride (10.9 mL, 98 mmol) in dimethoxyethane (50 mL) dropwise over 15 min. After 18 h, the resulting brown mixture was filtered and the black residue was washed with hexane (100 mL). The filtrate was washed with ice-cold hydrochloric acid (0.5 N, 100 mL), ice-cold sodium hydroxide solution (5%, 100 mL), saturated sodium chloride solution (100 mL), dried over anhydrous MgSO<sub>4</sub>, and then concentrated in vacuo to give the crude 3-substituted-4,4-dichlorocyclobutenone. The residue was directly used in the next step without any purification. To a suspension of zinc dust (25.60 g, 392 mmol) in absolute ethanol (100 mL) at 0 °C was added glacial acetic acid (11.2 mL, 196 mmol) dropwise over 5 min. Then a solution of 3-phenyl-4,4-dichlorocyclobutenone (8.35 g, 39 mmol) in absolute ethanol (10 mL) was added over 10 min. The reaction mixture was stirred for 2.5 h and then filtered and washed with a mixture of diethyl ether and pentane (1:1, 250 mL). The filtrate was washed with hydrochloric acid (1 N, 100 mL), water (100 mL) and saturated sodium chloride (100 mL). After extraction with a mixture of diethyl ether and pentane (1:1, 3x300 mL) the organic layers were washed with saturated sodium bicarbonate solution (500 mL), dried over MgSO<sub>4</sub> and concentrated in vacuo. The residue was finally purified chromatographically over silica gel column using AcOEt/Pentane affording the cyclobutenone **18** as a yellow solid (2.4 g, 40%). <sup>1</sup>H NMR (400 MHz, Chloroform-*d*) δ 3.52 (s, 2H), 6.37 (s, 1H), 7.48–7.52 (m, 3H), 7.60–7.63 (m, 2H).

These data are in agreement with the previously reported spectral data.<sup>114</sup>

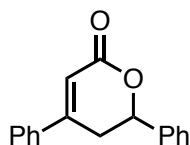
### Synthesis of lactone **20** with Ni(COD)<sub>2</sub> as catalyst



Chemical Formula: C<sub>17</sub>H<sub>14</sub>O<sub>2</sub>

A flame-dried Schlenk tube was charged with cyclobutenone **18** (28.9 mg, 0.20 mmol, 1 equiv.) and benzaldehyde **19** (23.3 mg, 0.22 mmol, 1.1 equiv.) in anhydrous and degassed toluene (1 mL) under a nitrogen atmosphere in a glove box. The mixture was cooled down to 0 °C before Ni(cod)<sub>2</sub> (8.3 mg, 0.06 mmol, 0.3 equiv.) was added. The solution was allowed to reach room temperature and stirred for 16 h. All volatiles were removed in vacuo. The residue was concentrated in vacuo and purified chromatographically over silica gel column using n-hexane/EtOAc (80:20) provided lactone **20** as a white solid (16 mg, 31%).

### Synthesis of lactone **20** with Ni(TMDA)(*o*-tolyl)Cl as catalyst

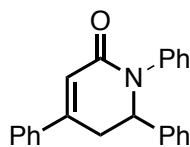


Chemical Formula: C<sub>17</sub>H<sub>14</sub>O<sub>2</sub>

Under a nitrogen atmosphere in a glove box, the cyclobutenone **18** (20 mg, 0.2 mmol, 1 equiv.), benzaldehyde **19** (44 mg, 0.6 mmol, 3 equiv.), Ni(TMDA)(*o*-tolyl)Cl (33 mg, 0.16 mmol, 0.8 equiv.) and dppBz (22 mg, 0.16 mmol, 0.8 equiv.) were added into a 8 mL microwave tube with 3 mL of toluene. The resultant mixture was stirred in a microwave reactor for 6 hours at 60 °C, concentrated in vacuo and the resulting residue was analysed by <sup>1</sup>H NMR (39%). <sup>1</sup>H NMR (400 MHz, Chloroform-*d*) δ 3.04–3.06 (m, 2H), 5.53–5.57 (m, 1H), 6.48–6.48 (m, 1H), 7.36–7.50 (m, 8H), 7.55–7.57 (m, 2H).

These data are in agreement with the previously reported spectral data.<sup>115</sup>

### Synthesis of lactam **22** with Yttrium(III) triflate as catalyst

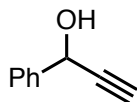


Chemical Formula: C<sub>23</sub>H<sub>19</sub>NO

In a 10 mL round bottom flask was added under nitrogen atmosphere, the cyclobutenone **18** (20 mg, 0.2 mmol, 1 equiv.), imine **21** (44 mg, 0.6 mmol, 3 equiv.), Yttrium(III) triflate (6.5 mg, 0.02 mmol, 0.1 equiv.) and IPr (4 mg, 0.02 mmol, 0.1 equiv.) in DCE (4 mL). The resultant mixture was stirred for 24 hours at 60 °C, concentrated in vacuo and finally purified chromatographically over silica gel column using AcOEt/heptane (3:7) to afford the compound **22** (6 mg, 15%). <sup>1</sup>H NMR (400 MHz, Chloroform-*d*) δ 3.12–3.09 (m, 1H), 3.62–3.59 (m, 1H), 5.26–5.23 (m, 2H), 6.56–6.57 (m, 1H), 7.20 (t, *J* = 7.5 Hz 1H), 7.44–7.46 (m, 1H), 7.26–7.51 (m, 12H).

## 5.5. Chapter IV

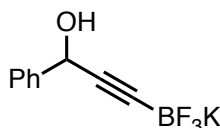
### Synthesis of 1-Phenylprop-2-yn-1-ol **31**



Chemical Formula: C<sub>9</sub>H<sub>8</sub>O

To a stirring solution of ethynylmagnesium bromide (0.5 M in THF, 90 mL, 1.1 equiv.) at -78 °C was added benzaldehyde (3 mL, 30 mmol, 1 equiv.). The reaction mixture was stirred for 10 minutes before warming to room temperature over 2 hours. NH<sub>4</sub>Cl (sat. aq., 50 mL) was added and the solvent phases separated. The aqueous phase was extracted with EtOAc (3x 100mL) and the combined organic phases dried over anhydrous MgSO<sub>4</sub> then concentrated *in vacuo*. The resulting dark mixture was purified by flash column chromatography on silica gel using n-hexane/EtOAc (80:20) to afford the title compound **31** as a gold coloured oil (3.5, 88%). <sup>1</sup>H NMR (400 MHz, Chloroform-*d*) δ<sub>H</sub> ppm 2.29 (d, 1H, J = 2.0 Hz), 2.70 (d, 1H, J = 6.0 Hz), 5.50 (dd, 1H, J = 2.0, 6.0 Hz), 7.46 – 7.43 (m, 3H), 7.62 – 7.55 (m, 2H).

### Synthesis of Potassium (3-hydroxy-3-phenylprop-1-yn-1-yl)trifluoroborate **32**

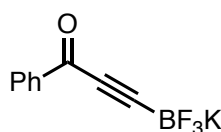


Chemical Formula: C<sub>9</sub>H<sub>7</sub>BF<sub>3</sub>KO

To a solution of 1-Phenylprop-2-yn-1-ol **31** (2.0 g, 19 mmol, 1 equiv.) in THF (190 mL) at -78 °C, *n*butyllithium ~2.5 M in hexanes, (16.7 mL, 42 mmol, 2.2 equiv.) was added dropwise. The mixture was stirred for 1 hour before adding 2-isopropoxy-4,4,5,5-tetramethyl-1,3,2-dioxaborolane (<sup>i</sup>PrOBPin) (6.33 mL, 57 mmol, 3 equiv.) dropwise and allowing it to warm to -20 °C over a period of 2 hours. Potassium hydrogen difluoride (17.7 g, 228 mmol, 12 equiv.) dissolved in H<sub>2</sub>O (60 mL) was added slowly and the flask was allowed to warm to room temperature. The resulting mixture was concentrated to dryness *in vacuo* and the product was separated from excess inorganic material by addition of acetone and vigorous stirring for 1 hour followed by filtration. The filtrate was concentrated *in vacuo* and redissolved in the minimum amount of acetone affording a saturated solution. The product was precipitated by adding diethyl

ether and isolated by filtration followed by washing with diethyl ether. The precipitate was dried *in vacuo* to give the ynol trifluoroborate **32** salt as a colourless solid (3.2 g, 71%). **M.p.** = 234 °C; **<sup>1</sup>H NMR (400 MHz, DMSO-*d*<sup>6</sup>)**  $\delta_{\text{H}}$  ppm 5.16 (d, *J* = 5.5 Hz, 1H), 5.59 (d, *J* = 5.5 Hz, 1H), 7.20 – 7.27 (m, 1H), 7.28 – 7.35 (m, 2H), 7.41 – 7.48 (m, 2H); **<sup>19</sup>F NMR (376 MHz, DMSO-*d*<sup>6</sup>)**  $\delta_{\text{F}}$  ppm -131.9 – -131.4 (m, br); **<sup>11</sup>B NMR (128 MHz, DMSO-*d*<sup>6</sup>)**  $\delta_{\text{B}}$  ppm -2.0; **<sup>13</sup>C NMR (101 MHz, DMSO-*d*<sup>6</sup>)**  $\delta_{\text{C}}$  ppm 64.0, 90.8, 127.0, 127.4, 128.3, 144.1

### Synthesis of Potassium (3-oxo-3-phenylprop-1-yn-1-yl)trifluoroborate **23**



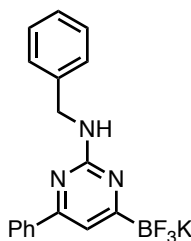
Chemical Formula: C<sub>9</sub>H<sub>5</sub>BF<sub>3</sub>KO

To a stirring suspension of manganese(IV) oxide (7.3 g, 84 mmol, 10 equiv.) in acetone (50 mL) was added portion-wise ynol trifluoroborate **32** (2 g, 8.4 mmol, 1 equiv.) at room temperature for 4 hours. The reaction mixture was then filtered through a bed of Celite and the filtrate concentrated *in vacuo*. The solid residue was redissolved in the minimum amount of acetone affording a saturated solution. The product was precipitated by adding diethyl ether and isolated by filtration followed by washing with diethyl ether. The precipitate was dried *in vacuo* to give the ynone trifluoroborate salt as a colourless solid (1.5 g, 75%). **M.p.** = 169 - 170 °C; **<sup>1</sup>H NMR (400 MHz, DMSO-*d*<sup>6</sup>)**  $\delta_{\text{H}}$  ppm 7.53 – 7.60 (m, 2H), 7.64 – 7.71 (m, 1H), 8.04 – 8.10 (m, 2H); **<sup>19</sup>F NMR (376 MHz, DMSO-*d*<sup>6</sup>)**  $\delta_{\text{F}}$  ppm -132.8 – -133.3 (m); **<sup>11</sup>B NMR (128 MHz, DMSO-*d*<sup>6</sup>)**  $\delta_{\text{B}}$  ppm -1.9 (q, *J* = 33.0 Hz); **<sup>13</sup>C NMR (101 MHz, DMSO-*d*<sup>6</sup>)**  $\delta_{\text{C}}$  ppm 88.6, 129.2, 129.4, 134.3, 137.2, 178.7.

## General procedure A: Freebasing and condensation of *N*-alkyl guanidine hydrochloride salts **25** with **23**

To a stirring suspension of alkylguanidine hydrochloride (2.4-2.5 eq) in toluene was added potassium carbonate (2.4-2.5 eq). The mixture was heated at 80 °C for 2 h, then **23** (1.0 eq) was added and the mixture was heated at reflux for 16 h. The mixture was cooled to room temperature and concentrated *in vacuo*, followed by dissolving in acetone and filtering to remove residual salts. The resultant acetone solution was concentrated to afford a saturated solution and Et<sub>2</sub>O was added slowly. The aminopyrimidine trifluoroborate precipitate was then collected by filtration and dried thoroughly *in vacuo*.

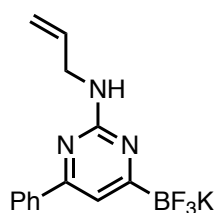
### Preparation of 2-(benzylamino)-4-phenylpyrimidin-6-yl trifluoroborate **25a**



Chemical Formula: C<sub>17</sub>H<sub>14</sub>BF<sub>3</sub>KN<sub>3</sub>

Following general procedure using benzylguanidine hydrochloride (200 mg, 1.08 mmol), potassium carbonate (147 mg, 1.06 mmol), **23** (100 mg, 0.42 mmol) and toluene (10 mL). The title compound was obtained as a colourless solid (114 mg, 74%). **M.p.** = 234-235 °C (dec); **<sup>1</sup>H NMR (400 MHz, DMSO-*d*<sup>6</sup>)** δ<sub>H</sub> ppm 4.61 (d, 2H, J = 6.0 Hz), 7.09 (s, 1H), 7.10 – 7.25 (m, 2H), 7.29 (t, 2H, J = 7.5 Hz), 7.37 – 7.47 (m, 5H), 7.99 (dd, 2H, J = 8.0, 1.5 Hz); **<sup>13</sup>C NMR (101 MHz, DMSO-*d*<sup>6</sup>)** δ<sub>C</sub> ppm 44.2, 108.5, 126.3 (x2C), 127.3, 128.0, 128.5, 129.4, 138.7, 141.5, 159.6, 162.1; **<sup>19</sup>F NMR (376 MHz, DMSO-*d*<sup>6</sup>)** δ<sub>F</sub> ppm -142.6; **<sup>11</sup>B NMR (128 MHz, DMSO-*d*<sup>6</sup>)** δ<sub>B</sub> ppm 1.3; **FTIR (neat)** ν<sub>max</sub> / cm<sup>-1</sup> 3432 (m), 3063 (w), 3033 (w), 2945 (w), 1534 (s), 1026 (s), 953 (s); **HRMS (ESI-TOF)** *m/z* [M-K]<sup>-</sup> calculated for C<sub>17</sub>H<sub>14</sub><sup>11</sup>BF<sub>3</sub>N<sub>3</sub> 328.1238, found 328.1251.

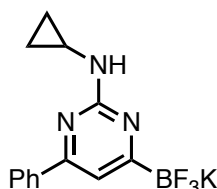
### Preparation of 2-((*N*-allyl)amino)-4-phenylpyrimidin-6-yl trifluoroborate 25b



Chemical Formula: C<sub>13</sub>H<sub>12</sub>BF<sub>3</sub>KN<sub>3</sub>

Following general procedure A using allylguanidine hydrochloride (115 mg, 0.85 mmol), potassium carbonate (117 mg, 0.85 mmol), **23** (82 mg, 0.35 mmol) and toluene (6 mL). The title compound was obtained as a colourless solid (60 mg, 54%). **M.p.** = 204-205 °C (dec); **<sup>1</sup>H NMR (400 MHz, DMSO-d<sub>6</sub>)** δ<sub>H</sub> ppm 3.97 – 4.06 (m, 2H), 5.00 – 5.08 (m, 1H), 5.16 – 5.25 (m, 1H), 5.98 (ddt, 1H, J = 17.0, 10.5, 5.5 Hz), 6.69 (s, 1H), 7.08 (s, 1H), 7.40 – 7.51 (m, 3H), 8.02 (dd, 2H, J = 8.0, 1.5 Hz); **<sup>13</sup>C NMR (101 MHz, DMSO-d<sub>6</sub>)** δ<sub>C</sub> ppm 43.7, 109.0, 114.8, 116.4, 126.8, 129.0, 129.8, 139.1, 159.9, 162.3; **<sup>19</sup>F NMR (377 MHz, DMSO-d<sub>6</sub>)**: δ<sub>F</sub> ppm -142.6; **<sup>11</sup>B NMR (128 MHz, DMSO-d<sub>6</sub>)** δ<sub>B</sub> ppm 1.6; **FTIR (neat)** ν<sub>max</sub> / cm<sup>-1</sup> 3383, 1645, 1601, 1534, 1033; **HRMS (ESI-TOF)** *m/z* [M-K]<sup>-</sup> calculated for C<sub>13</sub>H<sub>12</sub><sup>11</sup>BF<sub>3</sub>N<sub>3</sub> 278.1082, found 278.1091.

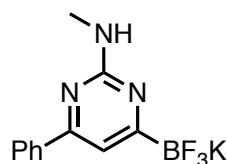
### Preparation of 2-((*N*-cyclopropyl)amino)-4-phenylpyrimidin-6-yl trifluoroborate 25c



Chemical Formula: C<sub>13</sub>H<sub>12</sub>BF<sub>3</sub>KN<sub>3</sub>

Following general procedure A using cyclopropylguanidine hydrochloride (145 mg, 1.07 mmol), potassium carbonate (147 mg, 1.06 mmol), **23** (100 mg, 0.42 mmol) and toluene (10 mL). The title compound was obtained as a pale-yellow solid (100 mg, 75%). **M.p.** = 168-170 °C (dec); **<sup>1</sup>H NMR (400 MHz, DMSO-d<sub>6</sub>)** δ<sub>H</sub> ppm 0.44 – 0.57 (m, 2H), 0.65 – 0.77 (m, 2H), 2.77 – 2.85 (m, 1H), 6.80 (s, 1H), 7.11 (s, 1H), 7.42 – 7.49 (m, 3H), 8.03 – 8.10 (m, 2H); **<sup>13</sup>C NMR (101 MHz, DMSO-d<sub>6</sub>)** δ<sub>C</sub> ppm 6.9, 24.4, 106.4, 127.2, 129.2, 131.0, 137.5, 159.3, 163.9; **<sup>19</sup>F NMR (377 MHz, DMSO-d<sub>6</sub>)** δ<sub>F</sub> ppm -142.6; **<sup>11</sup>B NMR (128 MHz, DMSO-d<sub>6</sub>)** δ<sub>B</sub> ppm 1.5; **FTIR (neat)** ν<sub>max</sub> / cm<sup>-1</sup> 3373, 1672, 1532, 1347, 1058; **HRMS: (ESI-TOF)** *m/z* [M-K]<sup>-</sup> calculated for C<sub>13</sub>H<sub>12</sub><sup>11</sup>BF<sub>3</sub>N<sub>3</sub> 278.1082, found 278.1094.

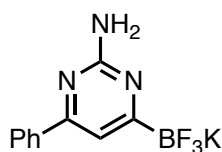
### Preparation of 2-((*N*-methyl)amino)-4-phenylpyrimidin-6-yl trifluoroborate 25e



Chemical Formula: C<sub>11</sub>H<sub>10</sub>BF<sub>3</sub>KN<sub>3</sub>

Following general procedure A using methylguanidine hydrochloride (116 mg, 1.06 mmol), potassium carbonate (147 mg, 1.06 mmol), **23** (100 mg, 0.42 mmol) and toluene (10 mL). The title compound was obtained as a pale yellow solid (30 mg, 25%). **M.p.** = 154-155 °C (dec); **<sup>1</sup>H NMR (400 MHz, DMSO-d<sub>6</sub>)** δ<sub>H</sub> ppm 2.83 – 2.91 (m, 3H), 6.48 (s, 1H), 7.06 (s, 1H), 7.37 – 7.52 (m, 3H), 7.97 – 8.10 (m, 2H); **<sup>13</sup>C NMR (101 MHz, DMSO-d<sub>6</sub>)** δ<sub>C</sub> ppm 28.5, 108.7, 126.8, 129.0, 129.8, 139.3, 160.1, 163.2; **<sup>19</sup>F NMR (377 MHz, DMSO-d<sub>6</sub>)** δ<sub>F</sub> ppm -142.6; **<sup>11</sup>B NMR (128 MHz, DMSO-d<sub>6</sub>)** δ<sub>B</sub> ppm 1.8; **FTIR (neat)** ν<sub>max</sub> / cm<sup>-1</sup> 3357, 1662, 1542, 1308, 1080; **HRMS: (ESI-TOF)** *m/z* [M-K]<sup>-</sup> calculated for C<sub>11</sub>H<sub>10</sub><sup>11</sup>BF<sub>3</sub>N<sub>3</sub> 252.0925, found 252.0936.

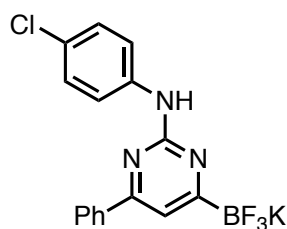
### Preparation of Potassium (2-amino-4-(naphthalen-2-yl)pyrimidin-6-yl)trifluoroborate 25f



Chemical Formula: C<sub>10</sub>H<sub>8</sub>BF<sub>3</sub>KN<sub>3</sub>

To a stirring suspension of **23** (100 mg, 0.35 mmol) in toluene at room temperature was added *N*-carbamimidoyl pivalate (250 mg, 1.75 mmol) in one portion. The mixture was heated at reflux for 48 hours, then cooled to room temperature and concentrated *in vacuo*. The residue was then suspended in acetone, and Et<sub>2</sub>O was added slowly from a dropping funnel (typically ~10 times the volume of acetone). The mixture was then filtered and the resultant solid was washed with Et<sub>2</sub>O then dried *in vacuo* to provide the product **25f** as a tan solid (92 mg, 80%). **M.p.** = 235-236°C (dec); **<sup>1</sup>H NMR (400 MHz, DMSO-d<sub>6</sub>)** δ<sub>H</sub> ppm 6.08 (br, 2H), 7.07 (s, 1H), 7.40 – 7.49 (m, 3H), 7.96 – 8.01 (m, 2H); **<sup>13</sup>C NMR (101 MHz, DMSO-d<sub>6</sub>)** δ<sub>C</sub> ppm 109.2, 126.8, 129.0, 129.8, 139.2, 160.6, 163.6; **<sup>19</sup>F NMR (376 MHz, DMSO-d<sub>6</sub>)** δ<sub>F</sub> ppm -142.6; **<sup>11</sup>B NMR (128 MHz, DMSO-d<sub>6</sub>)** δ<sub>B</sub> ppm 1.5; **FTIR (neat)** ν<sub>max</sub> / cm<sup>-1</sup> 3467 (w), 3305 (w), 3189 (w), 1526 (s), 954 (s); **HRMS (ESI-TOF)** *m/z* [M-K]<sup>-</sup> calculated for C<sub>14</sub>H<sub>10</sub><sup>11</sup>BF<sub>3</sub>N<sub>3</sub> 288.0925, found 288.0930

## Preparation of 2-((4-chlorophenyl)amino)-4-phenylpyrimidin-6-yl trifluoroborate 25d



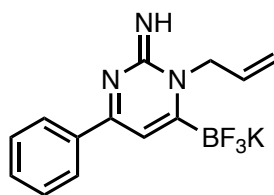
Chemical Formula:  $C_{16}H_{11}BClF_3KN_3$

To a slurry of **23** (174 mg, 0.74 mmol) in toluene was added (4-chlorophenyl)guanidine **24d** (150 mg, 0.88 mmol). The mixture was heated at reflux for 16 h then cooled to room temperature and concentrated *in vacuo*. The crude mixture was dissolved in acetone, and Et<sub>2</sub>O was added. The resultant precipitate was collected. Cooling the mixture to 0 °C provided a second crop of product. The solids were combined, washed with Et<sub>2</sub>O and dried *in vacuo* to give the title compound as a yellow solid (178 mg, 62%). **M.p.** = 156-157 °C (dec); **<sup>1</sup>H NMR (400 MHz, DMSO-*d*<sup>6</sup>)** δ<sub>H</sub> ppm 7.31 (d, 2H, J = 9.0 Hz), 7.33 (s, 1H), 7.29 – 7.32 (m, 3H), 7.98 (d, 2H, J = 9.0 Hz), 8.08 (dd, 2H, J = 8.0, 1.0 Hz), 9.53 (br, 1H); **<sup>13</sup>C NMR (101 MHz, DMSO-*d*<sup>6</sup>)** δ<sub>C</sub> ppm 110.9, 119.4, 123.4, 126.6, 128.2, 128.8, 129.9, 138.3, 140.9, 159.6, 160.0; **<sup>19</sup>F NMR (376 MHz, DMSO-*d*<sup>6</sup>)** δ<sub>F</sub> ppm -142.7; **<sup>11</sup>B NMR (128 MHz, DMSO-*d*<sup>6</sup>)** δ<sub>B</sub> ppm 1.5; **FTIR (neat)** ν<sub>max</sub> / cm<sup>-1</sup> 3414 (w), 3338 (br), 3338 (w), 1522 (s), 1490 (s), 1059 (m); **HRMS (ESI-TOF)** *m/z* [M-K]<sup>-</sup> calculated for C<sub>16</sub>H<sub>11</sub><sup>11</sup>B<sup>35</sup>ClF<sub>3</sub>N<sub>3</sub> 348.0692, found 348.0702.

### General procedure B: Ring alkylation of 25f

To a stirring suspension of **25f** (1.0 eq) in acetone at room temperature was added alkyl halide (1.0 eq). The reaction mixture was heated at 50 °C for 16 h, then cooled to room temperature and concentrated *in vacuo*, giving a saturated solution. Et<sub>2</sub>O was added and the resultant precipitate was collected, washed with Et<sub>2</sub>O and dried thoroughly *in vacuo* to afford the corresponding alkylated pyrimidine trifluoroborate salt.

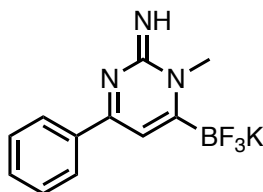
### Preparation of 1-allyl-2-(1*H*)-4-phenylpyrimidinimin-6-yl trifluoroborate 26b



Chemical Formula: C<sub>13</sub>H<sub>12</sub>BF<sub>3</sub>KN<sub>3</sub>

Following general procedure B, using **25f** (70 mg, 0.25 mmol), allyl bromide (22  $\mu$ L, 0.25 mmol) and acetone (8 mL). The title compound was obtained as a colourless solid (40 mg, 50%). **M.p** = 173-174 °C (dec); **<sup>1</sup>H NMR (400 MHz, DMSO-*d*<sup>6</sup>)**  $\delta_{\text{H}}$  ppm 4.96 (d, 2H *J* = 3.0 Hz), 5.21 (d, 1H, *J* = 17.5 Hz), 5.26 (d, 1H, *J* = 11.0 Hz), 5.83 – 5.95 (m, 1H), 7.04 (s, 1H), 7.48 (s, 1H), 7.54 – 7.67 (m, 3H), 8.08 – 8.22 (m, 2H); **<sup>13</sup>C NMR (101 MHz, DMSO-*d*<sup>6</sup>)**  $\delta_{\text{C}}$  ppm 52.1, 109.9, 118.5, 128.0, 129.3, 130.4, 132.8, 134.5, 155.7, 166.8; **<sup>19</sup>F NMR (377 MHz, DMSO-*d*<sup>6</sup>)**  $\delta_{\text{F}}$  ppm -140.7; **<sup>11</sup>B NMR (128 MHz, DMSO-*d*<sup>6</sup>)**  $\delta_{\text{B}}$  ppm 0.6; **FTIR (neat)**  $\nu_{\text{max}}$  / cm<sup>-1</sup> 3367, 1636, 1597, 1556, 1362; **HRMS: (ESI-TOF)** *m/z* [M-K]<sup>-</sup> calculated for C<sub>13</sub>H<sub>12</sub><sup>11</sup>BF<sub>3</sub>N<sub>3</sub>. 278.1082, found 278.1096.

### Preparation of 1-methyl-2-(1*H*)-4-phenylpyrimidinimin-6-yl trifluoroborate 26a



Chemical Formula: C<sub>11</sub>H<sub>10</sub>BF<sub>3</sub>KN<sub>3</sub>

Following general procedure B, using **25f** (70 mg, 0.25 mmol), iodomethane (15  $\mu$ L, 0.25 mmol) and acetone (8 mL). The title compound was obtained as a colourless solid (68 mg, 93%). **M.p** = 175-177 °C (dec); **<sup>1</sup>H NMR (400 MHz, DMSO-*d*<sup>6</sup>)**  $\delta_{\text{H}}$  ppm 3.77 (s, 3H), 6.90 (s, 1H), 7.45 (s, 1H), 7.55 – 7.67 (m, 3H), 8.11 – 8.21 (m, 2H); **<sup>13</sup>C NMR (101 MHz, DMSO-*d*<sup>6</sup>)**  $\delta_{\text{C}}$  ppm 38.6, 109.4, 127.8, 129.2, 132.5, 134.6, 156.5, 166.3; **<sup>19</sup>F NMR (377 MHz, DMSO-*d*<sup>6</sup>)**  $\delta_{\text{F}}$  ppm -141.5; **<sup>11</sup>B NMR (128 MHz, DMSO-*d*<sup>6</sup>)**  $\delta_{\text{B}}$  ppm 0.6; **FTIR (neat)**  $\nu_{\text{max}}$  / cm<sup>-1</sup> 3367, 1639, 1599, 1562, 1360; **HRMS: (ESI-TOF)** *m/z* [M-K]<sup>-</sup> calculated for C<sub>11</sub>H<sub>10</sub><sup>11</sup>BF<sub>3</sub>N<sub>3</sub> 252.0925, found 252.0932.

## References

- <sup>1</sup> A.-L. Auvinet, J.P.A. Harrity, *Angew. Chem. Int. Ed.* **2011**, 50, 2769.
- <sup>2</sup> D. L. Comins, S. O'Connor, R. S. Al-awar, *Comprehensive Heterocyclic Chemistry III Vol. 7* (Eds: A. Katritzky, E.F.V Scriven, C. A. Ramsden, J.K. Taylor), **2008**.
- <sup>3</sup> G. D. Henry, *Tetrahedron* **2004**, 60, 6043 – 6061.
- <sup>4</sup> R. Pingaew, S. Prachayasittikul, S.Ruchirawat, *Molecules* **2010**, 15, 988 – 996.
- <sup>5</sup> M. Vrabel, M. Hocek, L. Havran, M. Fojta, I. Votru ba, B. Klepetarova, R. Pohl, L. Rulisek, L. Zendlova, P. Hobza, I. H. Shih, E. Mabery, R. Mackman, *Eur. J. Inorg. Chem.* **2007**, 1752 – 1769.
- <sup>6</sup> J. A. Joule, K. Mills, *Heterocyclic Chemistry* (Eds: Fifth), **2010**.
- <sup>7</sup> Y. M. Choi, N. Kucharczyk, R. D. Sofia, *J. Label. Compd. Radiopharm.* **1987**, 24, 1 – 14.
- <sup>8</sup> F. Bohlmann, D. Rahtz, *Chem. Ber.* **1957**, 90, 2265 – 2272.
- <sup>9</sup> M. Movassaghi, M. D. Hill, O. K. Ahmad, *J. Am. Chem. Soc.* **2007**, 129, 10096 – 10097.
- <sup>10</sup> B. M. Trost, Gutierrez, A. C. *Org. Lett.* **2007**, 9, 1473 – 1476.
- <sup>11</sup> S. Liu and L. S. Liebeskind *J. Am. Chem. Soc.* **2008**, 130, 6918 – 6919.
- <sup>12</sup> F. Fringuelli, A. Taticchi, *The Diels-Alder Reaction: Selected Practical Methods*, **2002**.
- <sup>13</sup> J. Sauer, *Angew. Chem. Int Ed. Engl.* **1967**, 6, 16.
- <sup>14</sup> I. Fleming, *Frontier Orbitals and Organic Chemical Reactions*, John Wiley & Sons, Chichester, **1976**.
- <sup>15</sup> E. A. Aydin, **2012**, *Diels-Alder reactions of phencyclone and coumarin derivatives and click chemistry of novel BODIPY dyes for fluorescence Detection*, Ph.D. thesis, Univeristy of Sheffield, Sheffield.
- <sup>16</sup> R.B. Woodward, F. Sondheimer, D. Taub, K. Heusler, W. M. Mclamore, *J. Am. Chem. Soc.* **1952**, 74, 4223 – 4251.
- <sup>17</sup> M. Gates, G. Tschudi, *J. Am. Chem. Soc.* **1952**, 74, 1109 – 1110.
- <sup>18</sup> M. Gregoritz, F. P. Brandl, *Eur. J. Pharm. Biopharm.* **2015**, 97, 438 – 453.
- <sup>19</sup> M. Behforouz, M. Ahmadian, *Tetrahedron* **2000**, 56, 5259 – 5288.
- <sup>20</sup> S. Jayakumar, M. P. S. Ishar and M. P. Mahajan, *Tetrahedron* **2002**, 58, 379 – 471.
- <sup>21</sup> B. Groenendaal, E. Ruijter, R. V. A. Orru, *Chem. Commun.* **2008**, 5474 – 5489.
- <sup>22</sup> D. L. Boger, *Chem. Rev.* **1986**, 86, 781 – 793.
- <sup>23</sup> H. Neunhoeffer, P. F. Wiley, *Chemistry of Heterocyclic Compounds*, Wiley, **1978**, vol 33.
- <sup>24</sup> D. L. Boger, *Tetrahedron*, **1983**, 39, 2912 – 2922.

- 
- <sup>25</sup> (a) S. M. Winreb, F.Z. Basha, S. Hibino, N. A. Khatri, D. Kim, W. E. Pye, T. T. Wu, *J. Am. Chem. Soc.* **1982**, *104*, 536 – 544 (b) F. Z. Basha, S. Hibino, D. Kim, D. W. E. Pye, T. T. Wu, S. M. Weinreb, *Ibid. J. Am. Chem. Soc.* **1980**, *102*, 3962 – 3964.
- <sup>26</sup> D. L. Boger, J. S. Panek, *J. Am. Chem. Soc.* **1985**, *107*, 5745 – 5754.
- <sup>27</sup> D. L. Boger, J. S. Panek, *J. Org. Chem.* **1981**, *46*, 2179 – 2182.
- <sup>28</sup> S. P. J. T. Bachollet, J. F. Vivat, D. C. Cocker, H. Adams, J. P. A. Harrity, *Chem. Eur. J.* **2014**, *20*, 12889 – 12893.
- <sup>29</sup> J. F. Vivat, H. Adams, J. P. A. Harriy, *Org. Lett.* **2010**, *136*, 160 – 163.
- <sup>30</sup> S. R. LaPlante, L. D. Fader, K. R. Fandrick, D. R. Fandrick, O. Hucke, R. Kemper, S. P. F. Miller, and P. J. Edwards, *J. Med. Chem.* **2011**, *54*, 7005 – 7022.
- <sup>31</sup> S. R. LaPlante P. J. Edwards, L. D. Fader, A. Jakalian, O. Hucke, *ChemMedChem.* **2011**, *7*, 505 – 513.
- <sup>32</sup> G. Bringmann, Y. Reichert, V. Kane, *Tetrahedron* **2004**, *60*, 3539 – 3574.
- <sup>33</sup> J. Porter and al, *Bioorg. Med. Chem. Lett.* **2009**, *19*, 1767 – 177.
- <sup>34</sup> M. B. Kim, K. E. Giesler, Y. A. Tahirovic, V. M. Truax, D. C. Liotta, L. J. Wilson, *Expert Opin. Investig. Drug* **2016**, *25*, 1377 – 1392.
- <sup>35</sup> R. Ratz and H. Schroeder, *J. Org. Chem.* **1958**, *23*, 1931 – 1934.
- <sup>36</sup> F. H. Case, *J. Org. Chem.*, **1965**, *30*, 931 – 933.
- <sup>37</sup> S. P. J. T. Bachollet, D. Volz, B. Fiser, S. Minch, F. Rönicke, J. Carrillo, H. Adams, U. Schepers, E. Gúmez - Bengoa, S. Bräse, J. P. A. Harrity, *Chem. Eur.J.* **2016**, *22*, 12430 – 12438.
- <sup>38</sup> A. S. Vieira, P. F. Fiorante, T. L. S. Hough, F. P. Ferreira, D. S. Lüdtké H. A. Stefani, *Org. Lett.* **2008**, *10*, 5215 – 5218.
- <sup>39</sup> A. Kajal, S. Bala, S. Kamboj, N. Sharma, V. Saini, *Journal of Catalysts.* **2013**, 1 – 14.
- <sup>40</sup> B. E. Love, T. S. Boston, B. T. Nguye, J. R. Rorer, *Organic Preparations and Procedure Int.*, **1999**, *31*, 399 – 405.
- <sup>41</sup> a) B. E. Love, J. Ren, *J. Org. Chem.* **1993**, *58*, 5556 – 5557 b) B. E. Love, P. S. Rajee, T. C. Williams, *Synlett.* **1994**, *8*, 491 – 493.
- <sup>42</sup> G. C. Look, M. M. Murphy, D. A. Campbell, M. A. Gallop, *Tetrahedron Lett.* **1995**, *36*, 2937 – 2940.
- <sup>43</sup> J. Ritter, *J. Am. Chem. Soc.* **1933**, *55*, 3322 – 3326.
- <sup>44</sup> A. Nishinaga, S. Yamazaki, T. Matsuura, *Tetrahedron Lett.* **1988**, *29*, 4115 – 4118.
- <sup>45</sup> J. S. M. Samec, A. H. Éll, J-E. Bäckvall, *Chem. Eur. J.* **2005**, *11*, 2327 – 2334.
- <sup>46</sup> E. Zhang, H. Tian, S. Xu, X. Yu, Qing Xu, *Org. Lett.* **2013**, *15*, 2704 – 2707.

- 
- <sup>47</sup> K. Gopalaiah, A. Saini, *Cat. Lett.* **2016**, *9*, 1648 – 1654.
- <sup>48</sup> F. Bottaro, A. Takallou, A. Chehaiber, R. Madsen, *Eur. J. Org. Chem.* **2019**, 7164 – 7168.
- <sup>49</sup> a) M. Haruta, N. Yamada, T. Kobayashi, S. Iijima, *J. Catal.* **1989**, *115*, 301 – 309 b) M. Haruta, *Chem. Rec.* **2003**, *3*, 75 – 87.
- <sup>50</sup> a) H. Tsunoyama, H. Sakurai, Y. Negishi, T. Tsukuda, *J. Am. Chem. Soc.* **2005**, *127*, 9374 – 9375 b) C. Milone, R. Ingoglia, G. Neri, A. Pistone, S. Galvagno, *Appl. Catal.* **2001**, *211*, 251 – 257.
- <sup>51</sup> S. Biella, M. Rossi, *Chem. Commun.* **2003**, 378 – 379.
- <sup>52</sup> H. Sun, F-Z. Su, J. Ni, Y. Cao, H-Y. He, K-N. Fan, *Angew. Chem.* **2009**, *121*, 4454 – 4457.
- <sup>53</sup> Z. Opre, D. Ferri, F. Krumeich, T. Mallat, A. Baiker, *Journal of Catalysis* **2006**, *241*, 287 – 295.
- <sup>54</sup> S. Sebti, A. Solhy, R. Tahir, A. Smahi, *Appl. Catal. A.* **2002**, *235*, 273 – 281.
- <sup>55</sup> a) J. Zhang, G. Leitus, Y. Ben-David, D. Milstein, *J. Am. Chem. Soc.* **2005**, *127*, 10840 – 10841 b) R. Yamaguchi, C. Ikeda, Y. Takahashi, K. I. Fujita, *J. Am. Chem. Soc.* **2009**, *131*, 8410 – 8412 c) D. Spasyuk, D. G. Gusev, *Organometallics* **2012**, *31*, 5239 – 5242 d) S. Musa, S. Fronton, L. Vaccaro, D. Gelman, *Organometallics* **2013**, *32*, 3069 – 3073.
- <sup>56</sup> G. Jaiswal, V. G. Landge, D. Jagadeesan, E. Balaraman, *Green Chem.* **2016**, *18*, 3232 – 3238.
- <sup>57</sup> J. Bain, P. Cho, A. Voutchkova-Kostal, *Green Chem.* **2015**, *17*, 2271 – 2280.
- <sup>58</sup> F. Cavani, F. Trifiro, A. Vaccari, *Catal. Today* **1991**, *11*, 173 – 301.
- <sup>59</sup> A. V. Iosub, S. S. Stahl, *Org. Lett.* **2015**, *17*, 4404 – 4407.
- <sup>60</sup> V. Pascanu, G. González Miera, A. K. Inge, B. Martín-Matute, *J. Am. Chem. Soc.* **2019**, *141*, 7223 – 7234.
- <sup>61</sup> J. L. C. Rowsell, O. M. Yaghi, *Microporous Mesoporous Mater.* **2004**, *73*, 3 – 14.
- <sup>62</sup> H. Li, M. Eddaoudi, M. O'Keeffe, O. M. Yaghi, *Nature*, **1999**, *402*, 276 – 279.
- <sup>63</sup> a) B. F. Abrahams, B. F. Hoskins, R. Robson, *J. Am. Chem. Soc.* **1991**, *113*, 3606 – 3607. b) S. R. Batten, R. Robson, *Angew. Chem. Int. Ed.* **1998**, *37*, 1460 – 1494 c) B. Chen, M. Eddaoudi, S. T. Hyde, M. O. Keffe, O. M. Yaghi, *Science* **2002**, *295*, 469 – 472.
- <sup>64</sup> Q. Wang, D. Astruc, *Chem. Rev.* **2020**, *120*, 1438 – 1511.
- <sup>65</sup> Y. Q. Tian, Y. M. Zhao, Z. X. Chen, G. N. Zhang, L. H. Weng, D. Y. Zhao, *Chem. Eur. J.* **2007**, *13*, 4146 – 4154.
- <sup>66</sup> A. Corma, H. Garcia, F. X. Llabres i Xamena, *Chem. Rev.* **2010**, *110*, 4606 – 4655.
- <sup>67</sup> F. Song, C. Wang; W. Lin, *Chem. Commun.* **2011**, *47*, 8256 – 8258.
- <sup>68</sup> T. Ishida, M. Nagaoka, T. Akita and M. Haruta, *Chem. Eur. J.* **2008**, *14*, 8456 – 846.

- 
- <sup>69</sup> N. Yuan, V. Pascanu, Z. Huang, A. Valiente, N. Heidenreich, S. Leubner, A. K. Inge, Jakob G. Norbert, S. Persson, B. Martín-Matute, X. Zou, *J. Am. Chem. Soc.* **2018**, *140*, 8206 – 8217.
- <sup>70</sup> L. Chen, Z. Gao, Y. Li, *Catal. Today* **2015**, *245*, 122 – 128.
- <sup>71</sup> a) F. Carson, V. Pascanu, A. Bermejo Gómez, Y. Zhang, A. E. Platero-Prats, X. Zou, B. Martín-Matute, *Chem. Eur. J.* **2015**, *21*, 10896 – 10902 b) V. Pascanu, P. R. Hansen, A. Bermejo Gómez, C. Ayats, A. E. Platero-Prats, M. J. Johansson, M. À. Pericàs, B. Martín-Matute, *ChemSusChem*. **2015**, *8*, 123 – 130 c) V. Pascanu, Q. Yao, A. Bermejo Gómez, M. Gustafsson, Y. Yun, W. Wan, L. Samain, X. Zou, B. Martín-Matute, *Chem. Eur. J.* **2013**, *19*, 17483 – 17493.
- <sup>72</sup> A. Valiente, S. Carrasco, A. Sanz-Marco, C.-W. Tai, A. Bermejo Gómez, B. Martín-Matute, *ChemCatChem*. **2019**, *11*, 3933 – 3939.
- <sup>73</sup> T. D. Bennett, A. K. Cheetham, *Acc. Chem. Res.* **2014**, *47*, 1555 – 1562.
- <sup>74</sup> T. D. Bennett, A. L. Goodwin, M. T. Dove, D. A. Keen, M. G. Tucker, E. R. Barney, A. K. Soper, E. G. Bithell, J. C. Tan, A. K. Cheetham, *Phys. Rev. Lett.* **2010**, *104*, No. 115503, 1 – 4
- <sup>75</sup> K. W. Chapman, D. F. Sava, G. J. Halder, P. J. Chupas, T. M. Nenoff, *J. Am. Chem. Soc.* **2011**, *133*, 18583 – 18585
- <sup>76</sup> P. Horcajada, C. Serre, M. Vallet-Regi, M. Sebban, F. Taulelle, G. Férey, *Angew. Chem., Int. Ed.* **2006**, *45*, 5974 – 5978.
- <sup>77</sup> O. A. Kholdeeva, I. Y. Skobelev, I. D. Ivanchikova, K. A. Kovalenkob, V. P. Fedin, A. R. B. Sorokin, *Catal. Today* **2014**, *238*, 54 – 61.
- <sup>78</sup> L. Zhu, X.-Q. Liu, H.-L. Jiang, L.-B. Sun, *Chem. Rev.* **2017**, *117*, 8129 – 8176.
- <sup>79</sup> A. Dhakshinamoorthy, M. Alvaro, H. Garcia, *ChemCatChem* **2010**, *2*, 1438 – 1443.
- <sup>80</sup> A. Dhakshinamoorthy, M. Alvaro, H. Garcia, *J. Catal.* **2009**, *267*, 1 – 4.
- <sup>81</sup> G.-J. Chen, H.-C. Ma, W.-L. Xin, X.-B. Li, F.-Z. Jin, J.-S. Wang, M.-Y. Liu, Y.-B. Dong, *Inorg. Chem.* **2017**, *56*, 654 – 660.
- <sup>82</sup> J.-Yi Tan, J.-X. Shi, P.-H. Cui, Y.-Y. Zhang, N. Zhang, J.-Y. Zhang, W. Deng, *Microporous and Mesoporous Mater.* **2019**, *287*, 152 – 158.
- <sup>83</sup> C. Xu, H. Liu, D. Li, J.-H. Su, H.-L. Jiang, *Chem. Sci.* **2018**, *9*, 3152 – 3158.
- <sup>84</sup> S. Carrasco, A. Sanz-Marco, B. Martín-Matute, *Organometallics* **2019**, *38*, 3429 – 3435.
- <sup>85</sup> D. Feng, Z.-Y. Gu, J.-R. Li, H.-L. Jiang, Z. Wei, H.-C. Zhou, *Angew. Chem. Int. Ed.* **2012**, *51*, 10307 – 10310.
- <sup>86</sup> M. Gutierrez, B. Cohen, F. Sánchez, A. Douhal, *Phys. Chem. Chem. Phys.* **2016**, *18*, 27761 – 27774.
- <sup>87</sup> L. Shen, S. Liang, W. Wu, R. Liang, L. Wu, *Dalton Trans.* 2013, **42**, 13649 – 13657.

- 
- <sup>88</sup> T. N. Poudel, R. J. I. Tamargo, H. Cai, Y. R. Lee, *Asian J. Org. Chem.* **2018**, *7*, 985 –1005.
- <sup>89</sup> M. C. Bonifacio, C. R. Robertson, J.-Y. Jung, B. T. J. King, *J. Org. Chem.* **2005**, *70*, 8522 – 8526
- <sup>90</sup> W. M. Shu, K. L. Zheng, J. R. Ma, A. X. Wu, *Org. Lett.* **2015**, *17*, 5216 – 5219.
- <sup>91</sup> S. M. B. Maezono, T. N. Poudel, Y. R. Lee, *Org. Biomol. Chem.* **2017**, *15*, 2052 – 2062.
- <sup>92</sup> J. Gong, F. Xie, H. Chen, Y. Hu, *Org. Lett.* **2010**, *12*, 3848 – 3851.
- <sup>93</sup> H. Chen, F. Xie, J. Gong, Y. Hu, *J. Org. Chem.* **2011**, *76*, 8495 – 8500.
- <sup>94</sup> S. J. Hein, D. Lehnerr, H. Arslan, F. J. Uribe-Romo, W. R. Dichtel, *Acc. Chem. Res.* **2017**, *50*, 2776 – 2788.
- <sup>95</sup> W. Reppe, W. J. Schweckendiek, *Justus Liebigs Ann. Chem.* **1948**, *560*, 104 – 116.
- <sup>96</sup> G. Hilt, S. Lüers, K. Harms, *J. Org. Chem.* **2004**, *69*, 624 – 630.
- <sup>97</sup> a) M. W. Davies, C. N. Johnson, J. P. A. Harrity, *Chem. Commun.* **1999**, 2107 – 2108; b) M. W. Davies, C. N. Johnson, J. P. A. Harrity, *J. Org. Chem.* **2001**, *66*, 3525 – 3532.
- <sup>98</sup> a) M. A. Huffman, L. S. Liebeskind, *J. Am. Chem. Soc.* **1990**, *112*, 8617 – 8618; b) M. A. Huffman, L. S. Liebeskind, *J. Am. Chem. Soc.* **1991**, *113*, 2771 – 2772; c) A.-L. Auvinet, J.P.A. Harrity, *Angew. Chem. Int. Ed.* **2011**, *50*, 2769
- <sup>99</sup> T. Stalling, **2014**, *Synthetic and Mechanistic Studies on Ni-catalysed Benzannulation Reactions*, Postdoctoral Research, Univeristy of Sheffield, Sheffield.
- <sup>100</sup> H. Zhang, Y. Luo, D. Li, Q. Yao, S. Dong, X. Liu, X. Feng, *Org. Lett.* **2019**, *7*, 2388 – 2392.
- <sup>101</sup> V. Sharma, N. Chitranshi, A. K. Agarwal, *Int. J. Med. Chem.* **2014**, 202784.
- <sup>102</sup> A. L. Marzinzik, E. R. Felder, *J. Org. Chem.* **1998**, *63*, 723 – 727.
- <sup>103</sup> O. K. Ahmad, M. D. Hill, M. Movassaghi, *J. Org. Chem.* **2009**, *74*, 8460 – 8463.
- <sup>104</sup> M. Lin, Q. Chen, Y. Zhu, X. Chen, J. Cai, Y. Pan, Z. Zhan, *Synlett*, **2011**, 1179 – 1183.
- <sup>105</sup> N. Deibl, K. Ament, R. Kempe, *J. Am. Chem. Soc.* **2015**, *137*, 12804 – 12807.
- <sup>106</sup> S. P. J. T. Bachollet, D. Volz, B. Fiser, S. Minch, F. Röncke, J. Carrillo, H. Adams, U. Schepers, E. Gúmez - Bengoa, S. Bräse, J. P. A. Harrity, *Chem. Eur. J.* **2016**, *22*, 12430 –12438.
- <sup>107</sup> C. C. Chen, M. Y. Wu, H. Y. Chen, and M. Wu, *J. Org. Chem.* **2017**, *82*, 6071–608.
- <sup>108</sup> F. Bottaro, A. Takallou, A. Chehaiber, R. Madsen, *Eur. J. Org. Chem.* **2019**, *42*, 7164 – 7168.
- <sup>109</sup> Y. Zhang, F. Lu, H.-Y. Zhang, J. Zhao, *Catal. Lett.* **2017**, *147*, 20 – 28.
- <sup>110</sup> S. Belkharchacha, H. Elayadia, H. Ighachanea, S. Sebtic, M. A. Alib, H. B. Lazreka, *J. Chem. Res.* **2018**, *42*, 614 – 618.

- <sup>111</sup> R. Nongrum, G. K. Kharmawlong, Jims W. S. Rani, N. Rahman, A. Dutta, R. Nongkhlaw *J. Hetero. Chem.* **2019**, *56*, 2873 – 2883.
- <sup>112</sup> S. Das, S. Mallick, S. De Sarkar, *J. Org. Chem.* **2019**, *84*, 12111 – 12119.
- <sup>113</sup> L.-L. Zhao, W. Liu, Z. Zhang, H. Zhao, Q. Wang, X. Yan, *Org. Lett.* **2019**, *21*, 10023 – 10027.
- <sup>114</sup> Y. Li, Z. Huang, X. Wu, P.-F. Xu, J. Jin, Y. Zhang, J. Wang, *Tetrahedron* **2012**, *68*, 5234 – 5240.
- <sup>115</sup> T. Bai, S. Ma, G. Jia, *Tetrahedron* **2007**, *63*, 6210 – 6215.

## Appendix

X-ray crystal structures of compounds 12aa, 31a, 31e and 32e are provided below.

### X-ray crystal structure data for compound 12aa

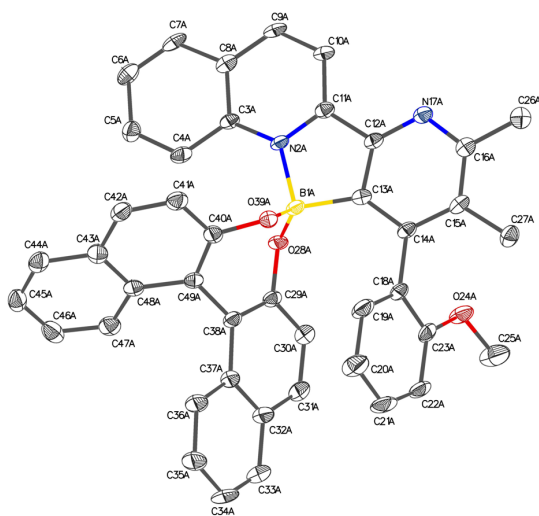


**Table 1 Crystal data and structure refinement for 2018ncs0765t.**

Identification code	2018ncs0765t
Empirical formula	C <sub>50</sub> H <sub>39</sub> BN <sub>2</sub> O <sub>3</sub>
Formula weight	726.64
Temperature/K	100.15
Crystal system	monoclinic
Space group	P2 <sub>1</sub>
a/Å	6.8740(4)
b/Å	32.7563(18)
c/Å	16.3196(11)
α/°	90
β/°	92.276(6)

$\gamma/^\circ$	90
Volume/ $\text{\AA}^3$	3671.7(4)
Z	4
$\rho_{\text{calc}}/\text{g}/\text{cm}^3$	1.314
$\mu/\text{mm}^{-1}$	0.081
F(000)	1528.0
Crystal size/ $\text{mm}^3$	$0.12 \times 0.025 \times 0.02$
Radiation	MoK $\alpha$ ( $\lambda = 0.71075$ )
2 $\Theta$ range for data collection/ $^\circ$	3.524 to 55.054
Index ranges	$-8 \leq h \leq 8, -42 \leq k \leq 42, -21 \leq l \leq 21$
Reflections collected	22769
Independent reflections	22769 [ $R_{\text{int}} = \text{Merged}, R_{\text{sigma}} = 0.0466$ ]
Data/restraints/parameters	22769/1/1018
Goodness-of-fit on $F^2$	1.006
Final R indexes [ $I \geq 2\sigma(I)$ ]	$R_1 = 0.0587, wR_2 = 0.1417$
Final R indexes [all data]	$R_1 = 0.0794, wR_2 = 0.1515$
Largest diff. peak/hole / $e \text{\AA}^{-3}$	0.35/-0.36
Flack parameter	1.3(8)

**Table 2 Fractional Atomic Coordinates ( $\times 10^4$ ) and Equivalent Isotropic Displacement Parameters ( $\text{\AA}^2 \times 10^3$ ) for 2018ncs0765t.  $U_{\text{eq}}$  is defined as 1/3 of of the trace of the orthogonalised  $U_{ij}$  tensor.**

Atom	x	y	z	U(eq)	
O24A	5742(5)	3933.1(10)	7857.8(18)	27.7(7)	
O28A	4052(4)	4938.0(9)	5895.2(16)	19.7(7)	
O39A	505(4)	4860.7(10)	5977.5(16)	20.3(7)	
N2A	2339(5)	5493.8(12)	6562(2)	17.8(8)	
N17A	2277(5)	5184.0(12)	8646(2)	19.8(8)	
C3A	2364(6)	5817.0(14)	6029(2)	17.1(9)	
C4A	2444(7)	5758.7(15)	5174(3)	21.4(10)	
C5A	2360(7)	6087.6(16)	4659(3)	24.3(10)	
C6A	2275(7)	6488.8(16)	4968(3)	25.0(11)	
C7A	2257(7)	6549.9(16)	5783(3)	24.7(10)	
C8A	2281(6)	6221.8(15)	6343(3)	19.7(9)	
C9A	2214(6)	6279.1(15)	7198(3)	21.3(10)	
C10A	2212(6)	5950.7(15)	7708(3)	20.3(10)	
C11A	2280(6)	5558.9(14)	7367(2)	18.2(9)	
C12A	2311(6)	5177.6(15)	7829(2)	17.9(9)	
C13A	2415(6)	4838.7(15)	7320(2)	18.4(9)	
C14A	2523(6)	4459.9(15)	7717(2)	17.6(9)	
C15A	2449(6)	4450.0(15)	8574(3)	19.0(9)	

---

C16A	2311(6)	4815.3(16)	9014(2)	18.9(9)
C18A	2676(7)	4071.9(15)	7230(3)	23.0(10)
C19A	1197(8)	3965.1(16)	6671(3)	30.7(11)
C20A	1295(8)	3604.6(17)	6218(3)	40.3(14)
C21A	2860(9)	3355.2(17)	6324(3)	38.2(13)
C22A	4373(7)	3452.2(15)	6872(3)	27.0(11)
C23A	4271(7)	3812.5(14)	7322(2)	21.6(10)
C25A	7297(9)	3654(2)	8021(4)	43.3(14)
C26A	2224(7)	4820.7(17)	9928(2)	24.7(10)
C27A	2443(7)	4055.9(16)	9048(3)	25.7(10)
C29A	4285(6)	4586.2(14)	5464(2)	19.2(9)
C30A	5961(7)	4354.6(16)	5645(3)	25.5(10)
C31A	6277(8)	4006.2(17)	5217(3)	32.4(12)
C32A	4934(8)	3861.2(16)	4618(3)	31.4(12)
C33A	5217(9)	3490.6(18)	4187(3)	40.9(14)
C34A	3860(10)	3348.9(18)	3626(3)	44.8(15)
C35A	2137(9)	3566.5(17)	3469(3)	39.9(14)
C36A	1818(8)	3934.0(16)	3861(3)	29.3(11)
C37A	3232(7)	4094.8(15)	4431(3)	25.0(10)
C38A	2965(7)	4480.1(14)	4833(2)	19.9(9)
C40A	152(7)	4920.5(15)	5156(2)	21.1(10)
C41A	-1519(7)	5149.1(15)	4910(3)	25.0(10)
C42A	-1897(7)	5237.8(16)	4108(3)	25.6(11)
C43A	-555(7)	5132.3(15)	3509(3)	24.5(10)
C44A	-791(7)	5259.8(16)	2679(3)	27.1(11)
C45A	594(8)	5176.0(16)	2130(3)	29.3(11)
C46A	2276(8)	4963.7(17)	2376(3)	30.8(12)
C47A	2528(7)	4827.1(16)	3168(3)	24.9(10)
C48A	1103(7)	4897.1(14)	3748(3)	22.8(10)
C49A	1361(7)	4761.6(14)	4589(2)	20.7(9)
B1A	2329(7)	4988.1(16)	6372(3)	18.5(10)
O24B	10584(5)	7294.8(11)	7326.5(18)	27.5(7)
O28B	9126(4)	6250.6(9)	9261.2(16)	20.5(7)
O39B	5579(4)	6328.6(10)	9100.1(16)	18.5(7)
N2B	7363(5)	5703.1(12)	8540(2)	17.3(8)
N17B	7356(5)	6020.5(13)	6461(2)	19.0(8)
C1S	7407(8)	3988.5(17)	1940(3)	31.9(12)
C2S	6220(8)	3732.0(18)	1440(3)	37.2(13)
C3B	7349(6)	5376.3(15)	9071(2)	18.0(9)
C3S	6961(9)	3554.8(17)	755(3)	40.1(13)
C4B	7390(6)	5432.1(16)	9926(3)	22.2(10)
C4S	8848(9)	3620.6(17)	557(3)	37.8(13)
C5B	7236(7)	5098.2(16)	10430(3)	23.7(10)
C5S	10037(8)	3871.9(17)	1052(3)	33.5(12)
C6B	7099(6)	4700.2(16)	10113(3)	23.7(10)

---

C6S	9303(8)	4047.3(16)	1733(3)	30.8(11)
C7B	7128(7)	4641.5(15)	9288(3)	22.8(10)
C7S	6592(10)	4194(2)	2668(4)	53.9(17)
C8B	7242(6)	4976.3(15)	8742(3)	20.4(10)
C8S	2344(8)	7280.8(17)	3217(3)	32.6(12)
C9B	7225(6)	4921.3(15)	7887(3)	20.1(9)
C9S	3792(8)	7428.5(17)	3755(3)	35.5(12)
C10B	7277(6)	5252.1(15)	7377(3)	19.9(9)
C10S	3338(10)	7600.5(19)	4498(3)	42.6(15)
C11B	7324(6)	5641.1(15)	7730(2)	17.5(9)
C11S	1415(10)	7621.0(18)	4715(3)	42.1(14)
C12B	7349(6)	6023.9(15)	7278(2)	17.0(9)
C12S	-10(9)	7473.0(18)	4191(3)	40.1(14)
C13B	7419(6)	6363.5(15)	7797(2)	17.5(9)
C13S	452(8)	7307.5(17)	3449(3)	33.5(12)
C14B	7485(6)	6742.6(15)	7408(3)	20.4(10)
C14S	2858(10)	7095(2)	2423(3)	55.2(18)
C15B	7408(6)	6755.5(16)	6546(3)	21.8(10)
C16B	7371(6)	6387.2(16)	6097(2)	20.0(10)
C18B	7586(7)	7130.2(14)	7893(2)	21.0(10)
C19B	6120(7)	7225.0(14)	8420(3)	26.2(10)
C20B	6133(8)	7591.1(16)	8852(3)	35.0(13)
C21B	7625(8)	7862.1(16)	8761(3)	31.2(12)
C22B	9134(7)	7775.4(16)	8256(3)	26.7(10)
C23B	9116(7)	7409.6(14)	7826(3)	21.6(10)
C25B	12046(8)	7592.4(18)	7169(3)	35.1(13)
C26B	7351(7)	6383.3(16)	5180(3)	24.3(10)
C27B	7291(8)	7148.2(16)	6076(3)	28.7(11)
C29B	9397(6)	6612.8(14)	9666(2)	19.8(9)
C30B	11060(7)	6840.6(15)	9495(3)	23.8(10)
C31B	11436(7)	7198.9(16)	9900(3)	28.1(11)
C32B	10103(7)	7354.3(16)	10455(3)	28.3(11)
C33B	10413(8)	7738.0(17)	10854(3)	35.6(13)
C34B	9077(9)	7891.9(17)	11362(3)	39.1(13)
C35B	7364(9)	7675.3(17)	11489(3)	35.2(13)
C36B	7038(8)	7306.4(16)	11130(3)	26.9(10)
C37B	8429(7)	7127.1(15)	10622(2)	23.9(10)
C38B	8143(7)	6731.4(15)	10258(2)	21.1(9)
C40B	5311(6)	6284.9(14)	9919(2)	19.6(10)
C41B	3668(7)	6057.2(15)	10149(3)	22.3(10)
C42B	3331(7)	5990.9(16)	10949(3)	23.7(10)
C43B	4682(7)	6122.5(15)	11569(3)	23.4(10)
C44B	4452(7)	6029.4(16)	12412(3)	26.9(11)
C45B	5792(8)	6146.3(16)	12998(3)	29.6(11)
C46B	7464(7)	6354.8(16)	12780(3)	27.7(11)

C47B	7731(7)	6455.6(15)	11977(3)	23.8(10)
C48B	6332(7)	6353.1(15)	11346(2)	21.3(10)
C49B	6541(6)	6457.7(14)	10503(2)	18.4(9)
B1B	7383(7)	6206.0(16)	8746(3)	19.5(11)

**Table 3 Anisotropic Displacement Parameters ( $\text{\AA}^2 \times 10^3$ ) for 2018ncs0765t. The Anisotropic displacement factor exponent takes the form:  $-2\pi^2[h^2a^{*2}U_{11}+2hka^*b^*U_{12}+\dots]$ .**

Atom	$U_{11}$	$U_{22}$	$U_{33}$	$U_{23}$	$U_{13}$	$U_{12}$
O24A	27.7(18)	13.9(19)	40.8(19)	-3.2(14)	-7.0(13)	1.0(15)
O28A	25.5(16)	11.2(17)	22.3(15)	-3.7(12)	1.1(11)	-1.2(13)
O39A	25.6(17)	15.4(18)	19.9(15)	-0.7(12)	-0.1(11)	-0.6(14)
N2A	21(2)	10(2)	22.5(19)	0.0(14)	-0.1(13)	2.0(16)
N17A	20(2)	15(2)	24(2)	-1.0(15)	-1.0(14)	0.3(17)
C3A	17(2)	10(2)	24(2)	-1.2(16)	-0.6(15)	-3.7(18)
C4A	24(3)	12(3)	29(2)	-0.3(17)	4.2(17)	-3(2)
C5A	27(2)	23(3)	23(2)	4.2(18)	2.1(17)	0(2)
C6A	22(2)	16(3)	36(3)	7(2)	1.4(18)	-3(2)
C7A	23(3)	9(3)	42(3)	2.9(19)	-0.5(18)	-1(2)
C8A	12(2)	15(3)	31(2)	0.8(18)	-1.9(16)	-0.5(18)
C9A	19(2)	10(2)	35(3)	-3.8(18)	-1.1(17)	1.4(19)
C10A	20(2)	13(3)	27(2)	-4.1(17)	0.5(16)	3.1(19)
C11A	16(2)	14(3)	24(2)	-2.1(17)	-2.2(15)	-0.5(19)
C12A	15(2)	14(3)	24(2)	-0.7(17)	-1.1(15)	1.7(19)
C13A	17(2)	15(3)	23(2)	-1.9(17)	1.6(15)	1.2(19)
C14A	16(2)	12(2)	25(2)	0.6(17)	-2.0(15)	-1.6(19)
C15A	14(2)	14(2)	29(2)	4.2(18)	0.2(15)	0.0(19)
C16A	10(2)	21(3)	25(2)	0.6(18)	-0.8(15)	-0.1(19)
C18A	35(3)	10(2)	24(2)	3.8(17)	4.1(18)	-1(2)
C19A	40(3)	14(3)	38(3)	1(2)	-10(2)	2(2)
C20A	43(3)	22(3)	54(3)	-8(2)	-25(2)	1(3)
C21A	54(4)	12(3)	47(3)	-8(2)	-9(2)	3(3)
C22A	36(3)	10(3)	35(3)	0.9(18)	-0.8(19)	2(2)
C23A	26(2)	14(2)	25(2)	6.5(18)	2.0(17)	-1(2)
C25A	37(3)	29(3)	62(4)	-12(3)	-15(2)	8(3)
C26A	21(2)	27(3)	26(2)	1.0(19)	2.3(17)	-1(2)
C27A	29(3)	21(3)	27(2)	6.1(19)	-0.2(17)	-2(2)
C29A	23(2)	13(2)	22(2)	1.9(16)	6.6(16)	-0.1(19)
C30A	29(3)	22(3)	26(2)	1.1(18)	0.9(17)	4(2)
C31A	37(3)	28(3)	32(3)	3(2)	0(2)	16(2)
C32A	50(3)	17(3)	28(2)	-1.2(19)	6(2)	7(2)
C33A	63(4)	22(3)	38(3)	-1(2)	2(2)	18(3)
C34A	75(4)	12(3)	47(3)	-7(2)	3(3)	10(3)
C35A	68(4)	18(3)	33(3)	-7(2)	0(2)	-5(3)

C36A	42(3)	15(3)	31(3)	-2.8(19)	1.4(19)	-3(2)
C37A	38(3)	16(3)	22(2)	-0.5(18)	2.1(18)	2(2)
C38A	25(2)	12(2)	22(2)	1.5(17)	3.8(16)	1(2)
C40A	27(2)	16(3)	21(2)	-1.6(17)	0.8(16)	-5(2)
C41A	29(3)	17(3)	29(3)	-1.7(18)	1.5(17)	-2(2)
C42A	28(3)	18(3)	31(3)	1.2(19)	-2.7(18)	2(2)
C43A	30(3)	18(3)	25(2)	-2.1(18)	-4.1(17)	-7(2)
C44A	34(3)	17(3)	29(3)	2.2(18)	-4.2(19)	-6(2)
C45A	44(3)	21(3)	22(2)	3.1(19)	-4.3(19)	-9(2)
C46A	42(3)	28(3)	23(2)	-5(2)	5.5(19)	-11(3)
C47A	26(3)	19(3)	29(2)	-2.9(19)	-0.6(17)	-4(2)
C48A	33(3)	11(2)	24(2)	-3.1(17)	-1.2(17)	-7(2)
C49A	28(2)	12(2)	22(2)	-2.4(17)	-1.8(16)	-3(2)
B1A	22(3)	11(3)	23(2)	0.1(19)	-0.1(18)	2(2)
O24B	29.6(18)	15.9(18)	37.3(19)	-2.4(14)	5.5(13)	-1.0(15)
O28B	27.7(17)	12.9(18)	20.9(15)	-2.0(12)	0.5(11)	-0.8(14)
O39B	25.0(16)	11.3(17)	19.3(15)	-2.2(11)	1.1(11)	-1.9(14)
N2B	17.8(19)	10(2)	24.3(19)	-1.2(14)	1.0(13)	-0.5(15)
N17B	15.3(19)	19(2)	22.9(19)	-0.9(15)	-0.1(13)	-1.5(16)
C1S	43(3)	17(3)	36(3)	0(2)	4(2)	2(2)
C2S	39(3)	26(3)	48(3)	3(2)	3(2)	-6(3)
C3B	14(2)	13(3)	26(2)	2.2(17)	0.0(16)	0.2(18)
C3S	63(4)	20(3)	37(3)	3(2)	-1(2)	-4(3)
C4B	24(2)	14(3)	28(2)	0.8(18)	-3.6(17)	3(2)
C4S	58(4)	19(3)	37(3)	2(2)	12(2)	8(3)
C5B	25(2)	23(3)	23(2)	0.1(18)	-2.2(17)	4(2)
C5S	41(3)	20(3)	40(3)	12(2)	4(2)	4(2)
C6B	16(2)	21(3)	33(3)	9.1(19)	-2.5(17)	-2(2)
C6S	38(3)	22(3)	32(3)	9(2)	-4(2)	-2(2)
C7B	22(2)	9(2)	38(3)	-0.5(18)	-4.4(18)	0(2)
C7S	60(4)	45(4)	58(4)	-12(3)	21(3)	-3(3)
C8B	14(2)	18(3)	29(2)	-0.4(18)	-0.4(16)	0.1(19)
C8S	45(3)	16(3)	36(3)	9(2)	-1(2)	0(2)
C9B	17(2)	11(2)	33(2)	-3.7(17)	2.1(16)	-1.7(19)
C9S	37(3)	22(3)	47(3)	10(2)	0(2)	-4(2)
C10B	20(2)	17(3)	23(2)	-5.2(17)	0.7(16)	-4.1(19)
C10S	60(4)	26(3)	41(3)	4(2)	-12(3)	-8(3)
C11B	15(2)	15(2)	23(2)	0.3(17)	1.2(15)	-0.7(19)
C11S	69(4)	20(3)	38(3)	2(2)	0(3)	6(3)
C12B	10(2)	14(3)	27(2)	-1.3(17)	2.9(15)	-1.1(18)
C12S	45(3)	30(3)	45(3)	11(2)	5(2)	3(3)
C13B	16(2)	16(3)	21(2)	-4.5(17)	2.7(15)	-0.1(19)
C13S	41(3)	20(3)	38(3)	8(2)	-7(2)	-2(2)
C14B	18(2)	19(3)	24(2)	0.5(18)	0.5(16)	-1.3(19)
C14S	64(4)	65(5)	37(3)	-9(3)	0(3)	5(4)

C15B	18(2)	21(3)	26(2)	2.5(18)	1.8(16)	-3(2)
C16B	15(2)	22(3)	23(2)	-1.7(18)	1.5(16)	0(2)
C18B	30(3)	9(2)	23(2)	3.9(17)	-2.4(17)	3(2)
C19B	32(3)	10(3)	37(3)	1.9(18)	7.6(19)	2(2)
C20B	54(3)	16(3)	37(3)	-1(2)	22(2)	4(3)
C21B	52(3)	12(3)	30(3)	-0.4(19)	5(2)	0(2)
C22B	37(3)	16(3)	27(2)	2.6(19)	-1.7(18)	-2(2)
C23B	28(2)	14(3)	22(2)	3.7(17)	-0.8(17)	4(2)
C25B	30(3)	29(3)	47(3)	-5(2)	10(2)	-9(2)
C26B	23(2)	24(3)	26(2)	-0.3(19)	0.3(16)	0(2)
C27B	41(3)	21(3)	24(2)	4.5(19)	1.4(19)	-2(2)
C29B	27(2)	13(2)	19(2)	2.9(16)	-3.5(16)	0(2)
C30B	24(2)	21(3)	26(2)	5.4(18)	-0.2(17)	1(2)
C31B	30(3)	20(3)	34(3)	5(2)	-3.0(19)	-9(2)
C32B	37(3)	20(3)	28(2)	1.8(19)	-10.0(19)	-3(2)
C33B	48(3)	15(3)	42(3)	4(2)	-12(2)	-6(3)
C34B	57(4)	14(3)	45(3)	-4(2)	-12(2)	-3(3)
C35B	52(3)	19(3)	34(3)	-6(2)	-2(2)	8(3)
C36B	38(3)	15(2)	28(2)	-1.9(18)	-1.3(18)	1(2)
C37B	33(3)	17(3)	22(2)	-0.3(18)	-5.6(17)	2(2)
C38B	25(2)	17(2)	20(2)	3.0(17)	-5.7(16)	-2(2)
C40B	24(2)	12(2)	22(2)	-3.0(17)	2.1(16)	4(2)
C41B	28(3)	14(3)	24(2)	-2.8(18)	-3.2(17)	0(2)
C42B	24(2)	18(3)	29(2)	1.1(19)	2.6(17)	-3(2)
C43B	28(3)	16(3)	26(2)	-3.9(18)	3.4(17)	2(2)
C44B	35(3)	20(3)	25(2)	2.7(19)	7.1(18)	-3(2)
C45B	42(3)	22(3)	25(2)	2.4(19)	0.8(19)	3(2)
C46B	35(3)	24(3)	24(2)	-7.1(19)	-5.0(18)	4(2)
C47B	28(3)	15(3)	28(2)	-0.4(18)	0.1(17)	0(2)
C48B	27(2)	14(2)	23(2)	-2.4(17)	1.2(16)	6(2)
C49B	20(2)	9(2)	26(2)	-3.0(16)	4.5(16)	3.3(18)
B1B	26(3)	7(3)	25(3)	-3.5(19)	2.5(19)	-4(2)

**Table 4 Bond Lengths for 2018ncs0765t.**

Atom Atom	Length/Å	Atom Atom	Length/Å
O24A C23A	1.369(6)	N2B C11B	1.336(5)
O24A C25A	1.424(7)	N2B B1B	1.681(6)
O28A C29A	1.363(5)	N17B C12B	1.335(5)
O28A B1A	1.452(6)	N17B C16B	1.340(6)
O39A C40A	1.368(5)	C1S C2S	1.410(8)
O39A B1A	1.448(6)	C1S C6S	1.373(7)
N2A C3A	1.371(6)	C1S C7S	1.493(8)
N2A C11A	1.333(5)	C2S C3S	1.375(8)

---

N2A B1A	1.685(7)	C3B C4B	1.406(6)
N17A C12A	1.335(5)	C3B C8B	1.417(7)
N17A C16A	1.348(6)	C3S C4S	1.367(8)
C3A C4A	1.411(6)	C4B C5B	1.376(7)
C3A C8A	1.423(6)	C4S C5S	1.395(8)
C4A C5A	1.366(7)	C5B C6B	1.404(7)
C5A C6A	1.409(7)	C5S C6S	1.366(7)
C6A C7A	1.346(6)	C6B C7B	1.362(6)
C7A C8A	1.410(6)	C7B C8B	1.417(7)
C8A C9A	1.411(6)	C8B C9B	1.406(6)
C9A C10A	1.360(6)	C8S C9S	1.388(8)
C10A C11A	1.401(6)	C8S C13S	1.372(8)
C11A C12A	1.459(6)	C8S C14S	1.488(8)
C12A C13A	1.390(6)	C9B C10B	1.368(7)
C13A C14A	1.400(6)	C9S C10S	1.383(8)
C13A B1A	1.621(6)	C10B C11B	1.398(6)
C14A C15A	1.403(6)	C10S C11S	1.384(9)
C14A C18A	1.505(6)	C11B C12B	1.455(6)
C15A C16A	1.400(7)	C11S C12S	1.364(8)
C15A C27A	1.505(6)	C12B C13B	1.397(6)
C16A C26A	1.495(6)	C12S C13S	1.376(7)
C18A C19A	1.384(7)	C13B C14B	1.396(6)
C18A C23A	1.391(7)	C13B B1B	1.633(6)
C19A C20A	1.396(7)	C14B C15B	1.407(6)
C20A C21A	1.356(8)	C14B C18B	1.496(6)
C21A C22A	1.381(7)	C15B C16B	1.411(7)
C22A C23A	1.394(6)	C15B C27B	1.498(7)
C29A C30A	1.401(6)	C16B C26B	1.496(6)
C29A C38A	1.389(6)	C18B C19B	1.386(7)
C30A C31A	1.360(7)	C18B C23B	1.402(7)
C31A C32A	1.401(8)	C19B C20B	1.391(7)
C32A C33A	1.420(7)	C20B C21B	1.369(8)
C32A C37A	1.421(7)	C21B C22B	1.380(7)
C33A C34A	1.362(9)	C22B C23B	1.388(7)
C34A C35A	1.397(9)	C29B C30B	1.402(6)
C35A C36A	1.385(7)	C29B C38B	1.376(6)
C36A C37A	1.420(7)	C30B C31B	1.367(7)
C37A C38A	1.437(6)	C31B C32B	1.409(7)
C38A C49A	1.480(6)	C32B C33B	1.428(7)
C40A C41A	1.416(7)	C32B C37B	1.406(7)
C40A C49A	1.371(6)	C33B C34B	1.359(8)
C41A C42A	1.356(6)	C34B C35B	1.397(8)
C42A C43A	1.414(7)	C35B C36B	1.358(7)
C43A C44A	1.421(6)	C36B C37B	1.417(7)
C43A C48A	1.418(7)	C37B C38B	1.436(7)

---

C44A C45A	1.361(7)	C38B C49B	1.486(6)
C45A C46A	1.394(8)	C40B C41B	1.417(7)
C46A C47A	1.371(7)	C40B C49B	1.371(6)
C47A C48A	1.407(7)	C41B C42B	1.353(6)
C48A C49A	1.447(6)	C42B C43B	1.413(7)
O24B C23B	1.374(6)	C43B C44B	1.423(6)
O24B C25B	1.431(6)	C43B C48B	1.422(7)
O28B C29B	1.367(5)	C44B C45B	1.356(7)
O28B B1B	1.444(6)	C45B C46B	1.395(7)
O39B C40B	1.363(5)	C46B C47B	1.371(6)
O39B B1B	1.446(6)	C47B C48B	1.421(6)
N2B C3B	1.378(6)	C48B C49B	1.431(6)

**Table 5 Bond Angles for 2018ncs0765t.**

Atom Atom Atom Angle/°	Atom Atom Atom Angle/°		
C23A O24A C25A	117.6(4)	C6S C1S C2S	118.3(5)
C29A O28A B1A	119.2(3)	C6S C1S C7S	121.4(5)
C40A O39A B1A	120.8(3)	C3S C2S C1S	119.9(5)
C3A N2A B1A	130.0(3)	N2B C3B C4B	121.5(4)
C11A N2A C3A	120.2(4)	N2B C3B C8B	118.8(4)
C11A N2A B1A	109.8(3)	C4B C3B C8B	119.7(4)
C12A N17A C16A	115.4(4)	C4S C3S C2S	120.8(5)
N2A C3A C4A	121.7(4)	C5B C4B C3B	119.4(4)
N2A C3A C8A	119.3(4)	C3S C4S C5S	119.7(5)
C4A C3A C8A	119.0(4)	C4B C5B C6B	121.5(4)
C5A C4A C3A	119.9(4)	C6S C5S C4S	119.6(5)
C4A C5A C6A	121.1(4)	C7B C6B C5B	119.5(4)
C7A C6A C5A	119.6(4)	C5S C6S C1S	121.7(5)
C6A C7A C8A	121.8(5)	C6B C7B C8B	121.0(4)
C7A C8A C3A	118.4(4)	C7B C8B C3B	118.7(4)
C7A C8A C9A	122.6(4)	C9B C8B C3B	119.5(4)
C9A C8A C3A	118.9(4)	C9B C8B C7B	121.7(4)
C10A C9A C8A	120.1(4)	C9S C8S C14S	120.3(5)
C9A C10A C11A	118.7(4)	C13S C8S C9S	117.9(5)
N2A C11A C10A	122.8(4)	C13S C8S C14S	121.8(5)
N2A C11A C12A	111.8(4)	C10B C9B C8B	120.2(4)
C10A C11A C12A	125.4(4)	C10S C9S C8S	121.0(5)
N17A C12A C11A	120.2(4)	C9B C10B C11B	118.1(4)
N17A C12A C13A	127.8(4)	C9S C10S C11S	119.7(5)
C13A C12A C11A	112.0(4)	N2B C11B C10B	123.0(4)
C12A C13A C14A	115.8(4)	N2B C11B C12B	111.7(4)
C12A C13A B1A	109.1(4)	C10B C11B C12B	125.2(4)
C14A C13A B1A	135.0(4)	C12S C11S C10S	119.4(5)

---

C13A C14A C15A	118.6(4)	N17B C12B C11B	120.0(4)
C13A C14A C18A	120.6(4)	N17B C12B C13B	127.6(4)
C15A C14A C18A	120.9(4)	C13B C12B C11B	112.3(4)
C14A C15A C27A	122.2(4)	C11S C12S C13S	120.5(5)
C16A C15A C14A	119.8(4)	C12B C13B B1B	108.7(4)
C16A C15A C27A	117.9(4)	C14B C13B C12B	115.7(4)
N17A C16A C15A	122.6(4)	C14B C13B B1B	135.5(4)
N17A C16A C26A	115.6(4)	C8S C13S C12S	121.5(5)
C15A C16A C26A	121.8(4)	C13B C14B C15B	118.7(4)
C19A C18A C14A	119.8(4)	C13B C14B C18B	121.1(4)
C19A C18A C23A	118.2(4)	C15B C14B C18B	120.2(4)
C23A C18A C14A	122.0(4)	C14B C15B C16B	119.5(4)
C18A C19A C20A	120.9(5)	C14B C15B C27B	122.4(4)
C21A C20A C19A	119.7(5)	C16B C15B C27B	118.0(4)
C20A C21A C22A	121.2(5)	N17B C16B C15B	122.5(4)
C21A C22A C23A	118.9(5)	N17B C16B C26B	115.8(4)
O24A C23A C18A	116.9(4)	C15B C16B C26B	121.7(4)
O24A C23A C22A	122.0(4)	C19B C18B C14B	119.9(4)
C18A C23A C22A	121.1(4)	C19B C18B C23B	118.0(4)
O28A C29A C30A	117.5(4)	C23B C18B C14B	122.1(4)
O28A C29A C38A	120.5(4)	C18B C19B C20B	121.2(5)
C38A C29A C30A	121.9(4)	C21B C20B C19B	119.6(5)
C31A C30A C29A	119.5(4)	C20B C21B C22B	121.0(5)
C30A C31A C32A	121.9(5)	C21B C22B C23B	119.2(5)
C31A C32A C33A	122.4(5)	O24B C23B C18B	116.0(4)
C31A C32A C37A	118.8(4)	O24B C23B C22B	123.0(4)
C33A C32A C37A	118.8(5)	C22B C23B C18B	121.0(4)
C34A C33A C32A	121.4(5)	O28B C29B C30B	117.5(4)
C33A C34A C35A	120.1(5)	O28B C29B C38B	120.5(4)
C36A C35A C34A	120.5(5)	C38B C29B C30B	121.9(4)
C35A C36A C37A	120.6(5)	C31B C30B C29B	120.0(4)
C32A C37A C38A	119.6(4)	C30B C31B C32B	120.4(5)
C36A C37A C32A	118.5(4)	C31B C32B C33B	121.5(5)
C36A C37A C38A	121.9(4)	C37B C32B C31B	119.5(5)
C29A C38A C37A	117.8(4)	C37B C32B C33B	119.1(5)
C29A C38A C49A	120.1(4)	C34B C33B C32B	120.8(5)
C37A C38A C49A	122.1(4)	C33B C34B C35B	119.8(5)
O39A C40A C41A	117.6(4)	C36B C35B C34B	120.9(5)
O39A C40A C49A	121.3(4)	C35B C36B C37B	121.2(5)
C49A C40A C41A	121.1(4)	C32B C37B C36B	118.1(5)
C42A C41A C40A	120.6(4)	C32B C37B C38B	119.8(4)
C41A C42A C43A	120.7(5)	C36B C37B C38B	122.1(5)
C42A C43A C44A	122.3(5)	C29B C38B C37B	117.7(4)
C42A C43A C48A	118.8(4)	C29B C38B C49B	120.7(4)
C48A C43A C44A	118.8(4)	C37B C38B C49B	121.6(4)

C45A C44A C43A	120.8(5)	O39B C40B C41B	117.1(4)
C44A C45A C46A	120.3(4)	O39B C40B C49B	122.3(4)
C47A C46A C45A	120.4(4)	C49B C40B C41B	120.6(4)
C46A C47A C48A	121.0(5)	C42B C41B C40B	120.7(4)
C43A C48A C49A	119.6(4)	C41B C42B C43B	120.6(4)
C47A C48A C43A	118.5(4)	C42B C43B C44B	122.1(4)
C47A C48A C49A	121.7(4)	C42B C43B C48B	119.2(4)
C40A C49A C38A	121.3(4)	C48B C43B C44B	118.8(4)
C40A C49A C48A	118.0(4)	C45B C44B C43B	121.5(5)
C48A C49A C38A	120.6(4)	C44B C45B C46B	120.1(4)
O28A B1A N2A	102.2(3)	C47B C46B C45B	120.3(4)
O28A B1A C13A	118.6(4)	C46B C47B C48B	121.5(5)
O39A B1A O28A	116.0(4)	C43B C48B C49B	119.0(4)
O39A B1A N2A	111.2(4)	C47B C48B C43B	117.6(4)
O39A B1A C13A	109.6(4)	C47B C48B C49B	123.3(4)
C13A B1A N2A	97.0(3)	C40B C49B C38B	120.3(4)
C23B O24B C25B	117.2(4)	C40B C49B C48B	119.2(4)
C29B O28B B1B	117.6(3)	C48B C49B C38B	120.4(4)
C40B O39B B1B	121.0(3)	O28B B1B O39B	116.3(4)
C3B N2B B1B	129.4(3)	O28B B1B N2B	102.5(4)
C11B N2B C3B	120.3(4)	O28B B1B C13B	118.5(4)
C11B N2B B1B	110.3(3)	O39B B1B N2B	110.6(4)
C12B N17B C16B	115.8(4)	O39B B1B C13B	109.7(4)
C2S C1S C7S	120.2(5)	C13B B1B N2B	96.9(3)

**Table 6 Hydrogen Atom Coordinates ( $\text{\AA} \times 10^4$ ) and Isotropic Displacement Parameters ( $\text{\AA}^2 \times 10^3$ ) for 2018ncs0765t.**

Atom	$x$	$y$	$z$	$U(\text{eq})$	
H4A	2555.45		5491	4957.28	26
H5A	2359.3		6045.1	4083.36	29
H6A	2231.15		6714.69	4602.22	30
H7A	2225.97		6821.36	5986.58	30
H9A	2169.77		6547.34	7417.66	26
H10A	2165.73		5986.44	8284.74	24
H19A	100.58		4139.41	6593.86	37
H20A	269.62		3534.25	5836.2	48
H21A	2915.88		3109.52	6016.77	46
H22A	5465.67		3276.21	6939.89	32
H25A	8193.45		3767.34	8443.35	65
H25B	7996.08		3606.79	7517.63	65
H25C	6770.49		3394.31	8213.82	65
H	989.86		4701.43	10089.55	37
HA	2316.26		5103.04	10124.31	37

---

HB	3310.01	4661.36	10168.23	37
H27A	1343.2	4054.65	9412.57	39
H27B	3663.27	4030.35	9375.52	39
H27C	2317.77	3826.05	8665.43	39
H30A	6870.22	4440.31	6063.66	31
H31A	7442.04	3856.71	5327.73	39
H33A	6375.74	3338.23	4292.64	49
H34A	4085.22	3101.55	3341.46	54
H35A	1177.73	3461.61	3090.79	48
H36A	643.43	4079.68	3747.94	35
HC	-2382.63	5241.23	5311.28	30
HD	-3076.4	5372.15	3947.02	31
HE	-1929.15	5405.34	2504.53	33
H45A	415.08	5262.53	1576.72	35
H46A	3253.23	4913.36	1993.46	37
H47A	3681.06	4683.02	3326.64	30
H2S	4909.56	3681.72	1574.84	45
H3S	6151.37	3384.56	415.51	48
HF	7523.27	5698.12	10152.88	27
H4S	9348.76	3495.91	83.45	45
HG	7221.41	5137.74	11006.81	28
HH	11347.87	3920.59	916.8	40
HI	6987.9	4473.67	10471.79	28
HJ	10126.4	4214.51	2073.13	37
H7B	7070.44	4371.75	9074.4	27
H7SA	6700.95	4491.01	2605.59	81
H7SB	7321.63	4108	3165.84	81
H7SC	5219.36	4119.36	2708.51	81
H9B	7176.92	4653.56	7663.62	24
H9S	5115.66	7411.13	3611.72	43
H10B	7281.92	5218.5	6798.54	24
HK	4341.27	7704.2	4856.54	51
HL	1090.9	7737.29	5225.31	51
HM	-1331.05	7484.14	4340.02	48
HN	-562.93	7209.59	3088.53	40
H14A	4247.18	7026.2	2440.21	83
H14B	2576.66	7288.94	1977.34	83
H14C	2089.27	6845.9	2328.01	83
H19B	5088.18	7036.59	8487.67	31
HO	5111.95	7652.76	9207.81	42
HP	7621.65	8113.65	9050.78	37
HQ	10171.47	7963.85	8202.64	32
HR	12963.21	7479.95	6783.86	53
HS	12746.65	7663.62	7684.35	53
HT	11430.18	7837.48	6932.37	53

H26A	6069.22	6470.57	4961.52	36
H26B	7622.13	6106.35	4987.86	36
H26C	8349.82	6570.44	4989.29	36
H27D	6246.66	7130.35	5651.43	43
H27E	8533.28	7198.44	5819.08	43
H27F	7018.05	7372.92	6451.19	43
HU	11924.49	6745.9	9096.54	29
HV	12603.17	7344.03	9806.55	34
HW	11569.15	7887.6	10763.11	43
HX	9305.9	8145.83	11630.15	47
HY	6414.21	7787.67	11831.27	42
HZ	5855.92	7166.05	11220	32
H41B	2794.5	5949.99	9737.88	27
H0AA	2174.9	5854.69	11095.99	28
H1AA	3334.58	5882.12	12566.92	32
H2AA	5591.48	6086.06	13557.31	35
H3AA	8421.13	6427.3	13189.75	33
H4AA	8879.11	6597.15	11838.65	29

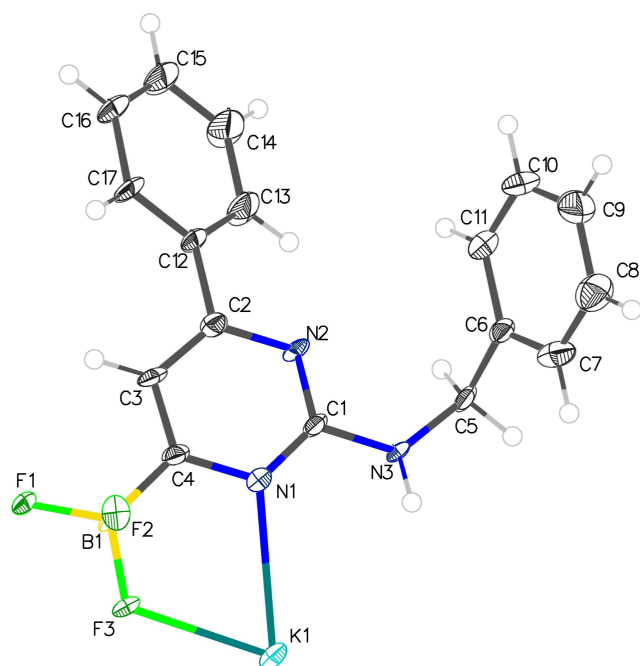
#### Crystal structure determination of 2018ncs0765t

**Crystal Data** for  $C_{50}H_{39}BN_2O_3$  ( $M=726.64$  g/mol): monoclinic, space group  $P2_1$  (no. 4),  $a = 6.8740(4)$  Å,  $b = 32.7563(18)$  Å,  $c = 16.3196(11)$  Å,  $\beta = 92.276(6)^\circ$ ,  $V = 3671.7(4)$  Å<sup>3</sup>,  $Z = 4$ ,  $T = 100.15$  K,  $\mu(\text{MoK}\alpha) = 0.081$  mm<sup>-1</sup>,  $D_{\text{calc}} = 1.314$  g/cm<sup>3</sup>, 22769 reflections measured ( $3.524^\circ \leq 2\theta \leq 55.054^\circ$ ), 22769 unique ( $R_{\text{int}} = ?$ ,  $R_{\text{sigma}} = 0.0466$ ) which were used in all calculations. The final  $R_1$  was 0.0587 ( $I > 2\sigma(I)$ ) and  $wR_2$  was 0.1515 (all data).

---

## X-ray crystal structure data for compound 31a

ORTEP of 6, thermal ellipsoids are shown at 50% probability



### Crystal structure determination of compound 31a

Crystals of 32a were grown from a saturated acetone solution, allowing slow evaporation.

**Crystal Data** for  $C_{17}H_{14}BF_3KN_3$  ( $M = 367.22$  g/mol): monoclinic, space group  $P2_1/c$  (no. 14),  $a = 18.251(5)$  Å,  $b = 10.005(3)$  Å,  $c = 9.1105(18)$  Å,  $\beta = 94.150(16)^\circ$ ,  $V = 1659.2(7)$  Å<sup>3</sup>,  $Z = 4$ ,  $T = 100$  K,  $\mu(\text{MoK}\alpha) = 0.355$  mm<sup>-1</sup>,  $D_{\text{calc}} = 1.470$  g/cm<sup>3</sup>, 4270 reflections measured ( $4.476^\circ \leq 2\theta \leq 46.598^\circ$ ), 2330 unique ( $R_{\text{int}} = 0.0897$ ,  $R_{\text{sigma}} = 0.1525$ ) which were used in all calculations. The final  $R_1$  was 0.0678 ( $I > 2\sigma(I)$ ) and  $wR_2$  was 0.1452 (all data).

**Table 1 Crystal data and structure refinement for ojH388k.**

Identification code	ojH388k
Empirical formula	C <sub>17</sub> H <sub>14</sub> BF <sub>3</sub> KN <sub>3</sub>
Formula weight	367.22
Temperature/K	100
Crystal system	monoclinic
Space group	P2 <sub>1</sub> /c
a/Å	18.251(5)
b/Å	10.005(3)
c/Å	9.1105(18)
α/°	90
β/°	94.150(16)
γ/°	90
Volume/Å <sup>3</sup>	1659.2(7)
Z	4
ρ <sub>calc</sub> /cm <sup>3</sup>	1.470
μ/mm <sup>-1</sup>	0.355
F(000)	752.0
Crystal size/mm <sup>3</sup>	0.61 × 0.21 × 0.025
Radiation	MoKα (λ = 0.71073)
2Θ range for data collection/°	4.476 to 46.598
Index ranges	-14 ≤ h ≤ 20, -9 ≤ k ≤ 11, -10 ≤ l ≤ 10
Reflections collected	4270
Independent reflections	2330 [R <sub>int</sub> = 0.0897, R <sub>sigma</sub> = 0.1525]
Data/restraints/parameters	2330/199/226
Goodness-of-fit on F <sup>2</sup>	1.021
Final R indexes [I>=2σ (I)]	R <sub>1</sub> = 0.0678, wR <sub>2</sub> = 0.1209
Final R indexes [all data]	R <sub>1</sub> = 0.1523, wR <sub>2</sub> = 0.1452
Largest diff. peak/hole / e Å <sup>-3</sup>	0.44/-0.44

**Table 2 Fractional Atomic Coordinates (×10<sup>4</sup>) and Equivalent Isotropic Displacement Parameters (Å<sup>2</sup>×10<sup>3</sup>) for ojH388k. U<sub>eq</sub> is defined as 1/3 of of the trace of the orthogonalised U<sub>ij</sub> tensor.**

Atom	x	y	z	U(eq)
K1	4804.9(7)	2868.2(15)	5155.8(15)	20.5(4)
F1	5722.0(16)	4324(4)	727(3)	23.6(10)
N1	6075(3)	4493(5)	4782(5)	17.9(13)
C1	6653(3)	4283(6)	5805(6)	16.6(15)
B1	5562(4)	4735(8)	2153(8)	16.5(16)
F2	5350.8(17)	6104(4)	2087(4)	24.4(9)
N2	7360(3)	4100(6)	5533(5)	21.3(14)

C2	7517(3)	4156(7)	4114(7)	20.5(16)
F3	4923.1(17)	3994(4)	2490(3)	21.8(9)
N3	6485(2)	4228(5)	7237(5)	20.0(14)
C3	6962(3)	4334(6)	3002(7)	17.6(15)
C4	6240(3)	4500(6)	3351(6)	16.8(14)
C5	7052(3)	4058(7)	8443(6)	21.8(16)
C6	7437(3)	5366(7)	8943(6)	20.4(15)
C7	7084(4)	6267(7)	9760(7)	28.0(17)
C8	7439(4)	7439(8)	10294(8)	37.0(19)
C9	8161(4)	7658(9)	9991(8)	51(2)
C10	8512(4)	6751(10)	9158(8)	52(2)
C11	8157(4)	5597(9)	8628(7)	42(2)
C12	8301(3)	3998(8)	3825(7)	28.5(18)
C13	8770(3)	3262(8)	4785(7)	37(2)
C14	9508(4)	3134(10)	4535(8)	58(3)
C15	9791(4)	3781(10)	3362(8)	55(3)
C16	9328(3)	4536(9)	2420(8)	45(2)
C17	8585(3)	4647(8)	2643(7)	32(2)

**Table 3 Anisotropic Displacement Parameters ( $\text{\AA}^2 \times 10^3$ ) for ojH388k. The Anisotropic displacement factor exponent takes the form:  $-2\pi^2[h^2a^{*2}U_{11}+2hka^*b^*U_{12}+\dots]$ .**

Atom	$U_{11}$	$U_{22}$	$U_{33}$	$U_{23}$	$U_{13}$	$U_{12}$
K1	18.4(8)	25.5(9)	19.0(7)	1.5(8)	9.9(6)	-0.1(8)
F1	12.6(18)	44(3)	15.1(18)	-2.4(19)	6.6(15)	-1.8(18)
N1	16(3)	23(4)	16(2)	0(3)	5(2)	-3(3)
C1	16(3)	20(4)	15(3)	1(3)	8(2)	-3(3)
B1	15(4)	22(4)	13(3)	0(3)	10(3)	2(3)
F2	30(2)	23(2)	20(2)	-0.6(18)	0.3(17)	2.4(18)
N2	13(3)	32(4)	21(3)	-8(3)	12(2)	-1(3)
C2	16(3)	26(4)	20(3)	-5(3)	6(2)	-2(3)
F3	13.2(18)	34(3)	19.2(19)	1.0(19)	8.5(15)	-6.2(17)
N3	9(3)	36(4)	16(2)	-7(3)	9(2)	0(3)
C3	14(3)	16(4)	24(3)	-2(3)	11(2)	-6(3)
C4	14(3)	17(4)	20(3)	0(3)	6(2)	-5(3)
C5	17(3)	38(4)	12(3)	6(3)	8(3)	1(3)
C6	16(3)	31(4)	15(3)	8(3)	3(3)	-2(3)
C7	17(4)	31(4)	37(4)	8(3)	6(3)	1(3)
C8	41(4)	35(5)	36(4)	6(4)	8(3)	-4(3)
C9	46(4)	71(6)	35(5)	6(4)	-1(4)	-32(4)
C10	27(4)	93(7)	37(5)	2(5)	10(4)	-29(4)
C11	26(4)	80(6)	23(4)	0(4)	9(3)	-15(4)
C12	12(3)	57(5)	17(3)	-4(3)	7(3)	1(3)
C13	21(3)	66(6)	26(4)	2(4)	10(3)	13(4)

C14	21(4)	118(8)	34(4)	2(5)	6(3)	24(5)
C15	20(4)	113(8)	33(4)	-9(5)	14(3)	6(4)
C16	19(4)	91(7)	28(4)	-9(4)	16(3)	-5(4)
C17	15(3)	59(6)	23(4)	1(4)	13(3)	-1(4)

**Table 4 Bond Lengths for ojH388k.**

Atom	Atom	Length/Å	Atom	Atom	Length/Å
K1	K1 <sup>1</sup>	4.337(3)	B1	C4	1.607(9)
K1	K1 <sup>2</sup>	4.6144(10)	N2	C2	1.346(7)
K1	K1 <sup>3</sup>	4.6145(10)	C2	C3	1.390(8)
K1	F1 <sup>2</sup>	2.785(4)	C2	C12	1.483(8)
K1	N1 <sup>1</sup>	3.093(5)	N3	C5	1.464(7)
K1	N1	2.872(5)	C3	C4	1.387(7)
K1	B1 <sup>2</sup>	3.412(8)	C5	C6	1.538(9)
K1	B1 <sup>1</sup>	3.528(7)	C6	C7	1.361(9)
K1	F2 <sup>4</sup>	2.700(4)	C6	C11	1.384(8)
K1	F2 <sup>1</sup>	2.748(4)	C7	C8	1.408(9)
K1	F3 <sup>2</sup>	2.824(4)	C8	C9	1.383(9)
K1	F3	2.699(3)	C9	C10	1.372(11)
F1	B1	1.413(7)	C10	C11	1.394(11)
N1	C1	1.372(7)	C12	C13	1.389(9)
N1	C4	1.359(7)	C12	C17	1.389(9)
C1	N2	1.343(7)	C13	C14	1.388(8)
C1	N3	1.363(7)	C14	C15	1.381(10)
B1	F2	1.423(9)	C15	C16	1.383(10)
B1	F3	1.434(8)	C16	C17	1.390(8)

<sup>1</sup>1-X,1-Y,1-Z; <sup>2</sup>+X,1/2-Y,1/2+Z; <sup>3</sup>+X,1/2-Y,-1/2+Z; <sup>4</sup>1-X,-1/2+Y,1/2-Z

**Table 5 Bond Angles for ojH388k.**

Atom	Atom	Atom	Angle/°	Atom	Atom	Atom	Angle/°
K1 <sup>1</sup>	K1	K1 <sup>2</sup>	94.63(5)	F3 <sup>3</sup>	K1	B1 <sup>1</sup>	86.16(15)
K1 <sup>1</sup>	K1	K1 <sup>3</sup>	103.49(5)	F3	K1	F2 <sup>1</sup>	133.34(12)
K1 <sup>3</sup>	K1	K1 <sup>2</sup>	161.62(7)	F3	K1	F2 <sup>4</sup>	66.60(11)
F1 <sup>3</sup>	K1	K1 <sup>2</sup>	90.91(8)	F3	K1	F3 <sup>3</sup>	161.09(10)
F1 <sup>3</sup>	K1	K1 <sup>1</sup>	133.43(9)	B1	F1	K1 <sup>2</sup>	103.8(4)
F1 <sup>3</sup>	K1	K1 <sup>3</sup>	74.50(7)	K1	N1	K1 <sup>1</sup>	93.22(13)
F1 <sup>3</sup>	K1	N1	89.35(13)	C1	N1	K1 <sup>1</sup>	119.5(4)
F1 <sup>3</sup>	K1	N1 <sup>1</sup>	167.08(13)	C1	N1	K1	114.9(4)
F1 <sup>3</sup>	K1	B1 <sup>1</sup>	123.17(15)	C4	N1	K1 <sup>1</sup>	99.5(4)
F1 <sup>3</sup>	K1	B1 <sup>3</sup>	23.72(13)	C4	N1	K1	110.7(4)
F1 <sup>3</sup>	K1	F3 <sup>3</sup>	47.75(9)	C4	N1	C1	116.1(5)

---

N1	K1	K1 <sup>2</sup>	85.17(10)	N2	C1	N1	126.6(5)
N1 <sup>1</sup>	K1	K1 <sup>3</sup>	94.65(9)	N2	C1	N3	117.2(5)
N1 <sup>1</sup>	K1	K1 <sup>1</sup>	41.39(9)	N3	C1	N1	116.1(5)
N1	K1	K1 <sup>3</sup>	105.37(10)	K1 <sup>2</sup>	B1	K1 <sup>1</sup>	143.1(2)
N1	K1	K1 <sup>1</sup>	45.39(10)	F1	B1	K1 <sup>1</sup>	154.0(5)
N1 <sup>1</sup>	K1	K1 <sup>2</sup>	101.04(10)	F1	B1	K1 <sup>2</sup>	52.4(3)
N1	K1	N1 <sup>1</sup>	86.78(13)	F1	B1	F2	108.3(5)
N1 <sup>1</sup>	K1	B1 <sup>1</sup>	44.12(15)	F1	B1	F3	105.8(5)
N1	K1	B1 <sup>3</sup>	101.31(16)	F1	B1	C4	112.4(5)
N1 <sup>1</sup>	K1	B1 <sup>3</sup>	146.37(15)	F2	B1	K1 <sup>1</sup>	46.4(3)
N1	K1	B1 <sup>1</sup>	83.86(15)	F2	B1	K1 <sup>2</sup>	127.9(4)
B1 <sup>3</sup>	K1	K1 <sup>2</sup>	112.07(13)	F2	B1	F3	106.5(5)
B1 <sup>1</sup>	K1	K1 <sup>3</sup>	53.77(13)	F2	B1	C4	111.2(6)
B1 <sup>1</sup>	K1	K1 <sup>2</sup>	143.90(13)	F3	B1	K1 <sup>1</sup>	90.3(3)
B1 <sup>3</sup>	K1	K1 <sup>3</sup>	51.72(12)	F3	B1	K1 <sup>2</sup>	54.2(3)
B1 <sup>3</sup>	K1	K1 <sup>1</sup>	136.35(14)	F3	B1	C4	112.2(5)
B1 <sup>1</sup>	K1	K1 <sup>1</sup>	54.36(12)	C4	B1	K1 <sup>1</sup>	78.7(3)
B1 <sup>3</sup>	K1	B1 <sup>1</sup>	103.78(7)	C4	B1	K1 <sup>2</sup>	120.9(4)
F2 <sup>4</sup>	K1	K1 <sup>2</sup>	32.43(8)	K1 <sup>5</sup>	F2	K1 <sup>1</sup>	115.78(13)
F2 <sup>4</sup>	K1	K1 <sup>3</sup>	129.44(10)	B1	F2	K1 <sup>1</sup>	111.5(3)
F2 <sup>1</sup>	K1	K1 <sup>1</sup>	73.74(9)	B1	F2	K1 <sup>5</sup>	132.4(3)
F2 <sup>4</sup>	K1	K1 <sup>1</sup>	127.04(9)	C1	N2	C2	116.5(5)
F2 <sup>1</sup>	K1	K1 <sup>2</sup>	165.81(10)	N2	C2	C3	120.7(5)
F2 <sup>1</sup>	K1	K1 <sup>3</sup>	31.79(8)	N2	C2	C12	116.2(6)
F2 <sup>1</sup>	K1	F1 <sup>3</sup>	102.97(11)	C3	C2	C12	123.1(5)
F2 <sup>4</sup>	K1	F1 <sup>3</sup>	69.84(10)	K1	F3	K1 <sup>2</sup>	113.30(13)
F2 <sup>4</sup>	K1	N1	108.79(13)	B1	F3	K1	121.8(3)
F2 <sup>1</sup>	K1	N1 <sup>1</sup>	64.89(12)	B1	F3	K1 <sup>2</sup>	101.5(3)
F2 <sup>1</sup>	K1	N1	91.96(12)	C1	N3	C5	121.8(5)
F2 <sup>4</sup>	K1	N1 <sup>1</sup>	123.06(13)	C4	C3	C2	120.1(5)
F2 <sup>1</sup>	K1	B1 <sup>1</sup>	22.03(15)	N1	C4	B1	116.0(5)
F2 <sup>4</sup>	K1	B1 <sup>3</sup>	85.47(15)	N1	C4	C3	119.9(6)
F2 <sup>4</sup>	K1	B1 <sup>1</sup>	162.85(15)	C3	C4	B1	124.0(5)
F2 <sup>1</sup>	K1	B1 <sup>3</sup>	82.12(14)	N3	C5	C6	114.0(5)
F2 <sup>4</sup>	K1	F2 <sup>1</sup>	157.58(11)	C7	C6	C5	120.1(6)
F2 <sup>4</sup>	K1	F3 <sup>3</sup>	97.86(11)	C7	C6	C11	119.7(7)
F2 <sup>1</sup>	K1	F3 <sup>3</sup>	64.26(11)	C11	C6	C5	120.1(6)
F3 <sup>3</sup>	K1	K1 <sup>2</sup>	129.25(9)	C6	C7	C8	121.1(6)
F3 <sup>3</sup>	K1	K1 <sup>1</sup>	133.96(9)	C9	C8	C7	118.9(7)
F3 <sup>3</sup>	K1	K1 <sup>3</sup>	32.50(7)	C10	C9	C8	119.7(8)
F3	K1	K1 <sup>1</sup>	60.44(8)	C9	C10	C11	121.0(7)
F3	K1	K1 <sup>3</sup>	163.80(10)	C6	C11	C10	119.5(7)
F3	K1	K1 <sup>2</sup>	34.20(8)	C13	C12	C2	120.2(6)
F3	K1	F1 <sup>3</sup>	114.24(10)	C13	C12	C17	119.2(6)
F3 <sup>3</sup>	K1	N1	116.39(13)	C17	C12	C2	120.4(6)

F3	K1	N1 <sup>1</sup>	74.68(12)	C14	C13	C12	120.4(6)
F3	K1	N1	62.58(12)	C15	C14	C13	120.4(8)
F3 <sup>3</sup>	K1	N1 <sup>1</sup>	124.11(11)	C14	C15	C16	119.4(7)
F3 <sup>3</sup>	K1	B1 <sup>3</sup>	24.32(12)	C15	C16	C17	120.7(7)
F3	K1	B1 <sup>1</sup>	111.90(15)	C12	C17	C16	119.9(7)
F3	K1	B1 <sup>3</sup>	137.96(14)				

<sup>1</sup>1-X,1-Y,1-Z; <sup>2</sup>+X,1/2-Y,-1/2+Z; <sup>3</sup>+X,1/2-Y,1/2+Z; <sup>4</sup>1-X,-1/2+Y,1/2-Z; <sup>5</sup>1-X,1/2+Y,1/2-Z

**Table 6 Torsion Angles for ojH388k.**

A B C D	Angle/°	A B C D	Angle/°
K1 <sup>1</sup> F1 B1 K1 <sup>2</sup>	-136.4(9)	N2 C1 N3 C5	3.7(9)
K1 <sup>1</sup> F1 B1 F2	-124.2(4)	N2 C2 C3 C4	2.1(10)
K1 <sup>1</sup> F1 B1 F3	-10.3(5)	N2 C2 C12 C13	27.9(10)
K1 <sup>1</sup> F1 B1 C4	112.5(5)	N2 C2 C12 C17	-148.2(7)
K1 N1 C1 N2	132.0(5)	C2 C3 C4 N1	0.2(9)
K1 <sup>2</sup> N1 C1 N2	-118.5(6)	C2 C3 C4 B1	179.0(6)
K1 <sup>2</sup> N1 C1 N3	63.1(7)	C2 C12 C13 C14	-178.7(7)
K1 N1 C1 N3	-46.4(7)	C2 C12 C17 C16	177.3(6)
K1 N1 C4 B1	46.3(6)	F3 B1 F2 K1 <sup>3</sup>	-112.0(4)
K1 <sup>2</sup> N1 C4 B1	-50.8(6)	F3 B1 F2 K1 <sup>2</sup>	74.0(5)
K1 <sup>2</sup> N1 C4 C3	128.1(5)	F3 B1 C4 N1	-42.5(8)
K1 N1 C4 C3	-134.8(5)	F3 B1 C4 C3	138.7(6)
K1 <sup>1</sup> B1 F2 K1 <sup>2</sup>	131.2(3)	N3 C1 N2 C2	179.9(6)
K1 <sup>2</sup> B1 F2 K1 <sup>3</sup>	174.0(5)	N3 C5 C6 C7	74.9(7)
K1 <sup>1</sup> B1 F2 K1 <sup>3</sup>	-54.8(6)	N3 C5 C6 C11	-108.5(6)
K1 <sup>1</sup> B1 F3 K1	126.9(4)	C3 C2 C12 C13	-151.2(7)
K1 <sup>2</sup> B1 F3 K1 <sup>1</sup>	169.27(12)	C3 C2 C12 C17	32.7(10)
K1 <sup>2</sup> B1 F3 K1	-63.8(3)	C4 N1 C1 N2	0.7(10)
K1 <sup>2</sup> B1 C4 N1	43.1(5)	C4 N1 C1 N3	-177.7(6)
K1 <sup>1</sup> B1 C4 N1	-103.0(6)	C4 B1 F2 K1 <sup>2</sup>	-48.6(5)
K1 <sup>1</sup> B1 C4 C3	78.2(7)	C4 B1 F2 K1 <sup>3</sup>	125.4(4)
K1 <sup>2</sup> B1 C4 C3	-135.7(6)	C4 B1 F3 K1	14.1(7)
F1 B1 F2 K1 <sup>2</sup>	-172.6(3)	C4 B1 F3 K1 <sup>1</sup>	-112.9(5)
F1 B1 F2 K1 <sup>3</sup>	1.4(8)	C5 C6 C7 C8	176.7(6)
F1 B1 F3 K1 <sup>1</sup>	10.0(5)	C5 C6 C11 C10	-176.4(6)
F1 B1 F3 K1	137.0(4)	C6 C7 C8 C9	-0.8(10)
F1 B1 C4 N1	-161.6(6)	C7 C6 C11 C10	0.2(10)
F1 B1 C4 C3	19.6(9)	C7 C8 C9 C10	1.3(11)
N1 C1 N2 C2	1.5(10)	C8 C9 C10 C11	-1.0(12)
N1 C1 N3 C5	-177.7(6)	C9 C10 C11 C6	0.3(11)
C1 N1 C4 B1	179.6(5)	C11 C6 C7 C8	0.1(10)
C1 N1 C4 C3	-1.6(9)	C12 C2 C3 C4	-178.9(6)

---

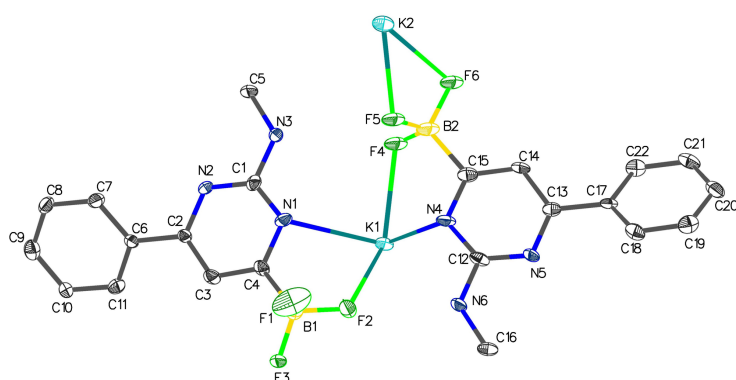
C1 N2 C2 C3	-2.9(10)	C12 C13 C14 C15	2.6(13)
C1 N2 C2 C12	178.0(6)	C13 C12 C17 C16	1.2(11)
C1 N3 C5 C6	82.9(7)	C13 C14 C15 C16	-1.3(13)
F2 B1 F3 K1 <sup>1</sup>	125.1(4)	C14 C15 C16 C17	0.0(13)
F2 B1 F3 K1	-107.9(5)	C15 C16 C17 C12	0.1(12)
F2 B1 C4 N1	76.8(7)	C17 C12 C13 C14	-2.5(11)
F2 B1 C4 C3	-102.0(7)		

<sup>1</sup>+X,1/2-Y,-1/2+Z; <sup>2</sup>1-X,1-Y,1-Z; <sup>3</sup>1-X,1/2+Y,1/2-Z

**Table 7 Hydrogen Atom Coordinates ( $\text{\AA} \times 10^4$ ) and Isotropic Displacement Parameters ( $\text{\AA}^2 \times 10^3$ ) for ojH388k.**

Atom	<i>x</i>	<i>y</i>	<i>z</i>	U(eq)
H3	6022.19	4295.73	7441.48	24
H3A	7077.71	4342.09	2002.16	21
H5A	7425.49	3422.76	8128.53	26
H5B	6824.36	3656.78	9294.03	26
H7	6590.36	6103.73	9974.37	34
H8	7186.3	8068.28	10852.51	44
H9	8412.32	8433.43	10358.26	61
H10	9005.74	6911.99	8938.58	62
H11	8406.14	4973.7	8055.25	51
H13	8584.13	2844.82	5618.07	45
H14	9819.85	2598.57	5173.73	69
H15	10297.86	3708.01	3202.93	66
H16	9520.79	4982.55	1611.93	54
H17	8272.35	5166.4	1989.25	39

## X-ray crystal structure data for compound 31e



### Crystal structure determination of compound 31e

Crystals of 31e were grown from a saturated acetone solution, allowing slow evaporation.

**Crystal Data** for  $C_{11}H_{10}BF_3KN_3$  ( $M=291.13$  g/mol): monoclinic, space group  $P2_1/c$  (no. 14),  $a = 17.226(8)$  Å,  $b = 17.878(9)$  Å,  $c = 9.023(4)$  Å,  $\beta = 96.749(11)^\circ$ ,  $V = 2759(2)$  Å<sup>3</sup>,  $Z = 8$ ,  $T = 100$  K,  $\mu(\text{MoK}\alpha) = 0.407$  mm<sup>-1</sup>,  $D_{\text{calc}} = 1.402$  g/cm<sup>3</sup>, 44917 reflections measured ( $3.296^\circ \leq 2\theta \leq 55.336^\circ$ ), 6407 unique ( $R_{\text{int}} = 0.1692$ ,  $R_{\text{sigma}} = 0.1227$ ) which were used in all calculations. The final  $R_1$  was 0.1171 ( $I > 2\sigma(I)$ ) and  $wR_2$  was 0.2700 (all data).

**Table 1 Crystal data and structure refinement for OJH383k.**

Identification code	OJH383k
Empirical formula	$C_{11}H_{10}BF_3KN_3$
Formula weight	291.13
Temperature/K	100
Crystal system	monoclinic
Space group	$P2_1/c$
$a/\text{Å}$	17.226(8)
$b/\text{Å}$	17.878(9)
$c/\text{Å}$	9.023(4)
$\alpha/^\circ$	90
$\beta/^\circ$	96.749(11)

$\gamma/^\circ$	90
Volume/ $\text{\AA}^3$	2759(2)
Z	8
$\rho_{\text{calc}}/\text{g}/\text{cm}^3$	1.402
$\mu/\text{mm}^{-1}$	0.407
F(000)	1184.0
Crystal size/ $\text{mm}^3$	$0.5 \times 0.1 \times 0.045$
Radiation	MoK $\alpha$ ( $\lambda = 0.71073$ )
2 $\Theta$ range for data collection/ $^\circ$	3.296 to 55.336
Index ranges	$-22 \leq h \leq 22, -23 \leq k \leq 23, -8 \leq l \leq 11$
Reflections collected	44917
Independent reflections	6407 [ $R_{\text{int}} = 0.1692, R_{\text{sigma}} = 0.1227$ ]
Data/restraints/parameters	6407/0/327
Goodness-of-fit on $F^2$	1.039
Final R indexes [ $I \geq 2\sigma(I)$ ]	$R_1 = 0.1171, wR_2 = 0.2386$
Final R indexes [all data]	$R_1 = 0.1759, wR_2 = 0.2700$
Largest diff. peak/hole / $e \text{\AA}^{-3}$	1.93/-1.56

**Table 2 Fractional Atomic Coordinates ( $\times 10^4$ ) and Equivalent Isotropic Displacement Parameters ( $\text{\AA}^2 \times 10^3$ ) for OJH383k.  $U_{\text{eq}}$  is defined as 1/3 of of the trace of the orthogonalised  $U_{ij}$  tensor.**

Atom	x	y	z	U(eq)
K1	5122.6(9)	5060.8(9)	2478.9(15)	24.2(4)
K2	5754.2(9)	7772.3(8)	7464.7(16)	22.9(4)
F1	6192(4)	6721(3)	-473(6)	62.8(17)
F2	5393(2)	5787(3)	29(4)	40.6(13)
F3	6244(2)	5606(3)	-1640(4)	36.4(12)
F4	5263(3)	5749(3)	5096(4)	41.1(7)
F5	5318(3)	6997(3)	5100(4)	41.1(7)
F6	4618(3)	6406(3)	6716(4)	41.1(7)
N1	6644(3)	5821(3)	2440(6)	17.6(12)
N2	7922(3)	5386(3)	3398(6)	16.1(11)
N3	7051(3)	5788(3)	4956(6)	22.9(13)
N4	4221(3)	6443(3)	2573(6)	19.7(12)
N5	2842(3)	6531(3)	1768(5)	15.5(11)
N6	3738(3)	6487(3)	93(6)	23.2(13)
C1	7218(4)	5653(4)	3546(7)	16.6(13)
C2	8071(4)	5234(3)	1992(6)	13.7(12)
C3	7520(4)	5373(4)	784(7)	18.4(14)
C4	6806(4)	5679(4)	1028(7)	16.6(13)
C5	7604(4)	5629(5)	6254(7)	28.1(17)
C6	8852(4)	4915(4)	1848(6)	14.8(12)
C7	9500(4)	5145(4)	2816(7)	19.2(14)
C8	10232(4)	4849(4)	2691(7)	20.4(14)
C9	10315(4)	4318(4)	1620(8)	23.0(15)

C10	9689(4)	4086(4)	665(7)	19.8(14)
C11	8945(4)	4384(4)	767(7)	18.3(13)
C12	3593(4)	6483(3)	1523(7)	17.6(14)
C13	2701(4)	6521(3)	3200(7)	17.2(13)
C14	3305(4)	6459(4)	4368(7)	18.4(14)
C15	4061(4)	6427(4)	4015(7)	20.2(14)
C16	3157(4)	6574(4)	-1176(7)	19.5(14)
C17	1879(4)	6624(3)	3493(6)	15.8(13)
C18	1373(4)	7023(4)	2511(7)	22.1(15)
C19	610(4)	7164(4)	2817(8)	23.7(15)
C20	351(4)	6885(4)	4096(7)	24.1(15)
C21	851(4)	6475(4)	5085(7)	24.2(15)
C22	1619(4)	6340(4)	4794(7)	20.8(14)
B1	6158(5)	5946(5)	-294(9)	23.3(17)
B2	4806(6)	6402(7)	5258(9)	41.1(7)

**Table 3 Anisotropic Displacement Parameters ( $\text{\AA}^2 \times 10^3$ ) for OJH383k. The Anisotropic displacement factor exponent takes the form:  $-2\pi^2[h^2a^{*2}U_{11}+2hka^*b^*U_{12}+\dots]$ .**

Atom	$U_{11}$	$U_{22}$	$U_{33}$	$U_{23}$	$U_{13}$	$U_{12}$
K1	24.3(8)	38.2(9)	10.4(6)	-2.5(6)	2.9(5)	-1.5(7)
K2	32.4(9)	20.1(7)	15.9(7)	1.6(6)	2.0(6)	1.4(6)
F1	90(5)	35(3)	55(3)	22(3)	-27(3)	9(3)
F2	22(2)	85(4)	15(2)	11(2)	2.4(17)	21(2)
F3	19(2)	78(4)	12.1(19)	-9(2)	-1.1(16)	9(2)
F4	36.4(15)	74(2)	11.6(11)	-6.6(12)	-1.1(10)	-10.8(14)
F5	36.4(15)	74(2)	11.6(11)	-6.6(12)	-1.1(10)	-10.8(14)
F6	36.4(15)	74(2)	11.6(11)	-6.6(12)	-1.1(10)	-10.8(14)
N1	18(3)	21(3)	12(3)	2(2)	-3(2)	0(2)
N2	13(3)	23(3)	11(2)	1(2)	-3(2)	2(2)
N3	13(3)	43(4)	12(3)	-2(2)	-1(2)	9(3)
N4	27(3)	24(3)	8(2)	-2(2)	1(2)	3(3)
N5	20(3)	18(3)	10(2)	1(2)	5(2)	-1(2)
N6	19(3)	41(4)	10(3)	1(2)	3(2)	8(3)
C1	15(3)	17(3)	18(3)	-1(2)	1(3)	-6(3)
C2	15(3)	16(3)	11(3)	0(2)	3(2)	-2(2)
C3	22(3)	22(3)	12(3)	3(3)	5(3)	-3(3)
C4	18(3)	19(3)	13(3)	5(2)	5(2)	0(3)
C5	20(4)	53(5)	10(3)	-3(3)	-1(3)	6(3)
C6	15(3)	18(3)	11(3)	-1(2)	3(2)	2(3)
C7	19(3)	23(3)	15(3)	-1(3)	0(3)	-4(3)
C8	14(3)	29(4)	18(3)	4(3)	-2(3)	-3(3)
C9	19(4)	25(4)	26(4)	4(3)	6(3)	0(3)
C10	14(3)	29(4)	16(3)	-3(3)	4(3)	0(3)

C11	18(3)	19(3)	16(3)	1(3)	-2(3)	1(3)
C12	29(4)	14(3)	11(3)	4(2)	5(3)	7(3)
C13	23(4)	13(3)	15(3)	-2(2)	1(3)	-1(3)
C14	26(4)	22(3)	7(3)	0(2)	2(3)	0(3)
C15	28(4)	19(3)	13(3)	2(3)	0(3)	-2(3)
C16	29(4)	18(3)	10(3)	3(2)	1(3)	1(3)
C17	22(3)	17(3)	8(3)	-3(2)	-1(2)	2(3)
C18	29(4)	24(4)	15(3)	7(3)	8(3)	-2(3)
C19	28(4)	19(3)	23(4)	0(3)	-2(3)	5(3)
C20	28(4)	26(4)	20(3)	-6(3)	11(3)	-1(3)
C21	37(4)	21(3)	16(3)	-1(3)	11(3)	-4(3)
C22	27(4)	16(3)	19(3)	2(3)	1(3)	2(3)
B1	19(4)	33(4)	18(4)	7(3)	0(3)	0(3)
B2	36.4(15)	74(2)	11.6(11)	-6.6(12)	-1.1(10)	-10.8(14)

**Table 4 Bond Lengths for OJH383k.**

Atom	Atom	Length/Å	Atom	Atom	Length/Å
K1	K1 <sup>1</sup>	4.623(3)	N2	C1	1.325(8)
K1	K1 <sup>2</sup>	4.449(3)	N2	C2	1.351(8)
K1	K2 <sup>3</sup>	4.024(3)	N3	C1	1.358(8)
K1	F2	2.652(5)	N3	C5	1.449(8)
K1	F2 <sup>2</sup>	2.781(5)	N4	C12	1.353(8)
K1	F3 <sup>2</sup>	2.668(5)	N4	C15	1.361(8)
K1	F4 <sup>1</sup>	2.768(5)	N5	C12	1.342(8)
K1	F4	2.648(4)	N5	C13	1.343(8)
K1	F6 <sup>1</sup>	2.744(6)	N6	C12	1.343(8)
K1	N1	2.956(6)	N6	C16	1.438(8)
K1	N4	2.926(6)	C2	C3	1.381(9)
K1	B2 <sup>1</sup>	3.311(11)	C2	C6	1.481(8)
K2	K2 <sup>4</sup>	4.615(2)	C3	C4	1.386(9)
K2	F1 <sup>4</sup>	2.981(7)	C4	B1	1.608(10)
K2	F1 <sup>5</sup>	2.690(5)	C6	C7	1.395(9)
K2	F2 <sup>4</sup>	3.396(5)	C6	C11	1.384(9)
K2	F5 <sup>4</sup>	2.610(4)	C7	C8	1.386(9)
K2	F5	2.581(5)	C8	C9	1.373(10)
K2	F6	3.152(5)	C9	C10	1.363(9)
K2	N1 <sup>4</sup>	2.947(6)	C10	C11	1.402(9)
K2	N4 <sup>4</sup>	3.002(6)	C13	C14	1.396(9)
K2	B1 <sup>4</sup>	3.512(9)	C13	C17	1.482(9)
K2	B2 <sup>4</sup>	3.488(10)	C14	C15	1.379(9)
F1	B1	1.397(10)	C15	B2	1.603(11)
F2	B1	1.411(9)	C17	C18	1.369(9)
F3	B1	1.381(9)	C17	C22	1.399(9)

F4	B2	1.425(13)	C18	C19	1.397(10)
F5	B2	1.398(12)	C19	C20	1.379(10)
F6	B2	1.391(9)	C20	C21	1.377(10)
N1	C1	1.353(8)	C21	C22	1.399(10)
N1	C4	1.360(8)			

<sup>1</sup>1-X,1-Y,1-Z; <sup>2</sup>1-X,1-Y,-Z; <sup>3</sup>+X,3/2-Y,-1/2+Z; <sup>4</sup>+X,3/2-Y,1/2+Z; <sup>5</sup>+X,+Y,1+Z

**Table 5 Bond Angles for OJH383k.**

Atom	Atom	Atom	Angle/°	Atom	Atom	Atom	Angle/°
K1 <sup>1</sup>	K1	K1 <sup>2</sup>	168.04(8)	N1 <sup>4</sup>	K2	F6	165.89(14)
K2 <sup>3</sup>	K1	K1 <sup>1</sup>	92.15(5)	N1 <sup>4</sup>	K2	N4 <sup>4</sup>	93.56(16)
K2 <sup>3</sup>	K1	K1 <sup>2</sup>	95.99(5)	N1 <sup>4</sup>	K2	B1 <sup>4</sup>	44.88(16)
F2 <sup>1</sup>	K1	K1 <sup>1</sup>	34.08(10)	N1 <sup>4</sup>	K2	B2 <sup>4</sup>	86.1(2)
F2	K1	K1 <sup>1</sup>	35.99(12)	N4 <sup>4</sup>	K2	K1 <sup>4</sup>	46.45(11)
F2	K1	K1 <sup>2</sup>	152.71(14)	N4 <sup>4</sup>	K2	K2 <sup>4</sup>	88.03(10)
F2 <sup>1</sup>	K1	K1 <sup>2</sup>	135.86(12)	N4 <sup>4</sup>	K2	F2 <sup>4</sup>	64.66(13)
F2 <sup>1</sup>	K1	K2 <sup>3</sup>	125.64(11)	N4 <sup>4</sup>	K2	F6	80.94(15)
F2	K1	K2 <sup>3</sup>	56.77(12)	N4 <sup>4</sup>	K2	B1 <sup>4</sup>	88.09(17)
F2	K1	F2 <sup>1</sup>	70.1(2)	N4 <sup>4</sup>	K2	B2 <sup>4</sup>	44.80(18)
F2	K1	F3 <sup>1</sup>	102.60(15)	B1 <sup>4</sup>	K2	K1 <sup>4</sup>	56.66(14)
F2	K1	F4 <sup>2</sup>	175.41(15)	B1 <sup>4</sup>	K2	K2 <sup>4</sup>	148.56(14)
F2	K1	F6 <sup>2</sup>	130.51(15)	B2 <sup>4</sup>	K2	K1 <sup>4</sup>	55.99(19)
F2	K1	N1	61.44(14)	B2 <sup>4</sup>	K2	K2 <sup>4</sup>	47.86(16)
F2 <sup>1</sup>	K1	N1	116.10(14)	B2 <sup>4</sup>	K2	B1 <sup>4</sup>	112.6(2)
F2 <sup>1</sup>	K1	N4	111.35(15)	K2 <sup>6</sup>	F1	K2 <sup>3</sup>	108.86(19)
F2	K1	N4	75.92(15)	B1	F1	K2 <sup>6</sup>	139.5(5)
F2	K1	B2 <sup>2</sup>	154.6(2)	B1	F1	K2 <sup>3</sup>	100.4(4)
F2 <sup>1</sup>	K1	B2 <sup>2</sup>	93.2(2)	K1	F2	K1 <sup>1</sup>	109.9(2)
F3 <sup>1</sup>	K1	K1 <sup>2</sup>	94.51(10)	K1 <sup>1</sup>	F2	K2 <sup>3</sup>	163.07(17)
F3 <sup>1</sup>	K1	K1 <sup>1</sup>	73.53(9)	K1	F2	K2 <sup>3</sup>	82.44(12)
F3 <sup>1</sup>	K1	K2 <sup>3</sup>	131.25(12)	B1	F2	K1	122.1(4)
F3 <sup>1</sup>	K1	F2 <sup>1</sup>	48.58(12)	B1	F2	K1 <sup>1</sup>	99.1(4)
F3 <sup>1</sup>	K1	F4 <sup>2</sup>	72.84(14)	B1	F2	K2 <sup>3</sup>	82.9(4)
F3 <sup>1</sup>	K1	F6 <sup>2</sup>	76.01(15)	B1	F3	K1 <sup>1</sup>	105.3(4)
F3 <sup>1</sup>	K1	N1	162.95(14)	K1	F4	K1 <sup>2</sup>	117.18(19)
F3 <sup>1</sup>	K1	N4	86.12(16)	B2	F4	K1	118.6(4)
F3 <sup>1</sup>	K1	B2 <sup>2</sup>	77.8(2)	B2	F4	K1 <sup>2</sup>	99.3(4)
F4	K1	K1 <sup>1</sup>	155.13(14)	K2	F5	K2 <sup>3</sup>	125.5(2)
F4	K1	K1 <sup>2</sup>	32.19(11)	B2	F5	K2 <sup>3</sup>	117.8(4)
F4 <sup>2</sup>	K1	K1 <sup>2</sup>	30.64(10)	B2	F5	K2	116.7(4)
F4 <sup>2</sup>	K1	K1 <sup>1</sup>	139.98(12)	K1 <sup>2</sup>	F6	K2	127.32(16)
F4	K1	K2 <sup>3</sup>	63.86(12)	B2	F6	K1 <sup>2</sup>	101.3(6)

---

F4 <sup>2</sup>	K1	K2 <sup>3</sup>	126.57(11)	B2	F6	K2	90.0(5)
F4	K1	F2	120.63(17)	K2 <sup>3</sup>	N1	K1	85.96(15)
F4	K1	F2 <sup>1</sup>	164.91(15)	C1	N1	K1	117.4(4)
F4 <sup>2</sup>	K1	F2 <sup>1</sup>	105.94(15)	C1	N1	K2 <sup>3</sup>	121.3(4)
F4	K1	F3 <sup>1</sup>	116.47(14)	C1	N1	C4	115.9(5)
F4	K1	F4 <sup>2</sup>	62.82(19)	C4	N1	K1	101.8(4)
F4	K1	F6 <sup>2</sup>	102.29(15)	C4	N1	K2 <sup>3</sup>	109.3(4)
F4 <sup>2</sup>	K1	N1	123.03(14)	C1	N2	C2	116.4(5)
F4	K1	N1	78.99(15)	C1	N3	C5	122.1(6)
F4 <sup>2</sup>	K1	N4	103.96(16)	K1	N4	K2 <sup>3</sup>	85.50(16)
F4	K1	N4	64.84(15)	C12	N4	K1	114.0(4)
F4 <sup>2</sup>	K1	B2 <sup>2</sup>	25.1(2)	C12	N4	K2 <sup>3</sup>	125.9(4)
F4	K1	B2 <sup>2</sup>	79.9(2)	C12	N4	C15	115.8(6)
F6 <sup>2</sup>	K1	K1 <sup>1</sup>	102.29(10)	C15	N4	K1	100.2(4)
F6 <sup>2</sup>	K1	K1 <sup>2</sup>	74.06(9)	C15	N4	K2 <sup>3</sup>	108.6(4)
F6 <sup>2</sup>	K1	K2 <sup>3</sup>	152.30(11)	C12	N5	C13	116.4(5)
F6 <sup>2</sup>	K1	F2 <sup>1</sup>	73.80(14)	C12	N6	C16	125.2(6)
F6 <sup>2</sup>	K1	F4 <sup>2</sup>	48.52(14)	N1	C1	N3	115.8(6)
F6 <sup>2</sup>	K1	N1	109.02(15)	N2	C1	N1	127.1(6)
F6 <sup>2</sup>	K1	N4	150.47(16)	N2	C1	N3	117.1(6)
F6 <sup>2</sup>	K1	B2 <sup>2</sup>	24.32(19)	N2	C2	C3	121.1(6)
N1	K1	K1 <sup>1</sup>	89.43(11)	N2	C2	C6	115.7(5)
N1	K1	K1 <sup>2</sup>	102.53(11)	C3	C2	C6	123.2(5)
N1	K1	K2 <sup>3</sup>	46.92(11)	C2	C3	C4	119.1(6)
N1	K1	B2 <sup>2</sup>	113.7(2)	N1	C4	C3	120.4(6)
N4	K1	K1 <sup>2</sup>	84.31(11)	N1	C4	B1	116.0(6)
N4	K1	K1 <sup>1</sup>	94.73(11)	C3	C4	B1	123.4(6)
N4	K1	K2 <sup>3</sup>	48.05(12)	C7	C6	C2	120.0(6)
N4	K1	N1	94.95(17)	C11	C6	C2	120.5(6)
N4	K1	B2 <sup>2</sup>	129.1(2)	C11	C6	C7	119.6(6)
B2 <sup>2</sup>	K1	K1 <sup>1</sup>	125.00(18)	C8	C7	C6	120.3(6)
B2 <sup>2</sup>	K1	K1 <sup>2</sup>	50.00(17)	C9	C8	C7	119.4(6)
B2 <sup>2</sup>	K1	K2 <sup>3</sup>	140.53(17)	C10	C9	C8	121.1(6)
K1 <sup>4</sup>	K2	K2 <sup>4</sup>	99.73(4)	C9	C10	C11	120.3(6)
F1 <sup>4</sup>	K2	K1 <sup>4</sup>	78.88(11)	C6	C11	C10	119.3(6)
F1 <sup>5</sup>	K2	K1 <sup>4</sup>	136.42(14)	N5	C12	N4	126.6(6)
F1 <sup>5</sup>	K2	K2 <sup>4</sup>	37.67(14)	N5	C12	N6	116.7(6)
F1 <sup>4</sup>	K2	K2 <sup>4</sup>	164.24(11)	N6	C12	N4	116.8(6)
F1 <sup>5</sup>	K2	F1 <sup>4</sup>	138.4(2)	N5	C13	C14	121.7(6)
F1 <sup>4</sup>	K2	F2 <sup>4</sup>	40.55(13)	N5	C13	C17	117.0(5)
F1 <sup>5</sup>	K2	F2 <sup>4</sup>	173.21(16)	C14	C13	C17	121.2(6)
F1 <sup>5</sup>	K2	F6	73.95(16)	C15	C14	C13	118.0(6)
F1 <sup>4</sup>	K2	F6	105.09(13)	N4	C15	C14	121.5(6)
F1 <sup>5</sup>	K2	N1 <sup>4</sup>	119.86(17)	N4	C15	B2	115.8(6)
F1 <sup>5</sup>	K2	N4 <sup>4</sup>	118.68(19)	C14	C15	B2	122.7(6)

F1 <sup>4</sup>	K2	N4 <sup>4</sup>	101.69(16)	C18	C17	C13	119.9(6)
F1 <sup>4</sup>	K2	B1 <sup>4</sup>	23.03(16)	C18	C17	C22	119.3(6)
F1 <sup>5</sup>	K2	B1 <sup>4</sup>	152.1(2)	C22	C17	C13	120.7(6)
F1 <sup>4</sup>	K2	B2 <sup>4</sup>	134.7(2)	C17	C18	C19	120.5(6)
F1 <sup>5</sup>	K2	B2 <sup>4</sup>	85.0(2)	C20	C19	C18	120.3(7)
F2 <sup>4</sup>	K2	K1 <sup>4</sup>	40.79(8)	C21	C20	C19	119.7(7)
F2 <sup>4</sup>	K2	K2 <sup>4</sup>	140.51(9)	C20	C21	C22	120.2(6)
F2 <sup>4</sup>	K2	B1 <sup>4</sup>	23.49(15)	C17	C22	C21	119.8(6)
F2 <sup>4</sup>	K2	B2 <sup>4</sup>	94.7(2)	K1 <sup>1</sup>	B1	K2 <sup>3</sup>	127.1(2)
F5	K2	K1 <sup>4</sup>	117.85(13)	F1	B1	K1 <sup>1</sup>	120.3(5)
F5 <sup>4</sup>	K2	K1 <sup>4</sup>	74.80(12)	F1	B1	K2 <sup>3</sup>	56.6(4)
F5 <sup>4</sup>	K2	K2 <sup>4</sup>	27.08(11)	F1	B1	F2	106.1(7)
F5	K2	K2 <sup>4</sup>	131.38(13)	F1	B1	C4	110.2(6)
F5 <sup>4</sup>	K2	F1 <sup>4</sup>	153.16(16)	F2	B1	K1 <sup>1</sup>	56.0(3)
F5	K2	F1 <sup>4</sup>	60.52(15)	F2	B1	K2 <sup>3</sup>	73.6(4)
F5	K2	F1 <sup>5</sup>	103.13(18)	F2	B1	C4	111.7(6)
F5 <sup>4</sup>	K2	F1 <sup>5</sup>	64.38(18)	F3	B1	K1 <sup>1</sup>	51.0(3)
F5 <sup>4</sup>	K2	F2 <sup>4</sup>	114.79(15)	F3	B1	K2 <sup>3</sup>	163.9(5)
F5	K2	F2 <sup>4</sup>	81.90(15)	F3	B1	F1	108.9(6)
F5	K2	F5 <sup>4</sup>	138.67(18)	F3	B1	F2	107.0(6)
F5 <sup>4</sup>	K2	F6	94.58(15)	F3	B1	C4	112.6(6)
F5	K2	F6	45.05(13)	C4	B1	K1 <sup>1</sup>	129.5(5)
F5 <sup>4</sup>	K2	N1 <sup>4</sup>	94.46(16)	C4	B1	K2 <sup>3</sup>	81.1(4)
F5	K2	N1 <sup>4</sup>	123.61(16)	K1 <sup>2</sup>	B2	K2 <sup>3</sup>	142.5(4)
F5	K2	N4 <sup>4</sup>	96.08(16)	F4	B2	K1 <sup>2</sup>	55.6(4)
F5 <sup>4</sup>	K2	N4 <sup>4</sup>	63.09(14)	F4	B2	K2 <sup>3</sup>	87.8(4)
F5	K2	B1 <sup>4</sup>	80.06(18)	F4	B2	C15	110.9(7)
F5 <sup>4</sup>	K2	B1 <sup>4</sup>	130.15(19)	F5	B2	K1 <sup>2</sup>	133.3(6)
F5	K2	B2 <sup>4</sup>	135.2(2)	F5	B2	K2 <sup>3</sup>	41.5(3)
F5 <sup>4</sup>	K2	B2 <sup>4</sup>	20.78(19)	F5	B2	F4	104.5(7)
F6	K2	K1 <sup>4</sup>	125.82(11)	F5	B2	C15	111.7(7)
F6	K2	K2 <sup>4</sup>	88.56(9)	F6	B2	K1 <sup>2</sup>	54.3(5)
F6	K2	F2 <sup>4</sup>	112.77(12)	F6	B2	K2 <sup>3</sup>	149.5(6)
F6	K2	B1 <sup>4</sup>	121.53(16)	F6	B2	F4	107.1(8)
F6	K2	B2 <sup>4</sup>	98.7(2)	F6	B2	F5	108.2(7)
N1 <sup>4</sup>	K2	K1 <sup>4</sup>	47.12(11)	F6	B2	C15	113.9(7)
N1 <sup>4</sup>	K2	K2 <sup>4</sup>	104.32(11)	C15	B2	K1 <sup>2</sup>	115.0(6)
N1 <sup>4</sup>	K2	F1 <sup>4</sup>	63.11(14)	C15	B2	K2 <sup>3</sup>	83.5(4)
N1 <sup>4</sup>	K2	F2 <sup>4</sup>	53.38(13)				

<sup>1</sup>1-X,1-Y,-Z; <sup>2</sup>1-X,1-Y,1-Z; <sup>3</sup>+X,3/2-Y,-1/2+Z; <sup>4</sup>+X,3/2-Y,1/2+Z; <sup>5</sup>+X,+Y,1+Z; <sup>6</sup>+X,+Y,-1+Z

**Table 6 Torsion Angles for OJH383k.**

A	B	C	D	Angle/°	A	B	C	D	Angle/°
K1	F2	B1	K1 <sup>1</sup>	120.5(5)	N1	C4	B1	F1	75.4(8)
K1	F2	B1	K2 <sup>2</sup>	-76.4(4)	N1	C4	B1	F2	-42.3(9)
K1 <sup>1</sup>	F2	B1	K2 <sup>2</sup>	163.02(18)	N1	C4	B1	F3	-162.7(6)
K1	F2	B1	F1	-123.4(5)	N2	C2	C3	C4	0.5(9)
K1 <sup>1</sup>	F2	B1	F1	116.0(5)	N2	C2	C6	C7	-35.2(8)
K1 <sup>1</sup>	F2	B1	F3	-0.1(6)	N2	C2	C6	C11	144.2(6)
K1	F2	B1	F3	120.4(5)	N4	C15	B2	K1 <sup>3</sup>	-121.4(5)
K1 <sup>1</sup>	F2	B1	C4	-123.8(5)	N4	C15	B2	K2 <sup>2</sup>	24.4(6)
K1	F2	B1	C4	-3.3(8)	N4	C15	B2	F4	-60.7(9)
K1 <sup>1</sup>	F3	B1	K2 <sup>2</sup>	-89.4(18)	N4	C15	B2	F5	55.4(10)
K1 <sup>1</sup>	F3	B1	F1	-114.1(6)	N4	C15	B2	F6	178.4(7)
K1 <sup>1</sup>	F3	B1	F2	0.1(6)	N5	C13	C14	C15	1.6(10)
K1 <sup>1</sup>	F3	B1	C4	123.3(5)	N5	C13	C17	C18	-27.7(9)
K1	F4	B2	K1 <sup>3</sup>	128.0(4)	N5	C13	C17	C22	154.6(6)
K1	F4	B2	K2 <sup>2</sup>	-60.8(4)	C1	N1	C4	C3	0.6(9)
K1 <sup>3</sup>	F4	B2	K2 <sup>2</sup>	171.21(15)	C1	N1	C4	B1	-174.7(6)
K1 <sup>3</sup>	F4	B2	F5	132.9(5)	C1	N2	C2	C3	1.8(9)
K1	F4	B2	F5	-99.1(5)	C1	N2	C2	C6	-178.2(5)
K1 <sup>3</sup>	F4	B2	F6	18.2(7)	C2	N2	C1	N1	-3.2(9)
K1	F4	B2	F6	146.3(5)	C2	N2	C1	N3	178.2(6)
K1	F4	B2	C15	21.4(9)	C2	C3	C4	N1	-1.8(10)
K1 <sup>3</sup>	F4	B2	C15	-106.6(6)	C2	C3	C4	B1	173.2(6)
K1 <sup>3</sup>	F6	B2	K2 <sup>2</sup>	-134.9(11)	C2	C6	C7	C8	179.9(6)
K1 <sup>3</sup>	F6	B2	F4	-18.5(7)	C2	C6	C11	C10	-179.4(6)
K1 <sup>3</sup>	F6	B2	F5	-130.7(7)	C3	C2	C6	C7	144.8(6)
K1 <sup>3</sup>	F6	B2	C15	104.5(8)	C3	C2	C6	C11	-35.8(9)
K1	N1	C1	N2	122.6(6)	C3	C4	B1	K1 <sup>1</sup>	79.4(8)
K1	N1	C1	N3	-58.8(7)	C3	C4	B1	K2 <sup>2</sup>	-149.1(6)
K1	N1	C4	C3	-128.1(6)	C3	C4	B1	F1	-99.7(8)
K1	N1	C4	B1	56.6(6)	C3	C4	B1	F2	142.6(7)
K1	N4	C12	N5	117.8(6)	C3	C4	B1	F3	22.1(10)
K1	N4	C12	N6	-63.3(7)	C4	N1	C1	N2	2.0(9)
K1	N4	C15	C14	-123.9(6)	C4	N1	C1	N3	-179.3(6)
K1	N4	C15	B2	58.4(7)	C5	N3	C1	N1	179.3(6)
K2 <sup>4</sup>	F1	B1	K1 <sup>1</sup>	-19.3(10)	C5	N3	C1	N2	-1.9(10)
K2 <sup>2</sup>	F1	B1	K1 <sup>1</sup>	116.8(4)	C6	C2	C3	C4	-179.5(6)
K2 <sup>4</sup>	F1	B1	K2 <sup>2</sup>	-136.2(8)	C6	C7	C8	C9	-0.9(10)
K2 <sup>4</sup>	F1	B1	F2	-79.0(9)	C7	C6	C11	C10	0.1(9)
K2 <sup>2</sup>	F1	B1	F2	57.2(5)	C7	C8	C9	C10	0.9(10)
K2 <sup>4</sup>	F1	B1	F3	35.9(11)	C8	C9	C10	C11	-0.4(10)
K2 <sup>2</sup>	F1	B1	F3	172.0(4)	C9	C10	C11	C6	-0.1(10)
K2 <sup>4</sup>	F1	B1	C4	159.9(5)	C11	C6	C7	C8	0.4(10)
K2 <sup>2</sup>	F1	B1	C4	-63.9(6)	C12	N4	C15	C14	-0.8(9)

K2 <sup>2</sup> F2 B1 K1 <sup>1</sup>	-163.02(18)	C12N4 C15B2	-178.4(7)
K2 <sup>2</sup> F2 B1 F1	-47.0(5)	C12N5 C13C14	-0.3(9)
K2 <sup>2</sup> F2 B1 F3	-163.2(5)	C12N5 C13C17	176.1(6)
K2 <sup>2</sup> F2 B1 C4	73.1(5)	C13N5 C12N4	-1.7(10)
K2 <sup>2</sup> F5 B2 K1 <sup>3</sup>	125.5(5)	C13N5 C12N6	179.4(6)
K2 F5 B2 K1 <sup>3</sup>	-54.3(9)	C13C14C15N4	-1.0(10)
K2 F5 B2 K2 <sup>2</sup>	-179.7(7)	C13C14C15B2	176.5(7)
K2 F5 B2 F4	-110.4(5)	C13C17C18C19	-176.1(6)
K2 <sup>2</sup> F5 B2 F4	69.3(6)	C13C17C22C21	176.9(6)
K2 <sup>2</sup> F5 B2 F6	-176.8(5)	C14C13C17C18	148.7(6)
K2 F5 B2 F6	3.5(10)	C14C13C17C22	-28.9(9)
K2 F5 B2 C15	129.6(5)	C14C15B2 K1 <sup>3</sup>	60.9(9)
K2 <sup>2</sup> F5 B2 C15	-50.6(9)	C14C15B2 K2 <sup>2</sup>	-153.2(6)
K2 F6 B2 K1 <sup>3</sup>	128.2(2)	C14C15B2 F4	121.6(7)
K2 F6 B2 K2 <sup>2</sup>	-6.7(12)	C14C15B2 F5	-122.2(8)
K2 F6 B2 F4	109.6(6)	C14C15B2 F6	0.7(12)
K2 F6 B2 F5	-2.5(7)	C15N4 C12N5	2.3(10)
K2 F6 B2 C15	-127.3(8)	C15N4 C12N6	-178.9(6)
K2 <sup>2</sup> N1C1 N2	-134.5(6)	C16N6 C12N4	-175.8(6)
K2 <sup>2</sup> N1C1 N3	44.1(7)	C16N6 C12N5	3.1(10)
K2 <sup>2</sup> N1C4 C3	142.1(5)	C17C13C14C15	-174.6(6)
K2 <sup>2</sup> N1C4 B1	-33.2(6)	C17C18C19C20	-1.8(11)
K2 <sup>2</sup> N4C12N5	-139.7(5)	C18C17C22C21	-0.8(10)
K2 <sup>2</sup> N4C12N6	39.2(8)	C18C19C20C21	1.0(10)
K2 <sup>2</sup> N4C15C14	147.4(5)	C19C20C21C22	-0.2(10)
K2 <sup>2</sup> N4C15B2	-30.2(7)	C20C21C22C17	0.0(10)
N1 C4B1 K1 <sup>1</sup>	-105.4(6)	C22C17C18C19	1.6(10)
N1 C4B1 K2 <sup>2</sup>	26.0(5)		

<sup>1</sup>1-X,1-Y,-Z; <sup>2</sup>+X,3/2-Y,-1/2+Z; <sup>3</sup>1-X,1-Y,1-Z; <sup>4</sup>+X,+Y,-1+Z

**Table 7 Hydrogen Atom Coordinates ( $\text{\AA} \times 10^4$ ) and Isotropic Displacement Parameters ( $\text{\AA}^2 \times 10^3$ ) for OJH383k.**

Atom	x	y	z	U(eq)
H3	6592.37	5978.81	5084.12	28
H6	4226.67	6431.75	-81.02	28
H3A	7628.05	5260.43	-199.58	22
H5A	8084.81	5914.86	6194.92	42
H5B	7724.58	5093.35	6286.93	42
H5C	7376.41	5771.78	7159.16	42
H7	9437.91	5507.08	3564.37	23
H8	10674.21	5010.83	3341.26	25
H9	10815.53	4109.59	1543.1	28
H10	9758.11	3720.21	-72.51	24

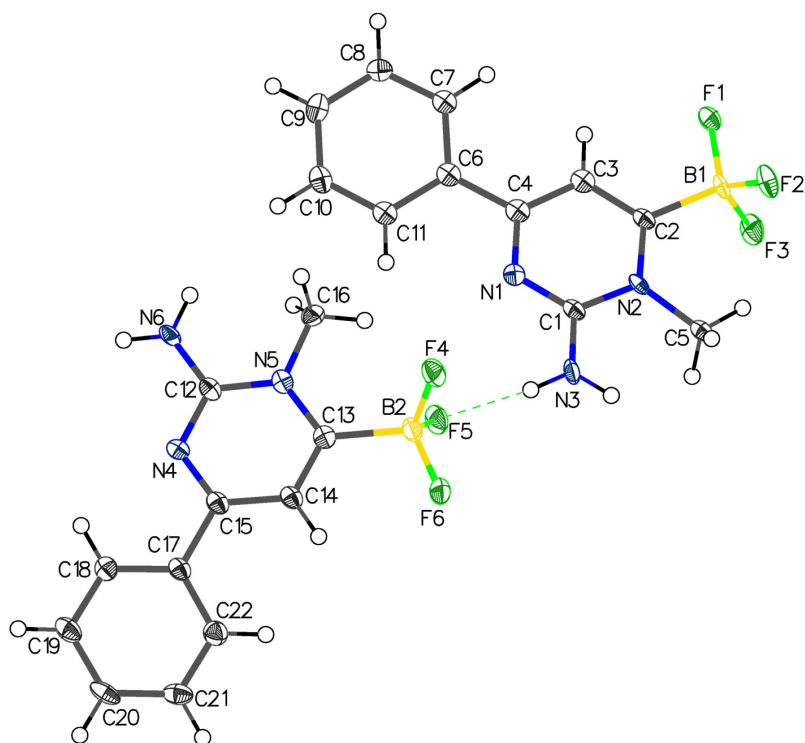
H11	8508.28	4223.18	101.13	22
H14	3198.08	6438.55	5376.85	22
H16A	3385.28	6839.94	-1970.63	29
H16B	2714.64	6861.45	-885.25	29
H16C	2974.88	6080.26	-1538.58	29
H18	1541.58	7206.02	1613.34	27
H19	268.2	7453.9	2141.62	28
H20	-170.79	6974.26	4293.55	29
H21	674.91	6282.87	5968.43	29
H22	1963.36	6057.3	5478.19	25

**Table 8 Solvent masks information for OJH383k.**

<b>Number</b>	<b>X</b>	<b>Y</b>	<b>Z</b>	<b>Volume</b>	<b>Electron count</b>	<b>Content</b>
1	0.156	0.250	-0.798	160.6	60.9	Solvent
2	0.844	0.750	-0.780	160.6	60.7	Solvent

## **X-ray crystal structure data for compound 32e**

**ORTEP of 10a, thermal ellipsoids are shown at 50% probability**



### Crystal structure determination of compound 32e

Crystals of 32e were grown from a saturated acetone solution, allowing slow evaporation.

**Crystal Data** for  $C_{11}H_{11}BF_3N_3$  ( $M=253.04$  g/mol): monoclinic, space group  $P2_1/n$  (no. 14),  $a = 17.8400(7)$  Å,  $b = 6.8724(3)$  Å,  $c = 19.3259(8)$  Å,  $\beta = 102.492(2)^\circ$ ,  $V = 2313.33(17)$  Å<sup>3</sup>,  $Z = 8$ ,  $T = 100.03$  K,  $\mu(\text{CuK}\alpha) = 1.055$  mm<sup>-1</sup>,  $D_{\text{calc}} = 1.453$  g/cm<sup>3</sup>, 12247 reflections measured ( $6.116^\circ \leq 2\theta \leq 133.71^\circ$ ), 3735 unique ( $R_{\text{int}} = 0.0706$ ,  $R_{\text{sigma}} = 0.0683$ ) which were used in all calculations. The final  $R_1$  was 0.1587 ( $I > 2\sigma(I)$ ) and  $wR_2$  was 0.3409 (all data).

**Table 1 Crystal data and structure refinement for OJH391v\_0m.**

Identification code	OJH391v_0m
Empirical formula	$C_{11}H_{11}BF_3N_3$
Formula weight	253.04
Temperature/K	100.03
Crystal system	monoclinic
Space group	$P2_1/n$
$a/\text{\AA}$	17.8400(7)
$b/\text{\AA}$	6.8724(3)
$c/\text{\AA}$	19.3259(8)
$\alpha/^\circ$	90
$\beta/^\circ$	102.492(2)
$\gamma/^\circ$	90

Volume/Å <sup>3</sup>	2313.33(17)
Z	8
ρ <sub>calc</sub> /cm <sup>3</sup>	1.453
μ/mm <sup>-1</sup>	1.055
F(000)	1040.0
Crystal size/mm <sup>3</sup>	0.2 × 0.034 × 0.025
Radiation	CuKα (λ = 1.54178)
2Θ range for data collection/°	6.116 to 133.71
Index ranges	-21 ≤ h ≤ 21, -7 ≤ k ≤ 8, -22 ≤ l ≤ 22
Reflections collected	12247
Independent reflections	3735 [R <sub>int</sub> = 0.0706, R <sub>sigma</sub> = 0.0683]
Data/restraints/parameters	3735/282/279
Goodness-of-fit on F <sup>2</sup>	1.419
Final R indexes [I ≥ 2σ (I)]	R <sub>1</sub> = 0.1587, wR <sub>2</sub> = 0.3370
Final R indexes [all data]	R <sub>1</sub> = 0.1701, wR <sub>2</sub> = 0.3409
Largest diff. peak/hole / e Å <sup>-3</sup>	0.58/-0.53

**Table 2 Fractional Atomic Coordinates (×10<sup>4</sup>) and Equivalent Isotropic Displacement Parameters (Å<sup>2</sup>×10<sup>3</sup>) for OJH391v\_0m. U<sub>eq</sub> is defined as 1/3 of the trace of the orthogonalised U<sub>ij</sub> tensor.**

Atom	x	y	z	U(eq)
F1	783(3)	4825(10)	4127(3)	31.3(15)
N1	3398(4)	3611(11)	3600(4)	15.2(15)
C1	3503(5)	3610(14)	4301(5)	16.7(11)
B1	1457(6)	4661(15)	4654(6)	15.0(18)
F2	1385(3)	3095(9)	5100(3)	27.9(14)
N2	2910(4)	3998(11)	4639(4)	13.7(15)
C2	2178(5)	4252(14)	4258(5)	16.7(11)
F3	1570(3)	6370(9)	5045(3)	27.0(14)
N3	4191(4)	3323(13)	4686(4)	21.9(18)
C3	2063(5)	4146(13)	3537(5)	16.1(8)
C4	2688(5)	3875(13)	3215(5)	16.1(8)
C5	3096(5)	4202(14)	5416(5)	16.7(11)
C6	2610(5)	3877(13)	2434(5)	16.1(8)
C7	1890(5)	3723(13)	1961(5)	16.1(8)
C8	1836(5)	3778(14)	1237(5)	17.9(19)
C9	2480(6)	3963(14)	958(5)	20.0(19)
C10	3193(6)	4094(14)	1417(5)	19.8(19)
C11	3267(5)	4061(13)	2146(5)	16.1(8)
B2	5799(6)	663(17)	3943(6)	19(2)
F4	5301(3)	-934(9)	3877(3)	27.7(14)
N4	6988(4)	972(11)	2157(4)	14.5(15)
F5	5386(3)	2399(9)	3956(3)	25.9(14)

N5	5838(4)	889(11)	2584(4)	15.4(15)
F6	6340(3)	487(11)	4562(3)	33.2(16)
N6	5824(4)	1077(12)	1378(4)	19.1(17)
C12	6220(5)	968(14)	2043(5)	16.3(17)
C13	6248(5)	744(13)	3276(5)	16.3(17)
C14	7024(5)	723(13)	3387(5)	17.2(11)
C15	7385(5)	873(14)	2814(5)	17.2(11)
C16	5001(5)	1022(15)	2411(5)	20(2)
C17	8231(5)	935(14)	2913(5)	17.2(11)
C18	8564(5)	786(14)	2328(5)	18.7(19)
C19	9352(5)	891(16)	2395(6)	25(2)
C20	9819(5)	1133(14)	3065(6)	22(2)
C21	9502(6)	1247(15)	3651(6)	24(2)
C22	8719(6)	1124(15)	3585(5)	23(2)

**Table 3 Anisotropic Displacement Parameters ( $\text{\AA}^2 \times 10^3$ ) for OJH391v\_0m. The Anisotropic displacement factor exponent takes the form:  $-2\pi^2[h^2a^{*2}U_{11}+2hka^*b^*U_{12}+\dots]$ .**

Atom	U <sub>11</sub>	U <sub>22</sub>	U <sub>33</sub>	U <sub>23</sub>	U <sub>13</sub>	U <sub>12</sub>
F1	13(3)	56(4)	26(3)	-5(3)	7(2)	3(3)
N1	20(3)	8(4)	19(3)	-1(3)	6(3)	-3(3)
C1	12(2)	16(3)	23(2)	-1(2)	5.5(18)	0(2)
B1	15(4)	13(4)	21(5)	0(3)	13(3)	0(4)
F2	30(3)	27(3)	33(3)	7(3)	20(3)	-1(3)
N2	11(3)	10(4)	21(3)	3(3)	7(3)	-2(3)
C2	12(2)	16(3)	23(2)	-1(2)	5.5(18)	0(2)
F3	28(3)	24(3)	34(3)	-6(2)	16(3)	4(3)
N3	16(3)	36(5)	17(4)	3(4)	10(3)	3(4)
C3	19.6(19)	6.4(17)	22.5(18)	0.9(16)	4.9(15)	0.2(16)
C4	19.6(19)	6.4(17)	22.5(18)	0.9(16)	4.9(15)	0.2(16)
C5	12(2)	16(3)	23(2)	-1(2)	5.5(18)	0(2)
C6	19.6(19)	6.4(17)	22.5(18)	0.9(16)	4.9(15)	0.2(16)
C7	19.6(19)	6.4(17)	22.5(18)	0.9(16)	4.9(15)	0.2(16)
C8	17(4)	14(5)	22(4)	0(4)	1(3)	4(4)
C9	32(4)	10(4)	19(4)	5(4)	8(3)	5(4)
C10	25(4)	11(4)	26(4)	3(4)	11(3)	0(4)
C11	19.6(19)	6.4(17)	22.5(18)	0.9(16)	4.9(15)	0.2(16)
B2	19(5)	20(5)	20(4)	-1(4)	9(3)	-3(4)
F4	28(3)	29(3)	28(3)	2(3)	12(3)	-7(3)
N4	15(3)	8(4)	21(3)	0(3)	4(3)	-1(3)
F5	24(3)	27(3)	30(3)	-5(3)	13(3)	4(2)
N5	18(3)	8(4)	21(3)	0(3)	8(3)	2(3)
F6	21(3)	61(5)	19(3)	-4(3)	8(2)	1(3)
N6	9(4)	25(4)	24(3)	-3(3)	6(3)	2(3)

C12	16(4)	12(4)	21(4)	3(4)	6(3)	0(4)
C13	21(4)	7(4)	22(4)	-4(4)	8(3)	-1(3)
C14	18(2)	12(2)	23(2)	0(2)	7.2(18)	-3(2)
C15	18(2)	12(2)	23(2)	0(2)	7.2(18)	-3(2)
C16	19(4)	23(5)	19(5)	-7(4)	3(4)	-2(4)
C17	18(2)	12(2)	23(2)	0(2)	7.2(18)	-3(2)
C18	20(4)	15(5)	22(4)	-2(4)	7(3)	1(4)
C19	16(4)	26(6)	34(5)	-2(5)	9(4)	3(4)
C20	11(4)	15(5)	41(5)	4(4)	6(3)	3(4)
C21	15(4)	21(5)	32(5)	-5(4)	-1(4)	2(4)
C22	22(4)	23(5)	25(4)	-3(4)	7(3)	-1(4)

**Table 4 Bond Lengths for OJH391v\_0m.**

Atom	Atom	Length/Å	Atom	Atom	Length/Å
F1	B1	1.402(13)	B2	F4	1.401(12)
N1	C1	1.327(12)	B2	F5	1.405(13)
N1	C4	1.335(12)	B2	F6	1.370(13)
C1	N2	1.384(11)	B2	C13	1.658(13)
C1	N3	1.304(12)	N4	C12	1.339(12)
B1	F2	1.403(12)	N4	C15	1.315(12)
B1	C2	1.657(13)	N5	C12	1.368(11)
B1	F3	1.387(12)	N5	C13	1.383(12)
N2	C2	1.364(12)	N5	C16	1.460(12)
N2	C5	1.474(11)	N6	C12	1.328(12)
C2	C3	1.365(13)	C13	C14	1.355(13)
C3	C4	1.402(13)	C14	C15	1.399(13)
C4	C6	1.486(13)	C15	C17	1.481(13)
C6	C7	1.410(13)	C17	C18	1.390(13)
C6	C11	1.408(12)	C17	C22	1.405(14)
C7	C8	1.383(13)	C18	C19	1.385(13)
C8	C9	1.377(13)	C19	C20	1.389(15)
C9	C10	1.386(14)	C20	C21	1.373(14)
C10	C11	1.386(13)	C21	C22	1.377(14)

**Table 5 Bond Angles for OJH391v\_0m.**

Atom	Atom	Atom	Angle/°	Atom	Atom	Atom	Angle/°
C1	N1	C4	118.5(8)	F4	B2	F5	110.0(8)
N1	C1	N2	121.8(8)	F4	B2	C13	111.0(8)
N3	C1	N1	119.3(8)	F5	B2	C13	109.2(8)
N3	C1	N2	118.8(8)	F6	B2	F4	108.9(9)
F1	B1	F2	109.3(8)	F6	B2	F5	109.4(8)

F1	B1	C2	107.8(7)	F6	B2	C13	108.3(8)
F2	B1	C2	109.7(8)	C15	N4	C12	118.4(8)
F3	B1	F1	109.2(8)	C12	N5	C13	119.7(8)
F3	B1	F2	109.7(8)	C12	N5	C16	118.5(8)
F3	B1	C2	111.1(8)	C13	N5	C16	121.8(7)
C1	N2	C5	118.1(7)	N4	C12	N5	122.4(8)
C2	N2	C1	120.7(8)	N6	C12	N4	118.1(8)
C2	N2	C5	121.1(7)	N6	C12	N5	119.4(8)
N2	C2	B1	121.3(8)	N5	C13	B2	120.7(8)
N2	C2	C3	117.3(8)	C14	C13	B2	121.8(8)
C3	C2	B1	121.4(8)	C14	C13	N5	117.5(8)
C2	C3	C4	120.1(9)	C13	C14	C15	120.2(9)
N1	C4	C3	121.3(8)	N4	C15	C14	121.7(8)
N1	C4	C6	115.8(8)	N4	C15	C17	116.3(8)
C3	C4	C6	122.8(8)	C14	C15	C17	122.0(8)
C7	C6	C4	122.0(8)	C18	C17	C15	119.7(8)
C11	C6	C4	119.9(8)	C18	C17	C22	118.0(9)
C11	C6	C7	118.0(8)	C22	C17	C15	122.2(8)
C8	C7	C6	120.6(9)	C19	C18	C17	121.5(9)
C9	C8	C7	121.1(9)	C18	C19	C20	119.1(9)
C8	C9	C10	118.9(9)	C21	C20	C19	120.3(9)
C11	C10	C9	121.5(9)	C20	C21	C22	120.6(9)
C10	C11	C6	119.9(9)	C21	C22	C17	120.4(9)

**Table 6 Torsion Angles for OJH391v\_0m.**

A	B	C	D	Angle/°	A	B	C	D	Angle/°
F1	B1	C2	N2	-179.0(8)	B2	C13	C14	C15	-177.4(9)
F1	B1	C2	C3	0.7(12)	F4	B2	C13	N5	59.5(12)
N1	C1	N2	C2	5.0(14)	F4	B2	C13	C14	-122.3(10)
N1	C1	N2	C5	-172.7(8)	N4	C15	C17	C18	-10.0(13)
N1	C4	C6	C7	166.2(8)	N4	C15	C17	C22	170.6(9)
N1	C4	C6	C11	-14.6(13)	F5	B2	C13	N5	-62.0(11)
C1	N1	C4	C3	0.0(13)	F5	B2	C13	C14	116.3(10)
C1	N1	C4	C6	179.5(8)	N5	C13	C14	C15	0.9(13)
C1	N2	C2	B1	178.4(8)	F6	B2	C13	N5	179.0(8)
C1	N2	C2	C3	-1.3(13)	F6	B2	C13	C14	-2.8(13)
B1	C2	C3	C4	177.5(8)	C12	N4	C15	C14	1.4(14)
F2	B1	C2	N2	-60.1(12)	C12	N4	C15	C17	-178.4(8)
F2	B1	C2	C3	119.6(10)	C12	N5	C13	B2	179.5(8)
N2	C2	C3	C4	-2.9(14)	C12	N5	C13	C14	1.2(13)
C2	C3	C4	N1	3.6(14)	C13	N5	C12	N4	-2.2(13)
C2	C3	C4	C6	-175.8(9)	C13	N5	C12	N6	179.0(9)
F3	B1	C2	N2	61.4(12)	C13	C14	C15	N4	-2.3(15)

F3	B1	C2	C3	-118.9(10)	C13C14C15C17	177.5(9)
N3	C1	N2	C2	-178.1(9)	C14C15C17C18	170.2(9)
N3	C1	N2	C5	4.2(13)	C14C15C17C22	-9.2(15)
C3	C4	C6	C7	-14.3(14)	C15N4 C12N5	0.8(14)
C3	C4	C6	C11	165.0(9)	C15N4 C12N6	179.7(9)
C4	N1	C1	N2	-4.3(13)	C15C17C18C19	178.2(9)
C4	N1	C1	N3	178.9(9)	C15C17C22C21	-177.6(9)
C4	C6	C7	C8	178.4(8)	C16N5 C12N4	175.9(9)
C4	C6	C11	C10	-179.0(9)	C16N5 C12N6	-2.9(13)
C5	N2	C2	B1	-4.0(13)	C16N5 C13B2	1.5(13)
C5	N2	C2	C3	176.4(8)	C16N5 C13C14	-176.8(8)
C6	C7	C8	C9	0.7(14)	C17C18C19C20	0.6(16)
C7	C6	C11	C10	0.3(14)	C18C17C22C21	2.9(15)
C7	C8	C9	C10	0.0(14)	C18C19C20C21	0.7(16)
C8	C9	C10	C11	-0.6(15)	C19C20C21C22	-0.1(16)
C9	C10	C11	C6	0.5(14)	C20C21C22C17	-1.8(16)
C11	C6	C7	C8	-0.8(14)	C22C17C18C19	-2.3(15)

**Table 7 Hydrogen Atom Coordinates ( $\text{\AA}\times 10^4$ ) and Isotropic Displacement Parameters ( $\text{\AA}^2\times 10^3$ ) for OJH391v\_0m.**

Atom	<i>x</i>	<i>y</i>	<i>z</i>	U(eq)
H3A	4578.98	3132.98	4479.7	26
H3B	4266.38	3319.69	5150.93	26
H3	1558.68	4255.6	3253.3	19
H5A	3282.07	2954.72	5632.71	25
H5B	2635.13	4594.65	5578.72	25
H5C	3495.71	5193.5	5553.59	25
H7	1438.5	3580.37	2141.99	19
H8	1345.28	3686.14	926.16	22
H9	2437.64	4000.07	459.86	24
H10	3639.56	4208.7	1227.71	24
H11	3760.74	4162.97	2450.26	19
H6A	6065.43	1149.91	1027.74	23
H6B	5318.42	1076.72	1288.56	23
H14	7325.26	606.44	3854.59	21
H16A	4843.67	2161.79	2109.77	31
H16B	4812.27	1150.73	2848.92	31
H16C	4785.55	-155.97	2158.59	31
H18	8243.4	608.61	1871.02	22
H19	9569.43	797.36	1989.38	29
H20	10359.54	1220.86	3116.87	27
H21	9826.58	1411.6	4106.63	28
H22	8508.62	1167.24	3995.75	27

